



Ismail, Nur Faezah (2020) *Investigation into the roles of neutrophil infiltration in bladder cancer using murine models*. PhD thesis.

<https://theses.gla.ac.uk/81552/>

Copyright and moral rights for this work are retained by the author

A copy can be downloaded for personal non-commercial research or study, without prior permission or charge

This work cannot be reproduced or quoted extensively from without first obtaining permission from the author

The content must not be changed in any way or sold commercially in any format or medium without the formal permission of the author

When referring to this work, full bibliographic details including the author, title, awarding institution and date of the thesis must be given

Enlighten: Theses

<https://theses.gla.ac.uk/>
research-enlighten@glasgow.ac.uk

**Investigation into the roles of neutrophil infiltration in bladder
cancer using murine models**

Nur Faezah Binti Ismail

**Submitted in fulfilment of the requirements for the
Degree of PhD**



School of Medicine, Dentistry & Nursing

University of Glasgow

College of Medical, Veterinary and Life Sciences (MVLS)

July 2020

Abstract

Current literature suggested that the role of tumour infiltrating neutrophils could be pro- or anti-tumour and therefore double-edged. The heterogeneous nature of this population is dictated by environmental signals coming from the host and the tumour immune microenvironment. In bladder cancer, a high level of neutrophils is associated with poor prognosis. However, the functional role of neutrophil infiltration along the courses of bladder tumorigenesis is yet to be understood.

This study aimed to elucidate the roles of neutrophils in regulating bladder tumorigenesis using FGFR3-mutated and Cxcr2-deleted mouse models with wildtype (wt) mice as a control. FGFR3 is one of the most commonly mutated genes in bladder cancer. Cxcr2 is an essential receptor protein that mediates chemotaxis of neutrophils.

Bladder tumours were induced by a tobacco carcinogen N-butyl-N-(4-hydroxybutyl) nitrosamine (OH-BBN) for 10 weeks and tumour pathogenesis was analysed at the timepoint of 2, 12, 16 and 20 weeks from the start of treatment. A combined qualitative and quantitative approaches, namely haematoxylin and eosin (H&E) staining, immunohistochemistry (IHC), real-time PCR-based microarray were used to evaluate the changes in the urothelial and tumour histopathology, immune cell influx and gene expression in the tissue context.

Carcinogen-dependent bladder tumorigenesis was increased in Tg(UroII-hFGFR3IIIbS249C) (*FGFR3^{S249C}*) and in mice with Cxcr2 deletion in myeloid lineage, LysMCre Cxcr2^{fl/fl} (Cxcr2 flox) compared to wt. The tumour phenotype in *FGFR3^{S249C}* and Cxcr2 flox was more advanced and invasive. The acute inflammatory response was suppressed at the initial time of carcinogen treatment in both *FGFR3^{S249C}* and Cxcr2 flox with a significant reduction in neutrophils recruitment.

Further mechanistic evaluation of the immune cell recruitment in Cxcr2 flox showed changes in the levels of infiltrations of neutrophils, macrophages and T cells along the stages of tumour initiation and progression. Unexpectedly, Cxcr2 flox tumours were highly infiltrated with neutrophils as examined by H&E for their morphological appearance. However, many of them lacked expression of well-established markers for neutrophils. The increased level of neutrophils was in concomitant with that of tumour-infiltrating CD3⁺ T-cells.

Evaluation of the transcriptional changes showed that genes associated with immunity and inflammation were differently expressed in the bladder at the acute inflammation stage compared to bladder tumours in Cxcr2 flox compared to wt. Differences were also

observed in the gene expression between neutrophil-infiltrated and non-neutrophil infiltrated *Cxcr2* flox tumour samples.

Depletion of neutrophils using Ly6G monoclonal antibody (1A8) in the first 10 weeks of carcinogen treatment in wt mice reduced the recruitment of neutrophil at acute inflammation stage. The suppression of neutrophil recruitment at acute inflammation stage resulted in an increase of inflammation at a later stage of bladder tumorigenesis. Depletion of neutrophils in tumour-bearing mice was also attempted, however the effectiveness of depletion remained inconclusive.

The results in this study suggested that, firstly, bladder tumorigenesis was induced by the suppression of acute immune responses. Secondly, an increased level of neutrophil infiltrations resulted in an enhanced tumour progression. Thirdly, neutrophils influenced the levels of macrophages and T cells infiltrations, and this is likely to be caused by their regulation of gene expression associated with inflammation and immune signalling during early and late stages of bladder tumorigenesis. The results support further investigations towards clinical translation of FGFR3, CXCR2 and neutrophils, as therapeutic targets in bladder cancer.

Table of Contents	
Abstract	2
List of Tables	11
List of Figures	12
Acknowledgements	14
Author's Declaration	15
Publication	16
Chapter 1	17
Introduction	17
1.1 The bladder	18
1.1.1 Anatomy and function	18
1.1.2 The urothelium	18
1.2 Bladder cancer	18
1.2.1 Epidemiology	18
1.2.2 Symptoms	19
1.2.3 Risks and causes	19
1.2.4 Diagnosis	19
1.2.5 Types of bladder cancer and histopathological staging	20
1.2.6 Treatments	22
1.2.6.1 Treatments for NMIBC.....	22
1.2.6.2 Treatments for MIBC	22
1.2.6.3 Immunotherapy as a treatment for bladder cancer.....	22
1.2.6.4 Prognosis.....	23
1.3 Genetic alterations in bladder cancer	23
1.3.1 Fibroblast Growth Factor Receptor 3 (FGFR3)	23
1.3.1.1 FGFR3 expression and function	23
1.3.1.2 FGFR3 signalling	24
1.3.1.3 FGFR3 alteration in bladder cancer.....	24
1.4 Inflammation and immunity in non-cancer conditions	26
1.4.1 Acute inflammation in non-cancer conditions	26
1.4.2 Chronic inflammation in non-cancer conditions	26
1.4.3 Innate immune response in non-cancer conditions	27
1.4.4 Adaptive immune response in non-cancer conditions	27
1.5 Inflammation and immunity in cancer	27
1.5.1 Chronic inflammation in cancer	27
1.5.2 Chronic inflammation in bladder cancer	28
1.5.3 Cancer immunosurveillance	28
1.5.4 Cancer immunoediting	29
1.6 Innate and adaptive immune cells	29
1.6.1 Neutrophils	29
1.6.1.1 Function of neutrophils	29
1.6.6.2 Development and maintenance of neutrophils	30
1.6.6.3 Regulation of neutrophil function and migration	30

	5
1.6.6.4 Tumour-associated neutrophils (TANs)	31
1.6.6.5 Neutrophils in bladder cancer	32
1.6.2 Macrophages	33
1.6.2.1 Macrophages in non-cancer conditions	33
1.6.2.2 Tumour-associated macrophages (TAMs)	33
1.6.3 Myeloid derived suppressor cells (MDSCs).....	34
1.6.4 T cells	35
1.6.4.1 T cells in non-cancer conditions	35
1.6.4.2 Tumour-infiltrating T cells	35
1.7 CXCR2.....	36
1.7.1 CXCR2 Structure	36
1.7.2 CXCR2 expression	38
1.7.3 CXCR2 function	38
1.7.4 CXCR2 downstream signalling	39
1.7.5 Regulation of neutrophil transmigration by CXCR2	39
1.7.6 Known roles of CXCR2 in cancer	40
1.8 Murine models of bladder tumorigenesis.....	40
1.8.1 Carcinogen-induced models	40
1.8.2 Genetically modified mouse models	41
1.8.2.1 Cre-loxP	41
1.9 Research questions	43
1.10 Aim and objectives of the study	43
Chapter 2	44
Materials and Methods	44
2.1 Animal work.....	45
2.1.1 Mice	45
2.1.2 OH-BBN treatment.....	45
2.1.3 1A8 treatment	46
2.1.3.1 1A8-neutrophil depletion during the first ten weeks.....	46
2.1.3.2 1A8-neutrophil depletion in the tumours	46
2.1.5 Ultrasound imaging.....	46
2.1.6 Blood analysis	46
2.2 Histology.....	47
2.1.1 Tissue harvest, bladder weight and fixation.....	47
2.1.2 H&E.....	47
2.1.3 Immunohistochemistry (IHC)	47
2.1.4 Analysis of immune cell infiltrations in the tissue.....	48
2.3 RNAscope.....	51
2.4 Analysis of RNA expression	52
2.4.1 RNA extraction	52
2.4.2 cDNA synthesis	53
2.4.3 RNA array	53

	6
2.4.4 Taqman qRT-PCR.....	59
Table 2.5. List of TaqMan Gene Expression assay.....	59
2.5 Statistical analyses.....	59
Chapter 3	60
Effects of FGFR3 mutation on immune responses	60
3.1 Aim and objectives	61
3.2 Results	62
3.2.1 Carcinogen-dependent bladder tumorigenesis was increased in the presence of FGFR3 S249C mutation	62
3.2.2 Tumour phenotype was more severe in FGFR3 S249C bladders.....	65
3.2.3 Effects of FGFR3 mutations at 2 weeks	67
3.2.4 OH-BBN induced changes in the stroma and angiogenesis at 2 weeks.....	69
3.2.5 FGFR3 K644E mutation increased urothelial abnormalities at 12 weeks	71
3.2.6 Neutrophil infiltration following carcinogen treatment was suppressed in FGFR3 ^{S249C}	73
3.2.7 Neutrophil infiltration mildly increased in FGFR3-mutated mice at 12 weeks and 20 weeks	75
3.2.8 T-cells infiltration was not affected in FGFR3 mutated transgenic mice at 2 weeks.....	77
3.2.9 No alteration in tumour-infiltrating T cells in FGFR3-mutated mice	79
3.2.10 Effects of FGFR3 S249C mutation on immune signature gene expression in bladder cancer patients	81
3.2.10.1 FGFR3 S249C associated with a decrease in neutrophils' associated gene	82
3.2.10.2 FGFR3 S249C associated with a decrease in chemokines gene expression	84
3.2.10.3 FGFR3 S249C mutation associated with decreased in T cell population and activation genes.....	86
3.3 Discussion.....	88
3.3.1 Results summary	88
3.3.2 FGFR3 S249C mutation increased tumour occurrence and severity in carcinogen-dependent bladder tumorigenesis	88
3.3.3 FGFR3 S249C mutation suppressed acute inflammation	89
3.3.4 FGFR3 mutation associated with a lower expression of immune gene signatures in bladder cancer patients.....	90
3.4 Future directions.....	91
Chapter 4	92
Effects of Cxcr2 deletion in carcinogen-dependent bladder tumorigenesis	92
4.1 Aim & objectives	93
4.2 Results	94
4.2.2 Increase in bladder weight in Cxcr2 flox at 20 weeks of the OH-BBN course of treatment.....	97
4.2.3 Cxcr2 deletion in the myeloid-lineage increased tumour pathogenesis in OH-BBN-induced bladder tumour model.....	99

4.2.4 Cxcr2 flox showed an increase in invasiveness and squamous transformation	101
4.2.6 No significant difference in urothelial phenotype was observed at 12 weeks	105
4.2.7 Cxcr2 flox displayed pathological changes at 16 weeks.....	107
4.2.8 Senescence was retained in Cxcr2 flox mice at 2 weeks	109
4.2.9 Cxcr2 deletion in the myeloid lineage led to an impairment of the senescence pathway at 20 weeks.....	111
4.3 Discussion.....	113
4.3.1 Summary of results.....	113
4.3.2 Cxcr2 deletion in the myeloid cells enhanced bladder tumour occurrence and progression	113
4.3.3 Cxcr2 loss may dysregulate senescence leading to bladder tumorigenesis	114
4.3.4 Tumour occurrence was more frequent in male mice than female	115
Chapter 5	116
Effects on Immune cell infiltration upon Cxcr2 deletion.....	116
5.1.1 Hypotheses.....	117
5.1.2 Aim and objectives	117
5.2 Results	118
5.2.1 WBC populations at 2 weeks of carcinogen treatment	118
5.2.2 WBC populations at 16 weeks from the start of carcinogen treatment	120
5.2.3 Levels of neutrophils and lymphocytes in circulation were altered in the presence of tumour	122
5.2.4 Cxcr2 deletion increased monocytes infiltration in non-bladder tumour mice	124
5.2.5 Cxcr2 deletion resulted in impairment of neutrophil recruitment to the bladder tissue at 2 weeks of carcinogen treatment.....	126
5.2.6 Macrophage infiltration was decreased in Cxcr2 flox at 2 weeks	129
5.2.7 T cell infiltration in the bladder at 2 weeks of OH-BBN treatment.....	131
5.2.8 Neutrophil recruitment at 12 weeks from the start of carcinogen treatment	134
5.2.9 Changes in neutrophil infiltration at 16 weeks from the start of OH-BBN treatment.....	136
5.2.10 Cxcr2 flox bladders were highly infiltrated with macrophages at 16 weeks	138
5.2.11 T-cell infiltration was not affected in Cxcr2 flox at 16 weeks.....	140
5.2.12 Neutrophil infiltration was increased in the tumour of Cxcr2 flox	142
5.2.13 Discrepancy in neutrophil levels were observed when IHC markers were used	144
5.2.14 A low level of macrophage infiltration in the bladder tumour	146
5.2.15 Cxcr2 flox tumours were more T-cell infiltrated.....	148
5.3 Discussion.....	150

5.3.1 Summary of results	150
5.3.2 Acute inflammatory response was suppressed in Cxcr2 flox	150
5.3.3 Cxcr2 flox tumour was infiltrated with neutrophils and CD3+ T-cells	150
5.3.4 Discrepancy in the levels of neutrophils identified by markers and by morphology in tumour	151
5.3.5. Transient increase in macrophage infiltration at 16 weeks in Cxcr2 flox...	151
5.4 Limitation	152
5.5 Future works	152
Chapter 6	153
Transcriptional changes in the absence of Cxcr2 in the bladder	153
6.1.1 Hypotheses.....	154
6.1.2 Aim & Objectives	154
6.2 Results	155
6.2.1 Sample selection for RNA analysis at 2 weeks of carcinogen treatment	155
6.2.2 Expression of immune and inflammatory genes at 2 weeks of OH-BBN treatment.....	157
6.2.3 Expression of chemokine signalling genes at 2 weeks.....	159
6.2.4 Expression of signal transduction genes at 2 weeks	161
6.2.5 Expression of apoptosis-related genes at 2 weeks	163
6.2.6 Summary of altered gene expression at 2 weeks of OH-BBN treatment	165
6.2.7 Evaluation of the changes in the gene expression by qRT-PCR.....	167
6.2.8 Summary of the level of gene expression at 2 weeks of OH-BBN treatment using RNA array and TaqMan qRT-PCR	169
6.2.9 Sample selection for RNA analysis at 20 weeks	171
6.2.10 Expression of immune & inflammatory genes at 20 weeks	173
6.2.11 Expression of chemokine signalling genes at 20 weeks.....	175
6.2.12 Expression of signal transduction genes at 20 weeks	177
6.2.13 Expression of apoptosis genes at 20 weeks	179
6.2.14 Summary of the most altered genes at 20 weeks	181
6.2.15 Validation of Ccr2 expression in the tumour.....	185
6.2.16 Comparisons of gene expression levels between 2 weeks and 20 weeks sample	187
6.2.18 Tgf- β expression in tumour	189
6.3 Discussion.....	191
6.3.1 Summary of results.....	191
6.3.2 Differences in RNA analysis using RNA array-based and TaqMan-Assay based qRT-PCR	191
6.3.3 Differences in the expression level of genes at acute inflammation compared to late bladder tumorigenesis	192
6.3.4 Altered gene expression associated with tumour-infiltrating neutrophils in Cxcr2 flox.....	192
6.3.5 Tgf- β expression was associated with the presence of tumour cells.....	193

6.4 Future directions.....	193
Chapter 7	195
Effects of neutrophil depletion	195
7.1.1 Hypotheses.....	196
7.1.2 Aim and Objectives.....	196
7.2 Results	197
7.2.1 WBC levels in OH-BBN- and 1A8-treated mice at 2 weeks of treatments....	197
7.2.2 WBC levels in 1A8-treated mice at 20 weeks.....	199
7.2.3 Effects of neutrophil depletion in bladder tumorigenesis.....	201
7.2.4 Effects of neutrophil depletion in tumour-bearing mice	203
7.2.5 The effects of neutrophil depletion in tumour-bearing mice	205
7.2.6 Association between circulating and tissue-infiltrated neutrophils in 1A8/2A3 treated mice	207
7.2.7 The effects of neutrophil depletion on the tumour size	209
7.3 Discussion.....	211
7.3.1 Summary of results.....	211
7.3.2 Neutrophil depletion at acute inflammation stage enhanced inflammation at the later stage of bladder tumorigenesis	211
7.3.3 Potential causes of the lack of clear neutrophil depletion in tumour-bearing mice	211
7.4 Future direction.....	212
Chapter 8	213
General discussion.....	213
8.1 Overall summary of the findings.....	214
8.2 Proposed mechanism of inflammation-induced bladder tumour and progression	215
8.2.1 Suppression of acute inflammatory responses	217
8.2.2 An increase in local inflammation associated with tumour initiation in Cxcr2- deficient mice	217
8.2.3 Recruitment of pro-tumour neutrophils and tumour progression	218
8.2.4 Potential regulators of neutrophil recruitment to the tumour microenvironment in the absence of Cxcr2.....	220
8.2.5 Cxcr2 loss may dysregulate senescence leading to bladder tumorigenesis	222
8.3 Targeted therapy in bladder cancer	222
8.3.1 FGFR3-targeted therapy in bladder cancer	223
8.3.2 Neutrophil-targeted therapy in bladder cancer	223
8.3.3 CXCR2-targeted therapy in bladder cancer	224
8.4 Limitations.....	225
8.4.1 The use of LysM Cre mouse model in studying the functions of neutrophils.	225
8.4.2 Lack of metastasis formation.....	226

	10
8.5 Overall conclusions.....	226
8.6 Future directions.....	227
References.....	229

List of Tables

Table 2.1. Primary antibodies used for immunohistochemistry.....	49
Table 2.2. Secondary antibodies for immunohistochemistry.....	50
Table 2.3. List of probes for RNAscope.....	51
Table 2.4 List of cytokine genes for RNA array.....	55
Table 2.5. List of TaqMan Gene Expression assay.....	59
Table 3.1. Summary of the mouse cohorts and gross observation.....	63
Table 4.1 Table 4.1. Summary of the mouse cohorts and gross observations at the time of dissection.....	96
Table 6.1. Sample selection for RNA array analysis at 2 weeks of OH-BBN treatment.....	156
Table 6.2. Characteristics of the alterations in gene expression comparing Cxcr2 flox with wt bladders at 2 weeks of OH-BBN treatment.....	166
Table 6.3. Differences in the relative expressions of selected genes between RNA array and TaqMan qRT-PCR analysis.....	170
Table 6.4. Sample selection for RNA array analysis at 20 weeks from the start of OH-BBN treatment.....	172
Table 6.5. Tumour-infiltrating neutrophils associated with the downregulation of genes linked with cancer and inflammation in Cxcr2 flox.....	182
Table 6.6. Upregulated genes associated with cancer and inflammation in the presence of tumour-infiltrating neutrophils in Cxcr2 flox.....	184
Table 6.7. Comparison of gene expression at 2 weeks and 20 weeks from the start of carcinogen treatment.....	188

List of Figures

Figure 1.1. T staging of bladder cancer according to Tumour-Node-Metastasis system (TNM).....	21
Figure 1.2. FGFR3 structure.....	25
Figure 1.3. Tertiary structure of CXCR2.....	37
Figure 3.1. Histopathological analysis at 20 weeks from the start of OH-BBN treatment.....	64
Figure 3.2. Tumour characteristic of samples taken at 20 weeks from the start of OH-BBN treatment.....	66
Figure 3.3. Histopathological analysis on the urothelial abnormalities in samples taken at 2 weeks from the start of OH-BBN treatment.....	68
Figure 3.4. Histopathological analysis of stroma and angiogenesis presence in samples taken at 2 weeks of OH-BBN treatment.....	70
Figure 3.5. Histopathological analysis of samples taken at 12 weeks from the start of OH-BBN treatment.....	72
Figure 3.6. Infiltrations of neutrophils at 2 weeks from the start of OH-BBN treatment.....	74
Figure 3.7. Infiltrations of neutrophils at 12 and 20 weeks from the start of OH-BBN treatment.....	76
Figure 3.8. Infiltration of total T-cells (CD3 ⁺) at 2 weeks of OH-BBN treatment.....	78
Figure 3.9. Infiltration of T-cells (CD3 ⁺) in tumour samples at 20 weeks.....	80
Figure 3.10. <i>FGFR3</i> S249C mutation effects on neutrophils and monocytes gene expression in TCGA, Cell 2017 study.....	83
Figure 3.11. <i>FGFR3</i> S249C mutation effects on CXCR2 and ELR ⁺ chemokines.....	85
Figure 3.12. <i>FGFR3</i> S249C mutation effects on immunostimulatory and immunosuppressive genes expression.....	87
Figure 4.1. Schematic presentation of OH-BBN treatment for induction of bladder tumorigenesis.....	95
Figure 4.2. Bladder weight at 20 weeks from the start of OH-BBN treatment.....	98
Figure 4.3. Histopathological analysis of the bladder at 20 weeks from the start of OH-BBN treatment.....	100
Figure 4.4. The characteristics of the urothelial at 20 weeks from the start of OH-BBN treatment.....	102
Figure 4.5. Histopathological analysis of urothelial abnormalities at 2 weeks.....	104
Figure 4.6. Histopathological analysis of the bladders at 12 weeks from the start of OH-BBN treatment.....	106
Figure 4.7. Histopathological analysis of bladder at 16 weeks from the start of OH-BBN treatment.....	108
Figure 4.8. Expression of senescence-associated proteins at 2 weeks.....	110
Figure 4.9. Expression of senescence-associated proteins in bladder tumour at 20 weeks.....	112
Figure 5.1. Effects of <i>Cxcr2</i> deletion in circulation at 2 weeks of carcinogen treatment.....	119
Figure 5.2. Blood analysis at 16 weeks from the start of carcinogen treatment.....	121
Figure 5.3. WBC profiles at 20 weeks.....	123
Figure 5.4. Effects of <i>Cxcr2</i> deletion on systemic WBC at 20 weeks from the start of carcinogen treatment.....	125
Figure 5.5. Neutrophil infiltration at 2 weeks.....	127
Figure 5.6. Neutrophil infiltration in the bladder at 2 weeks.....	128
Figure 5.7. Macrophage infiltration at 2 weeks.....	130
Figure 5.8. T cell infiltration at 2 weeks.....	132
Figure 5.9. T-cell infiltration at 2 weeks of OH-BBN treatment.....	133
Figure 5.10. Neutrophil infiltration at 12 weeks from the start of carcinogen treatment.....	135
Figure 5.11. Neutrophil infiltration at 16 weeks from the start of carcinogen treatment.....	137
Figure 5.12. Macrophage infiltration at 16 weeks from the start of carcinogen	

Treatment.....	139
Figure 5.13. T-cell infiltration in samples taken at 16 weeks from the start of carcinogen treatment.....	141
Figure 5.14. Presence of neutrophils in tumour at 20 weeks from the start of carcinogen treatment.....	143
Figure 5.15. Expression of neutrophil markers in the tumour area.....	145
Figure 5.16. Presence of macrophages in the tumour area.....	147
Figure 5.17. T-cell infiltration in the tumour.....	149
Figure 6.1. Expression of immune and inflammatory genes at 2 weeks.....	158
Figure 6.2. Chemokines, interleukins and growth factor profile at 2 weeks after carcinogen treatment.....	160
Figure 6.3. Expression of signal transduction genes at 2 weeks after OH-BBN Treatment.....	162
Figure 6.4. Changes in the apoptosis-related genes at 2 weeks of treatment with OH-BBN.....	164
Figure 6.5. Expression of Egf, Spp1, Ido1 and Nos2 at 2 weeks.....	168
Figure 6.6. Expression of Immune and inflammatory cytokine genes in tumour bladder samples.....	174
Figure 6.7. Gene expression for chemokines, interleukins, growth factors and their receptors.....	176
Figure 6.8. Expression of genes related to signal transduction.....	178
Figure 6.9. Expression of apoptosis-associated genes.....	180
Figure 6.10. Expression of Ccr2 by qRT-PCR analysis.....	186
Figure 6.11. Tgf- β expression in bladder tumour samples of Cxcr2 flox and wt.....	190
Figure 7.1. Depletion of neutrophils in wt mice.....	198
Figure 7.2. WBC analysis of samples at 20 weeks from the start of OH-BBN and 1A8/2A3 treatments.....	200
Figure 7.3. Effects of neutrophil depletion in the bladder tissues at 2 and 20 weeks.....	202
Figure 7.4. WBC analysis of 1A8/2A3-treated mice.....	204
Figure 7.5. Tissue-infiltrated neutrophils in 1A8/2A3-treated and non-1A8/2A3 treated mice.....	206
Figure 7.6 Association between circulating neutrophils and tissue-infiltrated neutrophils in 1A8/2A3-treated mice.....	208
Figure 7.7. Bladder volumetric analysis of tumour-bearing mice treated with 1A8/2A3 for 2 weeks.....	210
Figure 8.1. Proposed mechanisms of suppression of acute inflammatory response enhanced bladder tumorigenesis.....	216

Acknowledgements

I want to express my deepest gratitude towards my supervisor, Dr Tomoko Iwata, for her endless support and guidance throughout this project. I am also indebted to my second supervisor Dr Jennifer Morton, Prof Owen Sansom and Tam Jamieson for providing me their valuable inputs and the animals for the project.

My special thanks also go to Colin Nixon and his team for their valuable assistance with the histology services. Thanks also to Saadia Karim who has kindly helped and trained me for the ultrasound imaging. My gratitude is also extended to the staffs at Beatson Animal Unit for their great help in handling the animals.

My heartfelt thanks go to Dr Seth Coffelt and the members of his research group especially Dr Anna Kilbey for helpful discussions and experimental support.

I am forever indebted to my parents, Ismail Ngah and Nik Yam Salleh, for their love, encouragement and enormous support that helped me reach this stage. Last but not least, thank you to my siblings, my colleague in Dr Iwata's lab, John Pritchard, and my friends in Glasgow and abroad for always been the ones that I could run to whenever in need.

This research will not be materialized without the funding from the Public Department of Malaysia (JPA).

Nur Faezah Binti Ismail

July 2020

Author's Declaration

I hereby declare that all work in this thesis, unless stated otherwise, is entirely my work.
No part of this thesis has been submitted for any other degree at any institute.

Nur Faezah Binti Ismail

July 2020

Publication

The work presented in Chapter 3 (Effects of FGFR3 mutation on immune responses) has resulted in the following publication in which Dr Mona Foth and I shared joint first name authorship;

Foth, M., **Ismail, N.F.B.**, Kung, J.S.C., Tomlinson, D., Knowles, M.A., Eriksson, P., Sjö Dahl, G., Salmond, J.M., Sansom, O.J. & Iwata, T. (2018) FGFR3 mutation increases bladder tumourigenesis by suppressing acute inflammation. *Journal of Pathology*, 246 (3), pp.331–343.

Chapter 1

Introduction

1.1 The bladder

1.1.1 Anatomy and function

The bladder is part of the urinary tract system alongside kidney, ureter and urethra. It functions as a storage tank of urine. The ability of the bladder to hold urine which contains toxic and noxious compounds is enabled by its highly adapted structure with a tight barrier on the luminal surface of the urothelium (Abraham & Miao, 2015; Baker & Southgate, 2011; Wu et al., 2009).

The bladder is a triangle-shaped, hollow and elastic organ. The main structure of the human bladder consists of three layers, which are the urothelium, the lamina propria and the detrusor smooth muscle supporting the bladder (Baker & Southgate, 2011).

1.1.2 The urothelium

The urothelium is also called transitional epithelium owing to its elastic feature that could contract in and out during storage and excretion of urine. The urothelium lines the bladder and serves as the first lining defence against foreign substances in the urine (Abraham & Miao, 2015).

The urothelial cells are formed up to seven layers in humans, and up to three layers in mice (Castillo-Martin et al., 2010). The urothelium is composed of three different types of cells, superficial (umbrella), intermediate and basal cells (Castillo-Martin et al., 2010). The umbrella cells are large with polarized and thick asymmetric unit membrane and comprise of uroplakin proteins that serve as a barrier for reabsorption of the urine (Kobayashi et al., 2015; Wu et al., 2009). Intermediate cells are limited in proliferative capacity but are known to be the precursor for umbrella cells. Basal cells are cuboidal in shape and are metabolically active (Kobayashi et al., 2015; Gandhi et al., 2013; Frazier et al., 2012).

These umbrella, intermediate and basal cells have a different expression of cytokeratin and p63. The umbrella cells are positive for CK18 and CK20 but negative for p63 (Castillo-Martin et al., 2010; Karni-Schmidt et al., 2011). Intermediate and basal cells express CK5, CK10, CK14 and p63 (Castillo-Martin et al., 2010; Karni-Schmidt et al., 2011). All layers express CK7 (Castillo-Martin et al., 2010).

1.2 Bladder cancer

1.2.1 Epidemiology

Bladder cancer is the 9th most common cancer in the world and 10th most common cancer in the UK (Antoni et al., 2017; Cancer Research UK, 2019). In the UK, bladder cancer accounts for 3% of total cancer cases reported from 2014-2016 (Cancer Research UK, 2019). Bladder cancer is more prevalent in males than females. Among the ageing

population, a median age at diagnosis is at 73 years old (Cumberbatch et al., 2018) and the mortality rate is higher in developing countries (Antoni et al., 2017).

1.2.2 Symptoms

The most common symptom of bladder cancer is the presence of blood in the urine (macroscopic haematuria) which present in approximately 80% of bladder cancer patients (Cancer Research UK, 2019; Yazbek-Hanna et al., 2016; Ok et al., 2005). Other symptoms include microscopic haematuria, frequent urinating, pain or difficulty in urinating due to urinary obstruction (dysuria), abdominal pain and weight loss (Cancer Research UK, 2019; Yazbek-Hanna et al., 2016; Ok et al., 2005).

1.2.3 Risks and causes

Tobacco smoking is a significant risk factor for bladder cancer (Burger et al., 2013; Freedman et al., 2011). Cigarette smoke contains a diverse and high concentration of carcinogens, such as 1,3-butadiene, benzene, aldehydes, aromatic amines, ethylene oxide and N-nitrosamines (Centres for Disease Control and Prevention, 2010).

Occupational exposure to industrial processing paints, dyes, metals, or petroleum products is the second major risk factor for bladder cancer (Redondo-Gonzalez et al., 2015; Burger et al., 2013). These harmful chemicals exert a carcinogenic effect on the entire urinary system, especially in direct contact with the urothelium (Burger et al., 2013; McConkey et al., 2010).

Age and gender have also been associated with bladder cancer, and the incidence rate is higher in older people and men (Letašiová et al., 2012; Kuper et al., 2002). Infection with parasitic flatworm *Schistosoma haematobium* is also associated with bladder cancer (Kiriluk et al., 2012; Mostafa et al., 1999). The infection is common in developing countries but rare in developed countries, and lead to the squamous cell carcinoma type of bladder cancer (Antoni et al., 2017; Michaud et al., 2007).

1.2.4 Diagnosis

One of the standard methods used to diagnose bladder cancer is cystoscopy. Cystoscopy is highly sensitive, but it has its limitation where it may fail to identify small papillary tumours and carcinoma in situ (CIS) (Cheung et al., 2013). The development of narrow-band imaging (NBI) cystoscopy has aimed to overcome the issue (Jocham et al., 2008). NBI uses computer-enhanced cystoscopes which intensify the colour contrast of urothelial lesions (Bryan et al. 2008) and makes the blood vessels in tumours easier to see (Cancer Research UK, 2019).

The most widely adopted non-invasive urine test is cytology which includes Bladder Tumour Associated Antigen (BTA) test, Nuclear Matrix Protein (NMP22) test and Mcm5 test (Kitamura and Tsukamoto, 2006; Van Rhijn *et al.*, 2014; Cancer Research UK, 2019). These tests can be used to detect high-grade tumours but are limited for their sensitivity in low-grade tumours (Lotan *et al.*, 2008). Fluorescence in situ hybridization (FISH) is also used to detect urinary cells that have chromosomal abnormalities, which are consistent with recurrence and progression to muscle-invasive bladder cancer (Kipp *et al.*, 2009). However, this test is costly and associated with some false-positive results (Nieder *et al.*, 2007; Cheung *et al.*, 2013).

1.2.5 Types of bladder cancer and histopathological staging

Majority of bladder cancer is classified as urothelial carcinoma (90%), and the remainder is composed of squamous cell carcinoma (8%) as well as adenocarcinoma (1-2%) (Cancer Research UK, 2019).

Urothelial carcinoma (UC) could be further subcategorized into non-muscle invasive (NMIBC) which comprised approximately 75% of the reported UC, and the remaining 25% has muscle-invasive bladder cancer (MIBC) (Cumberbatch *et al.*, 2018).

UC is pathologically staged based on TNM classification in which T stands for tumour characteristics, N for regional lymph node status and M for the presence of metastasis (Cancer Research UK, 2019; EAU Guidelines, 2019) (Figure 1.1).

The NMIBC patients are stratified into three groups; 1) low-risk tumours, 2) intermediate-risk tumours, and 3) high-risk tumours based on the risk of recurrence and progression to MIBC (Hurst *et al.*, 2017; EAU Guidelines, 2019).

The MIBC patients are all classified as high-grade and staged based on the TNM classifications (EAU Guidelines, 2019).

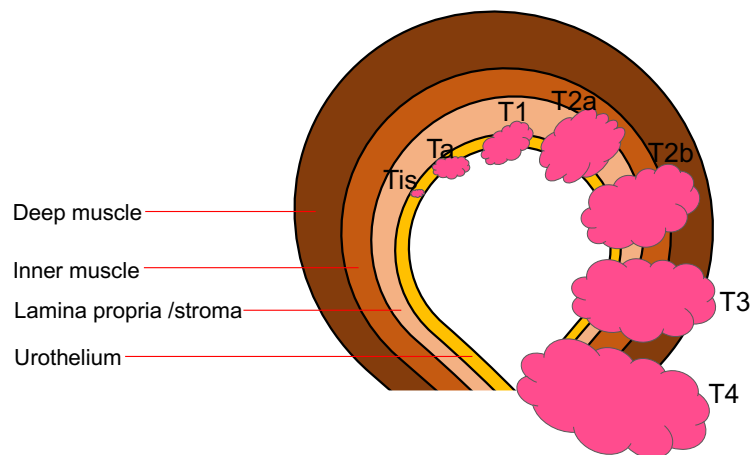


Figure 1.1. T staging of bladder cancer according to Tumour-Node-Metastasis system (TNM). The T stage is based on the invasiveness of the tumour cells (Tis-T4). Superficial lesion in the urothelium (CIS / Tis). Non-invasive papillary carcinoma (Ta) Tumour invades lamina propria (T1). Tumour invades superficial muscle layer (T2a). Tumour invades deep muscle (T2b). Tumour invades perivesical tissue surrounding the bladder wall (T3). Tumour invades neighbouring organs (T4) (Adapted from Cancer Research UK, 2020; Knowles and Hurst, 2015).

1.2.6 Treatments

1.2.6.1 Treatments for NMIBC

The management for low-risk NMIBC includes transurethral resection of bladder tumour (TURBT) followed by one chemotherapy instillation, and cystoscopy surveillance (EAU guidelines, 2019). For Intermediate-risk of NMIBC, patients need to undergo repeated TURBT treatments followed with cycles of chemotherapy or intravesical full-dose Bacillus Calmette-Guérin (BCG), and more prolonged and frequent cystoscopy surveillance than the low-risk NMIBC (Bellmunt *et al.*, 2017; EAU guidelines, 2019;). Meanwhile, for patients with high-risk NMIBC, full-dose of intravesical BCG is needed for one to three years, and radical cystectomy is offered for patients with the highest-risk of NMIBC (Cheung *et al.*, 2013; Bellmunt *et al.*, 2014; EAU guidelines, 2019).

1.2.6.2 Treatments for MIBC

The primary treatment for MIBC is neoadjuvant chemotherapy, followed by radical cystectomy (Cheung *et al.*, 2013). Chemotherapy involves a course of cisplatin-based chemotherapy, that is a combination of gemcitabine and cisplatin (GC) or methotrexate, vinblastine, doxorubicin (Adriamycin) and cisplatin (MVAC). During and after treatment, patients undergo a follow-up protocol to monitor tumour response, progression and recurrence (Bellmunt *et al.*, 2014). If the patients are not fit, radiotherapy may also be offered.

Depending on the fitness, patients with metastasis are treated with cisplatin-based chemotherapy as above as a first line (Cancer Research UK, 2019). The second line options are often clinical trials.

1.2.6.3 Immunotherapy as a treatment for bladder cancer

Intravesical instillation of BCG is the first immunotherapy that has been approved by the Food and Drug Administration (FDA) in 1990. BCG was shown to reduce the recurrence in NMIBC (Suttman *et al.*, 2006; Sylvester *et al.*, 2006).

Recently, five checkpoint inhibitors targeting PD1/PD-L1 have been approved by the FDA for the treatment of MBIC. These immune checkpoint inhibitors are being used as a first line therapy for cisplatin-ineligible advanced metastatic UC patients and as second line therapy for patients that are cisplatin-eligible, but tumour still grow after the cisplatin treatment (American Cancer Society, 2020; Ghatalia *et al.*, 2018). For example, two PD-1 inhibitors, Pembrolizumab and nivolumab, and three PD-L1 inhibitors, Avelumab, Durvalumab and Atezolizumab, are offered after the first-line cisplatin therapy (Massari *et al.*, 2018). The clinical trial outcome for approved checkpoint inhibitors was encouraging in treating bladder cancer patients, with an increased survival rate compared to

chemotherapy (Rosenberg et al., 2016). However, it was reported that only a small subset of patients benefitted from the immunotherapy (Hahn et al., 2017).

1.2.6.4 Prognosis

Like other cancers, the prognosis of bladder cancer is mainly associated with the pathological stages of cancer. NMIBC showed favourable prognosis but had a higher recurrence (31%) and approximately 25 - 75% of higher risk NMIBC developed MIBC (Cumberbatch et al., 2018; Sylvester et al., 2006). For MIBC, the 5-year survival rate of pT2 tumours is 60-70%, and 36%–58%, in pT3. At pT4 stage, or when tumour spread to nearby lymph nodes, a high percentage of relapse was recorded (Rosenberg & Hahn, 2009). Patients with metastasis also showed poor prognosis, with 5-year survival rates of 9% (Cancer Research UK, 2019).

1.3 Genetic alterations in bladder cancer

It has been proposed that urothelial carcinoma arises from two different pathways starting from early pre-tumour lesions; 1) papillary and superficial lesions that give rise to hyperplasia (non-invasive), and 2) dysplasia that leads to CIS (invasive) (Knowles, 2008). The superficial papillary lesion may be derived from the genetic instability induced by gain-of-function mutations of oncogenes, including FGFR3, PI3K, and HRAS and the deletions in chromosome 9q (Iyer & Milowsky, 2013; Castillo-Martin et al., 2010; Knowles, 2008; Jebar et al., 2005). In contrast, dysplasia/CIS is considered as a precursor of MBIC, derived from the genetic instability induced by loss-of-function of tumour suppressors, such as P53, RB and PTEN.

1.3.1 Fibroblast Growth Factor Receptor 3 (FGFR3)

1.3.1.1 FGFR3 expression and function

FGFR3 is a glycoprotein and belongs to tyrosine kinase receptors family, FGFRs (Sturla et al., 2003; Junker et al., 2008). It is normally expressed in the cartilage, central nervous system and testis (Iwata & Hevner, 2009; Plowright et al., 2000; Cancilla et al., 1999).

FGFR3 mediates signalling pathways that control cellular processes, such as proliferation, migration and differentiation (Iyer & Milowsky, 2013; Turner & Grose, 2010). It has also been shown to play a role in angiogenesis, wound healing and embryonic development (Chen et al., 2015; Kang et al., 2017).

FGFR3 negatively regulates bone development, and its overactivation causes dwarfism (Kang et al., 2017; Chen et al., 2005; Iwata, 2001; Iwata, 2000). The roles of FGFR3 are also known to be involved in tumorigenesis of bladder cancer and multiple myeloma. A high frequency of mutation in FGFR3 is associated with these cancer types (Kang et al., 2017; Iyer & Milowsky, 2013; Junker et al., 2008; Chen et al., 2005).

1.3.1.2 FGFR3 signalling

The extracellular portion of FGFR3 binds FGF-1-10,16-23 for its activation (Iwata & Hevner, 2009; Powers et al., 2000; Jaye et al., 1992) (Figure 1.2). FGFR3 activation causes dimerization and subsequent phosphorylation of tyrosine residues (Spivak-Kroizman *et al.*, 1994; Chen *et al.*, 2005; Ornitz and Itoh, 2015). The activated kinase binds to cytosolic adaptor proteins, triggering various intracellular signalling pathways for cell growth and differentiation including mitogen-activated protein kinases (MAPKs), STAT, phosphatidylinositol 3-kinase (PI3K), and PLC γ but not PKB/AKT (Spivak-Kroizman et al., 1994; Chen et al., 2005; Iwata and Hevner, 2009; Ornitz and Itoh, 2015).

1.3.1.3 FGFR3 alteration in bladder cancer

As stated above, FGFR3 is commonly mutated in bladder cancer, multiple myeloma, cervical cancer (Kang et al., 2017). FGFR3 mutations associated with bladder cancer include R248C, S249C in the ligand-binding domain, K652E in the kinase domain, and G372C and Y375C in the transmembrane domain (Billerey et al., 2001). K652E is equivalent to K644E in mice (Iwata et al., 2000). 70% of NMIBC show FGFR3 point mutations (Di Martino et al., 2016; Kang et al., 2017). High expression of FGFR3 was also linked with the low-grade NMBIC, with the high-recurrence rate (Kang et al., 2017). In contrast, FGFR3 mutations were not detected in CIS (Billerey *et al.*, 2001).

Overexpression of wild-type FGFR3 was observed in 40% of MIBC patients (Hahn et al., 2017). High expression of FGFR3 was also associated with poor prognosis in MIBC (Sjödahl et al., 2012).

Mutations and overexpression of FGFR3 lead to constitutive dimerization and activation of oncogenic signalling pathways, including RAS/MAPK, PI3K/AKT and STAT (Bernard-Pierrot et al., 2006).

It has been shown that FGFR3 mutation alone does not cause spontaneous bladder tumour in mice, but a combination of FGFR3 mutation with deletion of PTEN, an inhibitor for PI3K-AKT signalling, was shown to induce urothelial abnormalities (Foth et al., 2014).

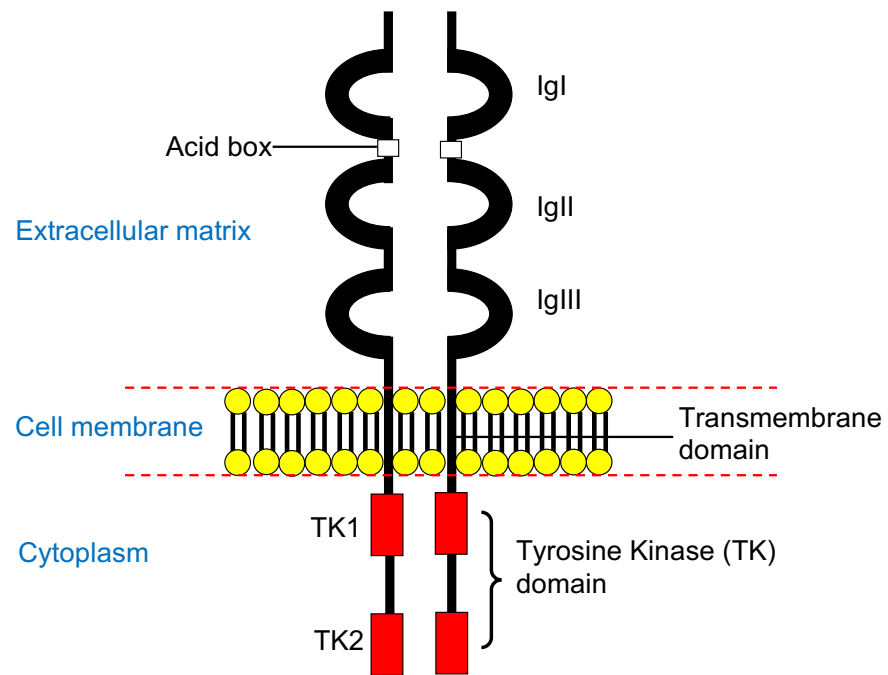


Figure 1.2. FGFR3 structure. FGFs bind to immunoglobulin domains (IgI,II, III) triggered receptor dimerization and conformational change which then lead to transphosphorylation of the tyrosine kinase . Subsequently, kinase binds to cytosolic adaptor proteins to trigger various intracellular signalling cascades including MAPKs, STATs, PI3K and PLC γ (Adapted from Turner and Grose, 2010).

1.4 Inflammation and immunity in non-cancer conditions

1.4.1 Acute inflammation in non-cancer conditions

Acute inflammation is a response to tissue stressor induced by infection or injury (Medzhitov, 2008; Freire and Dyke, 2013). A natural acute inflammatory response is self-limiting, with a balance of pro- and anti-inflammatory factors (Coussens and Werb, 2002; Freire and Dyke, 2013). The goal for the acute inflammatory response is to eradicate pathogen or foreign materials and induce subsequent tissue repair with minimal physical changes on the tissue (Sansbury & Spite, 2016). The degree of the response depends on the cause and persistence of the inflammation (Freire and Dyke, 2000).

During an acute inflammatory response, the recruitment of innate immune cells precedes the adaptive immune cells (Schreiber et al., 2011). The recruitment is initiated by the upregulation of inflammatory mediators by the mast and tissue-resident macrophages (Gilroy & Lawrence, 2008). The neutrophils are then recruited, followed by monocytes which then differentiate to phagocytosing macrophages at the site of inflammation (Sansbury & Spite, 2016).

Once the inciting agent is removed, the inflammation is resolved to avoid excessive inflammatory responses and chronic inflammation. The release of lipid mediators such as lipoxins, resolvins and prostaglandins (PGs) play a role as a “stop signal” for the influx of neutrophils, and for the macrophages to remove apoptotic neutrophils (Freire and Dyke, 2000; Gilroy and Lawrence, 2008). The number of macrophages correlates with the number of neutrophils at the inflammation site (Selders et al., 2017). Macrophages ingest apoptotic neutrophils before they egress towards the lymphatic system or undergo the apoptosis process (Freire and Dyke, 2000). Other inflammation resolving mediators, such as cytokines and fibroblasts, also aid in neutralizing the chemokine gradients to restore the homeostasis back to normal (Gilroy and Lawrence, 2008).

1.4.2 Chronic inflammation in non-cancer conditions

Dysregulated inflammation and failure to resolve pro-inflammatory mediators lead to chronic inflammation (Coussens and Werb, 2002; Freire and Dyke, 2013). The prolonged and excessive activation of cytokine and chemokine signalling cascade leads to the uncontrolled infiltration of leukocytes, which promote pathological changes in the tissue (Ptaschinski & Lukacs, 2017).

Chronic inflammation contributes significantly to the pathogenesis of Type II diabetes, asthma, neurological disorder, rheumatoid arthritis and cancer (Multhoff et al., 2012; Nathan & Ding, 2010; Kotas & Medzhitov, 2015).

1.4.3 Innate immune response in non-cancer conditions

As discussed in 1.4.1, innate immune response works as the first line of host defences against foreign materials. The system varies from non-specific barrier functions such as pulmonary, skin, and guts epithelial cells, to highly selective immune cells, including dendritic cells, macrophages, neutrophils and natural T-killer cells (Clark & Kupper, 2005). Some of the components such as dendritic cells and macrophages, which are also known as antigen-presenting cells (APCs), are critical factors in initiating and instructing adaptive immune response against pathogens (Clark and Kupper, 2005). APCs express pathogen-recognition receptors (PRR) on their cell surface that could recognize pathogen-associated molecular patterns (PAMP) (Courtney et al., 2018).

1.4.4 Adaptive immune response in non-cancer conditions

The adaptive immune response (acquired immunity) is a part of the immune system that provides a response to antigen and maintains pathogen-specific memory cells (Courtney et al., 2018; McComb et al., 2013). The adaptive immune system is mainly composed of T cells and B cells that mediate cellular immune response and antibody production, respectively (McComb *et al.*, 2013). Compared to the innate immune system, the adaptive immune system is more flexible but slower and dependent on the innate immune system for its initiation (Clark and Kupper, 2005). The flexibility of the adaptive immune system is enabled by the T cells which change at the DNA level during development, creating a variety of T and B cell receptors that could recognize almost any antigen (Clark & Kupper, 2005; McComb et al., 2013).

1.5 Inflammation and immunity in cancer

1.5.1 Chronic inflammation in cancer

Chronic inflammation is listed as one of the hallmarks of cancer (Hanahan & Weinberg, 2011). The immunologic components of chronic inflammation in cancer consists of pro-inflammatory cells, such as macrophages, neutrophils, lymphocytes, and pro-inflammatory and immunosuppressive cytokines, such as tumour necrosis factor-alpha (TNF α), transforming growth factor-beta (TGF- β), IL-1, IL6, IL-10 and PGH-2. These components are present in the tumour and in the stroma (Coussens and Werb, 2002; Multhoff, Molls and Radons, 2012; Sui *et al.*, 2017; Tesi, 2019).

Chronic inflammation contributes to tumorigenesis at all stages, from initiation, progression and to metastasis (Schreiber et al., 2011; Grivennikov et al., 2010a). At the initiation and pre-malignant stages, inflammatory cells induce genetic modification via the production of inflammatory cytokines, reactive oxygen species (ROS) and reactive nitrogen species (RNS) (Grivennikov et al., 2010a). At the tumour-promoting stage, the local inflammation by the pro-inflammatory cells and cytokines activate transcription

factors, such as NF-KB and STAT3, leading to the proliferation of tumour cells (Schreiber et al., 2011; Grivennikov et al., 2010a). At the later stage of tumorigenesis, the unresolved inflammation enhances angiogenesis, tissue invasion and immunosuppression, establishing an environment for the tumour progression and metastasis (Schreiber et al., 2011; Grivennikov et al., 2010a).

1.5.2 Chronic inflammation in bladder cancer

Bladder cancer is sensitive to acute inflammation and is promoted by chronic inflammation (Grivennikov et al., 2010a). Several factors trigger chronic inflammation in the bladder, including urinary tract infection (UTI), chemical and mechanical irritations such as cigarette smoke, and infections by *Schistosoma haematobium* (Sui et al., 2017; Michaud & Sc, 2007). These factors are known risks of bladder carcinogenesis (Michaud & Sc, 2007). Persistent chronic inflammation in the urothelium may lead to an increase in replicative potential of the urothelial cells, which may later result in the pathological changes of the urothelium, such as dysplasia, metaplasia, carcinoma *in situ* (CIS) (Sui et al., 2017; Clouston & Lawrentschuk, 2013; Takahashi et al., 2000). These lesions may subsequently progress to invasive carcinoma with the histological subtype of squamous cell carcinoma (Michaud & Sc, 2007).

1.5.3 Cancer immunosurveillance

Cancer immunosurveillance is a concept of how innate and adaptive immune systems function as a tumour suppressor (Dunn et al., 2004). The evidence of cancer immunosurveillance in mammals is largely based on the evidence from the use of mouse models in cancer (Vesely et al., 2011). For example, immunodeficient mice are shown to be susceptible to develop spontaneous and carcinogen-induced tumours. Tumours from immunodeficient mice are more immunogenic than those developed in immunocompetent mice (Engel et al., 1997; Smyth, Godfrey and Trapani, 2001; Dunn *et al.*, 2002).

Immune responses are influenced by the characteristics of tumours, such as cell type and origin, mechanism of transformation and inherent immunogenicity (Dunn et al., 2004). The lymphocytes and cytokines function as extrinsic factors in eradicating tumour initiation when the intrinsic factors failed to induce repair mutations and programmed cell death (Vesely et al., 2011; Smyth et al., 2001).

In additions to dendritic cells, macrophages, natural killer cells (NK cells) and natural killer T cells (NKT cells), studies have shown that $\alpha\beta$ T cells and $\gamma\delta$ T cells are also important in immunosurveillance (Girardi et al., 2003; Girardi et al., 2018; Smyth et al., 2001). NK cells, $\alpha\beta$ CD8 T cells and $\gamma\delta$ T cells express NKG2D-activating receptor that helps to distinguish between the tumour from non-tumour cells (Dunn et al., 2004). Effectors for cell cytotoxicity, and cytokines, such as perforin, interferon-gamma (IFN- γ) and Fas-Fas ligand

(FasL), are also critical in mediating the immune activities against neoplastic cells (Vesely et al., 2011; Smyth et al., 2001).

1.5.4 Cancer immunoediting

The concept of cancer immunoediting has been introduced to explain the changes in the immune system from host-protective to host-tumour promoting (Smyth et al., 2006; Dunn et al., 2004). It involves three main phases, firstly, elimination phase or the cancer immunosurveillance by the innate and adaptive immune systems, secondly, equilibrium in which surviving tumour variants enter the dormancy period, and lastly, the escape of tumour cells with reduced immunogenicity (Schreiber et al., 2011; Vesely et al., 2011; Smyth et al., 2006).

During the elimination phase, the innate and adaptive immune systems detect and eradicate the growth of abnormal cells (Schreiber et al., 2011; Vesely et al., 2011). Some abnormal cells could survive immune destruction and enter the equilibrium phase (Smyth et al., 2006). During this equilibrium phase, immune cells, such as CD4⁺ CD8⁺ T cells, and immunostimulatory factors, such as IL-12 and IFN- γ , still control and prevent the growth of these dormant tumour cells (Dunn et al., 2004). However, tumours develop ways to escape these regulations and limit the immune surveillance with the elimination of tumour-antigen, reduction of effector T cells infiltration, and immunosuppressive activities induced in the tumour microenvironment (Singel & Segal, 2016; Schreiber et al., 2011).

1.6 Innate and adaptive immune cells

1.6.1 Neutrophils

Neutrophils are polymorphonuclear cells (PMN). They are produced at a rate of 10^{11} cells daily and account for 50-70% of the total circulating leukocytes (Cheng et al., 2019; Rosales, 2018; Selders et al., 2017). Neutrophils have been reported to have a short half-life, which is only about 8 hours in humans (Dancey et al., 1976). However, later studies showed that the half-life of neutrophils is much longer, 91.2 hours in humans and 12.5 hours in mice (Pillay et al., 2010).

1.6.1.1 Function of neutrophils

Neutrophils act as the first responders to the damaged and inflamed sites. Neutrophils promote clearance of the pathogen and debris by phagocytosis (Freire and Dyke, 2000). The destructive potentials of neutrophils towards pathogens are based on the generation of oxidases, such as NADPH oxidase (NOX2), the release of cytotoxic granular constituents, such as myeloperoxidase (MPO), and formation of neutrophil extracellular traps (NETs) (Singel & Segal, 2016).

1.6.6.2 Development and maintenance of neutrophils

The term, granulopoiesis, refers to the development of neutrophils in the bone marrow under the control of G-CSF to arise from haematopoietic stem cells (HSC) (Görgens et al., 2013). HSCs differentiate to lymphoid-primed multipotent progenitors, and then to the granulocyte-monocyte progenitors (GMP) (Coffelt et al., 2016). The GMP undergoes a series of maturation steps to give rise to circulating neutrophils.

The stages of maturation consist of proliferative and non-proliferative phases (Ng et al., 2019; Rosales, 2018). During the proliferative stage, myeloblasts, derived from GMP, differentiate into promyelocytes and then to myelocytes. The myelocytes give rise to the non-proliferative metamyelocytes, which mature to banded neutrophils, and finally fully matured neutrophils (Ng et al., 2019).

The development of granules begins in myeloblast and early promyelocytes and ends by the generation of secretory vesicles in mature, hyper-segmented neutrophils (Lawrence et al., 2018; Koenig et al., 2017). The granules contain proteins, receptors, adhesion molecules, and inflammatory mediators that play vital roles in every aspect of neutrophil function. A sequence of granule formation starts from the formation of azurophilic granules in promyelocyte. This follows the formation of secondary, “specific” granules in myelocyte, tertiary granules predominantly filled with gelatinase in metamyelocyte, and lastly, secretory granules in mature neutrophils (Lawrence et al., 2018).

During abnormal immune reactions driven by chronic inflammation or tumour pressure, production and release of neutrophils from the bone marrow rapidly increase to accommodate their demand (Rankin, 2010; Coffelt et al., 2016). This is called “emergency granulopoiesis”

1.6.6.3 Regulation of neutrophil function and migration

Neutrophils express a diverse class of surface receptors, which include G-protein coupled receptors, Fc-receptors, adhesion receptors, cytokine receptors and innate immune receptors (Futosi et al., 2013).

Neutrophils express G-protein coupled receptors, CXC or CXC3C chemokine receptors, including CXCR1, CXCR2, CXCR4 and CX3CR1, which are essential for their recruitment towards inflammatory sites (Stadtman & Zarbock, 2012).

Neutrophils respond towards diverse inflammatory mediators, including selectins, chemokines, and integrins (Stadtman and Zarbock, 2012). Mechanisms of neutrophil recruitment to the inflammatory sites could be described in four major steps; 1) recognition of the inflammation signals, 2) rolling along the capillary wall, 3) adhesion on the

endothelium and 4) extravasation into the tissue (Bardoel et al., 2014). The recruitment of neutrophils is guided by the chemokine gradients (Ptaschinski & Lukacs, 2017).

An *in vivo* study using an inflammatory model showed that neutrophils recruitment occurs in two waves. The first wave is to initiate the innate response, and the second wave, to induce the signalling cascade for the adaptive response (Lombard et al., 2016).

Neutrophils in the first and second waves do not differ in their cytotoxic ability and phenotype (Lombard *et al.*, 2016). The accumulation of neutrophils during the first wave has been shown to lead to the accumulation of monocytes/macrophages (Freire and Dyke, 2000).

The recruited neutrophils at the inflamed site express a higher level of IL-6, IL-1B, TNF, CXCL1 and CXCL2, compared to circulating neutrophils (Sadik et al., 2011). The higher expression of these pro-inflammatory cytokines may lead to the amplification of inflammatory signalling in recruiting more neutrophils (Sadik et al., 2011). The presence of neutrophils at the inflamed sites triggers the production of host-chemoattractant, which orchestrate the recruitment of other inflammatory cells, such as macrophages (Freire and Dyke, 2013; Coffelt *et al.*, 2016).

1.6.6.4 Tumour-associated neutrophils (TANs)

The TANs are the term that defines neutrophils that infiltrate the tumour. The recruitment of the TANs is induced by several factors, including hypoxia and nutrient starvation in the tumour microenvironment (Coffelt et al., 2016; Singel & Segal, 2016; Massena et al., 2015; Christoffersson et al., 2012). High cellular proliferation and apoptosis in the tumour microenvironment can lead to the release of damage-associated molecular patterns (DAMP) which later attracts neutrophils recruitment (Powell & Huttenlocher, 2016a; Singel & Segal, 2016; Zhang et al., 2010). Neutrophils interact with tumour and the tumour-stroma to generate cross-signalling to other inflammatory cells, such as macrophages (Powell & Huttenlocher, 2016a; Silvestre-Roig et al., 2016; Singel & Segal, 2016).

The heterogeneity of TANs could be characterised by their biological characteristics and properties, including maturation status, proliferative capacity, tissue localisation, site of origin, and effector function (Ng et al., 2019; Singel & Segal, 2016; Fridlender et al., 2012a; Fridlender et al., 2009). The TANs are also characterised by population-based transcriptional profiling and epigenetic regulations (Ng et al., 2019).

Surface markers have been used to differentiate the TANs into three distinctive populations; 1) low-density mature TANs, 2) high-density mature TANs, and 3) low-density immature TANs (Hsu et al., 2019; Sagiv et al., 2015). Singhal et al. (2016) have reported that a subset of TANs possesses APCs markers (HLA-DR, CD14, CD206. CD86.

CCR7). However, they lack other APC markers in dendritic cells and macrophages (CD209, CD204, CD83, CD163, CD1c, CCR6). These APC-TANs augmented T cell responses against tumour in the early-stage lung adenocarcinoma, but the population decrease at the later stage. It was also shown that the APC-TANs originated from the immature neutrophil progenitors (CD11b⁺ CD15^{hi}CD10⁻CD16^{low}) and that their differentiation into either immune-stimulatory or immune-suppressive were likely to be regulated by IFN γ .

Under tumour pressure, G-CSF expands the granulopoiesis leading to the release of mature and immature neutrophils from the bone marrow to the bloodstream, then to the tumour sites or distant organ (Coffelt et al., 2016; Brandau et al., 2013). This aids metastasis-niche seeding (Singel and Segal, 2016). Circulating immature neutrophils have a higher half-life than mature neutrophils owing to high expression of survivin, an anti-apoptotic protein (Altzner et al., 2004). Similar to mature neutrophils, immature neutrophils are non-proliferative but migrate towards inflammatory stimuli at the same rate (Evrard et al., 2018).

The plasticity of TANs is described under the N1 and N2 classification, a nomenclature adopted from M1/M2 tumour-associated macrophages (TAM). N1 classifies TANs with an anti-tumour phenotype that aids host adaptive immunity. In contrast, N2 classifies pro-tumour TANs associated with the increase of angiogenesis and inflamed tumour microenvironment (Fridlender et al., 2012a; Fridlender et al., 2009; Andzinski et al., 2015). The pro-tumour TANs are also associated with the metastatic seeding and its progression (Coffelt et al., 2015; Steele et al., 2016).

Clinically, a higher neutrophil-to-lymphocyte ratio (NLR) is mostly associated with poor prognosis and tumour progression in several solid cancers, including pancreas, lung, colon and liver (Guthrie et al., 2013). However, in gastric cancer, NLR was associated with a higher survival rate (Caruso et al., 2002).

1.6.6.5 Neutrophils in bladder cancer

In bladder cancer, the higher TANs were associated with worse pathological grades of bladder tumours as well as the higher recurrence of NMIBC (Liu et al., 2018). Bladder cancer patients with high TANs and NLR also have a poor prognosis (Zhang et al., 2017). High circulating and tumour-infiltrating granulocytic myeloid cells were observed in bladder cancer patients (Eruslanov et al., 2012). The CD11b⁺ CD15⁺ HLA-DR⁻ population, was shown to induce the production of pro-inflammatory cells (Eruslanov *et al.*, 2012).

1.6.2 Macrophages

1.6.2.1 Macrophages in non-cancer conditions

Macrophages are a heterogeneous population of myeloid cells, and their differentiation, homeostasis and functions are mainly influenced by the surrounding environmental stimuli (Chow et al., 2011; Mosser & Edwards, 2008). The classical function of macrophages is phagocytosis that aids the removal of apoptotic and senescence cells, toxin and cellular debris (Mosser & Edwards, 2008; Murray & Wynn, 2011). Macrophages are also important as APCs to activate T cell immunity (Gordon, 2003).

The heterogeneity of macrophages depends on the differentiation of their precursor, monocytes (Lawrence & Natoli, 2011). Tissue-resident macrophages are known as sentinel cells that protect the host against a pathogen or environmental challenges and maintain homeostasis (Davies et al., 2013). Tissue-resident macrophages also involved in other physiological processes such as bone development, angiogenesis and regulation of metabolism (Davies *et al.*, 2013).

Macrophages are the primary source of pro-inflammatory cells for neutrophils recruitment in the bladder by secreting the CXCL1 and MIF (Schiwon et al., 2014).

1.6.2.2 Tumour-associated macrophages (TAMs)

The plasticity of macrophages in the tumour microenvironment is defined with the designation of M1 and M2 phenotypes, that represent the classical-activated and alternative-activated macrophages, respectively. M1 is pro-inflammatory and possess anti-tumorigenic properties. In contrast, M2 is anti-inflammatory and pro-tumorigenic (Aras & Raza Zaidi, 2017; Murdoch et al., 2008; Mantovani et al., 2002).

M1 macrophages are stimulated by LPS and by IFN- γ . They also express a high level of pro-inflammatory cytokines and MHC I and II, and cytotoxic factors (Grivennikov et al., 2010a; Ugel et al., 2015; Mantovani et al., 2002). The polarization of M2 is stimulated by IL4 and IL13, with downregulation of suppressive factors, such as IL12 (Aras & Raza Zaidi, 2017; Ugel et al., 2009; Grivennikov et al., 2010a; Mantovani et al., 2002).

Most TAMs are reported to resemble the M2 phenotype, which aids the tumour cell migration, invasion, metastasis and tissue remodelling (Mantovani et al., 2002; Condeelis and Pollard, 2006; Aras and Zaidi, 2017). However, recent evidence has suggested that these two phenotypes are interchangeable and often coexist. Therefore, these characteristics of macrophages remain to be better clarified (Martinez & Gordon, 2014; Gordon, 2003).

1.6.3 Myeloid derived suppressor cells (MDSCs)

MDSCs are heterogeneous cell populations that resulted from altered myelopoiesis (Ugel et al., 2015; Sica et al., 2012; Highfill et al., 2010). Humans and mice MDSCs are classified into three subpopulations; 1) polymorphonuclear/granulocyte MDSCs, 2) monocytic MDSCs, and 3) immature MDSCs (Ugel *et al.*, 2015).

The granulocyte MDSCs resemble immature neutrophils and lack expression of MHC II and CD86, the co-stimulatory factor for antigen processing and presentation (Movahedi et al., 2008; Hsu et al., 2019). The monocytic MDSCs have phenotype overlapping with the M2 TAM (Sica & Bronte, 2007).

MDSCs are known to negatively regulate the immune system by promoting the recruitment of T regulatory cells (Treg) via IFN- γ and IL10 (Huang et al., 2006). MDSCs were also shown to induce the transformation of fibroblasts to cancer-associated fibroblast, and that they skewed the macrophages to M2 TAM phenotype by downregulating the expression of IL12 (Ugel et al., 2015; Sica & Bronte, 2007). The immunosuppressive activities of MDSCs are associated with high expression of arginase 1, iNOS and ROS production (Greten et al., 2011; Highfill et al., 2010). The presence of MDSCs has been implicated in various immune dysregulated diseases associated with chronic inflammation especially cancer (Ugel et al., 2015; Greten et al., 2011).

The expansion and recruitment of MDSCs in the tumour microenvironment was associated with the tumour growth, angiogenesis and metastasis progression (Ye et al., 2010; Yang et al., 2008). Increase in the infiltration of MDSC leads to suppression of T cell activities in a melanoma mouse model (Meyera et al., 2011; Bronte et al., 2000).

Monocyte MDSC (CD14⁺HLADR^{-/low}) was associated with clinical stages and pathological grade of bladder cancer (Yuan et al., 2011).

In the tumour microenvironment, tumour cells induce overexpression of Csf2 (also known as GM-CSF), leading to the expansion of immature MDSC from haematopoietic cells (Stromnes et al., 2014). GM-CSF and G-CSF regulate the differentiation of myeloid precursors to monocytic MDSCs and granulocyte MDSCs, respectively (Ugel et al., 2015; Coffelt et al., 2016). Chemokines and cytokines are involved in the recruitment of MDSCs (Murdoch et al., 2008). Increased production of CCL2, CXCL12 and CXCL5 lead to the recruitment of MDSCs by binding to their respective receptors CCR2 and CXCR2 on MDSCs (Highfill et al., 2014; Sawanobori et al., 2008). High expression of CXCR2 expression in tumour-bearing mice was also shown to regulate the differentiation of haematopoietic cells to monocytic MDSCs (Han et al., 2019).

1.6.4 T cells

1.6.4.1 T cells in non-cancer conditions

T cell development occurs in the thymus (Burt & Verda, 2004). A state of differentiation is characterised by the expression of cell differentiation surface molecules (Burt & Verda, 2004; Zúñiga-Pflücker, 2004). The precursor cell, known as thymocyte, lack expression of CD4 or CD8, termed as a double-negative, before differentiating into double-positive CD4⁺CD8⁺ cells, and lastly single-positive cell of either CD4⁺ or CD8⁺ (Michie & Zúñiga-Pflücker, 2002). CD8⁺ T cells recognise peptides in association with MHC I molecules found on all nucleated cells, whereas CD4⁺ T cells recognise peptides presented by MHC II molecules (Blum et al., 2013). CD4⁺ and CD8⁺ T cells play a major role in maintaining adaptive and memory responses (Smyth et al., 2001).

The activation of T cells occurs in three major steps; 1) the engagement of antigen to TCR, 2) co-stimulation of pathogen-associated molecular patterns (PAMPs) on the surface of T cells, and 3) differentiation of T helper cells (CD4⁺) to effector T cells (CD8⁺) (Jain & Pasare, 2017; Smyth et al., 2001). In the first step, the APC presents the antigen peptide by binding MHC I and/or MHC II presented on T cells (Courtney et al., 2018). The binding led to the co-stimulation of PAMPs on TCR, which helps to distinguish the self-antigen from non-self-antigen (Jain & Pasare, 2017). The co-stimulation leads to stimulate the increase of innate cytokines for the differentiation of T helper cells to effector T cells (Jain & Pasare, 2017; Smyth et al., 2001).

1.6.4.2 Tumour-infiltrating T cells

The effectiveness of anti-tumour activities by T cells is influenced by various factors, including the trafficking of effector T cells to the tumour sites and their interactions with the checkpoint inhibitors (Singel and Segal, 2016).

Human cancers can be stratified into three immune profiles, based on the presence and cytotoxic activities of T cells (Chen & Mellman, 2013). The first profile is “immune desert” in which there are no T cells present in the tumour and/or its surrounding. The second is “immune excluded” in which T cells are present in adjacent to tumour area but unable to infiltrate into the tumour area. The third is “inflamed” which represents tumours with high infiltration of T cells but are inactive to kill the tumour cells.

A high level of tumour-infiltrating T cells was associated with an increase in the expression of immune-inhibitory molecules such as PD-L1, IDO, FOXP3, TIM3 and LAG3 in MIBC (Sweis et al., 2016).

1.7 CXCR2

1.7.1 CXCR2 Structure

CXCR2 is a G-protein coupled receptor (G-PCR) (Murphy, 1994). It has seven transmembrane regions with the N-terminus at the extracellular side, for the binding of the ligands, and the C-terminus in the cytoplasm for the guanine nucleotide exchange (Figure 1.3) (Roth & Hebert, 2000).

In humans, CXCR2 binds to 7 chemokines that are known as glutamic acid-leucine-arginine (ELR)-positive chemokines, CXCL1-3 and CXCL5-8 (Roth and Hebert, 2000). In mice, *Cxcr2* binds to the same chemokines, except that mice lack CXCL8, and *Cxcl6* is homologous to the human CXCL5 and CXCL6 (Sherwood et al., 2015). Both human and mouse CXCR2 have been proved to be equal in functions, which allow the use of animal models to test the human receptor roles (Mihara et al., 2005).

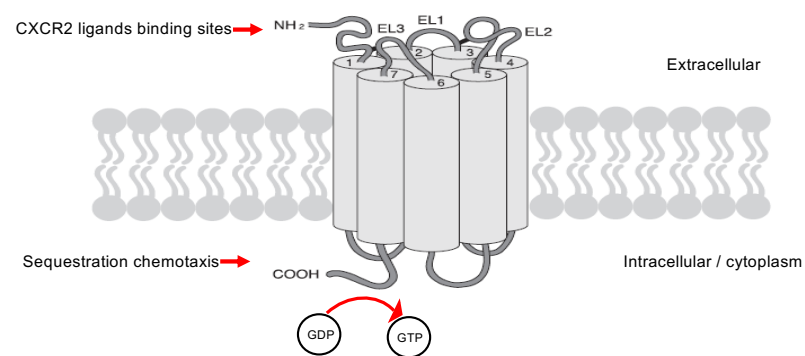


Figure 1.3. Tertiary structure of CXCR2. The transmembrane helical domains are indicated by the tubular structures, numbered 1 - 7. The seven hydrophobic regions of the receptors are embedded in the plasma membrane. Three extracellular loops are designated EL1-3. The free N-terminal tail is extracellular and for the binding site of CXCR2 ligands. The C-terminus is in the cytoplasm and contain serine and threonine for the phosphorylation, internalization and sequestration processes. Binding of CXCR2 to the ligands lead to the conversion of GDP to GTP. Adapted from (Cheng et al., 2019; Roth & Hebert, 2000).

1.7.2 CXCR2 expression

In general, chemokines are classified into two groups depending on their roles as either inflammatory or homeostatic (Moser & Loetscher, 2001). Inflammatory chemokines are produced under pathological conditions, such as inflammation, and involved in the trafficking of the leukocytes to the sites of inflammation. Homeostatic chemokines are continuously produced within tissues and play a regulatory role of inflammation (Zlotnik et al., 2011; Moser & Loetscher, 2001).

CXCR2 is classified as a homeostatic chemokine receptor. It is widely expressed in different haematopoietic and inflammatory cells such as eosinophils, natural killer cells, neutrophils, macrophages, mast cells, and monocytes as well as endothelial cells (Roth & Hebert, 2000; Murphy et al., 2000). CXCR2 is also expressed by non-haematopoietic keratinocytes and endothelial cells.

1.7.3 CXCR2 function

The binding of Cxcr2 ligands to their receptor activates multiple G-protein-mediated signalling cascades for the physiological and pathophysiological processes involved in inflammation and cell proliferation (Cheng et al., 2019; Han et al., 2015). The activation regulates the expression of multiple cytokines and chemokines to form a positive-feedback loop in enhancing the function of CXCR2 (Cheng *et al.*, 2019).

Cytokines are a small secreted protein that is important for immune and inflammatory responses (Zhang and An, 2007). The production of cytokine immune and inflammatory cells could enhance the tumour promotion and progression by providing the continuous growth factor and survival signals (Grivennikov et al., 2010a).

CXCR2 acts as a mediator of leukocyte recruitment to the sites of inflammation and its activation (Bizzarri et al., 2006; Baggiolini & Loetscher, 2000). The binding with its ligands mediates host defences by inducing chemotaxis and intracellular calcium mobilization in different leukocyte subsets (Wu et al., 2012; Roth & Hebert, 2000).

CXCR2 also regulates wound healing process via recruitment of neutrophil to the wound site (Devalaraja et al., 2000a; Milatovic et al., 2003). Several *in vivo* studies have also shown CXCR2 roles in inflammatory diseases including rheumatoid arthritis and multiple sclerosis (Liu et al., 2010; Coelho et al., 2008; Jacobs et al., 2010).

CXCR2 is also a key player in senescence pathways, including replicative senescence and oncogene-induced senescence (OIC) (Acosta et al., 2008; Acosta & Gil, 2009). Cxcr2 deletion could delay and impair both replicative and oncogenic-induced senescence (OIC) (Acosta and Gil., 2009). OIC is regarded as the first barrier of defence against cancer

development (Haugstetter et al., 2010). Oncogene-induced DNA damage response (DDR) and/or cytokine signalling were suggested to be involved in increasing the intrinsic senescence prior to DNA damage or early lesion expansion (Bartek et al., 2008). The loss of this senescence barrier contributes to the expansion of the lesion, which later becomes malignant. In vitro studies showed that CXCR2 is pivotal in maintaining oncogene-induced senescence where the expression of this receptor and its ligands were increased during this process (Acosta *et al.*, 2008).

1.7.4 CXCR2 downstream signalling

CXCR2 acts as guanine nucleotide exchange factors (GEF) for the heterotrimeric G proteins (Roth and Herbert, 2000). In the inactive, guanosine diphosphate (GDP)-bound state, heterotrimeric G proteins associate with the intracellular domains of CXCR2 (Roth and Herbert, 2000; Cheng et al., 2019). Binding of the ELR⁺ chemokine ligands to CXCR2 leads to its guanine nucleotide exchange activity, converting GDP to GTP of the G protein (Stadtman and Zarbock, 2012). The G protein then subsequently dissociates into α , β subunits to activate multiple downstream signalling cascades (Stadtman and Zarbock, 2012).

1.7.5 Regulation of neutrophil transmigration by CXCR2

CXCR2 and its ligands, CXC ELR⁺ chemokines, are pivotal for transmigration of neutrophils to the sites of inflammation (Köhler et al., 2011; Moser et al., 1993; Baggiolini & Loetscher, 2000). CXCL8 (also known as IL8) is the predominant ligand for CXCR2 in humans (Campbell et al., 2013).

The expression of CXCR2 increases proportionally during the maturation stage of neutrophils (Grassi et al., 2018). Mature neutrophils express a high level of CXCR2 and the level of CXCR2 decreases when neutrophils enter the senescent phase and apoptosis (Rankin, 2010). The decrease of CXCR2 expression is concomitant with the increase of CXCR4 expression, which is a mechanism for the homing of neutrophils back to the bone marrow (Sadik et al., 2011; Rankin, 2010).

CXCR2 mediates neutrophil migration via PI3K/AKT pathway (Cheng *et al.*, 2019). G-CSF regulates the CXCR2 and CXCR4 expression during the homeostasis by controlling the number of endothelial cells and osteoblast, the major sources for CXCR2 and CXCR4 ligands, respectively (Sadik et al., 2011; Semerad et al., 2005).

In cancer, both pro- and anti-tumorigenic properties of CXCR2 are mostly associated to its primary role as a chemotactic factor of neutrophils (Steele *et al.*, 2016; Steele *et al.*, 2015; Jamieson *et al.*, 2012; Acosta *et al.*, 2008).

1.7.6 Known roles of CXCR2 in cancer

Several *in vivo* cancer models have shown that CXCR2 and ELR⁺ chemokines are differentially expressed and regulated during the stages of cancer (Acosta and Gill, 2008; Acosta *et al.*, 2009; Jamieson *et al.*, 2012; Lee *et al.*, 2014). Cxcr2 was found to be highly expressed by endothelial cells, myeloid-derived cells, and the tumour cells themselves in the tumour microenvironment (Cheng *et al.*, 2019). The high expression correlates with CXCR2 abilities to modulate tumour-leukocyte interactions and suppression of anti-tumour immunity (Lee *et al.*, 2014; Cheng *et al.*, 2019).

High CXCR2 expression indicates poor prognosis in lung adenocarcinoma (Saintigny *et al.*, 2013). CXCR2-CXCL1-axis has been implicated in the migration and angiogenic effects of melanoma cells (Singh *et al.*, 2009). Depletion of Cxcl1/ Cxcr2 suppresses inflammation-driven tumorigenesis in the skin, intestine, and spontaneous adenocarcinoma formation in mice (Jamieson *et al.*, 2012).

CXCR2 was shown to promote metastasis in colon cancer (Yamamoto *et al.*, 2008). The crosstalk between Cxcr2-dependent neutrophils with other chemokines establishes mechanisms for the metastatic process in the pancreatic cancer mouse model (Steele *et al.*, 2016).

CXCR2 effect on tumour progression is tissue-dependent. Expression of CXCR2 in prostate cancer is upregulated in early pre-malignant cells but downregulated during tumour progression (Acosta *et al.*, 2008; Murphy *et al.*, 2005). At the pre-malignant stage, high expression of Cxcr2 and its ligands reinforced senescence by oncogenic K-ras (Acosta *et al.*, 2008). Anti-tumorigenic properties of CXCR2 was also evidenced in the pancreas, in which low CXCR2 expression was associated with advanced neoplastic lesions (Lesina *et al.*, 2016).

CXCR2 was reported to be pro-tumorigenic in bladder cancer (Zhang *et al.*, 2017; Gao *et al.*, 2015). High expression of CXCR2 and its ligands, CXCL2 and CXCL5 promotes the recruitment of MDSCs and tumour migration, invasion and invasion through PI3K/AKT signalling in bladder cancer patients.

1.8 Murine models of bladder tumorigenesis

1.8.1 Carcinogen-induced models

Spontaneous formation of bladder tumour is rare in murine models unless induced with carcinogen or with oncogenic genetic modification (Vasconcelos-Nóbrega *et al.*, 2012). Three main chemical carcinogens used to induce bladder cancer in mice are N-[4-(5-nitro-2-furyl)-2-thiazolyl] formamide (FANFT), N-butyl-N-(4-hydroxybutyl) nitrosamine (OH-BBN) and N-Methyl-N-nitrosourea (MNU) (Ahmad *et al.*, 2012). These carcinogens were

administered orally either via drinking water or via gavage (Ahmad et al., 2012; Vasconcelos-Nóbrega et al., 2012).

OH-BBN comes into contact with the bladder through urine (Vasconcelos-Nóbrega *et al.*, 2012). OH-BBN induces tumours that originate in the urothelium, as a form of urothelial dysplasia, papillary or nodular dysplasia, and subsequently leads to invasive carcinoma (Saito et al., 2018; Fantini et al., 2018).

Molecular alterations of bladder tumours induced by OH-BBN was shown to have similarities with high-grade, basal-like MIBC in humans (Fantini et al., 2018). However, driver mutations in human basal-like and luminal-like tumours, including FGFR3, were not induced by OH-BBN (Fantini et al., 2018; Saito et al., 2018).

1.8.2 Genetically modified mouse models

1.8.2.1 Cre-loxP

Cre-loxP technology has been successfully used in tissue- and cell-specific gene targeting in mouse models with conditional deleting, inserting, replacing, activating alteration of the levels of expression of a gene of interest (Smith, 2011; Akagi et al., 1997; Le & Sauer, 2001; Ahmad et al., 2012).

The standard gene modifications by Cre-loxP in the mouse requires two genetically engineered mouse lines, one with a Cre recombinase under the control of promotor that allows tissue-or cell-specific expression, and the other with a gene of interest flanked with loxP sites (Le & Sauer, 2001; Sauer & Henderson, 1988). These mouse strains are crossed to generate offspring with the context-specific gene modifications.

1.8.2.1.1 Bladder-specific promotor of expression

The Cre driver based on the expression of uroplakin 2 (Uro11), a protein expressed in the urothelium, has been extensively used to create conditional modulation of targeting gene in a bladder cancer mouse model (Kobayashi et al., 2015; Zhang et al., 1999). Uro11 promoter is urothelium specific and conditional expression of p53 driven by this promoter has successfully led to CIS and bladder tumour formation (De La Peña et al., 2011; Zhang et al., 1999).

1.8.2.1.2 Myeloid cell specific promotor of expression

Lysozyme (LysM) is an enzyme encoded by *Lyz2* gene and expressed in myeloblast, macrophages and neutrophils (Orthgiess et al., 2016; Cross et al., 1988). The efficiency of LysM-Cre recombinase-mediated deletion of loxP-flanked target genes were nearly 100% in granulocytes, 83-98% in mature macrophages, and 16% in CD11c⁺ splenic dendritic cells, but not in T and B cells (Clausen et al., 1999). LysM-Cre mice have been widely

used to target genes in myeloid cells specifically (Takahashi et al., 2010; Ye et al., 2003; Steele et al., 2015; Eash et al., 2010).

1.9 Research questions

The research questions addressed in this study were:

- 1) Does FGFR3 mutation influence inflammation during bladder tumorigenesis?
- 2) What is the role of inflammation during bladder tumorigenesis?
- 3) Does Cxcr2 play a role in the recruitment of immune cells to the urothelium, and in the bladder tumours?
- 4) What are the factors that regulate neutrophils, and what is the mechanism of tumour progression initiated and promoted by the myeloid cells?
- 5) Can we modulate neutrophil population in a murine model of bladder cancer, and will it lead to the regression of the tumour?

1.10 Aim and objectives of the study

The overall aim of this study was to investigate the roles of neutrophils in carcinogen-dependent bladder tumorigenesis.

The objectives were;

- 1) To characterise the effects of FGFR3 S249C & K644E mutations in carcinogen-induced bladder mouse models.
- 2) To characterise the effects of inflammation in bladder pathogenesis using a carcinogen-induced mouse model of Cxr2 deletion
- 3) To characterise the status of immune cell infiltrations at the stages of acute inflammation, tumour initiation and progression in the mouse model of Cxcr2 deletion.
- 4) To characterise the expression of genes that may have promoted bladder tumour progression and controlled the levels of neutrophil and immune cell infiltrations, in the presence and absence of Cxcr2.
- 5) To examine the effects of neutrophil depletion in the suppression of carcinogen-induced inflammation in the bladder, and in inflammation and tumour size in tumour-bearing mice.

Chapter 2

Materials and Methods

2.1 Animal work

2.1.1 Mice

Wild type animals (wt) were purchased from Charles River Laboratories.

Mice that expressed human FGFR3 IIIb isoform with an S249C mutation (*FGFR3^{S249C}*) were generated in collaboration amongst T. Iwata, M. Knowles and D. Tomlison (unpublished). *Fgfr3^{K644E}* mice express heterozygous *Fgfr3* K664E (UroIIICre *FGFR3^{+/K644E}*) (Iwata et al., 2000).

Mice with deleted *Cxcr2* in their myeloid lineage cells *LysMCre Cxcr2^{fl/fl}* (*Cxcr2* flox) were obtained from Dr Jennifer Morton (University of Glasgow, UK). The *Cxcr2* flox mice were generated using a Cre/loxP recombination system with lysozyme M promoter (*LysM*) (Clausen et al., 1999). Mice with deleted *Cxcr2* expression in the tissue *Cxcr2^{-/-}* (*Cxcr2* ko) were obtained from Thomas Jamieson (Beatson Institute for Cancer Research (BICR), UK). The generation of the *Cxcr2* ko was as previously described in Steele *et al.*, 2015.

All mice were of C57Bl/6J background apart from *Cxcr2* ko which were from Balb/c backcrossed with C57Bl/6J.

Mice were maintained at the BICR animal facility. All experiments were carried out in accordance with the Home Office Animal (Scientific Procedures) Act 1986 in the UK with Personal Licence No. I61A1FD21 under Project Licence No. 60/4271 and 70/9028.

2.1.2 OH-BBN treatment

Age-matched mice between 8-10 weeks old were used in this study. Mice were administered N-butyl- N-(4-hydroxybutyl)-nitrosamine (OH-BBN) (TCI, UK) at 0.05% v/v in drinking water for ten weeks which was freshly prepared three times a week. Mice were then subjected to another 10 weeks with normal drinking water.

Mice were monitored closely, and any clinical signs were recorded. Mice were sacrificed by Schedule 1 methods as per Home Office Guidelines at 2, 12, 16 and 20 weeks from the start of OH-BBN treatment. The gross observation was made to the bladders at dissection.

For *FGFR3^{S249C}* and *Fgfr3^{K644E}* mice, the OH-BBN treatment, monitoring and culling was performed by Dr Mona Foth (former PhD student in Dr Tomoko Iwata's lab).

2.1.3 1A8 treatment

2.1.3.1 1A8-neutrophil depletion during the first ten weeks

Neutrophil depletion was performed using 1A8 monoclonal antibody (anti-Ly6G, Bioxcell, US) with 2A3 (Rat IgG2a, Bioxcell, US) used as an isotype control.

Wt mice were injected interperitoneally (i.p) with 500 mg of either 1A8 monoclonal antibody (anti-Ly6G, Bioxcell, US) or 2A3 isotype control (Rat IgG2a, Bioxcell, US). The dosage was given three times per week for ten weeks, with concurrent OH-BBN administration in drinking water. The mice then were subjected to another 10 weeks with normal drinking water before culled.

2.1.3.2 1A8-neutrophil depletion in the tumours

Mice bearing tumour as detected using ultrasound imaging (described further in the next section, 2.1.5) were injected (i.p) with 500 µg of either 1A8 monoclonal antibody (anti-mLy-6G, Bioxcell, US) or 2A3 isotype control (Rat IgG2a, Bioxcell, US). The dosage was given three times per week for two weeks. Tumour size was monitored weekly during the treatment using the Vevo3100.

2.1.5 Ultrasound imaging

Recovery anaesthesia was used for ultrasound imaging purposes. Mice were anaesthetised using isoflurane through a Key Fill Vaporiser 5% connected to medical air and an active scavenging unit. The medical airflow level was set at level 0.8 and Isoflurane was supplied at level 4 to put the mouse asleep and maintained at level 2 during the procedure.

The *in vivo* imaging to detect and monitor bladder tumour growth was performed using Vevo 3100 ultrasound system with 25-55MHz transducer (Fujifilm VisualSonics Inc, Canada). Mice were examined for the presence of tumour from the 18th week from the start of OH-BBN treatment. The mice were imaged once a week, for 4-5 weeks or until the endpoint of the treatment. Where repeat imaging was necessary, mice body weight and the intake of appropriate fluid and food was monitored.

The bladder volume was analysed using Vevo LAB software (Fujifilm VisualSonics Inc, Canada).

2.1.6 Blood analysis

Blood sampling was performed either by tail vein sampling or cardiac puncture technique. Blood transferred to EDTA-containing tubes, and the white blood cell populations (WBC) were analysed using ProCyte Dx Hematology Analyzer (IDEXX).

2.2 Histology

2.1.1 Tissue harvest, bladder weight and fixation

The bladders were dissected free from any connective tissue and gently emptied of urine. The weight of each bladder was recorded in mg unit. Dissected bladders were placed in 10% neutral-buffered formalin for overnight fixation before processing.

The bladder tissue harvest of *FGFR3*^{S249C} and *Fgfr3*^{K644E} mice was performed by Dr Mona Foth.

2.1.2 H&E

Haematoxylin and eosin (H&E) staining was carried out on 4 µm formalin-fixed paraffin-embedded (FFPE) bladder tissue sections by the Beatson Histology Services.

Histopathological analyses of the bladder were performed by first setting the criteria by viewing all samples, then in cohort by cohort using the set criteria. The data presented in this study were from two independent scorers.

2.1.3 Immunohistochemistry (IHC)

IHC was performed on 4 µm FFPE bladder tissue sections using the ImmPRESS Detection Kit (Vector Laboratories, US). All primary antibodies (Table 2.1) were freshly prepared using antibody diluent (OP Quanto; Thermo Scientific, US) before incubation.

Slides were deparaffined by immersion in xylene for 3x5 minutes and then rehydrated in a grade of alcohol series; 100%, 70% and 50% for 2 minutes each. Slides were then rinsed under running tap water for 2 minutes.

Heat-induced epitope retrieval (antigen retrieval) was performed either by; 1) PT module (Thermo Scientific, US) with the boiling set for 30 min or 2) microwave with the boiling set for 1 min at full power and additional 10 min at 20% power. For antibodies needing pH <7 the antigen retrieval was performed in heat-induced epitope retrieval (HIER) Buffer L (Thermo Scientific, US), and for pH >7 in HIER Buffer H (Thermo Scientific, US). The sections were allowed to cool down for 5 minutes at room temperature before washing in 1X TBST for 5 minutes and under running tap water for 2 minutes.

Sections were incubated with 0.3% H₂O₂ (VWR Chemicals, US) in distilled water (v/v) for 15 minutes to reduce endogenous peroxidase activities, and then washed under running tap water for 2 minutes. Sections were next incubated with either 2.5% normal goat serum or 2.5% normal horse (Vector Laboratories, US), depending on the nature of the secondary and primary antibodies (Table 2.2), for 15-30 minutes.

The sections were incubated with the primary antibody at the appropriate concentration for either one hour at room temperature or overnight at 4°C (Table 2.1). The sections were washed with 1X TBST for 3X5 minutes followed with secondary antibody incubation for 30 minutes. The sections were next washed again with 1X TBST, 3X5 minutes.

Immunoreactivity was detected by incubating the slides with 3,3'-diaminobenzidine (DAB) substrate (Vector Laboratories, US) until colour development. The reaction was terminated by immersing the sections in 1x TBST followed with running tap water for 2 minutes and then counterstained with haematoxylin for 3 minutes and washed again under running tap water for 2 minutes. The sections were then subsequently, dehydrated in 50%, 70%, 100% ethanol series 2 minutes each, with final incubation in xylene 3x1 minute and then mounted with Pertex mounting medium (Histolab Products AB, Sweden).

Stained slides were scanned using Hamamatsu Nanozoomer slide scanner and analysed using a SlidePath Digital Image Hub (Leica Biosystems, Germany). Cells with brown reactive product in either cytoplasm or membrane were considered as positive for the marker.

2.1.4 Analysis of immune cell infiltrations in the tissue

The presence of immune cells in the stroma, muscle, tumour and CIS area was counted in randomly chosen 10 fields of the tissue area, with 100 x 100 µm dimension per field on the SlidePath Digital Image Hub. The presence of immune cells in the urothelium area was counted in the whole surface area.

Quantification of neutrophils was carried out based on the morphology following H&E staining, as well as by IHC staining with markers of neutrophils; Ly6G (1A8), NIMP, MPO and S100A9 (Table 2.1).

For macrophage quantification, we have used anti-F4/80, and for T cells, CD3, CD4, CD4 and CD8α antibodies were used (Table 2.1).

Table 2.1. Primary antibodies used for immunohistochemistry

Antibody	Source	Cat #	Species	Antigen retrieval	AR buffer	Dilution	Primary antibody incubation
CD3	Vector Laboratories	VP-RM01	rabbit mono	Microwave	HIER H (pH 8)	1:100	1 hour
CD4	eBioscience	14-9766	rat mono	Microwave	HIER H (pH 8)	1:200	1 hour
CD8 α	eBioscience	14-0808	rat mono	Microwave	HIER H (pH 8)	1:200	1 hour
CK14	BioLegend	905301	rabbit poly	Microwave	HIER L (pH 6)	1:2000	1 hour
CK5	AbCam	ab24647	rabbit poly	Microwave	HIER L (pH 6)?	1:2000	1 hour
CXCR2	R&D Systems	MAB2164	rat mono	Microwave	HIER L (pH 6)	1:200	Overnight at 4°c
F4/80	Abcam	ab6640	rat mono	Microwave	HIER L (pH 6)	1:400	1 hour
FoxP3	Abcam	ab54501	rabbit poly	Microwave	HIER H (pH 8)	1:500	1 hour
FoxP3	eBioscience	14-5773-82	Rat mono	Microwave	HIER H (pH 8)	1:200	1 hour
gH2aX	Universal Biologicals / Bethyl Lab	A300-081A	rabbit poly	PT Module	HIER L (pH 6)	1:5000	1 hour
Granzyme B	AbCam	ab4059	rabbit poly	Microwave	HIER H (pH 8)	1:800	1 hour
Ki67	Novacastra	NCL-Ki67p	rabbit poly	PT Module	HIER L (pH 6)	1:2000	1 hour
Ly6G (1A8)	Bioxcell	BE0075-1	rat mono	Microwave	HIER H (pH 8)	1:6000	1 hour
MPO (a-)	Dako	A0398	rabbit poly	Microwave	HIER H (pH 8)	1:1000	1 hour
NIMP	AbCam	ab2557	rat mono	10 mg/ml Proteinase K for 10 min at 37° c	TBS-Tween	1:50	1 hour
p21	Santa Cruz Biotechnology	sc-471	rabbit poly	Microwave	HIER L (pH 6)	1:200	1 hour
p53	Cell Signalling	2524S	Mouse mono	Microwave	HIER H (pH 8)	1:100	1 hour
S100A9	Abcam	ab105472	rat mono	Microwave	HIER L (pH 6)	1:100	1 hour

Table 2.2. Secondary antibodies for immunohistochemistry

Antibody	Source	Cat #	Blocking reagent	Secondary antibody incubation
Anti-Mouse IgG	Vector Laboratories	MP-7452	Normal Goat Serum	30 min
Anti-Rabbit IgG	Vector Laboratories	MP-7401	Normal Horse Serum	30 min
Normal Goat Serum	Vector Laboratories	MP-7404	Normal Goat Serum	30 min
Anti-Rat IgG, Mouse adsorbed	Vector Laboratories	MP-7444	Normal Goat Serum	30 min

2.3 RNAscope

Chromogenic in situ RNA analysis was performed using RNAscope 2.0 Detection Kit (Brown) (Advanced Cell Diagnostics, US) on 4 mm FFPE bladder tissue sections. The experiment for the RNAscope was performed with the technical support from Ke Shi (former MSc student in Dr Tomoko Iwata's lab).

In order to ensure the quality of the FFPE tissue used, one positive control and one negative control were included and performed in parallel with the sample for the probe of the gene tested. The endogenous RNA polymerase II polypeptide (Polr2a) was used as a positive control probe to assess both tissue RNA integrity and assay procedure (Table 2.3). Negative control probe that targets the bacterial DapB gene was used to assess the background signals. Label probe used was conjugated to HRP for the chromogenic detection with DAB.

Table 2.3. List of probes for RNAscope

Probe	Gene	Catalogue number	Accession No
Positive control probe	Polr2a	312471	NM_009089.2
Negative Control probe	DapB	310043	EF191515
Target probe	Tgfb1	407751	NM_011577.1

Tissue sections were first deparaffined in xylene 2x5 minutes followed with dehydration in 100% ethanol for 2x5 minutes. The sections were incubated with hydrogen peroxide for 10 minutes to reduce endogenous peroxidase activities, followed by rinsing in distilled water twice. Antigen retrieval was performed by incubating the tissue sections in RNAscope 1X Target Retrieval Reagents (Advanced Cell Diagnostics, US), maintained at boiling temperature (100°C) using a hot plate for 15 minutes. The slides were then rinsed in distilled water three times, rinsed in 100% ethanol three times and then treated with RNAscope Protease Plus at 40°C for 30 minutes in a HybEZ hybridisation oven (Advanced Cell Diagnostics, US). The sections were rinsed with distilled water three times.

Next, the sections were hybridised with warmed target probes in the HybEZ hybridisation oven for 2 hours and then immersed in RNAscope Wash Buffer for two times, 2 min each time. The sections were then incubated subsequently with preamplifier and amplifiers; AMP1, AMP2, AMP3, AMP4, AMP5 and AMP6 for 15-30 minutes, each. After each

hybridisation step, slides were washed with wash buffer three times. Chromogenic detection was performed by incubating the sections with a mixture of DAB-A and DAB-B (1:1) solutions for 10 minutes at room temperature, followed with washing steps in distilled water.

Counter-staining was performed in 50% haematoxylin for 2 minutes followed with washing with distilled water three times and then briefly dipped in 0.02% Ammonia water. The slides were then dehydrated in series of ethanol; 70% for 2 minutes and 95% for 2x2 minutes before incubated in xylene for 5 minutes and lastly mounted with Pertex mounting medium (Histolab Products AB, Sweden).

Quantification of the positive cells was done using the criteria; None/minimum, low, medium and high based on the number of the positive spot signals.

2.4 Analysis of RNA expression

The experiments for RNA array and Taqman qRT-PCR were performed with the technical supports from previous MSc and MRes students in Dr Tomoko Iwata's lab; Reda Stankunaite, Yaiza Cáceres Martell and Iria Fernández Botana.

2.4.1 RNA extraction

Bladder tissue samples were collected in RNAlater (Qiagen, Germany) and stored at -20°C until whole tissue extraction use.

The total RNA extraction from the bladder tissue was performed using the RNeasy Mini Kit (Qiagen, Germany). Tissue was first removed from RNAlater solution and transferred into 600 µl of RLT buffer for homogenisation. The tissue was homogenised by constant pipetting up and down and vortexed at high speed for 1 minute. The resultant lysate was then centrifuged at full speed for 3 minutes. The supernatant was removed and then transferred into a new centrifuge tube before mixed with 600 µl of 70% ethanol. The sample was then transferred into RNeasy spin column, 600 µl at a time, and centrifuged for 30 seconds at 10,000 rpm. The flow-through was discarded, and 700 µl of RW1 buffer was added. The sample was centrifuged for 30 seconds at 10,000 rpm and the flow-through was discarded. 500 µl of RPE buffer was added to the RNeasy spin column and centrifuged for 30 seconds at 10,000 rpm. The flow-through was discarded, and 500 µl of RPE buffer was added prior to centrifugation for 2 minutes at 10,000 rpm. The RNeasy spin column was transferred into a new collection tube and centrifuged for 1 minute at full speed to remove residual carried-over ethanol. The spin column was then once again placed into a new 1.5 ml collection tube, and 30 µl RNase free water was added into the spin column. The sample was centrifuged for 1 minute at 10,000 rpm. The eluted sample

from the previous step was pipetted back into the same spin column further centrifuged for 1 min at 10, 000 rpm.

The isolated RNA was quantified using NanoDrop Microvolume Spectrophotometer (ThermoFisher, US). The purity of the RNA was evaluated based on the ratio of absorbance at 260 and 280 nm. The samples with 260/280 ratio between 1.8 and 2.2 was considered pure RNA and use for further analysis.

In order to assess the integrity of the RNA, 500 ng of the sample was loaded on 1% Agarose gel in TAE buffer and run for 20 minutes at 50 V. RNA samples with two sharp bands, corresponding to 28S and 18S ribosomal RNA, and with the intensity ratio of the 28S:18S = 2:1, were considered intact and used for the further analysis. The remaining RNA sample was stored at -20°C / -80°C before used for reverse transcribed to complement DNA (cDNA).

2.4.2 cDNA synthesis

Genomic DNA elimination and reverse transcription of the RNA sample were performed using the RT² First Strand Kit (Qiagen, Germany).

Genomic DNA elimination was performed by incubating 0.5 µg RNA with Buffer GE to a final volume of 10 µl for 5 minutes at 42°C. The genomic DNA elimination mix was then incubated with a reverse-transcription mix containing Buffer BC3, Control P2, RE3 Reverse Transcriptase Mix and RNase free water to a final volume of 10 µl/reaction and at 42°C for 15 minutes. The reaction was stopped by incubating at 95°C for 5 minutes before mixed with 91 µl of RNase-free water. The resultant cDNA was then stored at -20°C or used immediately for RNA array or Taqman qRT-PCR.

2.4.3 RNA array

RNA array targeting 84 genes linked to cancer and inflammation was performed using RT² Profiler Mouse Cancer Inflammation & Immunity Crosstalk PCR Array (Qiagen, Germany).

The PCR components mix was prepared by mixing 1350 µl of 2X RT² SYBR Green Mastermix, 102 µl of cDNA synthesis reaction and 1248 µl of RNase-free water to the final volume of 2700 µl. Then, 25 µl of the PCR components mix was added and mixed to each well of the RT² Profiler PCR array.

The array was placed and ran using the StepOnePlus Real-Time PCR System (ThermoFisher, US). Thermal cycle conditions were set at 95°C for 10 minutes, followed

by 40 cycles of 95°C for 15 seconds, and 60°C for 1 minute. Fold changes between samples was determined using the $2^{-\Delta\Delta Ct}$ method.

The genes were stratified based on biological properties according to the RNA array (Table 2.4).

Table 2.4 List of genes for RNA array

Cytokine category	Gene	
Immune & Inflammatory Responses	Immunostimulatory Factors	Ifng
		Il2
		Il12a
		Il12b
		Il15
		Tnf
	Immunosuppressive Factors	Cd274 (Pdl1)
		Csf2 (GMCSF)
		Ctla4
		Cxcl12 (Sdf1)
		Cxcl5 (ENA-78, LIX)
		Ido1 (Ido)
		Il10
		Il13
		Il4
		Il5
		Mif
		Nos2 (iNOS)
		Pdc1 (PD-1),
		Ptgs2 (COX2)
		Tgfb1
		Vegfa
	Pro-inflammatory Genes	Ccl2 (MCP-1)
		Ccl20 (MIP-3A)
		Ifng
		Il1a
		Il1b
		Il2
		Il6
		Il12a
		Il12b
		Il17a
		Il22
		Il23a
		Ptgs2 (COX2)
		Tlr4
		Tnf
		Vegfa
		Il4
		Il10
	Anti-inflammatory Genes:	Il13
		Tgfb1
Enzymatic Modulators of Inflammation & Immunity	Aicda (Aid)	
	Gzma	
	Gzmb	
	Ido1 (Ido)	
	Nos2 (iNOS)	
Ptgs2 (COX2)		

Antigen Presentation		H2-D1
		H2-K1
Chemokines		Ccl2 (MCP-1)
		Ccl4 (MIP-1B)
		Ccl5 (RANTES)
		Ccl20 (MIP-3A)
		Ccl22 (MDC)
		Ccl28
		Cxcl1 (Gro1)
		Cxcl2 (Gro2)
		Cxcl5 (ENA-78, LIX)
		Cxcl9 (Mig)
		Cxcl10 (INP10)
		Cxcl11 (Itac, Ip9)
		Cxcl12 (Sdf1)
Interleukins		Il1a
		Il1b
		Il2
		Il4
		Il5
		Il6
		Il10
		Il12a
		Il12b
		Il13
		Il15
		Il17a
		Il22
	Il23a	
Chemokine & Interleukin Receptors		Ackr3 (Cxcr7)
		Ccr1
		Ccr2
		Ccr4
		Ccr5
		Ccr7
		Ccr9
		Ccr10
		Cxcr1 (Il8 α)
		Cxcr2 (Il8r β)
		Cxcr3
		Cxcr4
		Cxcr5
	Il1r1	
Other Cytokines		Kitl (SCF)
		Mif, Spp1
		Tnf
		Tnfsf10 (Trail)
Growth Factors & Receptors		Csf1 (Mcsf)
		Csf2 (GMCSF)
		Csf3 (Gcsf)
		Egf
		Egfr

		Igf1
		Tgfβ1
		Vegfa
Signal Transduction	Interferon Signalling	Gbp2b (Gbp1)
		Ifng
		Il6
		Irf1
	Interferon-Responsive Genes	Ccl2 (MCP-1)
		Ccl5 (RANTES)
		Cxcl9 (Mig)
		Cxcl10 (INP10)
		Gbp2b (Gbp1)
		Irf1
		Myd88
		Stat1
		Tlr3
		Tnfsf10 (Trail)
	NFκB Targets	Bcl2l1 (Bcl-XL)
		Ccl2 (MCP-1)
		Ccl5 (RANTES)
		Csf1 (Mcsf)
		Csf2 (GMCSF)
		Csf3 (Gcsf)
		Ifng
		Tnf
	STAT Targets	Ccl2 (MCP-1)
		Ccl4 (MIP-1B)
		Ccl5 (RANTES)
		Csf1 (Mcsf)
		Csf2 (GMCSF)
		Csf3 (Gcsf)
		Cxcl9 (Mig)
		Cxcl10 (INP10)
		Cxcl11 (Itac, Ip9)
		Cxcl12 (Sdf1)
		Il1b
		Il6
		Il10
		Il17a
		Il23a
		Myc
Toll-Like Receptor Signalling	Myd88	
	Tlr2	
	Tlr3	
	Tlr4	
	Tlr7	
	Tlr9	
Transcription Factors	Foxp3	
	Hif1a	
	Irf1	
	Myc,	
	Nfkb1	

		Stat1
		Stat3
		Trp53 (p53)
Apoptosis	Pro-Apoptotic	Fasl (Tnfsf6)
		Tnf
		Tnfsf10 (Trail)
		Trp53 (p53)
	Anti-Apoptotic	Bcl2
		Bcl2l1 (Bcl-XL)
		Myc
		Stat3

2.4.4 Taqman qRT-PCR

The TaqMan-based qRT-PCR was performed using TaqMan Fast Advanced Master Mix kit (Thermo Fisher Scientific, US) and TaqMan Gene Expression assay (Table 2.5) (Applied Biosystems, US).

Table 2.5. List of TaqMan Gene Expression assay

Gene	Assay ID
Gapdh	Mm99999915_g1
Chemokine receptor 2 (CCR2)	Mm00 438270_m1
Nos2	Mm00440502_m1
Ido1	Mm00492590_m1
Egf:	Mm00438696_m1
Spp1	Mm00436767_m1

The PCR reaction mix was prepared by mixing 10 μ l of TaqMan Fast Advanced Master Mix with 1 μ l of TaqMan Gene Expression assay of the targeted gene and 7 μ l of nuclease free water to the final volume of 18 μ l/reaction. The PCR mix was pipetted into a 96-well plate with 18 μ l/well and mixed with 2 μ l of cDNA template (2 ng/ μ l) or 2 μ l of nuclease-free water for the negative control. The samples were then placed in the StepOnePlus™ Real-Time PCR System (ThermoFisher, US). The cycling protocol was set at 50°C for 2 min, 95°C for 2 min, and 40 cycles of 95°C for 1 sec and 60°C for 20 sec.

The double delta Ct ($\Delta\Delta$ Ct) analysis was used to calculate the fold change of the mean values in each experimental condition. Triplicates for each sample was used for each individual experiment.

2.5 Statistical analyses

The statistical analysis was performed using GraphPad Prism software (Version 7, GraphPad Software, Inc.). The differences in the mean between the two groups were determined using a Mann-Whitney test for the non-parametric distribution of data. P-values less than 0.05 were considered significant.

Chapter 3

Effects of FGFR3 mutation on immune responses

3.1 Aim and objectives

This chapter aimed to determine the effects of FGFR3 mutations on immune responses during bladder tumorigenesis induced by carcinogen treatment.

The specific objectives were:

1. To study the effect of FGFR3 S249C and FGFR3 K644E mutations in carcinogen-induced bladder tumorigenesis.
2. To characterise the tumour characteristics and immune cell infiltration in the tumour microenvironment of *FGFR3*^{S249C} and *Fgfr3*^{K644E}.
3. To characterise the pathogenesis and immune responses at the acute inflammation stage and tumour initiation stage in *FGFR3*^{S249C} and *Fgfr3*^{K644E}.
4. To evaluate the association between FGFR3 S249C mutation and the mRNA expression of immune cell signatures using publicly available TCGA data.

3.2 Results

3.2.1 Carcinogen-dependent bladder tumorigenesis was increased in the presence of FGFR3 S249C mutation

In order to determine the effects of FGFR3 mutation in different stages of bladder tumorigenesis, mice were subjected to 0.05% OH-BBN treatment for 10 weeks followed by another 10 weeks with normal drinking water (Figure 3.1 A).

Gross observation of the bladder at 2 weeks, 12 weeks and 20 weeks from the start of OH-BBN treatment showed that a presence of tumour in bladder was only observed at 20 weeks samples (Table 3.1). Male wt bladders had a slightly higher occurrence of the tumour than female samples (20% and 14.8%, respectively). In *FGFR3*^{S249C}, the occurrence of the bladder tumour was comparable between males and females (Table 3.1). Two out of six male samples of *Fgfr3*^{K644E} had bladder tumour, while none was observed in females.

Next, microscopic observation of H&E staining was used to evaluate the histopathology of the bladder and the tumours.

FGFR3^{S249C} mice showed a significant increase of tumour occurrence compared to wt ($p = 0.0454$) (Figure 3.1I). The increase in the tumour occurrence was statistically significant in female *FGFR3*^{S249C} mice ($p = 0.0164$), but comparable in male *FGFR3*^{S249C} and male wt mice (Figure 3.1 J, K). Meanwhile, the presence of tumour was comparable in *Fgfr3*^{K644E} and wt. The presence of hyperplasia, atypia, dysplasia, carcinoma *in situ* (CIS) was comparable between wt, *FGFR3*^{S249C} and *Fgfr3*^{K644E}. Only small percentage of *FGFR3*^{S249C} (3.45%, $n = 1/22$) showed minimal changes in the urothelial compared to *Fgfr3*^{K644E} (27.27%, $n = 3/11$) and wt (10.64%, $n = 5/2=47$).

Table 3.1. Summary of the mouse cohorts and gross observation

Cohorts	Timepoints (weeks)	Cohort size (n)			Gross observation at time point (Tumour) (n)		
		Total	Male	Female	Total	Male	Female
Wildtype	2	17	8	9	17	None	None
	12	10	3	7	10	None	None
	20	47	20	27	47	4/20 (20%)	4/27 (14.8%)
<i>FGFR3</i> ^{S249C}	2	15	10	5	15	None	None
	12	10	3	7	10	None	None
	20	29	12	17	29	5/12 (41.7%)	7/17 (41.2%)
<i>Fgfr3</i> ^{K644E}	2	11	4	7	11	None	None
	12	8	3	5	8	None	None
	20	11	6	5	11	2/6 (33.3%)	None

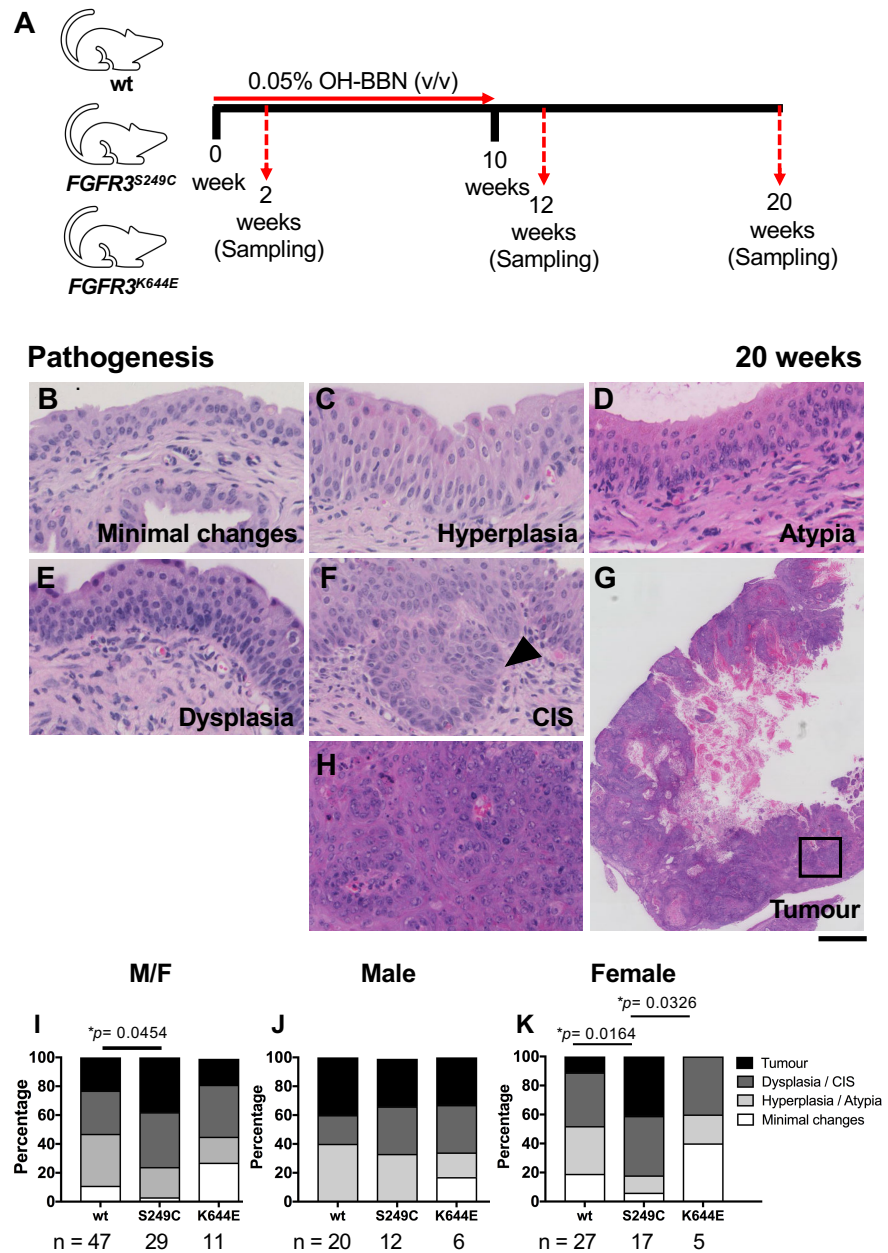


Figure 3.1. Histopathological analysis at 20 weeks from the start of OH-BBN treatment. Schematic presentation of OH-BBN treatment for induction of bladder tumorigenesis (A). Representative images of minimal changes (B), hyperplasia (C), atypia (D), dysplasia (E), CIS (F) (black arrowhead), and tumour (G). H is the magnified tumour area in G (black box). Scale bar represents 50 μm (B-F, H) and 1 μm (G). Percentage of each pathogenesis criterion was quantified in the combined male and female samples (H), male mice only (I) and female mice only (J). The number of samples used is indicated below each column. Statistical significance was determined by Mann-Whitney with * $p < 0.05$ and ** $p < 0.01$ indicated as significant.

3.2.2 Tumour phenotype was more severe in FGFR3 S249C bladders

Further histopathological analysis was performed to evaluate (1) invasiveness of urothelial cells and tumours, (2) lobular appearance of the urothelium-stroma boundary and (3) squamous transformation and keratinisation of the urothelium and tumour cells (Figure 3.2A-F).

An increase in the invasiveness of urothelial and tumour cells was observed in *FGFR3*^{S249C} mice compared to wt ($p = 0.023$) (Figure 3.2G). *FGFR3*^{S249C} mice also showed a more frequent formation of the lobulation in comparison to wt (Figure 3.2 J). The squamous transformation and keratinisation were also more prevalent in *FGFR3*^{S249C} compared to wt (Figure 3.2M). *Fgfr3*^{K644E} showed a similar level of invasiveness, lobulation and squamous transformation to wt.

The differences in the urothelial and tumour features were also observed in females when *FGFR3*^{S249C} were compared to wt (Figure 3.2I, L, O). However, the difference was not present in males (Figure 3.2H, K and N). *Fgfr3*^{K644E} showed a similar pattern in the severity of invasiveness, lobulation and squamous transformation to wt, regardless of gender (Figure 3G-O).

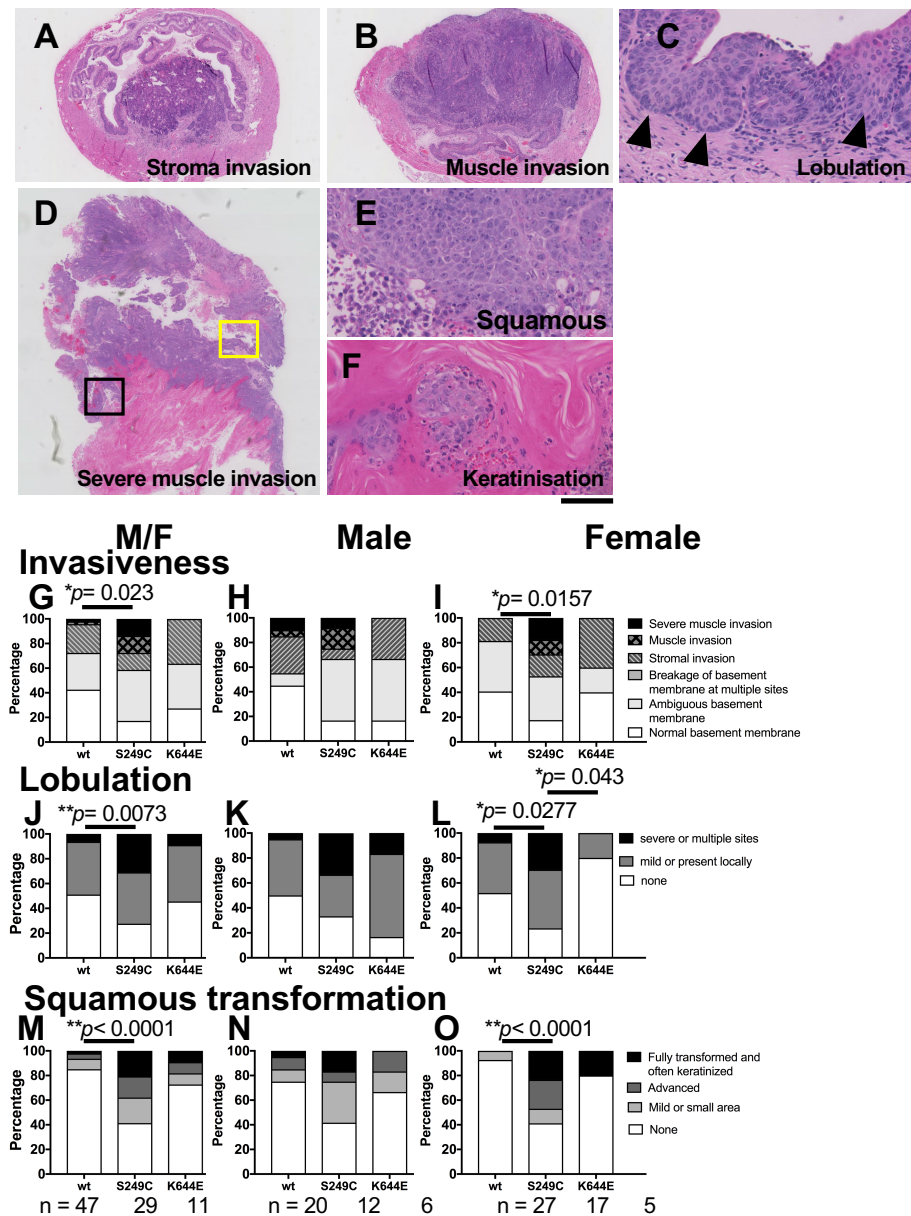


Figure 3.2. Tumour characteristic of samples taken at 20 weeks from the start of OH-BBN treatment. Representative image of stroma invasion (A), muscle invasion (B), lobulation (C) (black arrowhead), and severe muscle invasion (D). E and F are magnified area of squamous transformation (E) (black box) and keratinisation (yellow box) in the tumour area (D). Invasiveness of the urothelial and tumour cells (G-I), the lobulated appearance of urothelial cells (J-L), and squamous transformation of urothelial and tumour cells (M-O) were quantified. Scale bar represents 60 μm (C, E, F) and 1 μm (A, B, D).

3.2.3 Effects of FGFR3 mutations at 2 weeks

To further address the effects of *FGFR3* mutation in the initiation of bladder tumorigenesis, we have examined the pathogenesis of the bladder at 2 weeks of OH-BBN treatment.

The occurrence of hyperplasia was comparable among wt, *FGFR3*^{S249C} and *Fgfr3*^{K644E} (Figure 3.3A-C).

The presence of atypia and dysplasia was found to be decreased in *Fgfr3*^{K644E} compared to wt ($p = 0.0107$, Mann-Whitney) (Figure 3.3D).

No significant difference in the presence of atypia and dysplasia was observed in males (Figure 3.3B and E). In females, the prevalence of atypia and dysplasia was decreased in *FGFR3*^{S249C} ($p = 0.0075$, Mann-Whitney) and in *Fgfr3*^{K644E} ($p = 0.0119$, Mann-Whitney) compared to wt (Figure 3.3F).

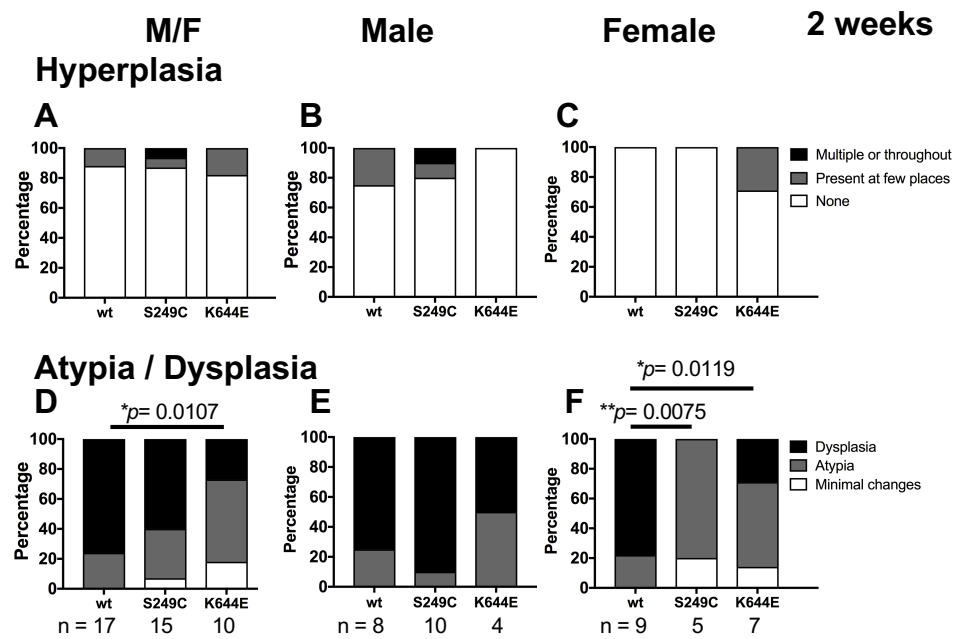


Figure 3.3. Histopathological analysis on the urothelial abnormalities in samples taken at 2 weeks from the start of OH-BBN treatment. Presence of hyperplasia (A-C), atypia and dysplasia (D-F).

3.2.4 OH-BBN induced changes in the stroma and angiogenesis at 2 weeks

The changes in the stroma characteristics were also investigated in 2 weeks samples. The stroma with area less than $<2 \text{ mm}^2$ were considered as thick and $>2 \text{ mm}^2$ were considered as very thick.

The stroma of the bladder showed an extensive thickening upon OH-BBN treatment (Figure 3.4B and C), and this was comparable among the three cohorts, wt, *FGFR3*^{S249C} and *Fgfr3*^{K644E} (Figure 3.4D-F).

The thickening of the stroma appeared in accordance with an increase in the formation of the blood vessel (angiogenesis) in the inner and outer stroma (Figure 3.4G, H). The presence of angiogenesis was at a similar frequency in wt, *FGFR3*^{S249C} and *Fgfr3*^{K644E} (Figure 3.4I-N).

3.2.5 FGFR3 K644E mutation increased urothelial abnormalities at 12 weeks

The histopathological changes of the urothelium were also evaluated in samples taken at 12 weeks from the start of OH-BBN treatment (10 weeks with OH-BBN, followed by 2 weeks with normal drinking water).

The occurrence of urothelial abnormalities; hyperplasia/atypia, dysplasia/CIS in *FGFR3*^{S249C} was comparable to wt (Figure 3.5A). However, the presence of dysplasia/CIS was found to be elevated in *Fgfr3*^{K644E} compared to wt ($p = 0.0128$, Mann-Whitney) (Figure 3.5A).

Compared to wt, *FGFR3*^{K644E} was found to have more prevalent lobulation ($p = 0.0296$, Mann-Whitney) (Figure 3.5G). The lobulation signify the growth of abnormal cell inside the urothelium lining towards the stroma.

The degree of invasiveness and squamous transformation were at a similar level in wt, *FGFR3*^{S249C} and *Fgfr3*^{K644E} (Figure 3.5D, J). Squamous differentiation in urothelial carcinoma reciprocated the malignant squamous epithelium and characterised by the presence of either keratin pearl formation, intercellular bridges or both (Gluck et al., 2014; Zhai et al., 2007).

The above differences in urothelial characteristics at 12 weeks were not seen in males (Figure 3.5B, E, H, K). However, in female samples, *Fgfr3*^{K644E} showed an increase in the pathogenesis and invasiveness compared to wt ($p = 0.0278$, Mann-Whitney) (Figure 3.5C and F).

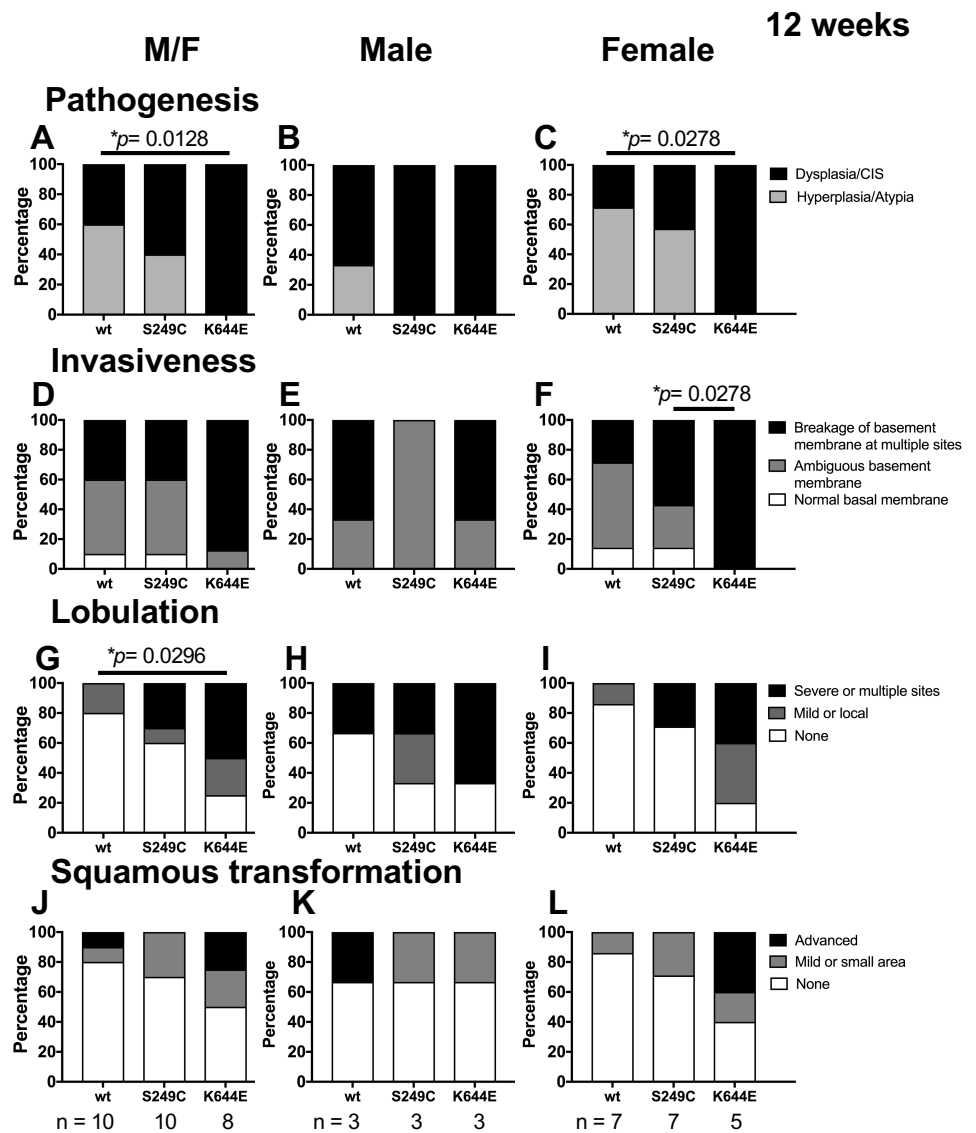


Figure 3.5. Histopathological analysis of samples taken at 12 weeks from the start of OH-BBN treatment. Pathogenesis (A-C), invasiveness (D-F), lobulation (G-I) and squamous transformation (J-L).

3.2.6 Neutrophil infiltration following carcinogen treatment was suppressed in *FGFR3*^{S249C}

We next asked whether the effects of *FGFR3* mutation was due to changes in the inflammatory response. Neutrophil infiltration was quantified by identifying the neutrophils based on their granular morphology and pinkish cytoplasm following H&E staining (Figure 3.6A-C).

At 2 weeks of OH-BBN treatment, *FGFR3*^{S249C} bladders showed a decrease in neutrophils infiltration in the urothelium ($p = 0.0466$), stroma ($p = 0.0063$), and muscle ($p = 0.0464$) compared to wt (Figure 3.6D, G, J). However, *Fgfr3*^{K644E} and wt showed a comparable level of neutrophil infiltration in the urothelium, stroma and bladder.

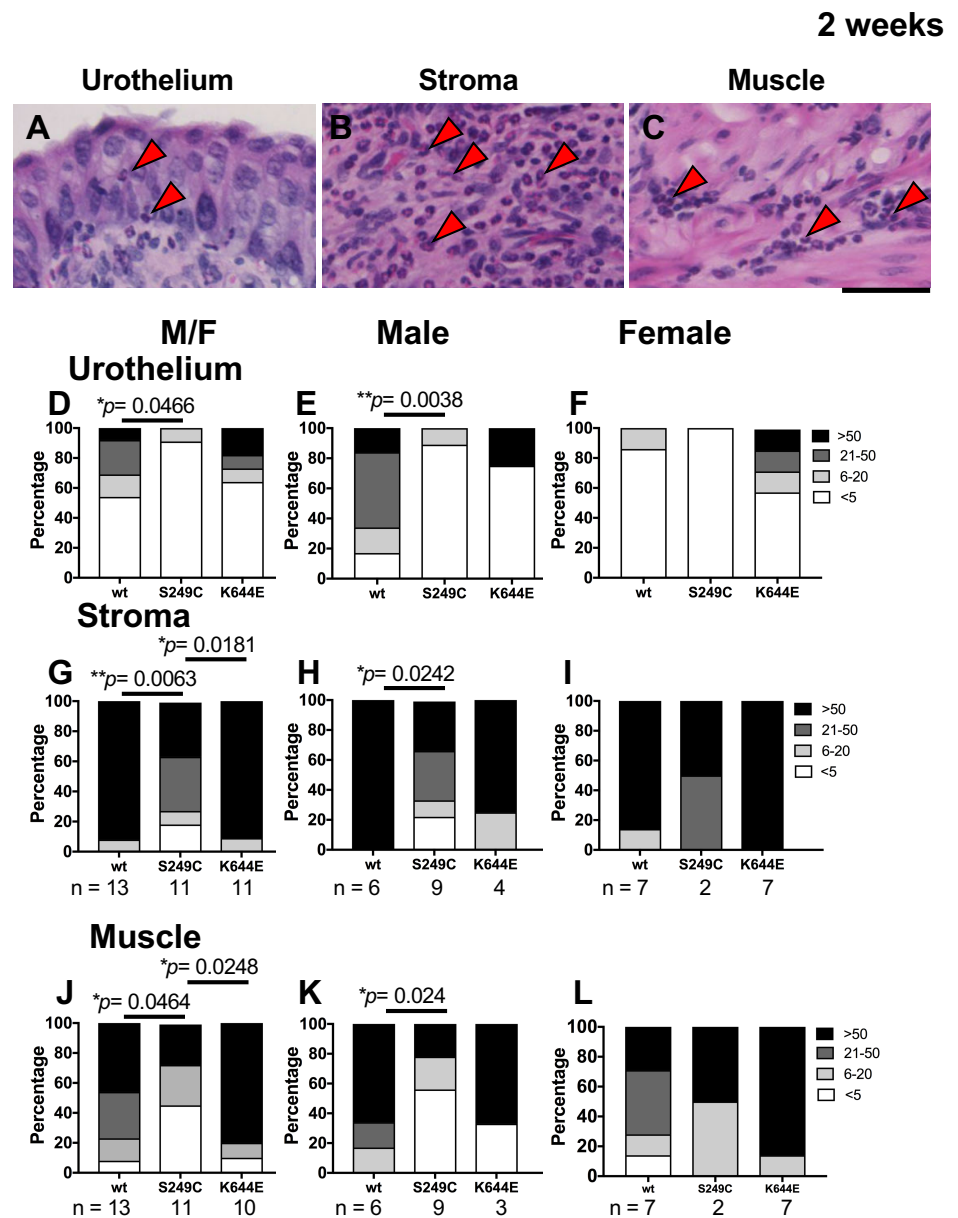


Figure 3.6. Infiltrations of neutrophils at 2 weeks from the start of OH-BBN treatment. Representative images of neutrophil infiltration in the urothelium, stroma and muscle in 2 weeks samples (A, B, C, respectively) under H&E staining. Presence of neutrophils was quantified in the urothelium (D-F), stroma (G-I), muscle (J-L). Scale bar represents 50 μ m (A-C).

3.2.7 Neutrophil infiltration mildly increased in FGFR3-mutated mice at 12 weeks and 20 weeks

We have also examined the level of neutrophil infiltration at 12 weeks timepoint when OH-BBN treatment had been ceased for 2 weeks.

The neutrophil infiltration in the urothelium and muscle was overall much less compared to 2 weeks samples. The level of infiltration was comparable between wt, *FGFR3*^{S249C} and *Fgfr3*^{K644E} (Figure 3.7A-I). However, *Fgfr3*^{K644E} showed a statistically significant increase of neutrophil infiltration in the stroma compared to wt ($p = 0.0229$, Mann-Whitney) (Figure 3.7D, F).

We have also quantified the neutrophil infiltration in the tumour area of samples taken at 20 weeks from the start of OH-BBN treatment. *Fgfr3*^{K644E} was excluded from this analysis due to the small number of samples. *FGFR3*^{S249C} showed a mild increase in the number of neutrophil infiltrations in the tumour area compared to wt (Figure 3.7J-L).

3.2.8 T-cells infiltration was not affected in FGFR3 mutated transgenic mice at 2 weeks

To further address the mechanism of increased bladder tumorigenesis in *FGFR3*^{S249C}, we have examined the T-cells infiltration at 2 weeks from the start of OH-BBN treatment. IHC was performed using CD3, a marker that recognizes all T-cells.

At 2 weeks, the infiltration of CD3⁺ T cells was observed to be low in the urothelium and very high (score 3) in the stroma and muscle, and this was comparable in wt and *FGFR3*^{S249C} (Figure 3.8A-I).

3.2.9 No alteration in tumour-infiltrating T cells in FGFR3-mutated mice

We next looked at the CD3⁺ T cell infiltration in tumour samples taken at 20 weeks from the start of OH-BBN treatment.

In general, CD3⁺ T cell infiltration observed to be higher in the stroma and tumour area while urothelium and stroma showed a mild presence of CD3⁺ T cells in both wt and *FGFR3*^{S249C} (Figure 3.9A-P). The difference in the presence of CD3⁺ T cells between *FGFR3*^{S249C} and wt was not statistically significant in the urothelium, stroma, CIS and tumour area (Figure 3.9E-P).

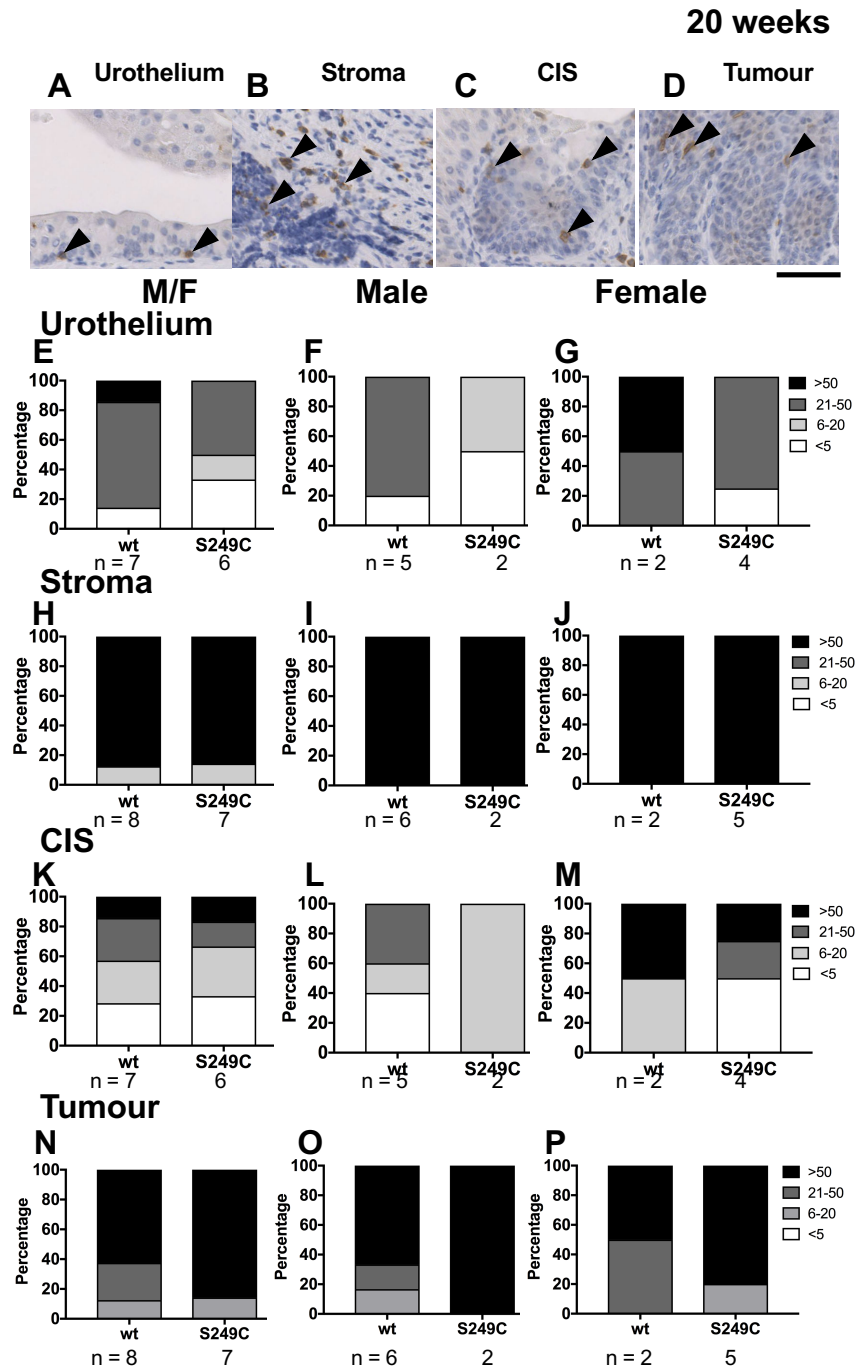


Figure 3.9. Infiltration of T-cells (CD3⁺) in tumour samples at 20 weeks. CD3⁺ (total T-cells) stained as brown (A-D) (black arrowheads). The number of CD3⁺ cells in the urothelium (E-G), stroma (H-J), CIS (K-M) and tumour area (N-P) was quantified and presented in percentage (Y-axis). Scale bar represent 100 μ m in A-D.

3.2.10 Effects of FGFR3 S249C mutation on immune signature gene expression in bladder cancer patients

In order to further explore the association between FGFR3 mutation and immune response signature gene expression, we have used data from publicly available genomic resources through cBioPortal. The data for FGFR3 mutational status and mRNA expression of the gene of interest were downloaded from cBioPortal (<http://www.cbioportal.org/public-portal/index.do>) of Bladder cancer TCGA Cell, 2017. The data set contained 404 tumours with complete mutation data. Out of these 404 tumours, only 31 have FGFR3 S249C mutation and used for the analysis comparing with the 347 FGFR3 wt tumours. The remaining n=26 samples from the TCGA data harboured the following mutations; FGFR3 E216K (n=1), FGFR3 G370C (n=5), FGFR3 G380R (n=2), FGFR3 H349D (n=1), FGFR3 K650E (n=1), FGFR3 L88WFS*10 (n=1), FGFR3 P358L (n=1), FGFR3 Q674 (n=1), FGFR3 R248C (n=2), FGFR3 S371C (n=2), FGFR3 V3061 (n=1), and FGFR3 4373C (n=8).

We have compared the association of FGFR3 S249C mutation with mRNA expression of genes associated with;

- 1) Neutrophil activities and monocytes: NIMP, MPO, S100A9, CD66B (CEACAM8) and CD68 – (Figure 3.10).
- 2) Neutrophil chemotaxis: CXCR2, CXCL1, CXCL2, CXCL3, CXCL5, CXCL6 and CXCL8 - (Figure 3.11).
- 4) T-cell populations, T cell cytotoxic activities and immunosuppressive activities: CD4, CD8A, GZMA, GZMB, PD-1, PD-L1, CTLA4 – (Figure 3.12).

The genes were chose based on the neutrophil-associated genes and immune signatures reported in the literature (Leach et al., 2017; Coffelt et al., 2016; Sjobahl et al., 2012) and discussion with pathologist (Dr Joshua Leach).

3.2.10.1 FGFR3 S249C associated with a decrease in neutrophils' associated gene

We compared the gene expression of neutrophils' surface receptor and enzymatic activities on samples with FGFR3 S249C (n=31) mutated and wt (n=347).

The expression of granulocyte marker (CD66B/CEACAM8) and NIMP was comparable between FGFR3 S249C and wt (Figure 3.10A, B). The gene expression of MPO which is the major component of azurophilic granule in neutrophils (Brinkmann et al., 2004), was significantly decreased in samples with FGFR3 S249C compared to wt ($p = 0.0004$) (Figure 3.10C). Meanwhile, the expression of S100A9 was unchanged in FGFR3 S249C compared to wt (Figure 3.6D).

We have also evaluated the association of FGFR3 S249C mutation with gene for monocytes (CD68). The expression of CD68 was comparable between FGFR3 S249 and wt samples (Figure 3.10E).

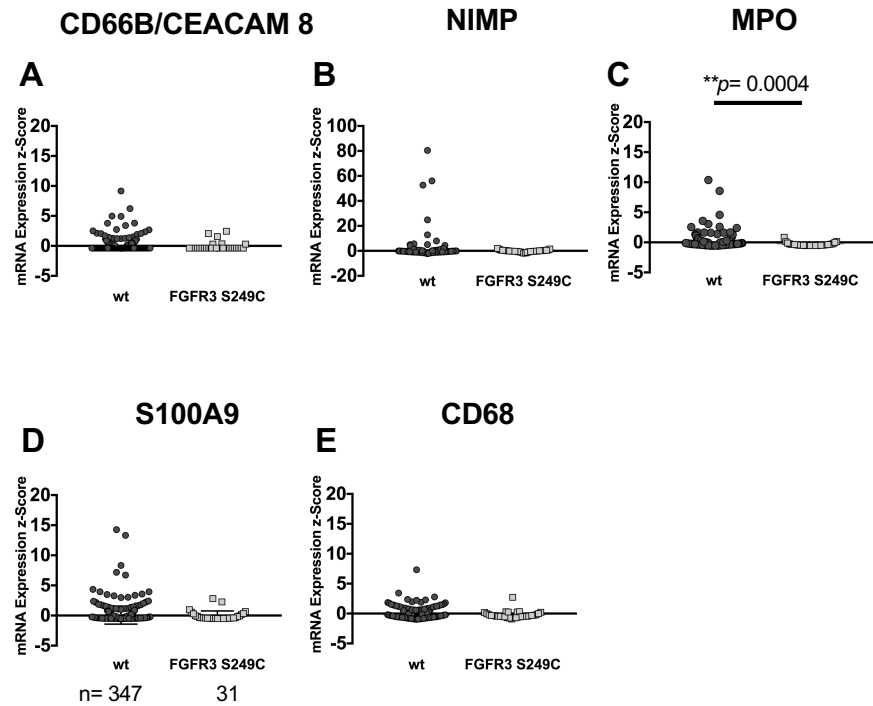


Figure 3.10. *FGFR3 S249C* mutation effects on neutrophils and monocytes gene expression in TCGA, Cell 2017 study. The *FGFR3 S249C* mutation compared to granulocyte gene expression (CD66B/CEACAM 8) (A), neutrophils' gene expression (NIMP, MPO, S100A9) (B-D) and monocytes (CD68) (E).

3.2.10.2 FGFR3 S249C associated with a decrease in chemokines gene expression

We next looked at the gene expression of neutrophil chemotactic surface receptor, CXCR2 and its ELR⁺ ligands; CXCL1-3, 5-8.

A significant decrease in the expression of CXCR2 ($p= 0.0336$) and three of its ligands, CXCL2 ($p= 0.0002$), CXCL3 ($p= 0.0003$) and CXCL5 ($p= 0.001$) was observed in FGFR3 S249C mutated compared to FGFR3 wt samples (Figure 3.11A, C-E). The expression of the other three CXCR2's ligands; CXCL1, CXCL6 and CXCL8 was comparable between FGFR3 S249C mutated and FGFR3 wt samples (Figure 3.11B, F, G).

FGFR3 mutation vs neutrophil chemoattractant mRNA expression

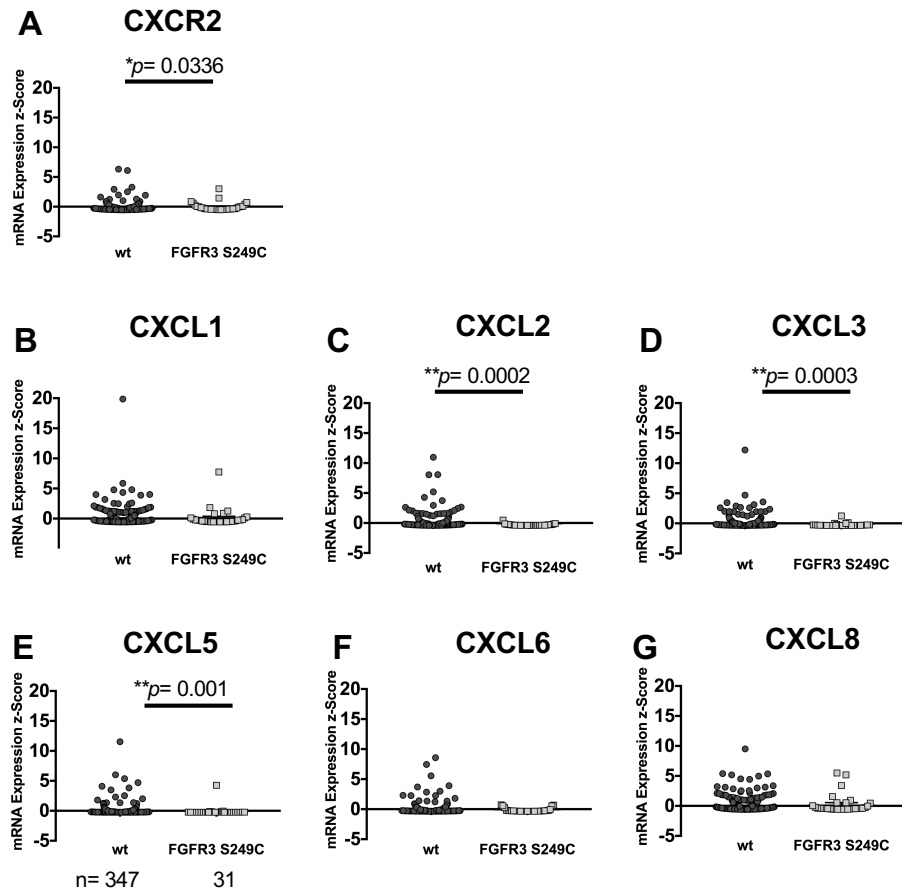


Figure 3.11. FGFR3 S249C mutation effects on CXCR2 and ELR⁺ chemokines. The FGFR3 S249C mutation compared to gene expression of CXCR2 (A) and CXCL1-8 (B-G).

3.2.10.3 FGFR3 S249C mutation associated with decreased in T cell population and activation genes

We then further analysed the expression of the gene for T-helper cells (CD4) and cytotoxic T-cells (CD8A) as well as the gene encoding cytotoxic activities for the CD8; GZMA and GZMB. The expression for CD4 was comparable between the FGFR3 S249C and FGFR3 wt cohorts (Figure 3.12A). However, a significant decrease was observed in the gene expression of CD8A ($p= 0.0082$) as well as GZMA ($p= 0.0275$) and GZMB ($p= 0.0005$) in FGFR3 S249C compared to FGFR3 wt samples (Figure 3.12B-D).

We next analysed the expression of genes associated with immunosuppression of the T-cells. FGFR3 S249C samples displayed significant decrease in the expression of PD-1, PD-L1 and CTLA4 ($p<0.0001$, $p= 0.0083$ and $p= 0.0003$, respectively).

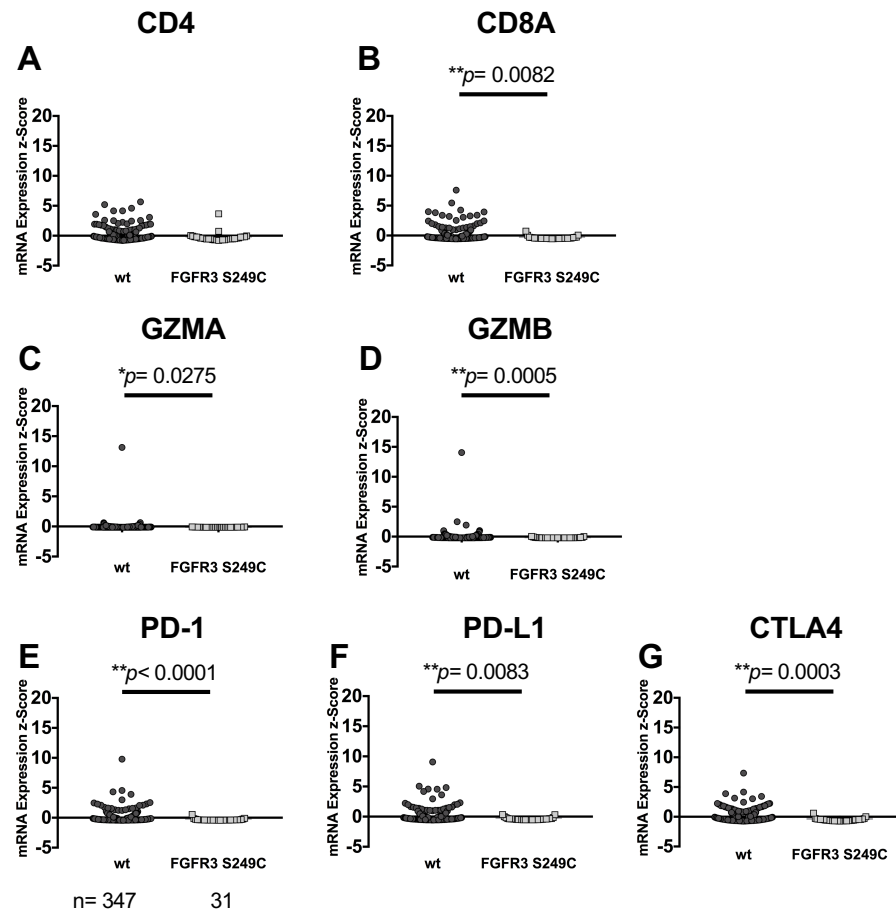


Figure 3.12. FGFR3 S249C mutation effects on immunostimulatory and immunosuppressive genes expression. The FGFR3 mutation compared to CD4 and CD8 T cells (A, B), cytotoxic enzymes, GZMA and GZMB (C, D) and immunosuppressive factors, PD-1, PD-L1 and CTLA4 (E-G).

3.3 Discussion

3.3.1 Results summary

We have shown that:

1. FGFR3 S249C mutation increased tumour occurrence and severity in carcinogen-dependent bladder tumorigenesis (Figure 3.1). The phenotype of urothelial and bladder tumour cells in FGFR3 S249C mice showed distinct characteristics with an increase in invasiveness, lobulation, as well as squamous transformation and keratinisation compared to wt (Figure 3.2).
2. Histopathological changes were suppressed in FGFR3 K644E at two weeks following carcinogen treatment (Figure 3.3). However, this was increased at 12 weeks, the time point which carcinogen has been ceased for two weeks (Figure 3.5).
3. Neutrophil infiltration was suppressed in *FGFR3^{S249C}* but not in *Fgfr3^{K644E}* at 2 weeks of carcinogen treatment (Figure 3.6).
4. *FGFR3^{S249C}* tumours were mildly more neutrophil-infiltrated than wt tumours (Figure 3.7).
5. FGFR3 mutation associated with lower expression of immune gene signatures in bladder cancer patients. A significant decrease in the gene expression of neutrophil azurophilic granule (MPO), neutrophil chemotactic factors (CXCR2, CXCL2, 3, 5), cytotoxic T-cells and their enzymatic activities (CD8A, GZMA and GZMB), and immunosuppressive factors (PD-1, PD-L1 and CTLA4) was observed in FGFR3 S249C mutated samples (Figure 3.10-3.12).

Altogether, the findings suggested that FGFR3 S249C mutation suppressed acute inflammatory responses in the bladder at the early time-point of carcinogen treatment in mice. The suppression was associated with the enhanced of the tumour progression. Furthermore, FGFR3 S249C and FGFR3 K644E mutations induced histopathological changes at differential time course, indicating different regulation of urothelial pathogenesis induced by these two FGFR3 mutations. The association of FGFR3 S249C with a decrease in immune cell signatures in bladder cancer patients further indicated its roles in modulating immune responses during bladder tumorigenesis.

3.3.2 FGFR3 S249C mutation increased tumour occurrence and severity in carcinogen-dependent bladder tumorigenesis

Inhibition of FGFR3 has been associated with a decrease in tumour cell proliferation and an increase in mouse survival in bladder cancer model ((Qing et al., 2009). Treatment with

anti-FGFR3 antibody (R3Mab) at 5 and 50 mg/kg dosage managed to decrease tumour volume (41 – 73%) in nude mice injected with RT112 cells that express wt FGFR3 (Qing et al., 2009).

The effects of mutant FGFR3 in inducing intracellular signalling and cellular transformation are specific to each mutation (Di Martino et al., 2009).

Fgfr3 K644E mutation alone did not play a causative role in inducing bladder tumorigenesis. However, with combination with other oncogenic signalling such as PTEN was able to induce urothelial tumorigenesis in mice (Foth et al., 2014).

The differences in the effect of S249C mutation and K644E mutation may be attributable to the effect on the activation of downstream signalling related to PLC γ 1 phosphorylation (di Martino et al., 2009). S249C mutation is a point mutation occurred in between the ligand Ig2 and Ig3 in the extracellular domain which is important for the ligand binding. Human K650/K652E mutation which is equivalent to K644E in mouse (Iwata et al., 2000) occurred in cytoplasmic tyrosine kinase domain that transmit the signal to the nucleus (Lievens et al., 2004). Phosphorylation of S249C FGFR3 is independent to the FGFs binding in contrast to the K652E FGFR3 which required stimulation with FGFs for the phosphorylation of PLC γ 1 (di Martino et al., 2009).

Squamous differentiation has been associated with increased of recurrence, poor prognosis and decrease sensitivity to adjuvant therapy in bladder cancer patients (Li et al., 2017; Gluck et al., 2014). The presence of squamous differentiation was observed in about 21% of urothelial carcinomas and associated with both poorly to moderate and well-differentiated of invasive and non-invasive phenotype, respectively (Zhai et al., 2007).

3.3.3 FGFR3 S249C mutation suppressed acute inflammation

A significant decrease in neutrophil infiltration was observed at 2 weeks of carcinogen treatment (Figure 3.6). In contrast, at 20 weeks from the start of carcinogen, a modest increase in neutrophil infiltration was observed in the tumour of FGFR3 S249C compared to wt (Figure 3.7). *Fgfr3*^{K644E} mice showed a significant increase in neutrophils infiltration at 12 weeks from the start of carcinogen treatment (Figure 3.7). T-cell infiltration was not affected in FGFR3 mutated mice upon carcinogen induction and at the later stage of bladder tumorigenesis (Figure 3.8 and 3.9).

The lack of neutrophils in *FGFR3*^{S249C} at the early time of carcinogen treatment could indicate suppression of acute inflammatory response. However, at a later stage, the effects of tumour progression likely led to neutrophil recruitment into the tumour microenvironment.

Neutrophils are important regulators for both the innate and adaptive immune response. Fibroblast growth factors, FGF1 and FGF2 are involved in neutrophil chemotaxis through FGFR2, but not FGFR3, as human neutrophils do not express FGFR3 (Haddad et al., 2011). Mechanistic effects of FGFR3 on neutrophils and other immune cells are largely unknown.

3.3.4 FGFR3 mutation associated with a lower expression of immune gene signatures in bladder cancer patients

FGFR3 alterations were associated with poor responses to immune checkpoint inhibitors (Ibrahim et al., 2019). Recent studies showed that FGFR3 mutation could be a tumour-intrinsic factor that drives T cell exclusion from MIBC tumour subset, leading to non-T cell inflamed phenotype (Ibrahim et al., 2019; Kilgour et al., 2016; Sweis et al., 2016). FGFR3 alterations in MIBC was associated with low expression of PD-L1 and low CD8 infiltration compared to wt FGFR3 (Kilgour *et al.*, 2016).

Beside PD-L1 and CD8, the expression of other immune cell signature involved in the T cell activation (GZMA), checkpoint T cell (TIGIT, ENTPD1, HAVCR2), checkpoint tumour cell (PVRIG), and MHC (HLA-DRA, HLA DRB) was also observed in MIBC (Borcoman et al., 2019). The reduction of expression was associated with the activation of the PI3K pathway (Borcomon *et al.*, 2019). PI3K is the downstream signalling for FGFR3 (Spivak-Kroizman *et al.*, 1994; Chen *et al.*, 2005; Ornitz and Itoh, 2015).

A similar observation was also reported in upper tract urothelial carcinoma with high expression of FGFR3, which correlated with a reduction of T cell infiltration in the tumour microenvironment (Robinson et al., 2019).

To the best of our knowledge, no study has reported the association of FGFR3 mutation with the gene expression for chemotactic factors for neutrophils.

In our mouse model, *Fgfr3* mutation was associated with the suppression of immune infiltration at the acute inflammatory stage induced by the carcinogen treatment. However, at the later stage of tumour growth, the infiltration of immune cells was not associated by *Fgfr3* mutation but instead the presence of the tumour and their progression (Foth et al., 2018). As discussed in the 3.3.4, the reduction of immune gene expression could be associated with the PI3K pathway as FGFR3 is the upstream of this pathway.

3.4 Future directions

Further evaluation should be performed on the effects of FGFR3 on the expression of T helper (CD4) and T effector (CD8) cells.

In order to better understand the role of FGFR3 mutation and immune response, our data presented in 3.2.10 need to be further analyzed based on the gender of the patients, grade and type of the tumour.

Chapter 4

Effects of Cxcr2 deletion in carcinogen-dependent bladder tumorigenesis

4.1 Aim & objectives

The study in this chapter aimed to investigate the effects of Cxcr2 deletion in carcinogen-dependent bladder tumorigenesis. The specific objectives were:

- 1) To characterise the effects of Cxcr2 deletion during the acute inflammation stage and late bladder tumorigenesis by gross observations of animals and the bladder at dissection, and by histopathological analysis.
- 2) To compare the differences in the tumour histopathology between male and female mice.
- 3) To determine the roles of Cxcr2 in regulating senescence-associated pathways in bladder tumorigenesis by immunohistochemistry (IHC).

4.2 Results

4.2.1 Cxcr2 deletion led to adverse gross observation induced by OH-BBN treatment

For the carcinogen-induced bladder tumorigenesis, wt, Cxcr2 flox, and Cxcr2 ko mice aged between 8-10 weeks were continuously subjected to 0.05% OH-BBN for 10 weeks (Figure 4.1). Mice were then subjected to another 10 weeks with normal drinking water to allow tumour development. Culling and bladder harvest was performed at 2, 12, 16 and 20 weeks from the start of OH-BBN treatment.

No sign of haematuria or bladder tumour was observed at 2 weeks, 12 weeks, or 16 weeks in wt, Cxcr2 flox, and Cxcr2 ko. At 20 weeks from the start of carcinogen treatment, haematuria was observed in male mice with 27.6% (n = 8/29) in Cxcr2 flox, 33.3% (n = 3/9) in Cxcr2 ko, and none in wt (n = 0/39). In contrast, none of the wt, Cxcr2 flox, or Cxcr2 ko female mice showed haematuria.

The gross observation also revealed that male Cxcr2 flox had the highest tumour incidence with 75.9% of the cases (n = 22/29), followed by Cxcr2 ko (33.3%, n = 3/9), in comparison to 23.1% (n = 9/39) in wt (Table 4.1). On the other hand, only female wt showed the presence of a bladder tumour with 18.5% of the cases (n = 5/27), while there were none for Cxcr2 flox or Cxcr2 ko.

In summary, the presence of haematuria and a bladder tumour at dissection were macroscopically observed at 20 weeks from the start of OH-BBN treatment (Table 4.1). Male Cxcr2 flox, but not Cxcr2 ko, have a higher percentage of haematuria and bladder tumour in comparison to wt. In contrast, a lower in tumour occurrence was observed in females of Cxcr2 flox and Cxcr2 ko compared to wt at 20 weeks from the start of OH-BBN.

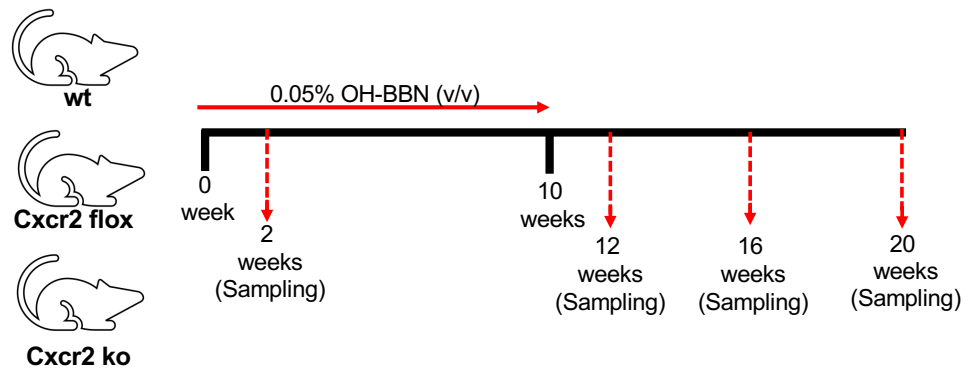


Figure 4.1. Schematic presentation of OH-BBN treatment for induction of bladder tumorigenesis. Cxcr2 flox and Cxcr2 ko mice were subjected to 0.05% OH-BBN in drinking water for 10 weeks, followed by another 10 weeks with normal drinking water. Wildtype “wt” (C57/Bl6 Charles River) mice were used as a control. The sampling of the bladder tissue was performed at 2, 12, 16, and 20 weeks from the start of OH-BBN treatment.

Table 4.1. Summary of the mouse cohorts and gross observations at the time of dissection. Mice from wt, Cxcr2 flox and Cxcr2 ko were treated with OH-BBN for 10 weeks with OH-BBN (followed with 10 weeks with normal drinking water). n/a indicate no sample available.

Genotype	Time from the start of OH-BBN treatment (weeks)*	Cohort size (n)			Haematuria (n)			Tumour (n)		
		Total	Male	Female	Total	Male	Female	Total	Male	Female
Wildtype	2	43	34	9	43	0/34 (0%)	0/9 (0%)	43	0/34 (0%)	0/9 (0%)
	12	15	8	7	15	0/8 (0%)	0/7 (0%)	15	0/8 (0%)	0/7 (0%)
	16	5	5	0	5	0/5 (0%)	0/0 (0%)	5	0/5 (0%)	0/0 (0%)
	20	70	43	27	66	0/39 (0%)	0/27 (0%)	66	9/39 (23.1%)	5/27 (18.5%)
Cxcr2 flox	2	47	34	13	47	0/34 (0%)	0/13 (0%)	47	0/34 (0%)	0/13 (0%)
	12	12	6	6	12	0/6 (0%)	0/6 (0%)	12	0/6 (0%)	0/6 (0%)
	16	5	5	0	5	0/5 (0%)	0/0 (0%)	5	0/5 (0%)	0/0 (0%)
	20	41	31	10	37	8/29 (27.6%)	0/8 (0%)	37	22/29 (75.9%)	0/8 (0%)
Cxcr2 ko	2	9	9	0	9	0/9 (0%)	0/0 (0%)	9	0/9 (0%)	0/0 (0%)
	12	0	0	0	n/a	n/a	n/a	n/a	n/a	n/a
	16	0	0	0	n/a	n/a	n/a	n/a	n/a	n/a
	20	16	9	7	16	3/9 (33.3%)	0/7 (0%)	16	3/9 (33.3%)	0/7 (0%)

4.2.2 Increase in bladder weight in Cxcr2 flox at 20 weeks of the OH-BBN course of treatment

We next analysed the weight of the dissected bladder tissues at dissection. Male Cxcr2 flox showed significantly higher bladder weight (65.7 mg, mean) in comparison to wt (44 mg, mean) ($p = 0.0002$, $n = 27$ Cxcr2 flox, $n = 39$ wt) (Figure 4.2). The mean for bladder weight of male Cxcr2 ko was comparable to wt. However, the data showed one outlier for Cxcr2 ko mouse. At gross examination, this particular Cxcr2 ko mouse had the heaviest bladder (4,000 mg) due to the presence of a big tumour and enlarged spleen which could be associated with the deletion of Cxcr2. The spleen was not harvested for histopathological examination.

In summary, the bladder weight supported the gross observation of increased tumour incidence in Cxcr2 flox mice in comparison to wt and Cxcr2 ko (Table 4.1, Figure 4.2).

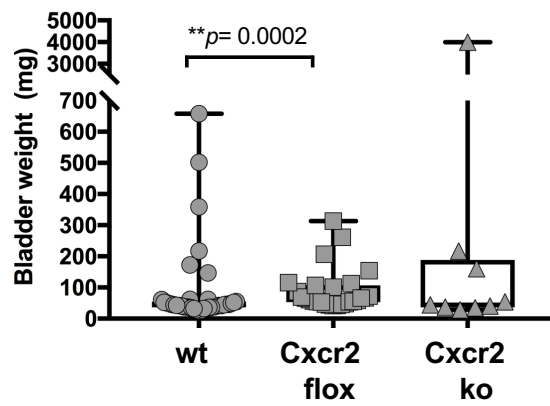


Figure 4.2. Bladder weight at 20 weeks from the start of OH-BBN treatment. Statistical significances were determined using the Mann-Whitney test for non-parametric distribution. The p -values of $**p < 0.001$ were considered significant.

4.2.3 Cxcr2 deletion in the myeloid-lineage increased tumour pathogenesis in OH-BBN-induced bladder tumour model

We next investigated the effects of Cxcr2 loss on bladder tumorigenesis at the histopathological level.

Microscopic observations of H&E stained sections revealed that the majority of mice in wt, Cxcr2 flox, and Cxcr2 ko developed abnormalities in the urothelium, including atypia, hyperplasia, dysplasia, and carcinoma in situ (CIS) in response to OH-BBN treatment (Figure 4.3A-C). The tumours occurred more frequently in the Cxcr2 flox compared to wt ($p = 0.0006$). Tumour pathogenesis was not significantly different when Cxcr2 ko and wt mice were compared (Figure 4.3A). Similar observations were obtained when males and females were compared individually (Figure 4.3B, C).

We also evaluated the size of the tumour developed at 20 weeks. A tumour size of more than $>3 \text{ mm}^2$ of the bladder tissues (examined in section) was considered to be 'big'. The remainder (tumour size $<3 \text{ mm}^2$) was considered to be 'small'. Cxcr2 flox showed a significantly higher occurrence of big tumours (60%) in comparison to wt (16.7%) ($p = 0.0473$) (Figure 4.3D). No significant difference was observed when the size of the tumour area (mm^2) was compared between wt, Cxcr2 flox and Cxcr2 ko (Mann-Whitney test) (Figure 4.3G-I).

Altogether, the histopathological analysis corresponded with the macroscopic observations at dissection of increased tumour occurrence in Cxcr2 flox compared to wt (Table 4.1).

4.2.4 Cxcr2 flox showed an increase in invasiveness and squamous transformation

Next, we evaluated the characteristics of the urothelial pathogenesis in more detail.

Cxcr2 flox and Cxcr2 ko bladders showed significantly higher invasiveness ($p < 0.0001$ and $p = 0.0106$, respectively) compared to wt (Figure 4.4A). Cxcr2 flox and Cxcr2 ko also showed a significant increase of squamous transformation compared to wt ($p < 0.0001$ and $p = 0.0485$, respectively) (Figure 4.4D).

Similar observations were obtained in males and females for invasiveness and squamous transformation (Figure 4.4B, C, E, and F).

No significant differences were observed in the presence of a lobulated pattern of the basal membrane of the urothelium (Figure 4.4G-I).

In summary, the results showed that Cxcr2 deletion in the myeloid lineage (Cxcr2 flox) resulted in the enhanced urothelial abnormalities and tumour pathology in comparison to wt (Fig 4.3 and 4.4). This indicated that Cxcr2 deletion in the myeloid lineage is pro-tumorigenic. In contrast, Cxcr2 deletion in the tissue (Cxcr2 ko) resulted in a similar bladder phenotype to wt.

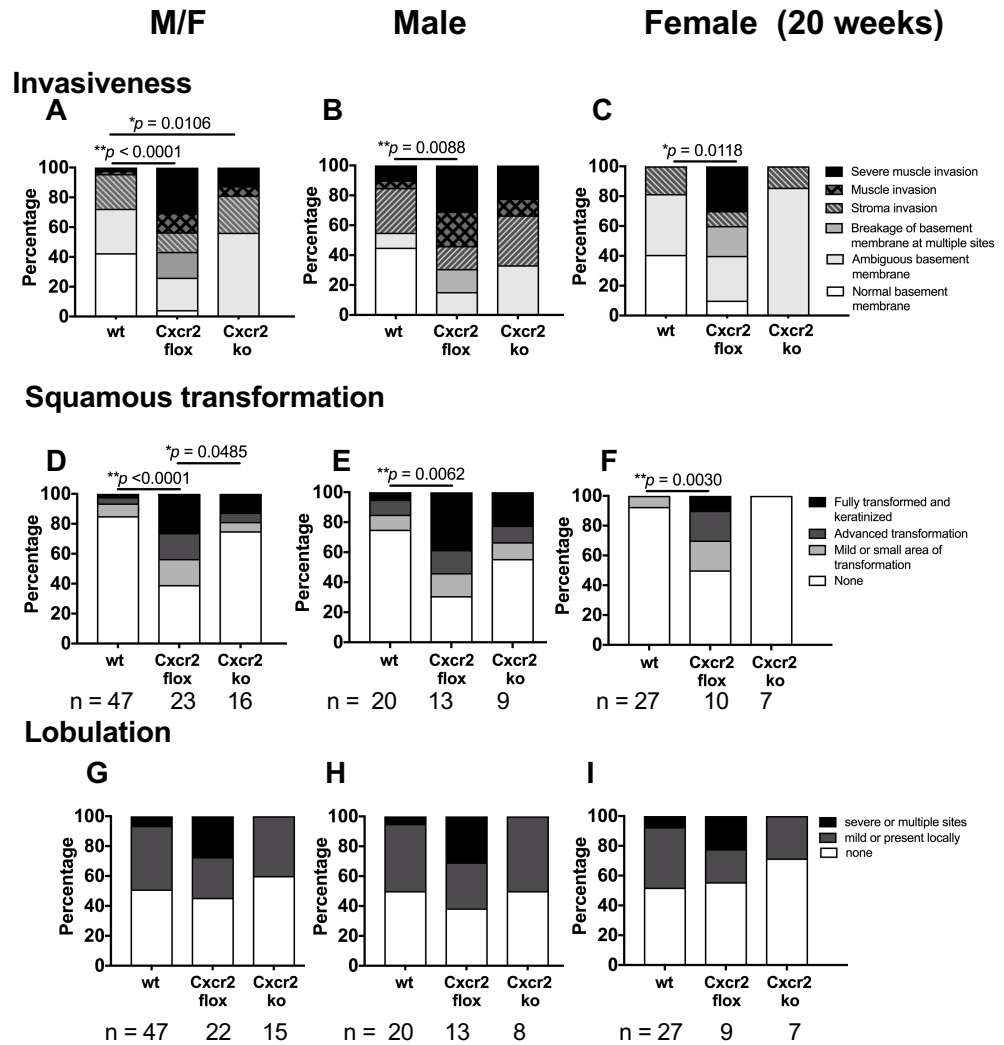


Figure 4.4. The characteristics of the urothelial at 20 weeks from the start of OH-BBN treatment. Invasiveness (A-C). Squamous transformation of the urothelial and tumour (D-F). Lobulated appearance of the basement membrane (G-I). Number of samples (n) analysed are as indicated below graph. The p-values (Mann-Whitney) are indicated where $*p < 0.05$ and $p < 0.01$ were considered significant.**

4.2.5 Stroma thickness was reduced in Cxcr2 flox at 2 weeks of OH-BBN treatment

Due to robust changes in the tumour occurrence and tumour phenotype in Cxcr2 flox and not in Cxcr2 ko, compared to wt, we next address the mechanism of increased bladder tumorigenesis in the Cxcr2 flox mice. Cxcr2 ko was also difficult to breed (personal communication with Dr Tomoko Iwata and Professor Jennifer Morton).

We examined the histopathological changes in the bladder tissue harvested at the earlier time points. At two weeks of the OH-BBN treatment, urothelial abnormalities, namely hyperplasia, atypia, and dysplasia, were observed at a comparable level in Cxcr2 flox and wt (Fig 4.5A-F).

The majority of Cxcr2 flox bladders showed a thinner stroma than wt ($p = 0.0165$) (Figure 4.5G). The difference was present in males ($p = 0.01648$) (Figure 4.4H) but not in females (Figure 4.5I).

Cxcr2 flox showed a mild decrease in the presence of the blood vessels, which could indicate angiogenesis, in the inner stroma compared to wt. However, the frequency was comparable in the outer stroma (Figure 4.5J-O).

4.2.6 No significant difference in urothelial phenotype was observed at 12 weeks

The changes in bladder characteristics were also investigated in the bladders at 12 weeks from the start of carcinogen treatment. The 12 weeks included 10 weeks of OH-BBN treatment and an additional two weeks of tap water.

Cxcr2 flox mice showed no statistically significant differences compared to wt in the urothelial phenotype, including hyperplasia, atypia, Dysplasia, and CIS, as well as invasiveness and lobulation (4.6A-I).

Altogether, the urothelial phenotype was comparable between Cxcr2 flox and wt at two weeks and 12 weeks (Figure 4.5 and 4.6). However, a significant decrease in stroma thickness observed in Cxcr2 flox at 2 weeks could indicate a dysregulation in the acute inflammatory response.

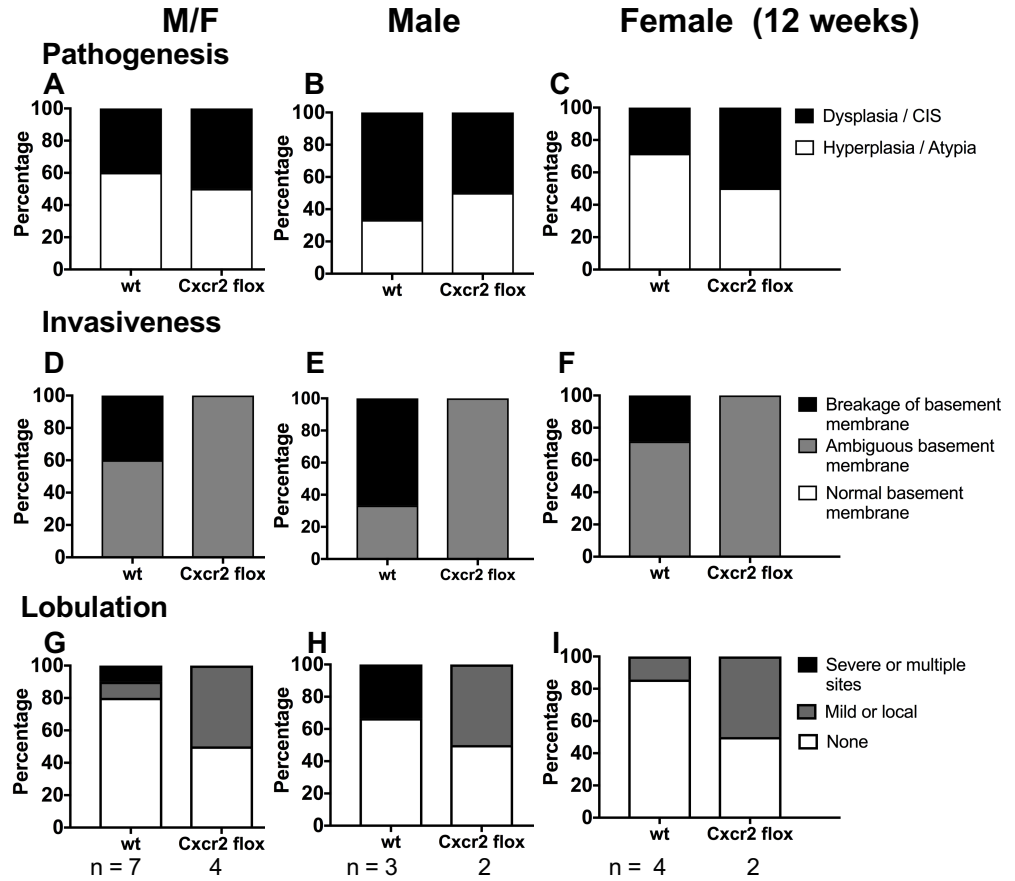


Figure 4.6. Histopathological analysis of the bladders at 12 weeks from the start of OH-BBN treatment. Pathogenesis (A-C), invasiveness of urothelial cells (D-F), and lobulation formation of basement membrane (G-I) were quantified as a percentage of each criterion.

4.2.7 Cxcr2 flox displayed pathological changes at 16 weeks

We next analysed the pathological changes at 16 weeks from the start of OH-BBN treatment, in which OH-BBN had been ceased for six weeks. A small sample size, $n = 5$ each for wt and Cxcr2 flox, was used.

All five wt samples at this timepoint only showed the presence of hyperplasia or atypia. In contrast, two out of five (40%) of male Cxcr2 flox showed the presence of a tumour. Furthermore, three out of five (60%) of Cxcr2 flox showed dysplasia or CIS (Figure 4.7A).

We next looked at the invasiveness of urothelial cells and lobulation of the basement membrane. Muscle invasion and stromal invasion were observed in one (20%) and two mice (40%) of Cxcr2 flox, respectively. Another two (40%) Cxcr2 flox mice showed ambiguous basal membrane. In contrast, all five (100%) wt mice showed ambiguous basal membranes (Figure 4.7B).

For the formation of lobulation at the basement membrane, three out of five (60%) Cxcr2 flox mice showed severe or multiple sites of lobulation, while another two showed mild or a local presence of lobulation. Wt, on the other hand, showed no presence of lobulation in all five out of five mice (Figure 4.7C).

We also observed a significant difference in the squamous transformation of the urothelium. Four out of five Cxcr2 flox bladders (80%) displayed a mild or small area of squamous transformation, while none of the wt showed a squamous transformation ($p = 0.0476$) (Figure 4.7D).

Taken altogether, the increase in bladder pathogenesis was evident in Cxcr2 flox compared to wt at 16 weeks, indicating that tumour initiation and promotion were enhanced in the absence of Cxcr2 expression.

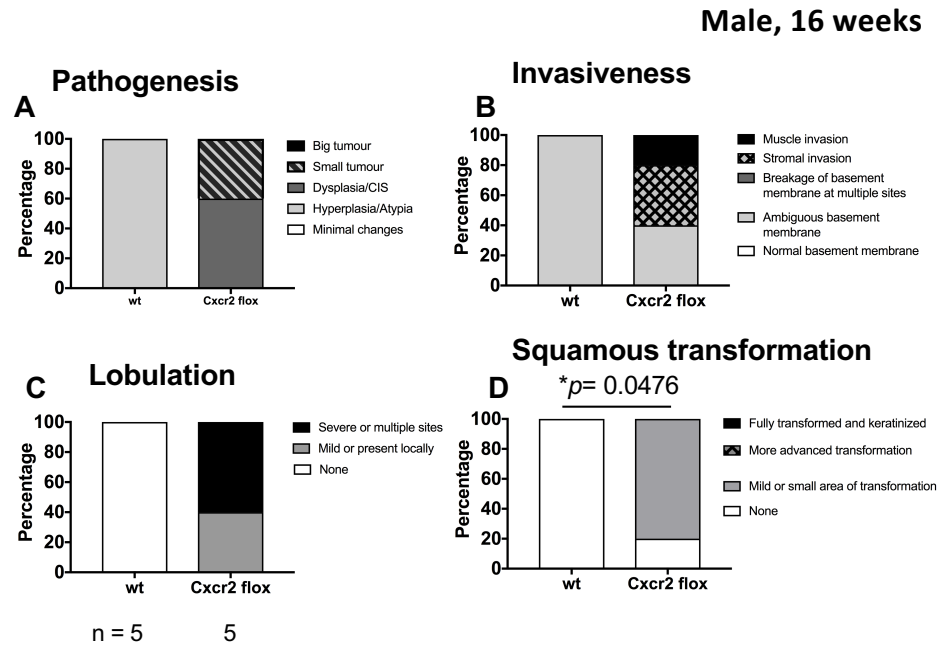


Figure 4.7. Histopathological analysis of bladder at 16 weeks from the start of OH-BBN treatment. Urothelial pathogenesis and tumour occurrence (A). Invasiveness of urothelial and bladder tumour cells (B). Formation of lobulation at basement membrane (C). Transformation of urothelial and bladder tumour cells (D). Mann-Whitney test was used to evaluate the statistical difference with $*p < 0.05$ was considered significant.

4.2.8 Senescence was retained in Cxcr2 flox mice at 2 weeks

Based on the report that showed depletion of Cxcr2 could delayed and impaired both replicative and oncogenic-induced senescence (OIC) (Acosta et al., 2009), we had also investigated the ability of Cxcr2 to reinforces senescence in abnormal cells in the bladder following carcinogen treatment. OIC is regarded as the first barrier of defence against cancer development (Haugstetter et al. 2010). Therefore, we hypothesized that loss of Cxcr2 in senescence pathway will influence the bladder tumour progression in a context dependent manner.

In order to address whether senescence plays a role in the phenotype observed in Cxcr2 flox mice, senescence-associated proteins was evaluated non-quantitatively in n=3 samples per cohort. The expression was first examined in samples at 2 weeks of OH-BBN treatment.

Four senescence-associated markers were used. γ H2aX is a marker to detect the presence of DNA damage (Hooten and Evans, 2017). p53 and p21 are the cell cycle regulator and inhibitor, respectively. p21 is known to be up-regulated as a downstream of p53 (El-Deiry et al., 1993). Ki67 is a marker for cell proliferation (Scholzen and Gerdes, 2000). The images were analysed qualitatively in n = 3 samples, in which scoring was performed in respect to the overall proportion of cells expressing positive staining in the tissue sections.

At two weeks, DNA damage was present and at a similar level in the urothelium of wt and Cxcr2 flox (Figure 4.8A, B). The expected increase in p53 (Figure 4.8C, D) and p21 expressions (Figure 4.8E, F) were also observed similarly in both cohorts. Only a few Ki67-positive cells were present in the urothelium of wt and Cxcr2 flox (Figure 4.8G, H).

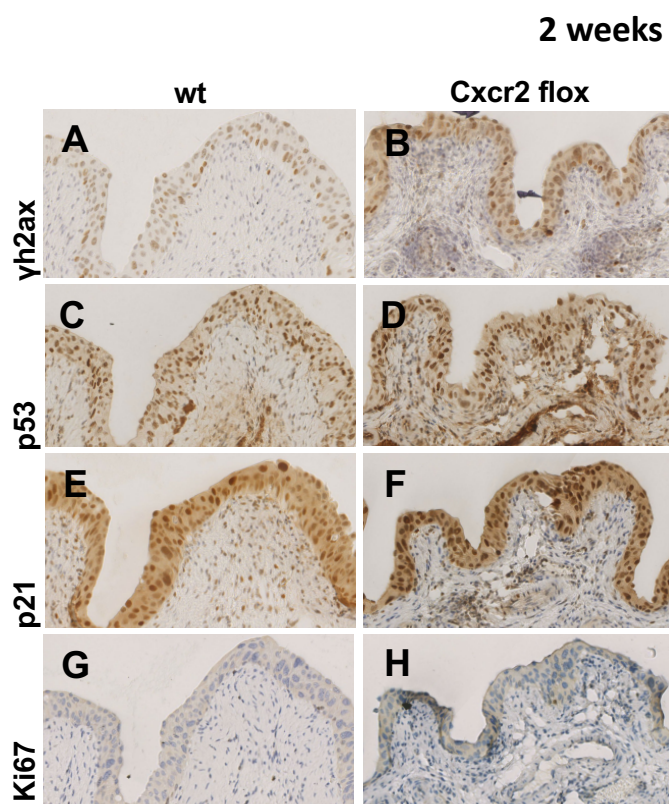


Figure 4.8. Expression of senescence-associated proteins at 2 weeks.

Representative images of γ H2aX (A and B), p53 (C and D), p21 (E and F), and Ki67 (G and H). IHC staining in wt (A, C, E, and G) and Cxcr2 flox (B, D, F, and H) bladder samples treated with OH-BBN for 2 weeks. N=3 samples were used for each cohort. Scale bar represents 100 μ m.

4.2.9 Cxcr2 deletion in the myeloid lineage led to an impairment of the senescence pathway at 20 weeks

We next analysed the cellular senescence in tumour samples taken at 20 weeks from the start of carcinogen treatment.

The DNA damage was still retained, as indicated by γ H2aX positivity, even after carcinogen treatment ceased for 10 weeks (Figure 4.9A-C).

We analysed the expression of p53 and p21 using consecutive sections. It was observed that these two protein expressions co-localized with γ H2aX positivity in the wild type (Figure 4.9D, G). Accordingly, some Ki67 positivity was observed in the corresponding tumour area (Figure 4.9J).

In Cxcr2 flox and Cxcr2 ko, the levels of expressions of γ H2aX and p53 were comparable to wt (Figure 4.9E, F). However, the expression of p21 was reduced in Cxcr2 flox and Cxcr2 ko compared to wt, regardless of sustained p53 expression (Figure 4.9H, I). Accordingly, increased Ki67 positivity was identified in tumours of Cxcr2 flox and Cxcr2 ko (Figure 4.9K, L).

Altogether, these data indicate that the senescence pathway was intact in wt at two weeks and 20 weeks from the start of OH-BBN treatment. The expression of p53 co-localized with γ H2aX at both time points. However, despite no changes in the p53 expression, that of p21 decreased in Cxcr2 flox and Cxcr2 ko tumour samples, leading to a concomitant increase in Ki67. This indicated that the loss of Cxcr2 expression led to dysregulation in the senescence pathway at the p53-p21 relay point and is likely to have enhanced the tumour progression (Figure 4.8 and 4.9).

Tumour, 20 weeks

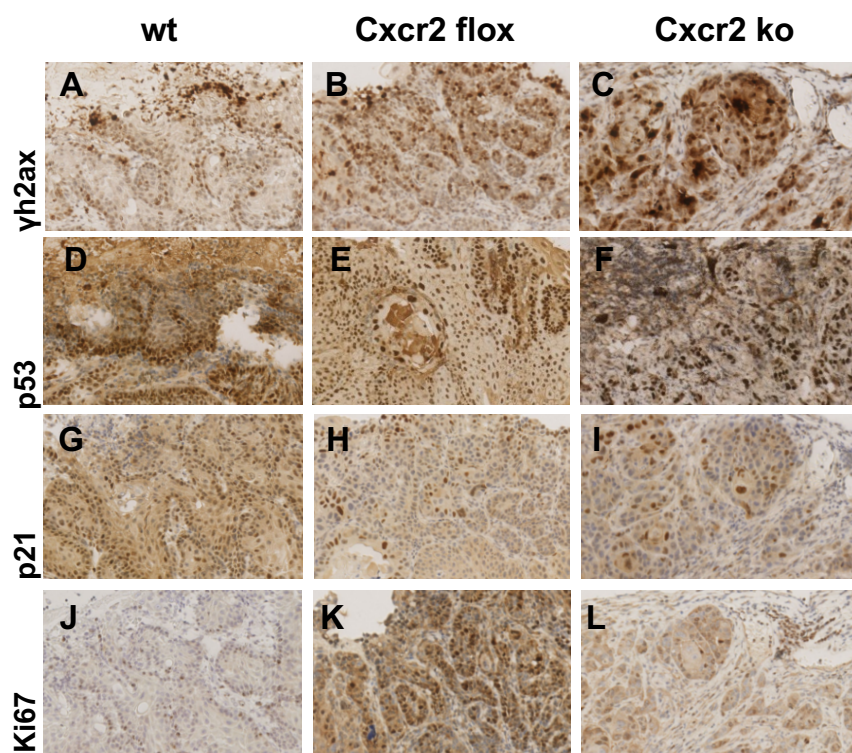


Figure 4.9. Expression of senescence-associated proteins in bladder tumour at 20 weeks. Representative images of γ H2ax (A, B, and C), p53 (D, E, and F), p21 (G, H, and I), and ki67 (J, K, and L). IHC staining in wt (A, D, G, and J), Cxcr2 flox (B, E, H, and K), and Cxcr2 ko (C, F, I, and L) bladder samples were evaluated. N=3 samples were used for each cohort. Scale bar represents 100 μ m.

4.3 Discussion

4.3.1 Summary of results

In summary, the results in this chapter showed that:

- 1) Deletion of *Cxcr2* in the myeloid cells (*Cxcr2* flox), but not in the tissue (*Cxcr2* ko), yielded a significant increase in the tumour occurrence and size of the tumour in comparison with wt (Table 4.1, Figure 4.2 and 4.3).
- 2) At 2 weeks of carcinogen treatment, wt and *Cxcr2* flox showed comparable urothelial abnormalities. However, the thickening of the stroma, indicative of inflammation, as well as angiogenesis, were less observed in *Cxcr2* flox compared to wt (Figure 4.4).
- 3) Tumour formation was observed at 16 weeks in *Cxcr2* flox, an an earlier time point in comparing to wt (Figure 4.7).
- 4) The senescence-associated pathway was similarly activated in *Cxcr2* flox and wt with the expression of γ -H2aX, p53, p21 but low Ki67 observed at 2 weeks of carcinogen treatment (Figure 4.8). However, at the later stage of bladder tumorigenesis, tumour cell proliferation occurred regardless of p53 expression in *Cxcr2* flox (Figure 4.9).
- 5) Male mice displayed severe urothelial pathogenesis and tumour occurrence compared to female mice (Figure 4.3 and 4.4).

Altogether, our results showed that *Cxcr2* deletion in the myeloid cells increased tumorigenesis in the bladder, indicated the ability of *Cxcr2* in inhibiting bladder tumorigenesis. Furthermore, the disparity between *Cxcr2* flox and *Cxcr2* ko indicated the tissue-dependent effect of *Cxcr2* in myeloid cells and in the bladder. Similar to humans, there was a higher incidence of tumour occurrence in male mice compared to female, regardless of genotype.

4.3.2 *Cxcr2* deletion in the myeloid cells enhanced bladder tumour occurrence and progression

CXCL1/CXCR2 have been implicated in the migration and angiogenic effects of melanoma cells (Singh et al., 2009) and their axis is essential in the metastasis of colon cancer (Yamamoto et al., 2008). *Cxcr2* deletion suppressed inflammation-driven tumorigenesis in the skin and intestine as well as spontaneous adenocarcinoma formation (Jamieson *et al.*, 2012). *Cxcr2* expression was also found to be higher in tumour tissue compared to adjacent non-cancerous tissue, and this correlates with their abilities to modulate tumour transformation, survival, growth, invasion, and metastasis by indirectly regulating angiogenesis and tumour-leukocyte interactions (Lee *et al.*, 2014).

Our results contradict most of the reported effects of Cxcr2 in the *in vivo* carcinogenesis models (discussed in Chapter 8 in more depth).

An increase in the incidence of developing bladder tumour in Cxcr2 flox mice indicated that the Cxcr2 expression in the myeloid cells was potentially anti-tumour, suppressing the bladder tumorigenesis. However, further deletion of the Cxcr2 in the bladder in Cxcr2 ko appeared to cancel out this tumour promoting effects of myeloid-specific deletion of Cxcr2, returning the level of tumorigenesis to that of the wt, which indicated the pro-tumour effect of epithelial (or bladder) Cxcr2. Myeloid cell-independent, bladder-specific effects of Cxcr2 deletion can be assessed by bladder-specific deletion of Cxcr2, for example, by use of UroIICre, in the future. As mentioned in 1.8.2.1.1, numerous studies have reported the usage of UroII promoter to create conditional modulation of targeting gene in bladder cancer mouse models (Kobayashi et al., 2015; Zhang et al., 1999). Thus, by crossing the UroII-Cre line to the line of mouse bearing the Cxcr2 gene flanked by the loxP sequences (floxed Cxcr2), we might be able to investigate the specific role of Cxcr2 expression in the bladder tissue.

The evaluation of the stromal thickness and angiogenesis at the 2 weeks of OH-BBN treatment in this study indicated suppression of acute inflammatory responses in the absence of Cxcr2. For the analysis of angiogenesis, IHC with markers, such as CD31 (PECAM-1) and VEGF (Murdoch et al., 2008) could be used in the future.

4.3.3 Cxcr2 loss may dysregulate senescence leading to bladder tumorigenesis

In normal cellular responses, DNA damage leads to either cell cycle arrest to repair the lesions or apoptosis. In DNA damage response pathways p53 is stabilized and its function as a transcription factor is activated, which leads to up-regulation of its downstream gene, p21. This downstream factor is an important inhibitor for cyclin-dependent kinases (CDKs) to induce senescence/cell cycle arrest at the G1/S phase (Bartek and Lukas, 2001). Thus, tumour cells in the Cxcr2 flox and Cxcr2 ko mice may have evaded the senescence by manipulating the defect in the p53-transcriptional activated p21 pathway.

The anti-proliferative effects and cell cycle inhibitory effects of Cxcr2 could be a result of its role in the regulation of the senescence pathway (Acosta et al., 2018). In its absence, tumour cells may have gained the ability to escape the senescence barrier, as observed in the immunohistochemistry analysis of senescence-associated proteins in Cxcr2 flox and Cxcr2 ko (Figure 4.9). An increase in cell proliferation has long been associated with tumour progression (Ventura et al., 2007). It has been suggested that the expression of Ki67 can be used as a prognostic marker for tumour recurrence and progression in

NMIBC (Ding et al., 2014). Its expression is associated with a higher grade and the risk of recurrence of NMIBC.

The IHC staining for the γ H2aX, p53, p21, and Ki67 should be further improved to reduce the background staining. The expression can be further analysed by an improved strategy using image analysis software (for example; QuPath or ImageJ) for semi-quantification analysis. The number of samples should be increased to at least n=2 more in each cohort.

4.3.4 Tumour occurrence was more frequent in male mice than female

Although both male and female mice received the same carcinogen treatment, tumour occurrence was observed to be higher in the male than in the female mice.

In humans, men are more likely to be diagnosed with this cancer (1 in 39) compared to women (1 in 110) (Cancer Research UK, 2019). This is associated with cigarette smoking and industrial or occupational chemical exposures, which were more common in men compared to women.

The elevated tumour occurrence could be linked to the intrinsic gender differences. Some studies have reported the association of sex hormones such as androgen and testosterone in promoting bladder cancer progression in human bladder tumours (Johnson et al., 2008; Miyamoto et al., 2007; Okajima et al., 1975). Transgenic castrated male mice and treated with OH-BBN showed an inhibition of bladder tumour growth and volume compared to non-castrated mice (Johnson et al., 2008). Female mice implanted with testosterone showed an increase of OH-BBN-induced bladder carcinogenesis (Okajima et al., 1975). Altered exposure of the primary sex hormone, oestrogen, has also been suggested to limit the risk of urothelial carcinoma incidence in women (George et al., 2013). It was suggested that sexual dimorphism exists in immune response, as seen in clinical studies of gastric cancer (Caruso et al., 2002). Female patients showed higher tumour-infiltrating neutrophils associated with a low mortality rate, but this was insignificant in male patients (Caruso *et al.*, 2002).

Chapter 5

Effects on Immune cell infiltration upon Cxcr2 deletion

5.1.1 Hypotheses

- 1) The loss of Cxcr2 will suppress the level of neutrophils in circulation and in the bladder during the acute inflammation stage induced by OH-BBN treatment, leading to overall suppression of immune infiltrations in the bladder tissue as a consequence.
- 2) At the late stage of tumorigenesis, the level of immune cells in circulation and in the bladder tissue might become independent of Cxcr2 loss, but instead, influenced by the presence of the bladder tumour.

5.1.2 Aim and objectives

This chapter aimed to investigate the effects of Cxcr2 loss in the recruitment of the myeloid cells and T-cell populations during bladder tumorigenesis. The specific objectives were:

1. To analyse the effects of Cxcr2 loss in the levels of immune cells in the blood
2. To analyse the effects of Cxcr2 loss in the levels of immune cells in the bladder tissue
3. To evaluate the above differences in the blood and in the bladder tissues
4. To evaluate how the above changes occur during the time course of carcinogen treatment
5. To evaluate how the above associated with the presence of tumours
6. To compare the populations of neutrophils identified by morphology to markers.

5.2 Results

5.2.1 WBC populations at 2 weeks of carcinogen treatment

Blood samples of wt and *Cxcr2* flox were withdrawn at 2 weeks from the start of OH-BBN treatment. The cell populations were evaluated in relative populations (percentage of each subset to total WBC), and the number of the cells in the blood (cells/ml).

In general, there was no significant difference in WBC populations between wt and *Cxcr2* flox mice (Figure 5.1).

However, a lower number of neutrophils in *Cxcr2* flox was observed in two out of three mice of this cohort in compared to wt (Fig 5.1A, D). These two particular *Cxcr2* flox mice also showed a higher number of lymphocytes and accordingly, a lower number of NLR in comparison to wt (Figure 5.1C, E).

It was also observed that the same two *Cxcr2* flox mice have a comparable number of monocytes and eosinophils, but a higher number of basophils compared to wt (Figure 5.1F-K).

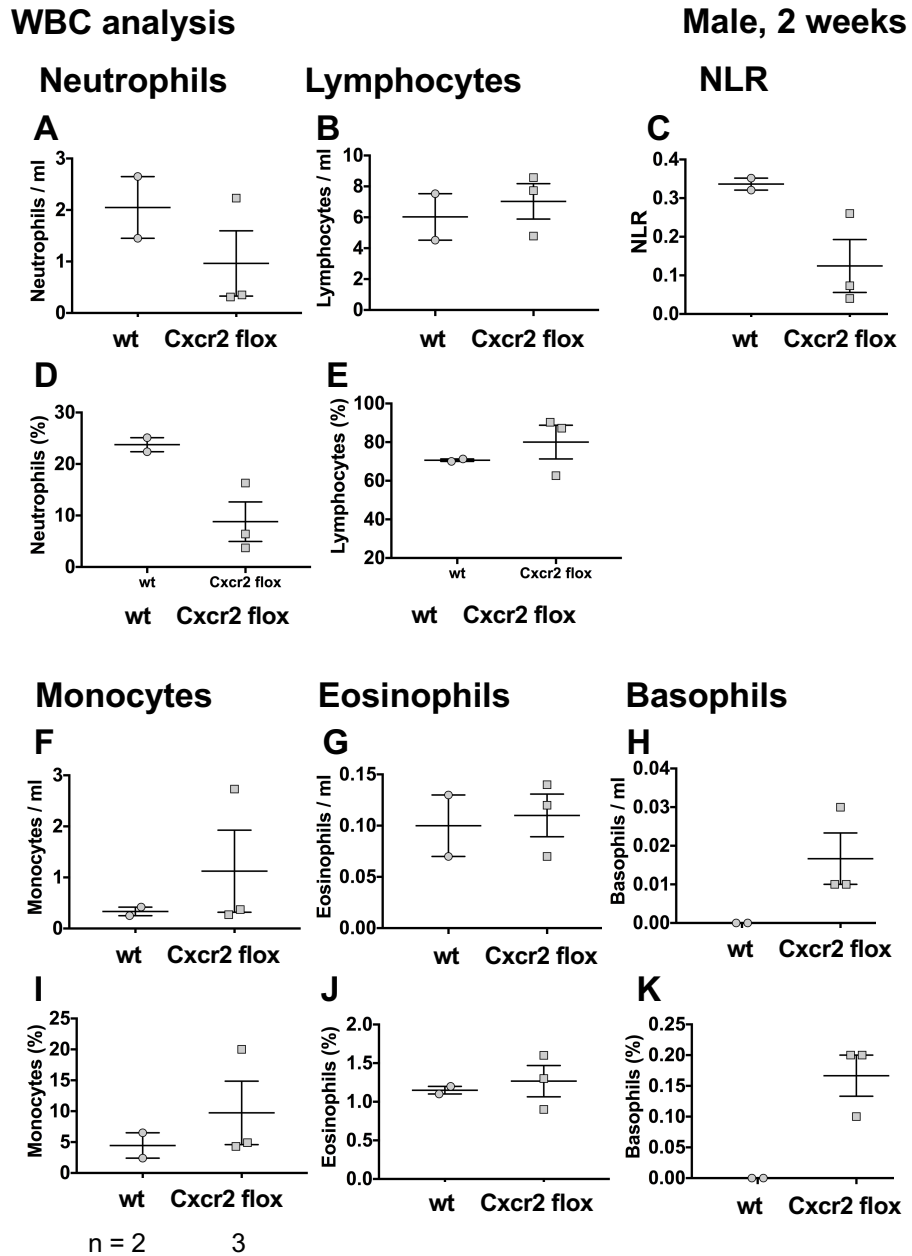


Figure 5.1. Effects of Cxcr2 deletion in circulation at 2 weeks of carcinogen treatment. Number of neutrophils, lymphocytes, NLR in blood (cells/ml) (A-C). Relative population of neutrophils and lymphocytes in whole WBC (%) (D, E). Number of monocytes, eosinophils and basophils in blood (cells/ml) (F-H). Relative population of neutrophils and lymphocytes in whole WBC (%) (I-K).

5.2.2 WBC populations at 16 weeks from the start of carcinogen treatment

We had also performed blood analysis on samples taken at 16 weeks, in which OH-BBN had been ceased for 6 weeks after 10 weeks of OH-BBN application.

The levels of neutrophils in *Cxcr2* flox mice were significantly lower in comparison to wt ($p = 0.0238$, Figure 5.2D). In contrast, lymphocytes were significantly increased in *Cxcr2* flox compared to wt ($p = 0.0317$, Figure 5.2B). Accordingly, the NLR was reduced in *Cxcr2* flox compared to wt ($p = 0.0317$, Figure 5.2C).

Cxcr2 flox also showed a significantly higher level of monocytes in comparison to wt ($p = 0.0159$, $p = 0.0079$, Figure 5.2F, I). On the other hand, the levels of eosinophils and basophils were comparable in *Cxcr2* flox and wt mice (Figure 5.2G, J, H, K).

WBC analysis

Male, 16 weeks

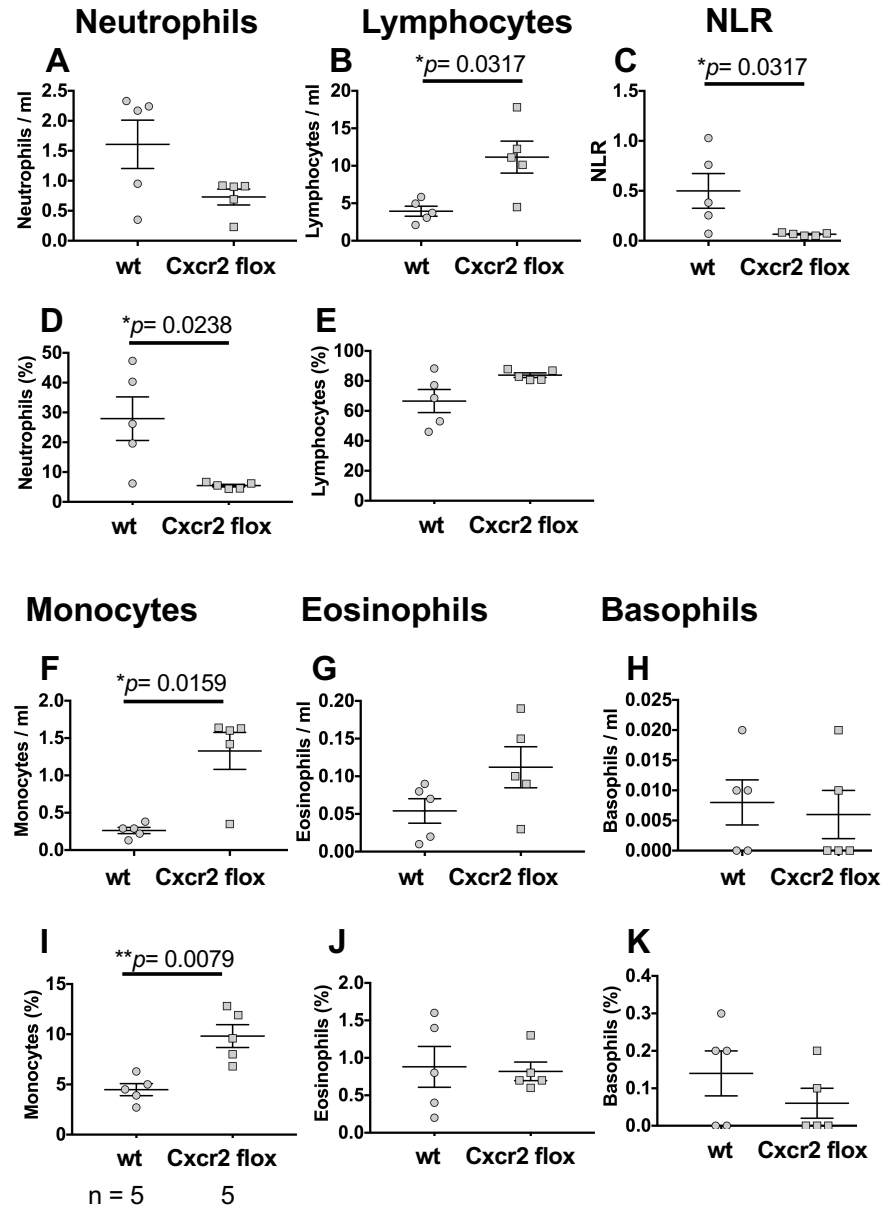


Figure 5.2. Blood analysis at 16 weeks from the start of carcinogen treatment.

Absolute number of neutrophils, lymphocytes, monocytes, basophils and eosinophils within blood (cell/ml) (A, B, F, G, J) and NLR (C). Relative number of neutrophils, lymphocytes, monocytes, basophils and eosinophils subset within whole WBC (%) (C, D, G, H, K, L). Relative number of monocyte and eosinophil population in whole WBC (%) (C, D, G, H, K, L). Number of samples (n) analysed are as indicated below graph. The p-values (Mann-Whitney) are indicated where $*p < 0.05$ and $**p < 0.005$ were considered significant.

5.2.3 Levels of neutrophils and lymphocytes in circulation were altered in the presence of tumour

We next analysed the blood profile in mice culled at 20 weeks from the start of OH-BBN treatment.

Overall, *Cxcr2* flox and wt mice showed a comparable level of circulating neutrophils, regardless of the presence of the tumour in the bladder (Figure 5.3A-D).

We have also compared the neutrophils number between mice that harboured bladder tumour with the non-bladder tumour in the same cohort. Wt mice with bladder tumour showed a significant increase in circulating neutrophils ($p = 0.0280$), and in relative to whole WBC populations ($p = 0.0105$) compared to their non-bladder tumour counterparts (Figure 5.3B, D). This difference was not observed between *Cxcr2* flox mice that harboured bladder tumour with their non-bladder tumour counterparts (Figure 5.3B, D).

In general, no significant changes were observed in the number of circulating lymphocytes between *Cxcr2* flox and wt mice (Figure 5.3E-H). However, in mice without bladder tumour, a decrease in circulating lymphocytes was observed in *Cxcr2* flox mice compared to the respective wt mice ($p = 0.0108$, Figure 5.3F).

We have also compared the NLR between *Cxcr2* flox and wt and observed no significant changes (Figure 5.3I, J). However, a significant increase in NLR was observed in wt mice that harboured bladder tumour in comparison to the wt mice without bladder tumour ($p = 0.049$, Figure 5.3J).

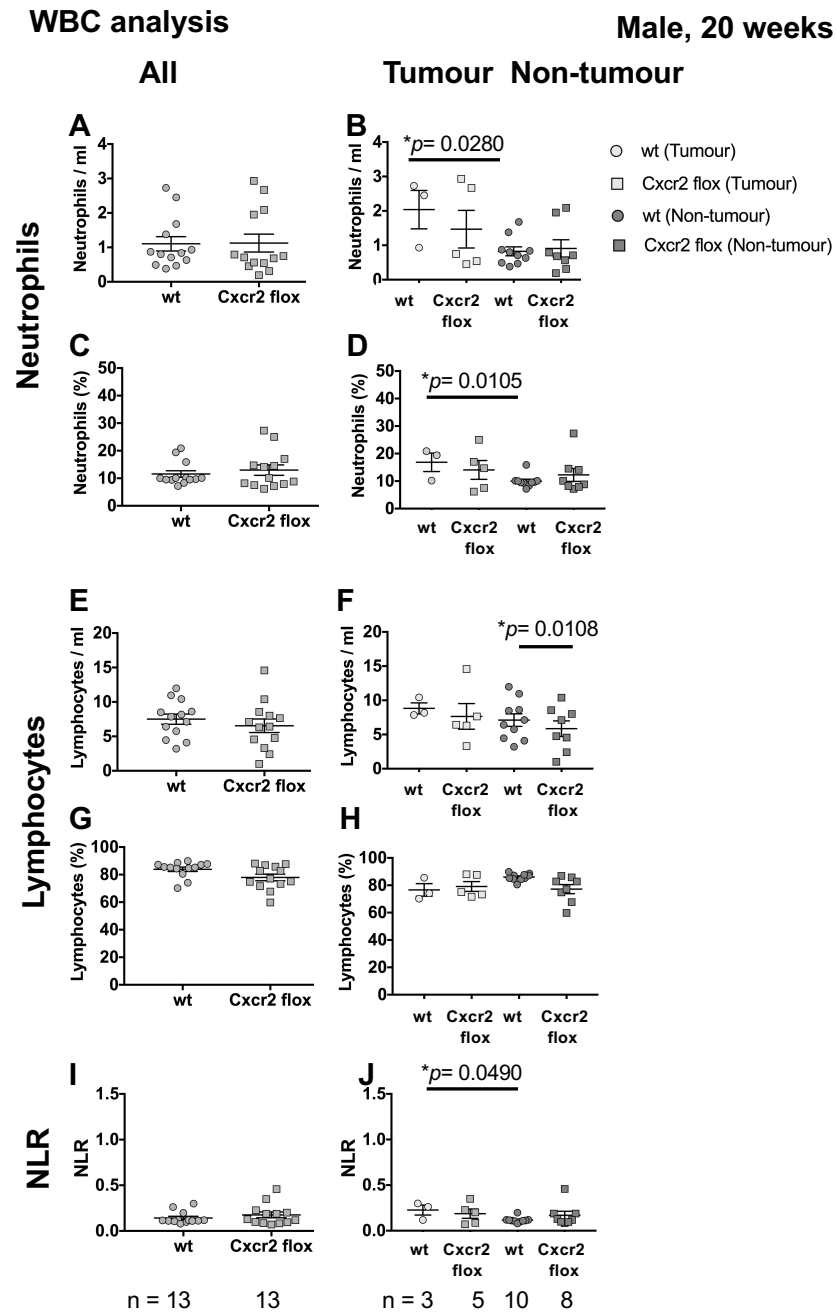


Figure 5.3. WBC profiles at 20 weeks. Number of neutrophils, lymphocytes, NLR in blood (cells/ml) (A, E, I). Relative population of neutrophils and lymphocytes in whole WBC (%) (C, D, G, H). Samples were taken at 20 weeks from the start of carcinogen treatment. Significant difference was evaluated using Mann-Whitney test with $*p < 0.05$ was considered significant.

5.2.4 Cxcr2 deletion increased monocytes infiltration in non-bladder tumour mice

We next analysed the differences in the number of circulating monocytes, eosinophils and basophils between Cxcr2 flox and wt at 20 weeks from the start of OH-BBN.

Cxcr2 flox mice showed a significant increase in circulating monocytes ($p = 0.0426$) as well as in relative to the whole WBC ($p = 0.0007$), compared to wt mice (Figure 5.4A, C).

Cxcr2 flox mice without bladder tumour demonstrated a significant increase in the circulating monocytes ($p = 0.0362$) and relative number to the whole WBC ($p = 0.0009$) compared to the wt mice without bladder tumour (Figure 5.4A, C).

In general, there was no significant difference observed in the number of circulating eosinophils between Cxcr2 flox and wt samples.

However, we did observe a significant increase in the number of absolute ($p = 0.0245$) and relative number ($p = 0.0315$) of eosinophils in wt mice that harboured bladder tumour in comparison to the wt mice without bladder tumour (Figure 5.4F, H).

Lastly, for circulating basophils, Cxcr2 flox mice showed a comparable number with wt mice, with or without the presence of bladder tumour (Figure 5.4I, K).

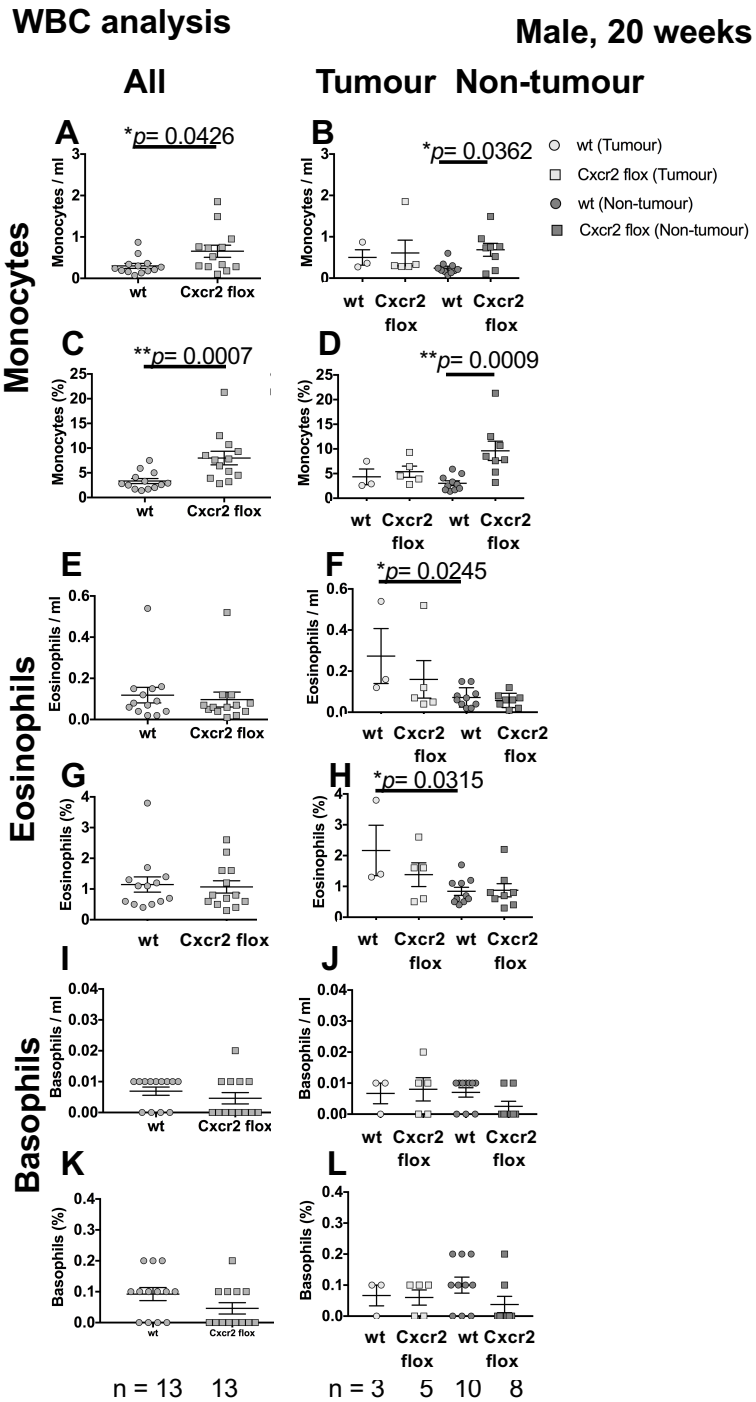


Figure 5.4. Effects of Cxcr2 deletion on systemic WBC at 20 weeks from the start of carcinogen treatment. Absolute number of monocytes, eosinophils and basophils in blood (cells/ml) (A, B, E, F, I, J) and relative number of monocytes, eosinophils and basophils (C, D, G, H, K, L). * $p < 0.05$ was considered significant (Mann-Whitney test).

5.2.5 Cxcr2 deletion resulted in impairment of neutrophil recruitment to the bladder tissue at 2 weeks of carcinogen treatment

We have evaluated the infiltration of neutrophil in the urothelium, stroma and muscle of the bladder samples treated with OH-BBN for 2 weeks. The neutrophils were recognized based on their granular morphology and pinkish cytoplasm following H&E staining, as well as by IHC with three different markers that are known to be expressed by neutrophils, 1A8, NIMP and S100A9 (Fig 5.5).

We found a significantly reduced level of neutrophil infiltration in the bladder urothelium ($p < 0.0001$), stroma ($p < 0.0001$), and muscle ($p = 0.0031$) of Cxcr2 flox compared to wt (Figure 5.6A).

A significant reduction of cells expressing 1A8 was also observed in the stroma ($p = 0.0043$) and the muscle ($p = 0.0455$) (Figure 5.6B). The quantification of 1A8-positive cells in the urothelium was not performed due to high background staining.

Similarly, Cxcr2 flox showed a significant reduction in the NIMP⁺ cells in the stroma ($p = 0.0159$) and the muscle ($p = 0.0159$) compared to wt (Figure 5.6C). High background staining was observed in the urothelium, which led to the exclusion of the quantification of NIMP expression in this area.

The number of cells expressing S100A9 was also significantly reduced in the urothelium ($p = 0.0152$), stroma ($p = 0.0022$) and muscle ($p = 0.0455$) in comparison to wt (Figure 5.6D).

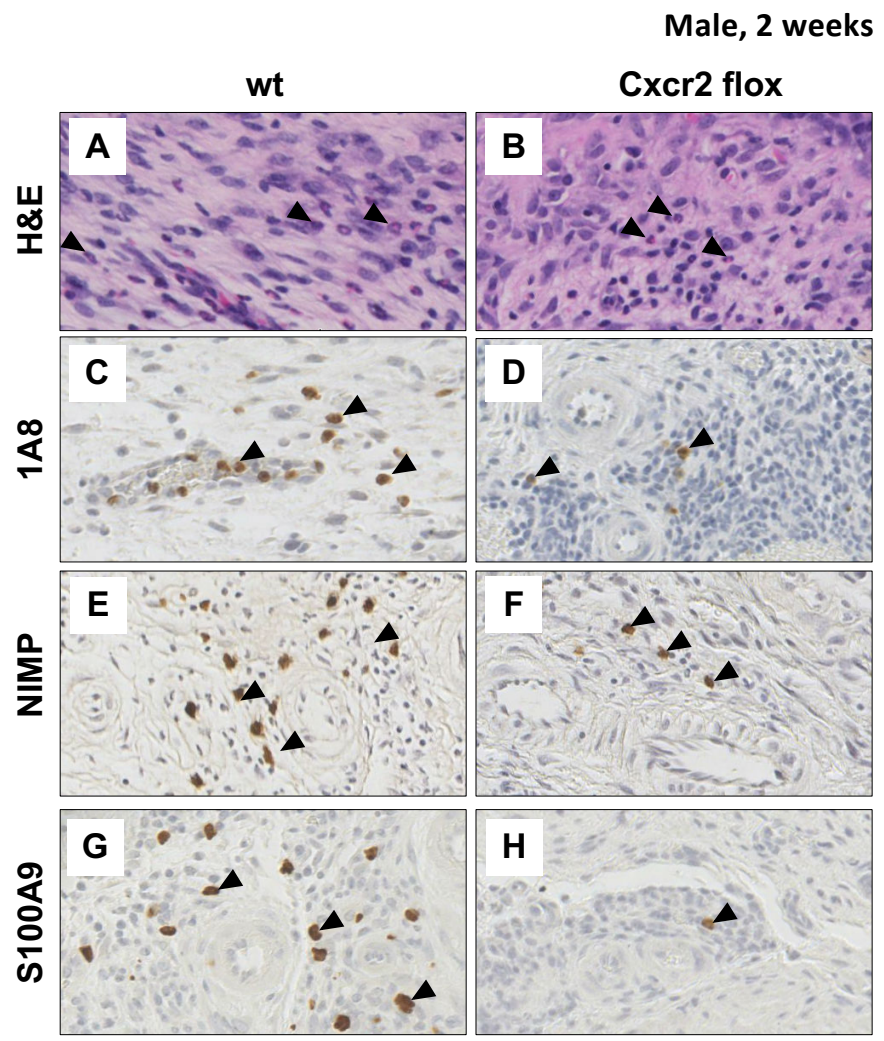


Figure 5.5. Neutrophil infiltration at 2 weeks. Representative images of H&E (A, B) and IHC staining for 1A8 (C, D), NIMP (E, F) and S100A9 (G, H) in wt and Cxcr2 flox samples. Black arrowheads indicate neutrophils in A&B, and positive cells in C-H (brown stained). Scale bar represents 50 μ m.

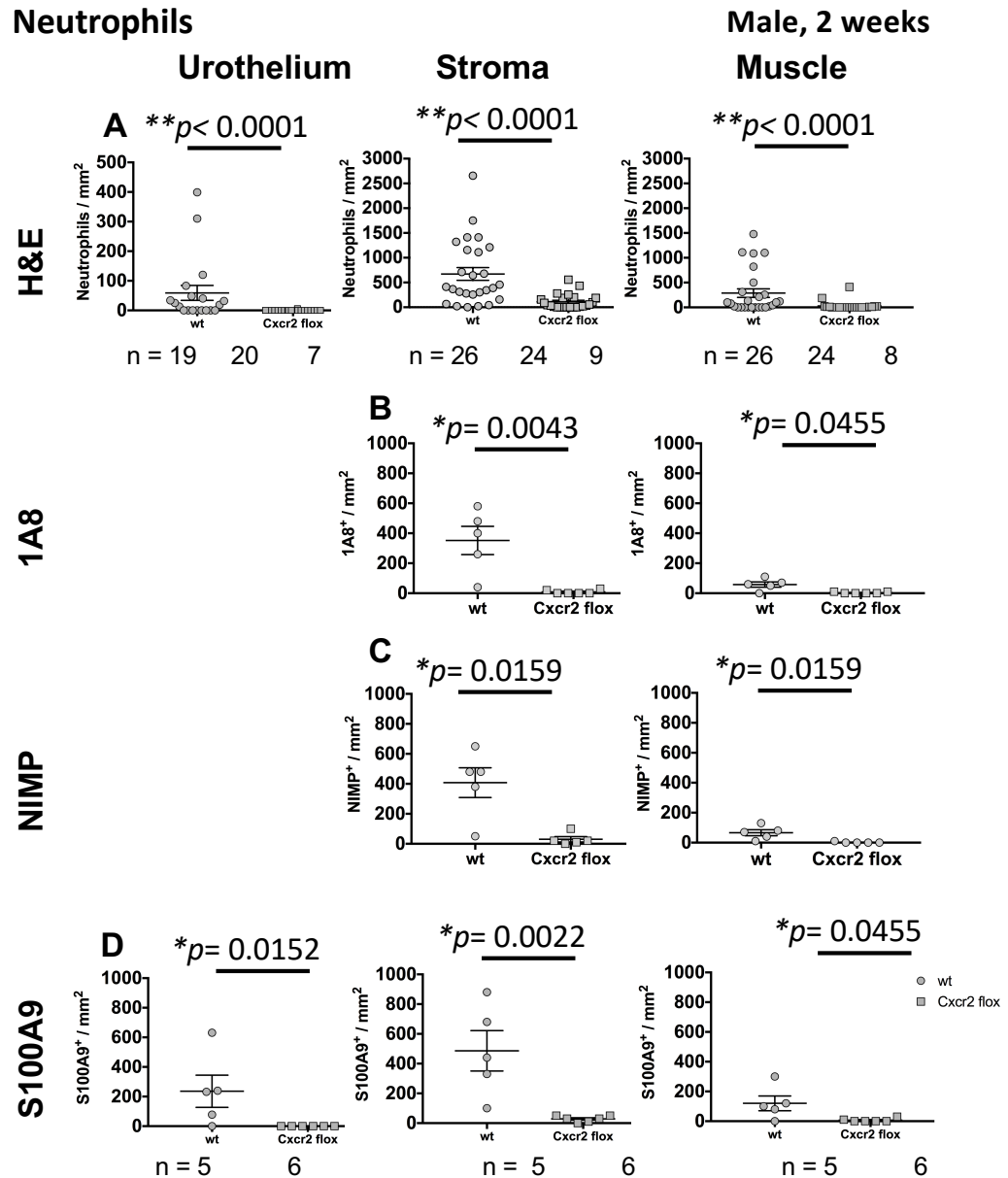


Figure 5.6. Neutrophil infiltration in the bladder at 2 weeks. Neutrophils were quantified in the urothelium, stroma and muscle following H&E staining (A-C) and IHC using 1A8 (D, E), NIMP (F, G), S100A9 (H-K). Bladder samples were harvested at 2 weeks after OH-BBN treatment. Significance asterisks: * = $p < 0.05$, ** = $p < 0.01$, Mann-Whitney test.

5.2.6 Macrophage infiltration was decreased in Cxcr2 flox at 2 weeks

LysM-Cre used in this study, to allow deletion of Cxcr2 in the myeloid cells, also target macrophages (Clausen *et al.*, 1999). Therefore, we have next quantified the macrophage infiltration in the bladder at 2 weeks of OH-BBN treatment. IHC was performed with F4/80 monoclonal antibody that is known to recognize macrophages (van der Beg and Kraal, 2005) (Figure 5.7 A, B).

A significant decrease in the number of macrophages was observed in the urothelium ($p=0.0043$) and stroma ($p=0.0043$) of Cxcr2 flox compared to wt (Figure 5.7C, D). The number of macrophages was comparable in the muscle of Cxcr2 flox and wt.

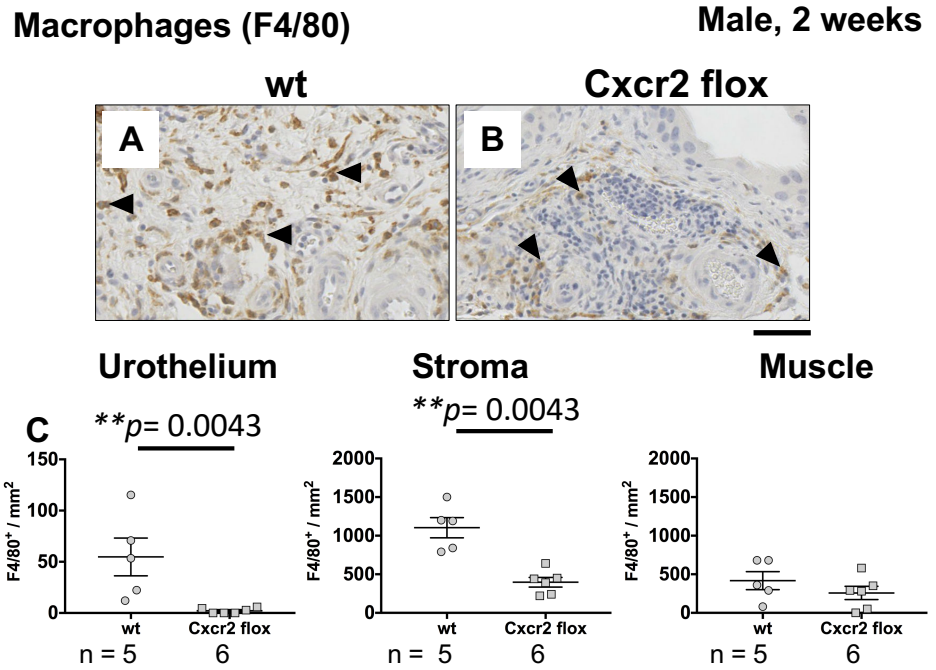


Figure 5.7. Macrophage infiltration at 2 weeks. Representative images of F4/80 IHC staining in wt (A) and Cxcr2 flox (B). Black arrowheads indicate positive cells (brown stained). Quantification of F4/80⁺ cells (cells/mm) in the urothelium (C), stroma (D) and muscle (E) in the bladder. Scale bar represents 50 μ m in A & B.

5.2.7 T cell infiltration in the bladder at 2 weeks of OH-BBN treatment

We hypothesized that the reduced levels of neutrophil and macrophage infiltration observed in *Cxcr2* flox might influence T cell infiltration. Four markers for T cell populations were used; CD3 to detect the total T cell population, CD4 for T helper cells, CD8 for cytotoxic T-cells and FoxP3 for T regulatory cells (Figure 5.8A-H). We have also further evaluated the expression of Granzyme B, an important mediator for the cytotoxic effect of CD8⁺ T cells (Shresta et al., 1998) (Figure 5.8I, J).

The infiltration of CD3⁺ T cells was comparable between *Cxcr2* flox and wt in the urothelium and the muscle but significantly reduced in the stroma ($p= 0.0041$) (Figure 5.9A).

Cxcr2 flox showed significant reduction in the infiltration of CD4⁺ T cells in the urothelium ($p= 0.0087$) and in the stroma ($p= 0.0173$) (Figure 5.9B). However, the number of CD4⁺ T cells was comparable in the muscle in *Cxcr2* flox and wt.

The infiltration of CD8⁺ T-cells between *Cxcr2* flox and wt was not statistically different (Figure 5.9C).

Cxcr2 flox showed a significant decrease of Foxp3⁺ T-cells in the urothelium ($p= 0.0025$), stroma ($p= 0.0025$), and muscle ($p= 0.0025$) in comparison to wt (Figure 5.9D).

The level of Granzyme B expression was significantly reduced in *Cxcr2* flox compared to wt in the urothelium ($p= 0.0476$), stroma ($p= 0.0195$) and muscle ($p= 0.0087$) (Figure 5.9M-O).

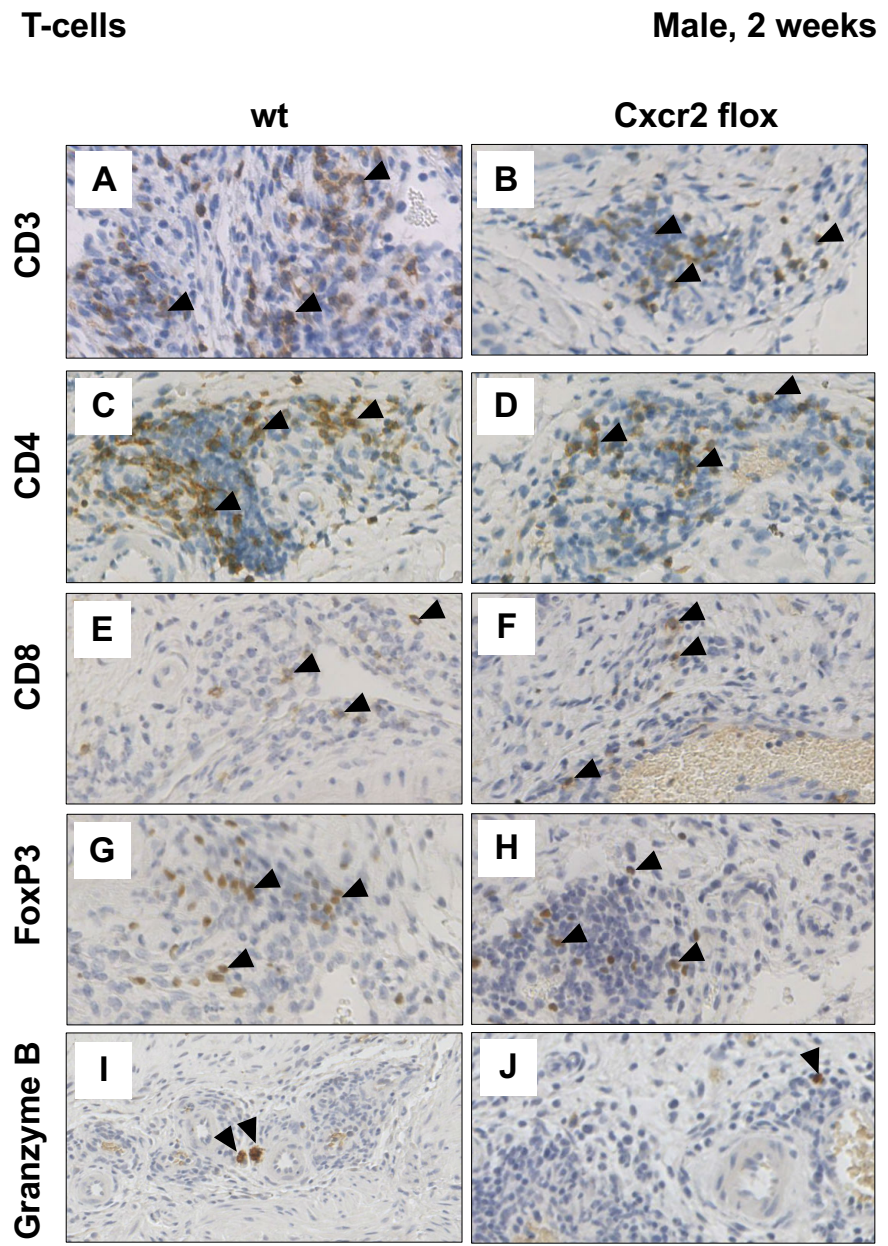


Figure 5.8. T cell infiltration at 2 weeks. Representative images of IHC staining for CD3 (A, B), CD4 (C, D), CD8 (E, F), FoxP3 and Granzyme B (I, J) in wt and Cxcr2 flox samples. Black arrowheads indicate positive cells (brown stained). Scale bar represents 50 μ m.

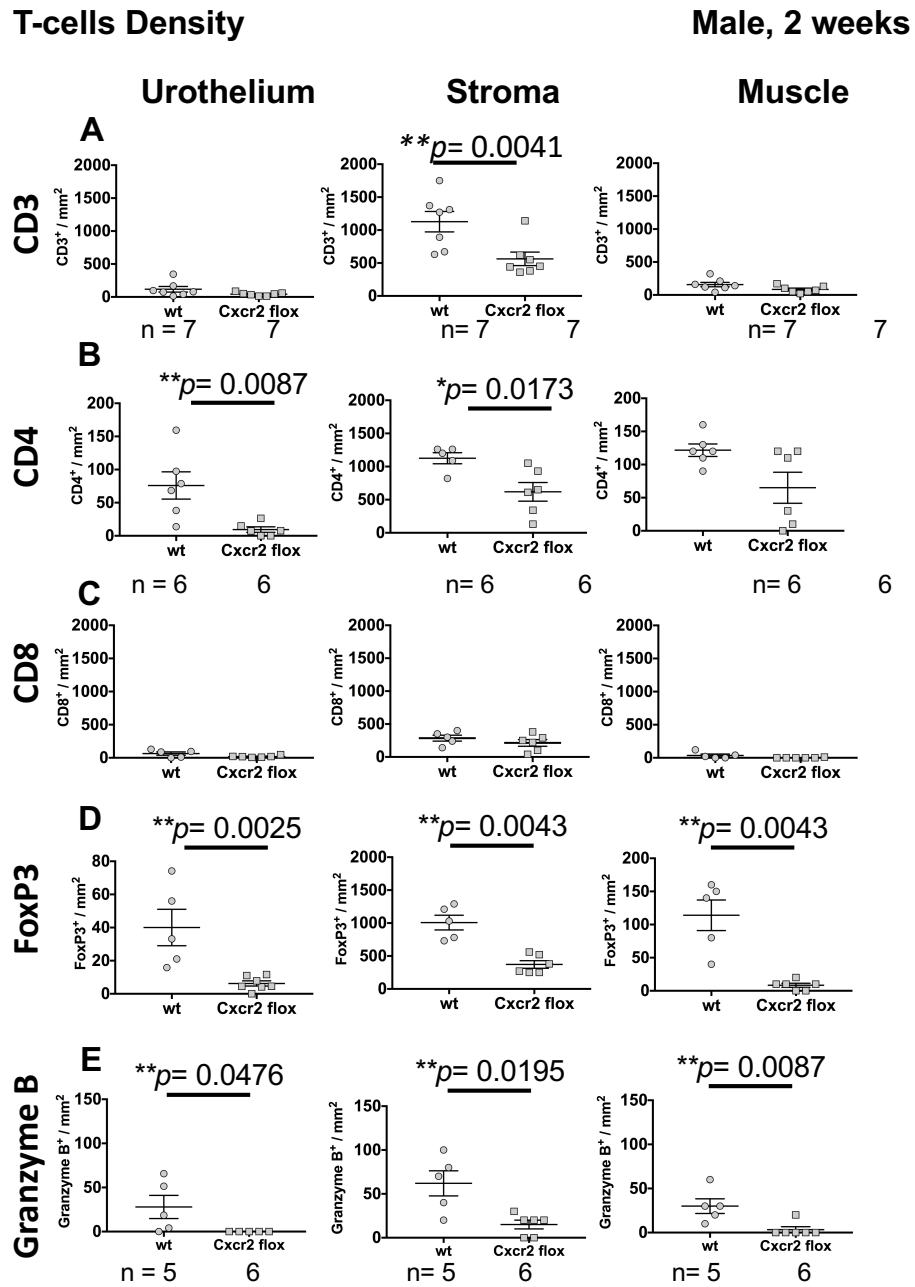


Figure 5.9. T-cell infiltration at 2 weeks of OH-BBN treatment. Quantification of CD3⁺ (A-C), CD4⁺ (D-F), CD8⁺ (G-I), FoxP3⁺ (J-L) T-cells and Granzyme B expression (M-O) in the urothelium, stroma and muscle in the bladder at 2 weeks of OH-BBN treatment. Significance asterisks: * = $p < 0.05$, ** = $p < 0.01$, Mann-Whitney test.

5.2.8 Neutrophil recruitment at 12 weeks from the start of carcinogen treatment

We next investigated the neutrophil infiltration after the carcinogen treatment.

Bladder samples were harvested at 12 weeks, in which OH-BBN was ceased for 2 weeks after the 10 weeks of application.

At this time point, the level of neutrophil infiltration in the urothelium, stroma and muscle were not significantly different between *Cxcr2* flox and wt (Figure 5.10).

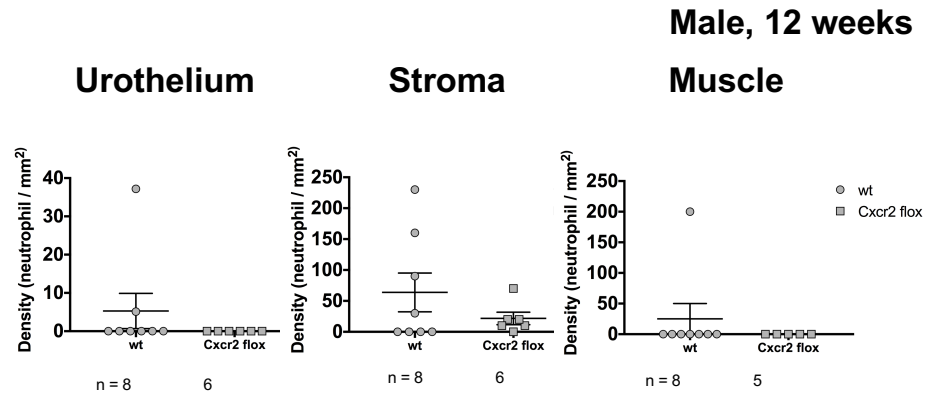


Figure 5.10. Neutrophil infiltration at 12 weeks from the start of carcinogen treatment. Presence of neutrophils in urothelium (A), stroma (B) and muscle (C) was quantified in H&E-stained tissue. No significant difference was observed between wt and Cxcr2 flox (Mann-Whitney test).

5.2.9 Changes in neutrophil infiltration at 16 weeks from the start of OH-BBN treatment

We have evaluated the tissue neutrophil infiltrations at 16 weeks (10 weeks with OH-BBN + 6 weeks with normal drinking water).

At 16 weeks, all wt samples (n = 5) and some Cxcr2 flox samples (n =3/5) were non-infiltrated with neutrophils (5.11A). However, two out of five Cxcr2 flox samples showed a high neutrophil density in the stroma (1160/mm² and 370/mm², Figure 5.11A). These two Cxcr2 flox samples were the samples observed with the presence of tumour in their bladder.

Consistent with the H&E results, all five wt and three out of five Cxcr2 flox samples had none or very few cells that were positive for the four markers tested (Figure 5.11B-E). Two Cxcr2 flox samples with bladder tumour were found to have a higher number of 1A8⁺, NIMP⁺, MPO⁺ and S100A9⁺ in the stroma and muscle compared to the wt.

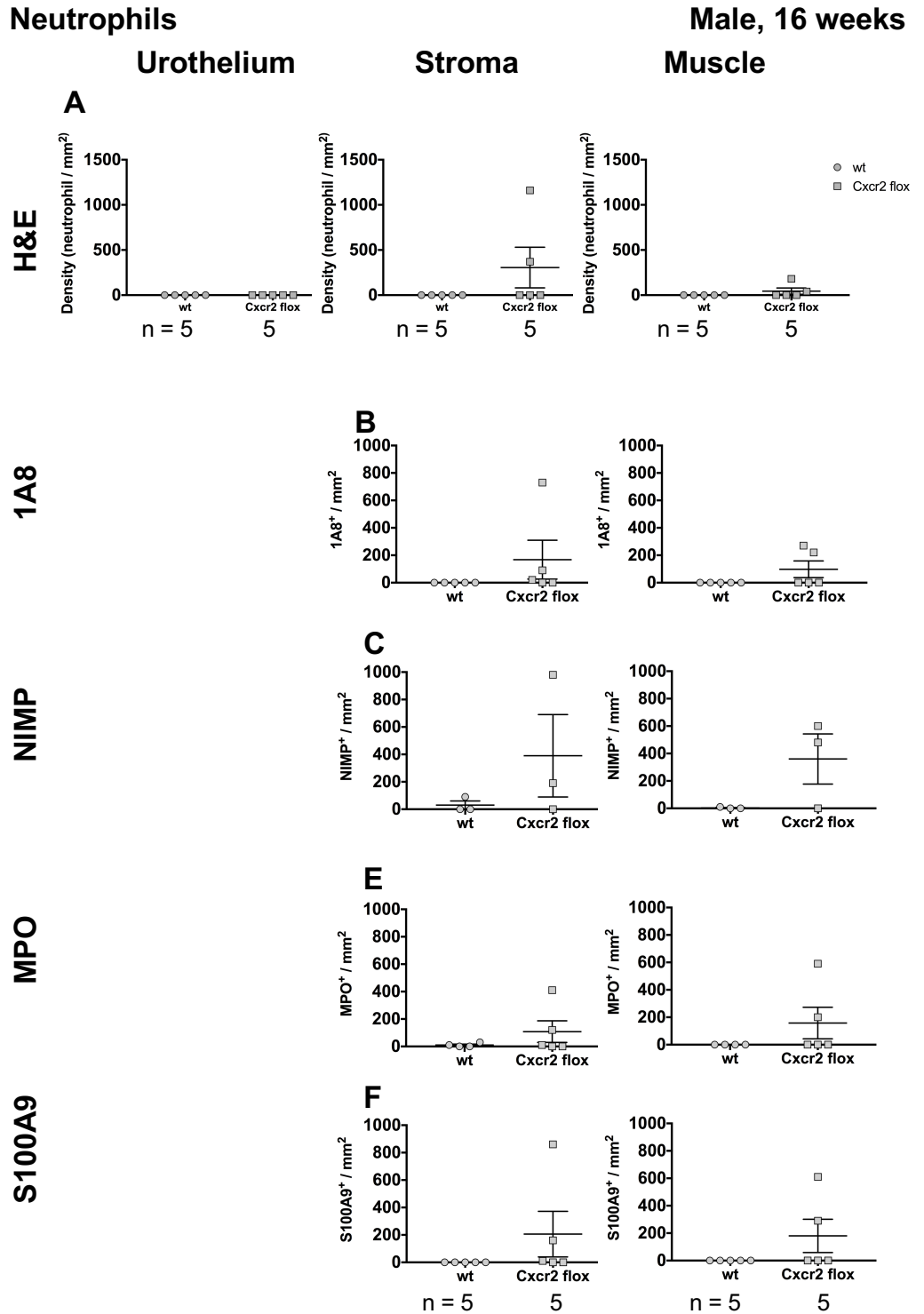


Figure 5.11. Neutrophil infiltration at 16 weeks from the start of carcinogen treatment. Quantification of neutrophils based on H&E staining (A), 1A8 (B), NIMP (C), MPO (E), and S100A9 (F) in the urothelium, stroma and muscle. No significant difference was observed between wt and Cxcr2 flox (Mann-Whitney test).

5.2.10 Cxcr2 flox bladders were highly infiltrated with macrophages at 16 weeks

We next quantified the macrophages in 16 weeks sample.

Cxcr2 flox showed a significant increase in the macrophage infiltrations in the stroma ($p=0.0286$) and muscle ($p=0.0286$) compared to wt (Figure 5.12).

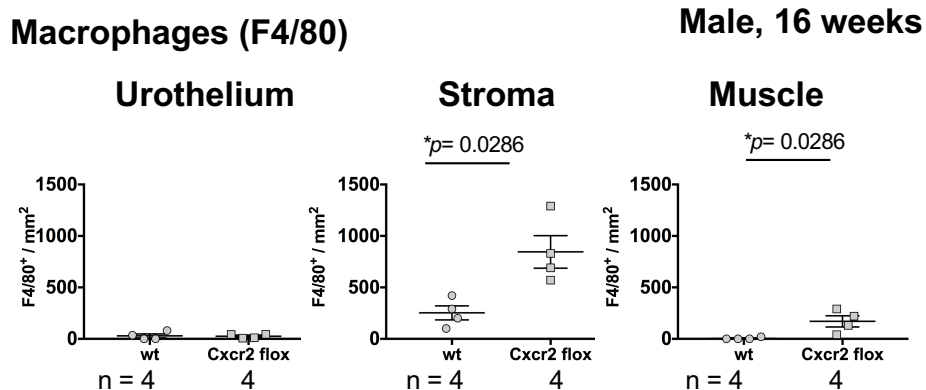


Figure 5.12. Macrophage infiltration at 16 weeks from the start of carcinogen treatment. Quantification of F4/80⁺ cells (cells/mm) in the urothelium (C), stroma (D) and muscle (E). Statistical difference was evaluated using Mann-Whitney test with **p* < 0.05 was considered significant.

5.2.11 T-cell infiltration was not affected in Cxcr2 flox at 16 weeks

We further quantified the immune cell infiltration at 16 weeks.

The levels of CD3⁺, CD4⁺ and CD8⁺ T-cell infiltration in the stroma and muscle were comparable between Cxcr2 flox and wt samples (Figure 5.13A-C).

Similarly, the expression of Granzyme B in the stroma and muscle of Cxcr2 flox was also at similar levels as wt samples (Figure 5.13D).

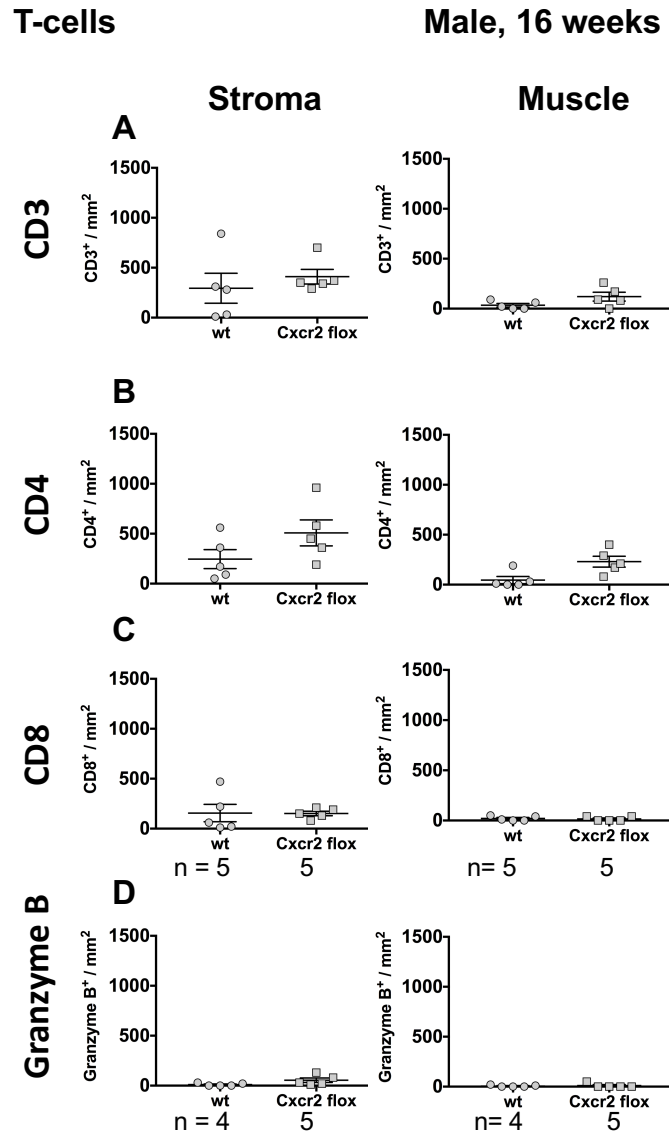


Figure 5.13. T-cell infiltration in samples taken at 16 weeks from the start of carcinogen treatment. Quantification of CD3⁺ (A-B), CD4⁺ (C, D), CD8⁺ (E, F), T-cells and Granzyme B expression (G-H) in the stroma and muscle. No significant difference was observed, Mann-Whitney test.

5.2.12 Neutrophil infiltration was increased in the tumour of Cxcr2 flox

Based on the scoring of neutrophils based on morphological examination on H&E, the neutrophil infiltration was not statistically different between wt, Cxcr2 flox and Cxcr2 ko in the tumour (5.13A). However, when we examined the big tumour samples, it was observed that 33.3% of Cxcr2 flox (n= 3/9) and Cxcr2 ko (n= 1/3) showed a higher number of neutrophil infiltrations compared to the wt (Figure 5.14A).

When samples with neutrophil infiltrated were analysed, Cxcr2 flox tumour showed an increase in neutrophil infiltrations compared to wt tumour ($p= 0.029$) (Figure 5.14B).

We also evaluated the levels of neutrophil infiltration in the stroma adjacent to the tumour area. No significant differences were observed across wt, Cxcr2 flox and Cxcr2 ko samples, regardless of tumour size (Figure 5.14C). Similarly, the neutrophil infiltration was comparable between wt, Cxcr2 flox and Cxcr2 ko when neutrophil infiltrated stroma samples were analysed individually (Figure 5.14D).

Neutrophils **Male, 20 weeks**

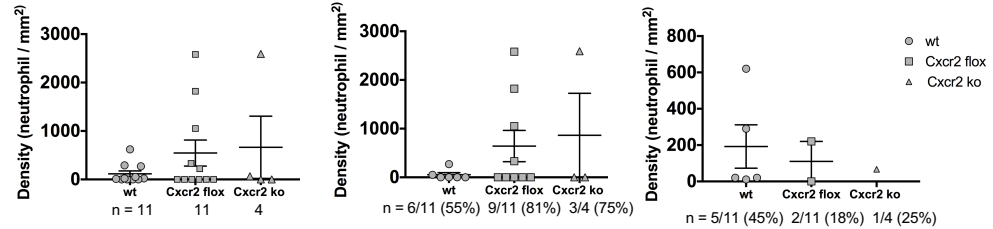
All

Big tumour

Small tumour

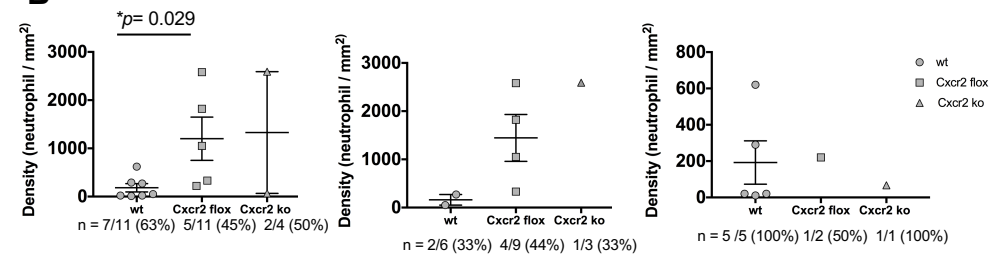
Tumour

A



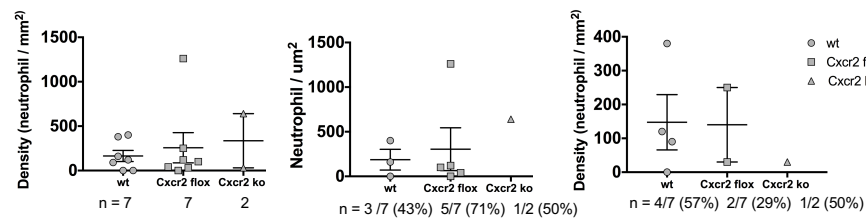
Neutrophil-infiltrated tumour

B



Stroma

C



Neutrophil-infiltrated stroma

D

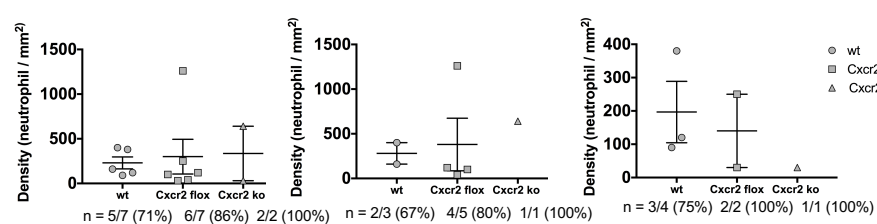


Figure 5.14. Presence of neutrophils in tumour at 20 weeks from the start of carcinogen treatment. Neutrophil infiltration was quantified in tumour area following H&E staining (A-F). Samples were taken at 20 weeks from the start of OH-BBN induction. Mann-Whitney test was used to evaluate the statistical significance. * $p < 0.05$ was considered significant.

5.2.13 Discrepancy in neutrophil levels were observed when IHC markers were used

We have also examined the levels of neutrophils using markers, including 1A8, NIMP, MPO and S100A9.

In contrast to our observations using morphological examination by H&E, 1A8⁺ cells were significantly reduced in the tumour area of Cxcr2 flox compared to that of wt ($p = 0.0385$, Figure 5.15A).

A mild decrease in the number of NIMP⁺, MPO⁺ and S100A9⁺ cells was observed in the tumour area of Cxcr2 flox tumour in comparison to that of wt (Figure 5.15B-D).

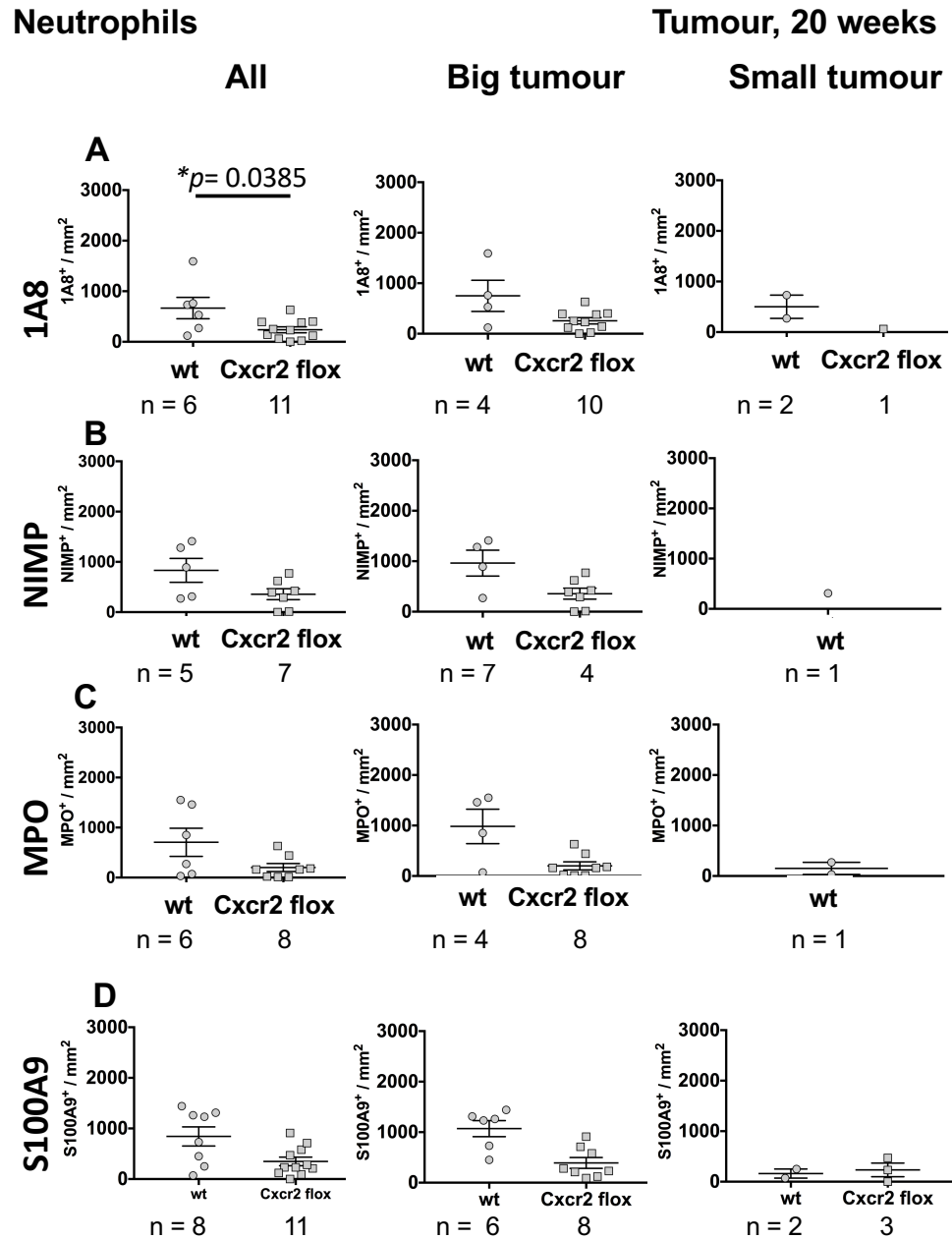


Figure 5.15. Expression of neutrophil markers in the tumour area. Quantification of 1A8⁺ (A) NIMP⁺ (B), MPO⁺ (C), and S100A9⁺ (D) cells in tumour area.

5.2.14 A low level of macrophage infiltration in the bladder tumour

We have examined the macrophage infiltration in tumour samples by IHC with F4/80 antibody.

Only a few macrophages were observed in most of the tumour samples in wt and Cxcr2 flox (Figure 5.16). The mean density (cell /mm²) was 98 ± 160 /mm² for wt tumour sample, and 65 ± 121 /mm² for Cxcr2 flox tumour sample.

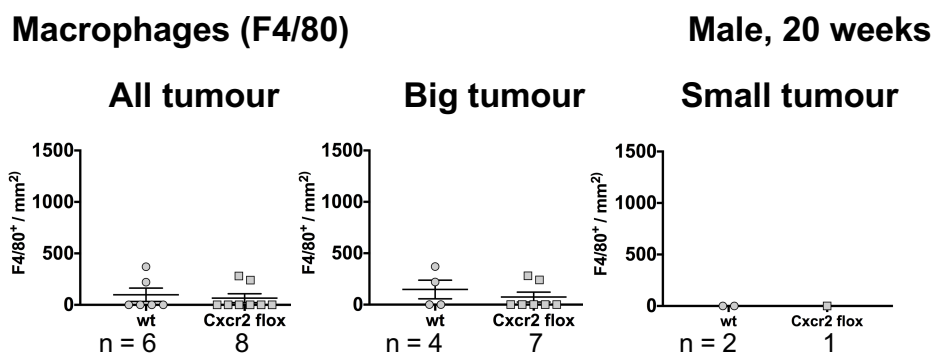


Figure 5.16. Presence of macrophages in the tumour area. Macrophages infiltration was quantified in the tumour area based on the expression of F4/80 IHC. Samples were taken at 20 weeks from the start of OH-BBN induction.

5.2.15 Cxcr2 flox tumours were more T-cell infiltrated

To determine whether the influx of neutrophils in the tumour has any influence on adaptive immune cells, we analysed the changes in the T-cell infiltration and the expression of Granzyme B.

A significant increase in CD3⁺ T-cell infiltration was observed in Cxcr2 flox compared to wt ($p= 0.0041$, Figure 5.17A). The mean density (cells/mm²) of CD3⁺ T-cell in Cxcr2 flox big tumour samples was higher compared to corresponding wt (536 ± 345 /mm², 251 ± 186 /mm², respectively).

However, the level of CD4⁺, CD8⁺ and FoxP3⁺ T-cell infiltrations in the tumour area was comparable between Cxcr2 flox and wt (Figure 5.17B-D).

The level of expression of Granzyme B in the tumour area of Cxcr2 flox samples was variable (Figure 5.17E).

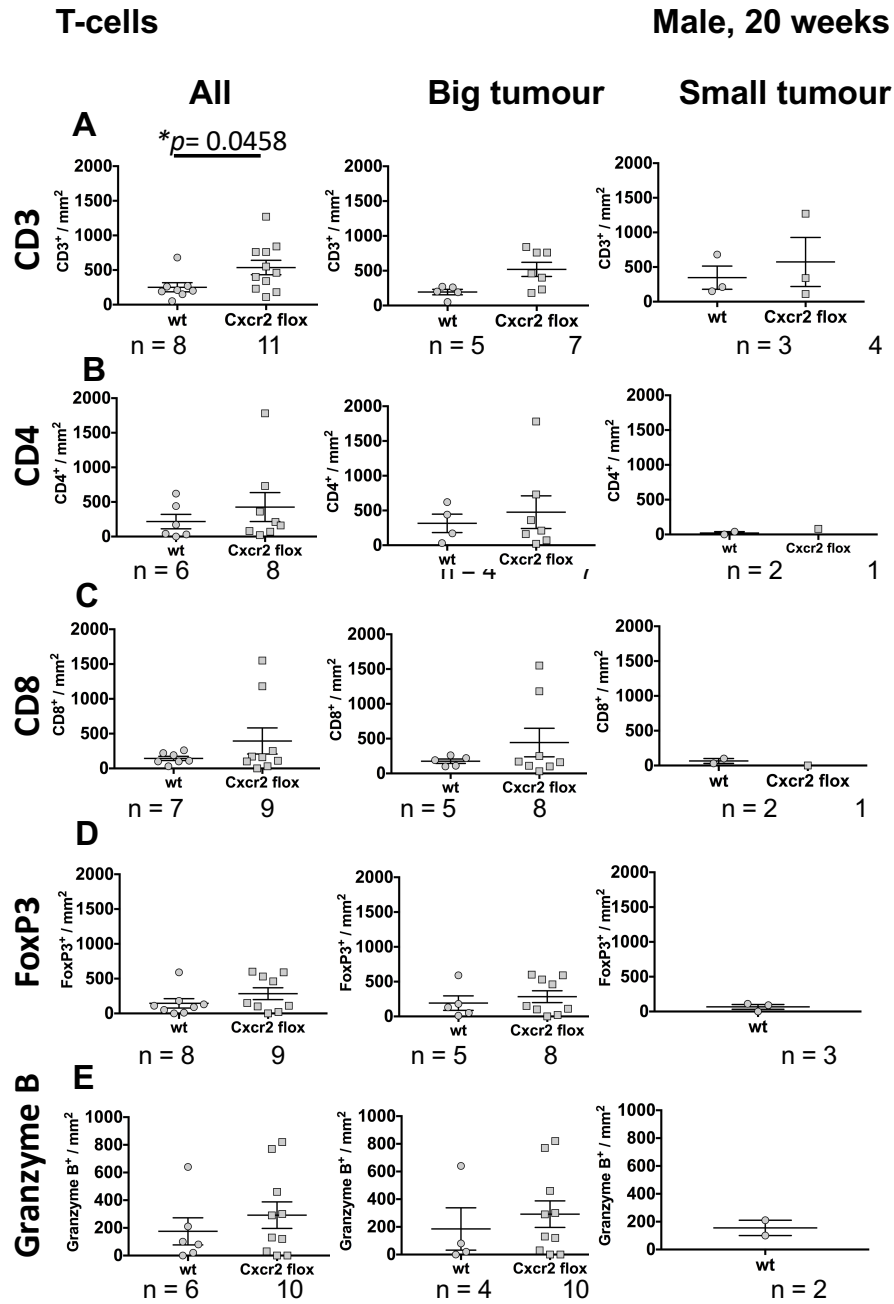


Figure 5.17. T-cell infiltration in the tumour. Presence of CD3⁺ (A), CD4⁺ (B), CD8⁺ (C), FoxP3⁺ (D) T-cells and Granzyme B expression (E) in tumour area were quantified. Statistical analysis was performed using Mann-Whitney test. $*p < 0.05$ was considered significant.

5.3 Discussion

5.3.1 Summary of results

Our results showed that:

- 1) Cxcr2 deletion affected infiltration of neutrophils, macrophages and T cells into the bladder tissue, but not in the blood circulation at 2 weeks (Figure 5.1, 5.6, 5.7 and 5.9).
- 2) By H&E, an increase of neutrophils, but not of monocytes, were observed in the tumour area of Cxcr2 flox comparing to wt (Figure 5.14 and 5.16). There was a discrepancy in the levels of neutrophils identified by morphology and by markers, observed in the tumours at 20 weeks (Figure 5.14 and 5.15). This discrepancy was not observed at 2 weeks and 16 weeks samples (Figure 5.6 and 5.11).
- 3) The level of tumour-infiltrating CD3⁺ was significantly increased in Cxcr2 flox compared to wt (Figure 5.17).
- 4) A transient increase in the level of macrophages in circulation and the bladder was observed in Cxcr2 flox comparing to wt at 16 weeks (Figure 5.2 and 5.12).

5.3.2 Acute inflammatory response was suppressed in Cxcr2 flox

Consistent with the known role of Cxcr2 as a chemotactic factor for myeloid cells, the suppression of neutrophil and macrophage recruitment was observed in the bladder in the absence of Cxcr2 at 2 weeks of carcinogen treatment.

Previous studies have shown that neutrophils are important in guiding the T cells to the inflammatory sites (Suttman et al., 2006; Lim et al., 2015). Thus, the significant decrease in T cells was likely to be caused by the reduced level of neutrophils and not by the direct effect of the lack of Cxcr2 function.

5.3.3 Cxcr2 flox tumour was infiltrated with neutrophils and CD3⁺ T-cells

Tumour could alter its microenvironment to recruit more neutrophils that are pro-tumour (Eruslanov *et al.*, 2014). These tumour-infiltrating neutrophils could influence the infiltration of other leukocytes that could contribute to tumour progression and metastasis (Coffelt et al., 2015; Eruslanov et al., 2014). Neutrophils in the early stage of lung cancer possess anti-tumour properties with a high level of pro-inflammatory factors including TNF- α and high level of cytotoxic reactive oxygen species (Mishalian et al., 2013). In contrast, neutrophils in advanced tumour downregulated these factors and induced suppressive T regulatory recruitment, hence favour tumour progression (Mishalian et al., 2013; Mishalian et al., 2014).

5.3.4 Discrepancy in the levels of neutrophils identified by markers and by morphology in tumour

In general, tumour-infiltrating neutrophils were shown to have low expression of granule proteins (primary, secondary, tertiary) and low respiratory burst (peroxidase) (Fridlender et al., 2012b; Shaul et al., 2016).

However, several tumour-infiltrating neutrophils subsets expressing different types of surface markers have been recently reported (Rosales, 2018; Silvestre-Roig et al., 2016; Yang et al., 2017). The transcriptional activation and expression levels of the surface molecules greatly influenced the functions of different phenotypes of tumour-infiltrating neutrophils (Eruslanov et al., 2014; Yang et al., 2017).

The consistency in the number of neutrophils identified morphologically and identified based on the expression of neutrophil markers in 2 weeks and 16 weeks samples supported our IHC and scoring as a methodology.

There is a possibility that the neutrophils recognised based on the morphology following H&E staining could also be eosinophils, as these cells are known to share almost identical morphology with neutrophils. However, our blood analysis showed a minimal number of eosinophils present in circulation (0.1867 ± 0.1442 /ml or 1.468 ± 1.468 % relative to the whole WBC). It is best to further confirm the presence of the eosinophil population at tissue level using IHC with eosinophil marker such as Siglec F (Finisguerra et al., 2015) in the future.

Overall, I hypothesise that the expression of common neutrophil markers was reduced in tumour-infiltrating neutrophils in the *Cxcr2* flox tumours; thus, phenotypically different from *Cxcr2* dependent (wt) neutrophils.

5.3.5. Transient increase in macrophage infiltration at 16 weeks in *Cxcr2* flox

Macrophages could lead to the trafficking of neutrophils (Mosser & Edwards, 2008; Schiwon et al., 2014). Tumour cells can alter circulating monocytes to favour their progression (Cassetta et al., 2019). The increase in this distinct population of macrophages was associated with poor prognosis in breast cancer patients (Cassetta et al., 2019).

I hypothesise that the increase of macrophages observed may be a part of the compensatory signalling in regulating the levels of neutrophils in the tumour in the absence of *Cxcr2* (discussed in Chapter 8 in more depth).

5.4 Limitation

We have tried to phenotype the neutrophil population in Cxcr2 flox tumour by flow cytometry. However, this was unsuccessful. We have encountered challenges in digesting and dissociating the bladder tissues into a single cell. The minimum number of cells needed to perform the flow cytometry analysis was never obtained.

One of the factors that could lead to the low of viability cells include the harmful enzymatic process during the digestion and dissociation steps for the flow cytometry analysis. We have used Collagenase IV (1mg/ml) and Dnase I (100 µg/ml) for 30 min incubation time to digest the cells. This might be too harsh and affect the cell membrane surface which then lead to spontaneous cell death. Unfortunately, we have limited number of tumour sample number thus further optimisation on the enzyme used and the timing for the enzyme digestion could not be performed.

5.5 Future works

A better strategy in phenotyping the tumour-infiltrating neutrophils in Cxcr2 flox could be performed using multiplex immunohistochemistry. This technique will allow the quantification of simultaneous cellular and sub-cellular level of proteins interest within the same FFPE tissue section (TsujiKawa et al., 2017).

We should address whether the increase in the macrophage populations observed at 16 weeks has led to the recruitment of neutrophils in Cxcr2 flox in the tumour at 20 weeks. Profiling the macrophages using multiplex immunohistochemistry for simultaneous identification of multiple monocytes/macrophages surface markers such as Ly6C and CCR2 will be useful in identifying the phenotypical changes.

Given that gamma delta T-cells could also express CD3 expression, it is likely that a portion of CD3+ T-cells in the tumour area of Cxcr2 flox could also be positive for gamma delta T-cells (Sjödahl et al., 2012). RNAscope (ACDBio) or flow cytometry analysis may be used to detect gamma delta T-cells, gated based on CD45+CD3+ TCR γδ+ (Daley et al., 2008; Takeuchi et al., 2011).

Chapter 6

Transcriptional changes in the absence of Cxcr2 in the bladder

6.1.1 Hypotheses

- 1) At 2 weeks of OH-BBN treatment, the loss of Cxcr2 expression in the bone marrow may alter the level of gene expression associated with inflammatory response and migration of immune cells.
- 2) In contrast to 2 weeks, at 20 weeks from the first administration of OH-BBN treatment, the tumour may alter its microenvironment by altering the signalling associated with chronic inflammation and immune suppression to advocate their growth and development.

6.1.2 Aim & Objectives

This chapter aimed to characterise the expression of genes that may have influenced the status of immune cell infiltrations in the acutely inflamed bladder (2 weeks) and bladder tumours (20 weeks), in the presence and the absence of Cxcr2.

The specific objectives were:

- 1) To evaluate the changes in the expression level of genes at 2 weeks of carcinogen treatment in wt and Cxcr2 flox.
- 2) To compare the level of gene expression in Cxcr2 flox tumour samples with and without neutrophil infiltration.
- 3) To compare the expression of genes at acute inflammation and later stages of bladder tumorigenesis.
- 4) To validate the changes in the expression of selected genes observed in RNA array using qRT-PCR
- 5) To examine whether pattern of gene expression correlated with a high infiltration of tumour-infiltrating neutrophils and T-cells observed in Cxcr2 flox tumours, indicating immunosuppression.
- 6) To determine the possible regulator(s) that could be associated with the increase of tumour-infiltrating neutrophils in the absence of Cxcr2.

6.2 Results

In this chapter, we have investigated the expression of genes previously known to be associated with cancer inflammation and immunity crosstalk by RNA array. The array contained 84 genes (Methods). Genes that showed ≥ 2 -fold differences ($\log_2 \geq 1$ or ≤ -1) and with standard deviation ≤ 1 between the biological replicates were considered. The expression of specific genes from the array was further evaluated using TaqMan Assay-based qRT-PCR.

6.2.1 Sample selection for RNA analysis at 2 weeks of carcinogen treatment

In order to characterise the gene expression at the acute inflammation stage, 2 bladder samples each from wt and Cxcr2 flox taken at 2 weeks from the start of carcinogen treatment were selected. The criteria for the selection were the inflammation status indicated by the thickness of the stroma, level of angiogenesis in the stroma and level of neutrophil infiltration in the urothelium, the stroma and the muscle (Table 6.1).

The expression for each of the 84 genes was compared to the housekeeping gene (Hsp90). The formula used was:

$$\text{Relative expression} = 2^{(-\Delta \text{ Ct value})}$$

*Where $\Delta \text{ Ct value} = \text{Ct value of the gene} - \text{ct value of housekeeping gene (Hsp90)}$.

The mean of relative expression for each gene in Cxcr2 flox and wt samples were compared.

Table 6.1. Sample selection for RNA array analysis at 2 weeks of OH-BBN treatment. Two biological replicates, each from wt and Cxcr2 flox, were used to investigate the expression levels of genes related to inflammation and immunity using the RNA array (Qiagen, Germany).

Cohort	Sample ID	Stroma thickness	Angiogenesis in the inner stroma	Angiogenesis in the outer stroma	Neutrophil infiltration in the urothelium	Neutrophil infiltration in the stroma	Neutrophil infiltration in the muscle
Wt	BBN 11-13	Very thickened	Mild increased	Notable increased	Non-infiltrated	Highly infiltrated	Non-infiltrated
Wt	BBN 11-17	Very thickened	Mild increased	Notable increased	Non-infiltrated	Highly infiltrated	Less infiltrated (22/mm ²)
Cxcr2 flox	ILYCX 39	Thickened	Mild increased	Notable increased	Non-infiltrated	Less infiltrated	Less infiltrated (22/mm ²)
Cxcr2 flox	ILYCX 41	Thickened	Notable increased	Notable increased	Non-infiltrated	Less infiltrated	Non-infiltrated

6.2.2 Expression of immune and inflammatory genes at 2 weeks of OH-BBN treatment

We first analysed the expression of genes categorised as "the immune & inflammatory responses" according to the RNA array. The genes were further classified into; 1) immunostimulatory factors, 2) immunosuppressive factors, 3) pro-inflammatory genes, 4) anti-inflammatory genes and 5) enzymatic modulators of inflammation & immunity.

Cxcr2 flox showed altered gene expression of Ido1, Il13 and Il5 compared to wt (Figure 6.1).

Ido1 is a catabolic enzyme that also acts as a signal transducer (Chen, 2011). In human, IDO1 was associated with immunosuppression of T cell activities (Stromness et al., 2014). Ido1 was upregulated in Cxcr2 flox by 3.03-log₂ fold, comparing to wt (Figure 6.1B).

Il13 and Il5 genes are immunosuppressive factors associated with inhibition of monokine production and an increase in inflammation (Quail et al., 2017; Zhang and An, 2007). The expression of Il13 and Il5 were upregulated by 2.02 and 1.57 log₂ fold, respectively, in Cxcr2 flox compared to wt (Figure 6.1B).

RNA array (Cxcr2 flox vs wt)
Immune & inflammatory responses

2 weeks

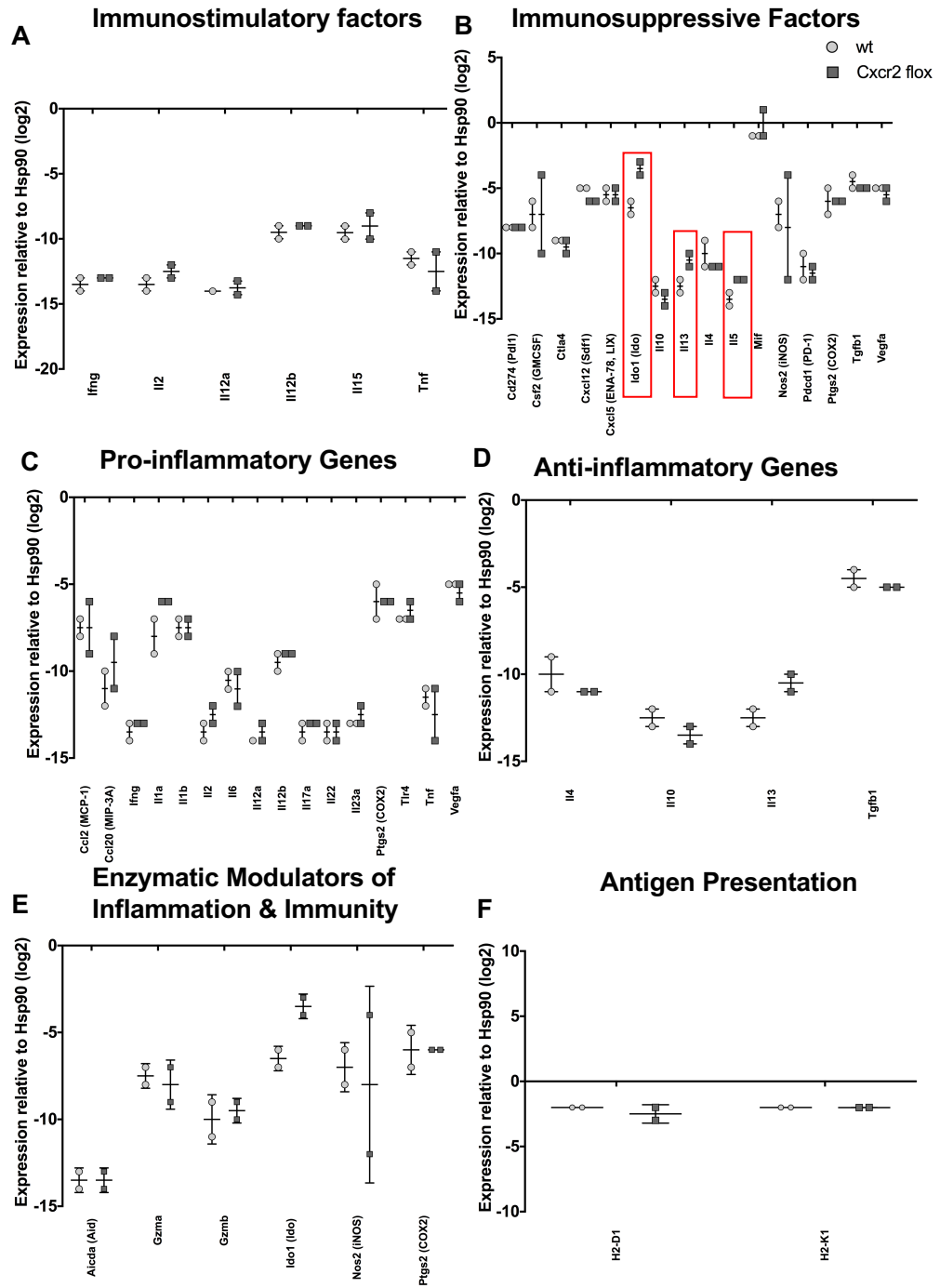


Figure 6.1. Expression of immune and inflammatory genes at 2 weeks. The relative expression of each gene was compared to the housekeeping gene (Hsp90) and presented in log2 fold. Two wt samples and two Cxcr2 flox bladder samples were used. Red box indicates the gene altered in Cxcr2 flox compared to wt.

6.2.3 Expression of chemokine signalling genes at 2 weeks

We next examined the expression of genes categorised as chemokines, interleukins, growth factors and their receptors.

Most of the genes (47 out of 55) showed a comparable level of expression in *Cxcr2* flox and wt (Figure 6.2).

Cxcr2 expression in *Cxcr2* flox was downregulated, as expected from the fact that the model lacked *Cxcr2* expression in the myeloid lineage (Figure 6.2C). *Cxcl1* is one of the ligands for *Cxcr2*. The expression of *Cxcl1* was upregulated by 2.51-fold in *Cxcr2* flox compared to wt (Figure 6.2A).

Ilr1 is an interleukin receptor. The expression of *Ilr1* was downregulated by 1.01 log₂ fold, in *Cxcr2* flox compared to wt (Figure 6.2C). *Il10* is interleukin produced by T-regulatory and T-helper cells (Denis et al., 2013). *Il10* expression was downregulated by 1.01 log₂ fold in *Cxcr2* flox in comparison to wt (Figure 6.2B).

We have also observed a downregulation by 4 log₂ fold in the expression of *Egf* in *Cxcr2* flox when compared to wt (Figure 6.2E).

RNA array (Cxcr2 flox vs wt)

2 weeks

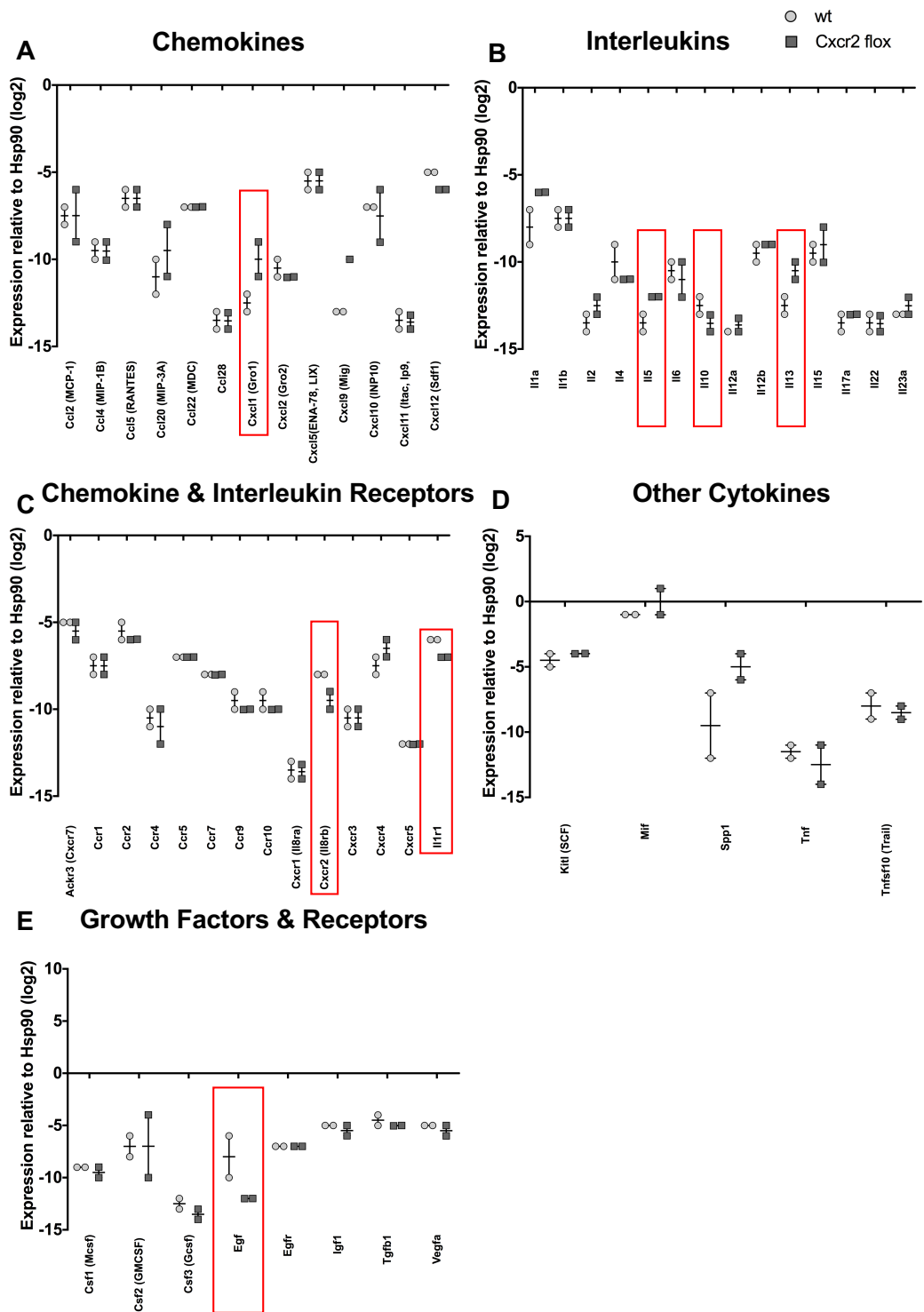


Figure 6.2. Chemokines, interleukins and growth factor profile at 2 weeks after carcinogen treatment. Relative expression to the housekeeping gene (Hsp90) for each gene as determined using RNA array. Data presented in log2 fold and for each individual mouse.

6.2.4 Expression of signal transduction genes at 2 weeks

Next, we analysed the expression of the genes related to signal transduction. These genes were further classified into; 1) interferon signalling, 2) interferon-responsive genes, 3) NFkB targets, 4) Stat targets, 5) toll-like receptor signalling and 6) transcription factors.

Tlr3 is a gene involved in interferon response and toll-like receptor signalling. The expression of Tlr3 was the only one observed to be altered in Cxcr2 flox with an upregulation by 1.51-log₂ fold compared to wt (Figure 6.3).

RNA array (Cxcr2 flox vs wt)

Signal Transduction

2 weeks

Interferon Signalling

Interferon-Responsive

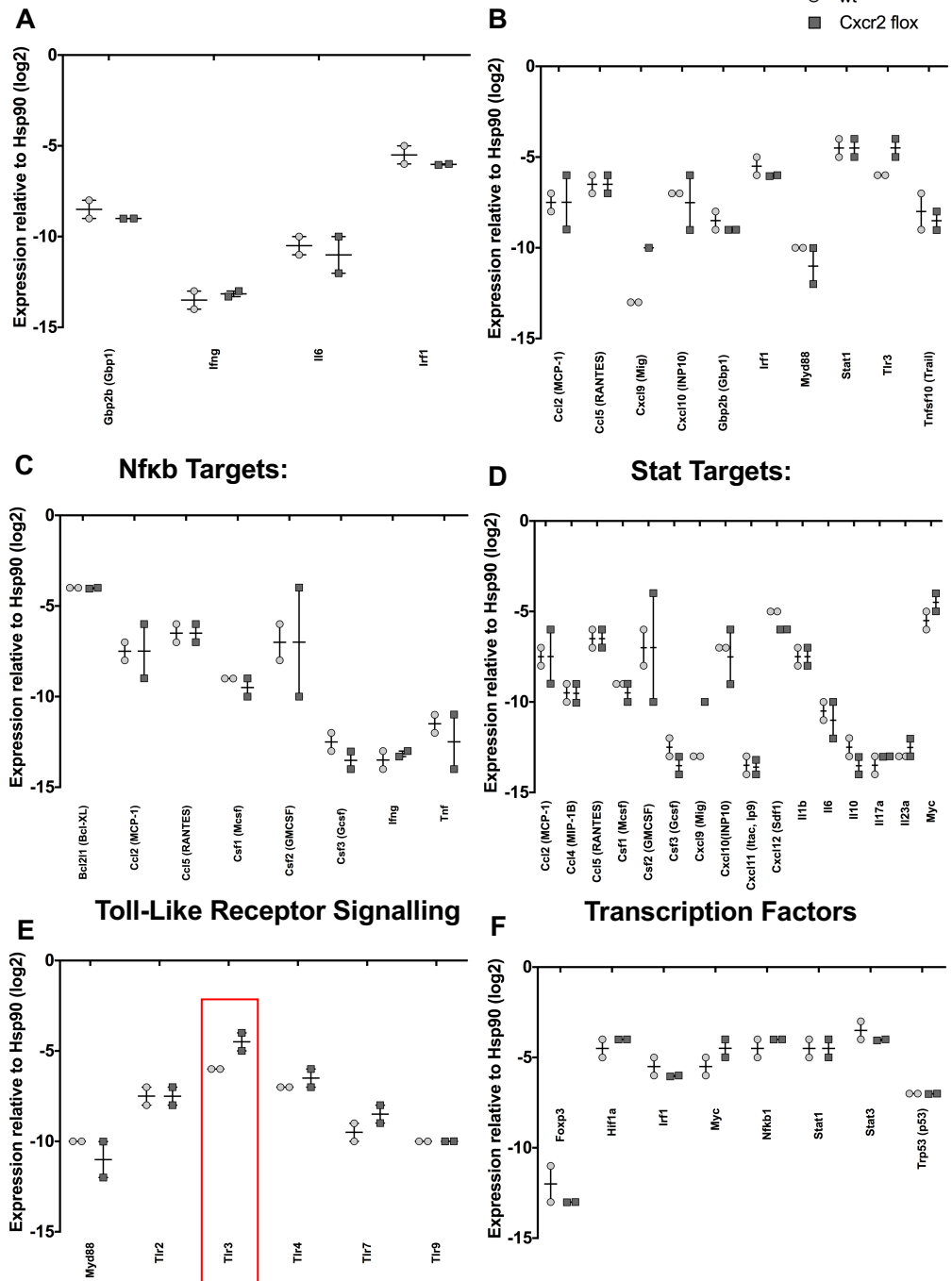


Figure 6.3. Expression of signal transduction genes at 2 weeks after OH-BBN treatment. The log2 fold in the gene expression as relative to housekeeping gene (Hsp90).

6.2.5 Expression of apoptosis-related genes at 2 weeks

We have further characterised the effects of *Cxcr2* deletion at 2 weeks of carcinogen treatment by analysing apoptosis-related genes.

The alteration in the expression of apoptotic molecules could be associated with the DNA damage induced by OH-BBN treatment. However, no notable changes were observed in the expression of pro-apoptosis and anti-apoptotic molecules in *Cxcr2* flox compared to wt (Figure 6.4).

RNA array (Cxcr2 flox vs wt)

Apoptosis

2 weeks

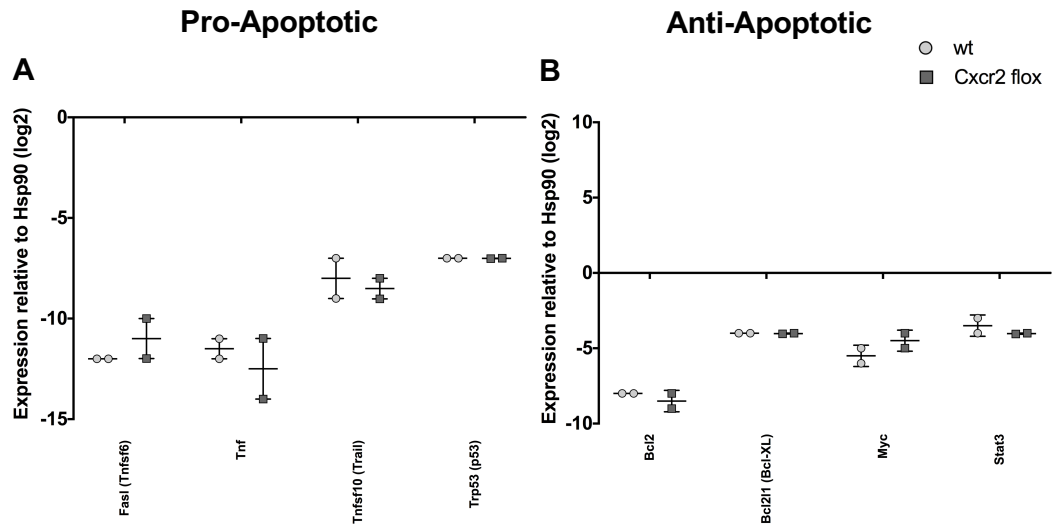


Figure 6.4. Changes in the apoptosis-related genes at 2 weeks of treatment with OH-BBN.

6.2.6 Summary of altered gene expression at 2 weeks of OH-BBN treatment

The most altered genes were listed based on the genes that showed ≥ 2 -fold differences ($\log_2 \geq 1$ or ≤ -1) and with standard deviation ≤ 1 between the biological replicates (Table 6.2).

The most upregulated gene in *Cxcr2* flox compared to wt was *Ido1* by 3.03- \log_2 fold (Table 6.2). The expression of one of *Cxcr2*'s dominant ligands, *Cxcl1*, was upregulated in *Cxcr2* flox compared to wt by 2.51- \log_2 fold. Two interleukin genes, *Il13* and *Il5*, also showed an upregulation by 2.02 and 1.57- \log_2 fold, respectively. The gene involved in neutrophil recruitment, *Tlr3*, was also upregulated by 1.51- \log_2 fold.

Egf expression was the most downregulated gene in *Cxcr2* flox bladder in comparison to wt (\log_2 fold= -4) (Table 6.2). The expression of *Cxcr2* was downregulated, as expected, in *Cxcr2* flox in comparison to wt (\log_2 fold= -1.49). One interleukin and interleukin receptor, *Il10* and *Il1r1*, respectively, showed downregulation by 1.01- \log_2 fold.

Table 6.2. Characteristics of the alterations in gene expression comparing Cxcr2 flox with wt bladders at 2 weeks of OH-BBN treatment. Fold changes was calculated based on $2^{-\Delta\Delta Ct}$ method and presented as log₂ value with the mean of endogenous control samples set to 0. ↓ indicates downregulation and ↑ upregulation. Two biological samples were used for each cohort.

Gene	Biological function	Wt	Cxcr2 flox	Fold difference (Cxcr2 flox vs wt)	Functional relevance
Ido1	Immunosuppressive factor, enzymatic modulator of inflammation & immunity	-6.53 ± 0.70	-3.50 ± 0.70	↑ 3.03	Immune-suppressive (Zou, 2005)
Cxcl1	Chemokine	-12.50 ± 0.71	-9.99 ± 1.41	↑ 2.51	Pro-angiogenic, neutrophils chemoattractant (Roth and Hebert, 2001)
Il13	Interleukin	-12.53 ± 0.69	-10.51 ± 0.70	↑ 2.02	Th2 cytokine, B cell proliferation, inhibition of monokine production (Berger, 2000; Zhang and An, 2007)
Il5	Interleukin	-13.57 ± 0.69	-12.00 ± 0.00	↑ 1.57	Th2 cytokine, eosinophil function (Berger; 2000; Zhang and An, 2007)
Tlr3	Toll-like receptor signalling	-6.00 ± 0.01	-4.49 ± 0.71	↑ 1.51	Neutrophils recruitment (Liu et al., 2016)
Egf	Growth factors & receptors	-8.01 ± 2.83	-12.00 ± 0.01	↓ 4.00	Bladder cancer cell proliferation (Izumi et al., 2012)
Cxcr2	Chemokine receptor	-7.99 ± 0.01	-9.49 ± 0.71	↓ 1.49	Neutrophil recruitment (Roth and Hebert, 2001)
Il 10	Interleukin	-12.52 ± 0.71	-13.53 ± 0.69	↓ 1.01	Anti-inflammatory (Turner <i>et al.</i> , 2014)
Il1r1	Interleukin receptor	-6.00 ± 0.00	-7.00 ± 0.01	↓ 1.01	Pro-inflammatory (Turner <i>et al.</i> , 2014)

6.2.7 Evaluation of the changes in the gene expression by qRT-PCR

We have further evaluated the expression of selected genes from the RNA array analysis using TaqMan quantitative real-time PCR analysis. Four OH-BBN-treated bladder samples, each from wt and Cxcr2 flox mice, were used. Two out of four of these samples were the RNA samples used in RNA array analysis. Non-OH-BBN treated samples (untreated) (n=3 each from wt and Cxcr2 flox) were also included to compare the basal expression of the selected genes in Cxcr2 flox and wt. We have used Gapdh as the housekeeping gene to be normalized the results from qRT-PCR. For the RNA array, there was a greater variation in the Ct value of Gapdh between the biological replicates of the same cohort. Hsp90 was used to normalize RNA array data, as it showed more consistent Ct value.

Four genes were selected for the TaqMan qRT-PCR analysis. Two of the genes selected were the most altered gene expression associated with immunosuppression (Ido1), growth factors (Egf). Two other genes, Spp1 and Nos2, were selected because of the high variation between the two biological samples of wt and Cxcr2 flox, respectively, used in the RNA array analysis.

The Egf expression detected using TaqMan qRT-PCR showed a downregulation by 3.1- \log_2 fold in Cxcr2 flox compared to wt, which was relatively similar to the fold change observed in the RNA array analysis (4- \log_2 fold) (Figure 6.5).

The expression of Spp1, Ido1 and Nos2 were at a comparable level in OH-BBN-treated Cxcr2 flox and wt bladder samples.

We have also compared the expression between untreated samples of Cxcr2 flox and wt. Generally, the expression of Egf, Spp1, Ido1 and Nos2 was comparable between the untreated Cxcr2 flox and untreated wt (Figure 6.5).

2 weeks

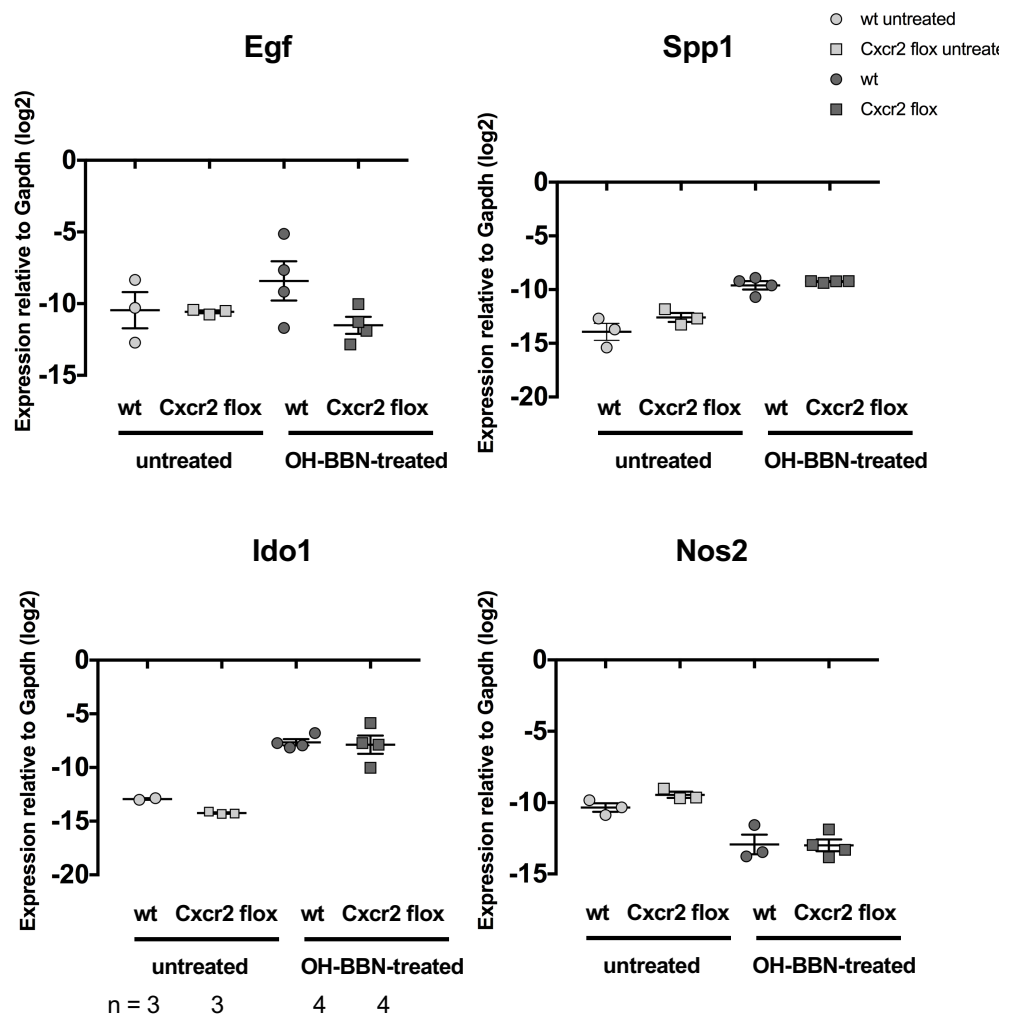


Figure 6.5. Expression of Egf, Spp1, Ido1 and Nos2 at 2 weeks. Total RNA from bladder tissue taken at 2 weeks from the start of OH-BBN was used to evaluate the expression of Egf, Spp1, Ido1 and Nos2 using TaqMan qRT-PCR. Untreated samples were the bladder samples without any OH-BBN treatment. Number of samples used is as indicated below the graph.

6.2.8 Summary of the level of gene expression at 2 weeks of OH-BBN treatment using RNA array and TaqMan qRT-PCR

In summary, only the expression of *Egf* analysed using TaqMan qRT-PCR was consistent with the RNA analysis dataset (Table 6.3). The expression of *Ido1* showed downregulation in RNA array analysis, but this was not seen in TaqMan qRT-PCR analysis. Similarly, the high variation of *Spp1* and *Nos2* expression between the two biological samples observed in RNA array analysis was not observed in TaqMan qRT-PCR analysis.

Table 6.3. Differences in the relative expressions of selected genes between RNA array and TaqMan qRT-PCR analysis. ↓ indicates downregulation and ↑ upregulation.

Gene	RNA array			TaqMan qRT-PCR		
	Wt	Cxcr2 flox	Fold difference (log ₂) (Cxcr2 flox vs wt)	Wt	Cxcr2 flox	Fold difference (log ₂) (Cxcr2 flox vs wt)
Egf	-8.01 ± 2.83	-12.00 ± 0.01	↓ 4.00	-8.41 ± 2.19	-11.51 ± 1.18	↓ 3.1
Ido1	-6.53 ± 0.70	-3.50 ± 0.70	↑ 3.03	-7.65 ± 0.59	-7.87 ± 1.70	↓ 0.22
Spp1	-9.56 ± 3.61	-5.01 ± 1.40	↑ 4.55	-9.60 ± 0.78	-9.26 ± 0.08	↑ 0.34
Nos2	-7.01 ± 1.43	-8.01 ± 5.67	↓ 1.00	-12.93 ± 1.20	-13.00 ± 0.82	↓ 0.07

6.2.9 Sample selection for RNA analysis at 20 weeks

The tumour samples taken at 20 weeks from the start of OH-BBN treatment were used to evaluate the changes in the expression of genes associated with inflammation and immunity. The characteristics of the tumour samples used to select the sample for RNA array analysis were the size of the tumour, invasiveness and the level of neutrophil infiltration in the tumour (Table 6.4). For Cxcr2 flox, one non-neutrophil infiltrated and one neutrophil infiltrated tumour were used in order to evaluate the effect of neutrophil infiltration in the tumour area. The two wt tumour samples were both non-neutrophil infiltrated.

The double delta Ct ($\Delta\Delta\text{Ct}$) analysis was used to calculate the fold change of the mean values in each experimental condition. The formula used was different from the one used in the analysis of the 2 weeks sample.

The formula used for the analysis of RNA in the tumour was as below:

$$\text{Fold change} = 2^{(-\Delta\Delta\text{Ct})}$$

*Where $\Delta\text{Ct} = \text{Ct gene test} - \text{Ct housekeeping gene (Hsp90)}$

$$\text{and } \Delta\Delta\text{Ct} = \Delta\text{Ct Cxcr2 flox} - \Delta\text{Ct wt}$$

Table 6.4. Sample selection for RNA array analysis at 20 weeks from the start of OH-BBN treatment. Two biological replicates tumour from wt and Cxcr2 flox were used for the RNA array analysis. Criteria for sample selection were based on tumour size, invasiveness and squamous transformation of urothelial and tumour cells, and level of neutrophil infiltration in the tumour area.

Cohort	Sample ID	Tumour size	Invasiveness	Neutrophil infiltration in the tumour (number of cells/tissue area)
Wt	BBN 12-26	Small tumour	Stroma invasion	Non-infiltrated
Wt	BBN 12-57	Big tumour	Stroma invasion	Non-infiltrated
Cxcr2 flox	NLA 14.1C	Small tumour	Stroma invasion	Non-infiltrated
Cxcr2 flox	NLA 14.1E	Small tumour	Muscle invasion	Highly infiltrated (520/mm ²)

6.2.10 Expression of immune & inflammatory genes at 20 weeks

Among the immunostimulatory factors, neutrophil infiltrated Cxcr2 flox tumour sample showed downregulation of *Ifng*, *Il12b* and *Tnf* compared to non-neutrophil infiltrated Cxcr2 flox tumour (Figure 6.6A).

Among the immunosuppressive factors, *Ctla4* expression was downregulated in the neutrophil infiltrated Cxcr2 flox tumour by 8.4 log₂-fold compared to non-neutrophil infiltrated Cxcr2 flox (Figure 6.6B). Other immunosuppressive factors that showed ≥ 2 -fold change in neutrophil infiltrated Cxcr2 flox tumour in comparison to non-neutrophil infiltrated Cxcr2 flox tumour were *Ido1*, *Il10*, *Il13*, *Pd-1* and *Ptgs2* (*Cox2*).

Neutrophil infiltrated Cxcr2 flox tumour sample also showed downregulation that produced ≤ -2 -fold change in 15 out of 16 pro-inflammatory cytokines compared to wt non-neutrophil infiltrated samples (Figure 6.6D).

Out of 4 anti-inflammatory cytokines assayed, two showed downregulation (*Il10* and *Il13*) while another two (*Il4* and *Tgfb1*) showed comparable expression in neutrophil infiltrated Cxcr2 flox tumour and non-neutrophil infiltrated Cxcr2 flox tumour.

Gzmb is an intracellular protease release by the cytotoxic T-cells to induce apoptosis in cancer cells (Shresta et al., 1998). The analysis on the expression of the enzymatic modulator of inflammation and immunity showed that the expression of *Gzmb* was upregulated in neutrophil infiltrated Cxcr2 flox tumour by log₂ fold= -4 compared to non-neutrophil infiltrated Cxcr2 flox tumour (Figure 6.6E).

The expression of antigen presentation- associated genes, *H2-D1* and *H2-K1*, was comparable between neutrophil infiltrated Cxcr2 flox tumour and non-neutrophil infiltrated Cxcr2 flox tumour.

**RNA array (Cxcr2 flox vs wt)
Immune & inflammatory responses**

Tumour (20 weeks)

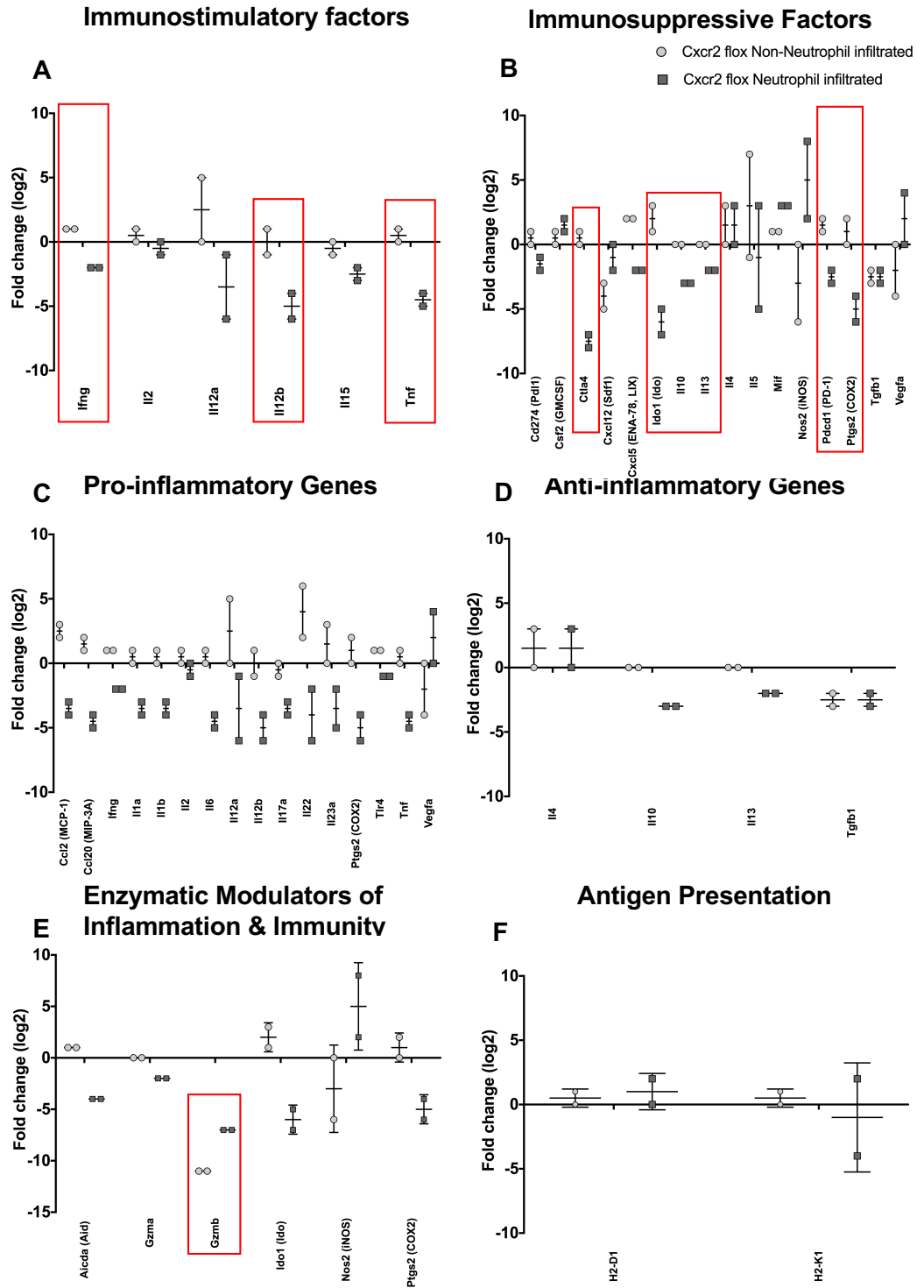


Figure 6.6. Expression of Immune and inflammatory cytokine genes in tumour bladder samples. Each circle/square represent data from each individual mouse. The fold change is presented in log₂ unit.

6.2.11 Expression of chemokine signalling genes at 20 weeks

Most of the genes were expressed at a comparable level in non-neutrophil infiltrated wt and non-neutrophil infiltrated Cxcr2 flox (Figure 6.7).

In contrast, 36 out of 54 genes analysed showed a downregulation in neutrophil infiltrated Cxcr2 flox tumour in comparison to the non-neutrophil infiltrated wt tumour (Figure 6.7).

A distinct difference was observed in the gene expression between neutrophil infiltrated, and non-neutrophil infiltrated Cxcr2 flox tumour. Several genes including Ccl2, Cxcl5, Ccr7, Cxcr4, Ccl2 and Egf showed downregulation, while an upregulation was observed in Cxcl12 and Mif (Figure 6.7).

The expression of Cxcr2 in non-neutrophil infiltrated Cxcr2 flox tumour was at a comparable level to the non-neutrophil infiltrated wt tumour (\log_2 fold=-0.02., Figure 6.7C). In contrast, the expression was downregulated to -1.99 \log_2 folds in neutrophil infiltrated Cxcr2 flox tumour compared to non-neutrophil infiltrated wt tumour.

RNA array (Cxcr2 flox vs wt)

Tumour (20 weeks)

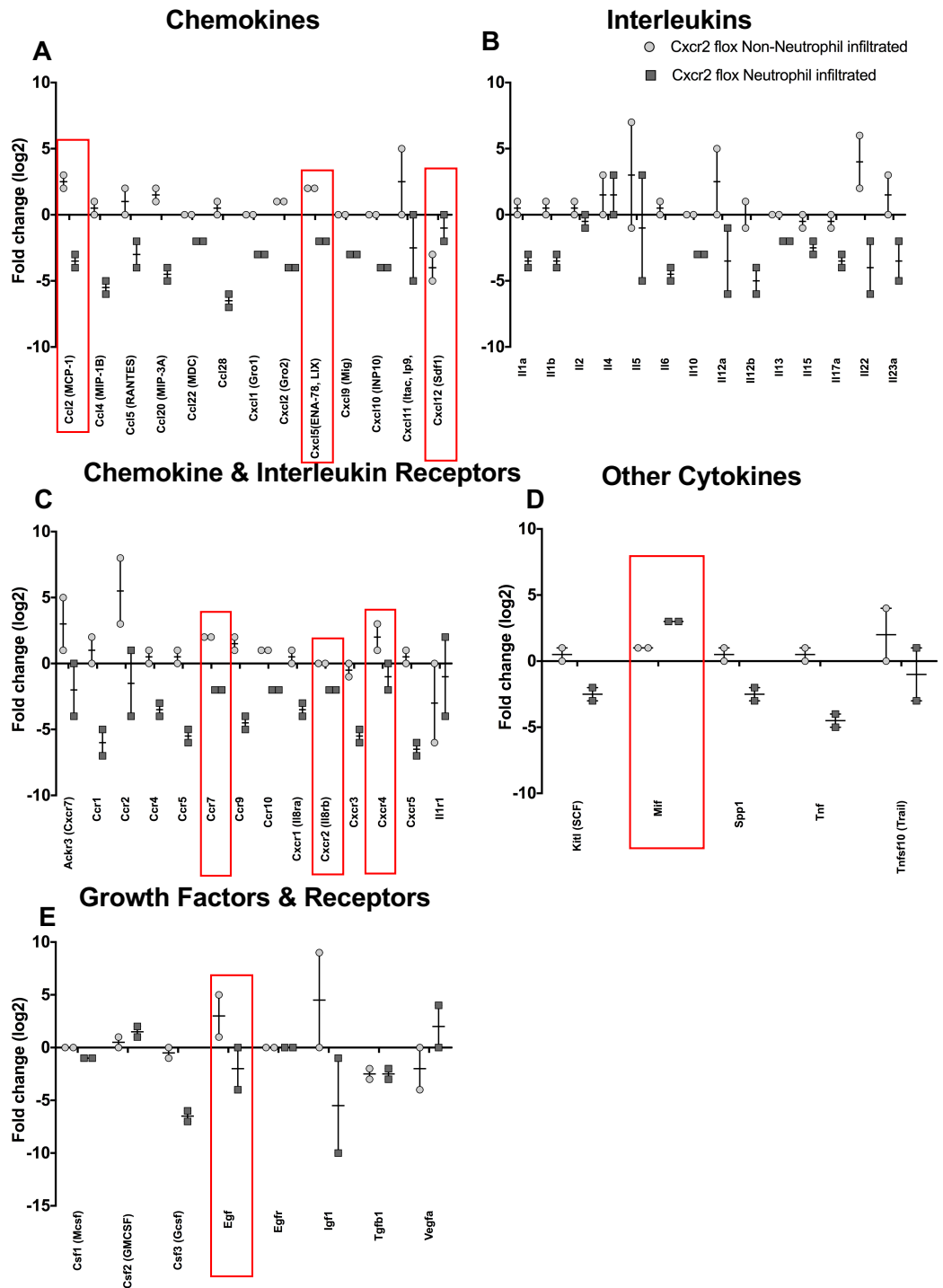


Figure 6.7. Gene expression for chemokines, interleukins, growth factors and their receptors.

6.2.12 Expression of signal transduction genes at 20 weeks

Generally, the expression of the genes involved in the signal transduction was comparable between non-infiltrated Cxcr2 flox tumour and non-infiltrated wt tumour (Figure 6.8).

In contrast, most of the genes were downregulated by at least ≤ 2 -fold change in neutrophil infiltrated Cxcr2 flox tumour compared to non-neutrophil infiltrated Cxcr2 flox and also non-neutrophil infiltrated wt tumour.

One of the most downregulated genes in neutrophil infiltrated Cxcr2 flox tumour include Myd88, which is an interferon-responsive gene and for toll-like receptor signalling (\log_2 fold = 5.05, Figure 6.8B). Downregulation was also observed in genes for NfKb and Stat targets, Csf3 and Il6 by 6.03 and 5.05- \log_2 fold, respectively (Figure 6.8C, D).

RNA array (Cxcr2 flox vs wt)

Signal Transduction

Tumour (20 weeks)

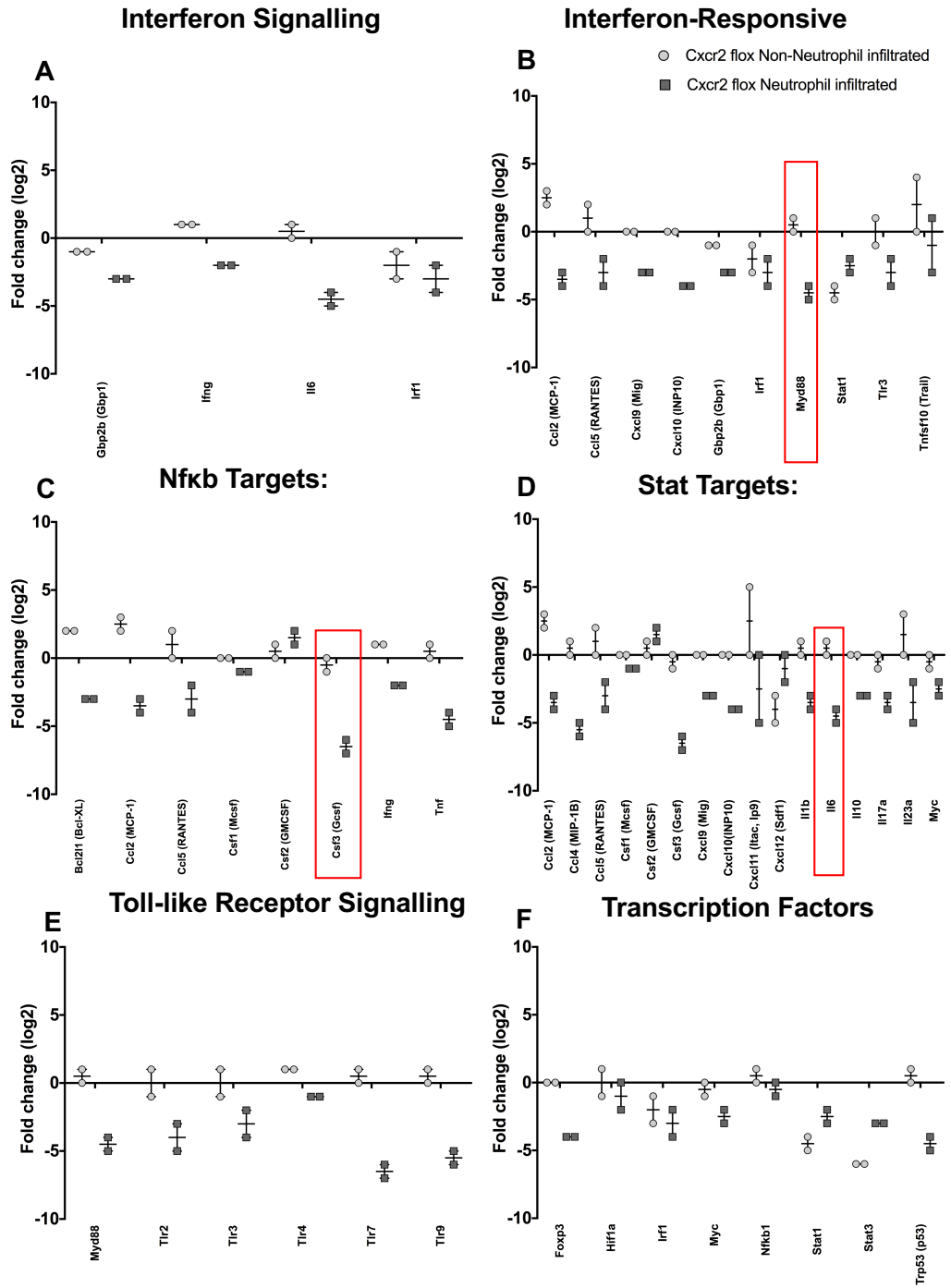


Figure 6.8. Expression of genes related to signal transduction. The genes were subcategorized as; interferon signalling (A), interferon-responsive (B), NfKb targets (C), Stat targets (D), toll-like receptor signalling (E) and transcription factors (F).

6.2.13 Expression of apoptosis genes at 20 weeks

A downregulation of pro-apoptotic genes Fasl, Tnf and Trp53 by 5.12, 5.01 and 5.02-log₂ fold, respectively, was observed in neutrophil infiltrated Cxcr2 flox tumour compared to non-neutrophil infiltrated CXCR2 flox tumour (Figure 6.9A).

Downregulation in the expression of the anti-apoptotic gene, Bcl2l1 (Bcl-XL), by 5.03-log₂ fold was also observed in neutrophil infiltrated Cxcr2 flox tumour compared to non-neutrophil infiltrated Cxcr2 flox tumour (Figure 6.9B). In contrast, the expression of the other two anti-apoptotic genes, Bcl2 and Stat3 was upregulated by 3.99-log₂ and 2.95-log₂ fold, respectively, in neutrophil infiltrated Cxcr2 flox tumour in comparison to non-neutrophil infiltrated Cxcr2 flox tumour.

RNA array (Cxcr2 flox vs wt)

Apoptosis

Tumour (20 weeks)

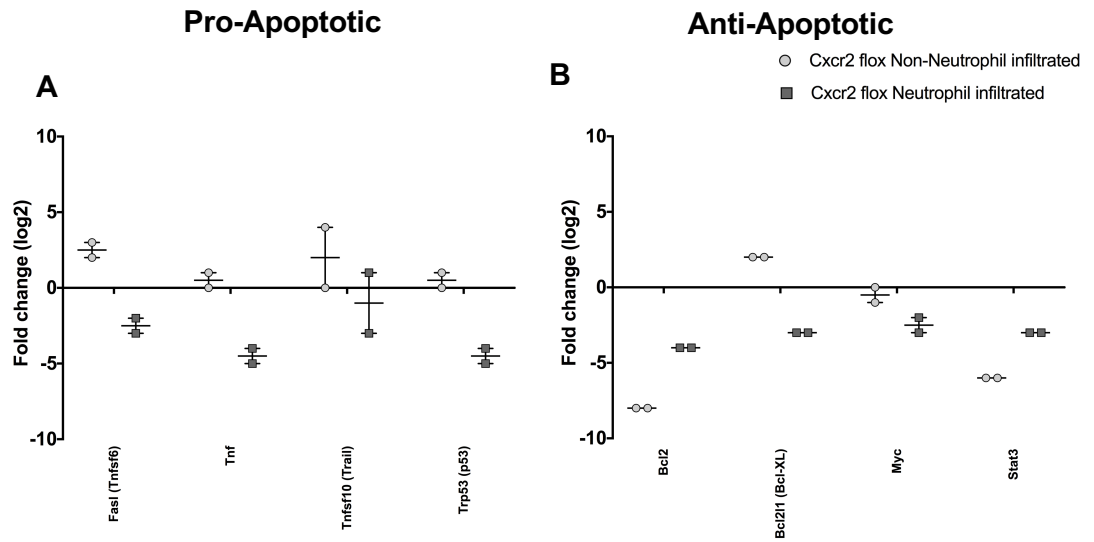


Figure 6.9. Expression of apoptosis-associated genes. The genes were subclassified as pro-apoptotic (A) and anti-apoptotic (B).

6.2.14 Summary of the most altered genes at 20 weeks

The expression of *Cxcr2* and its ligand, *Cx15*, was downregulated in neutrophil infiltrated *Cxcr2* flox tumour (log₂ fold= -2, -2.06, respectively) but not in non-neutrophil infiltrated *Cxcr2* flox tumour (Table 6.5).

Downregulation of immunosuppressive genes including *Ctla4*, *Pdcd1* (PD-1) and its ligand, *Cd274* (Pd-I1) was observed in *Cxcr2* flox neutrophil infiltrated tumour in comparison to non-neutrophil infiltrated *Cxcr2* flox and wt tumours (Table 6.5).

The expression of chemokines and chemokine receptor including *Ccl28* (log₂ fold = -7.04), *Ccl2* (log₂ fold = 6.02), *Ccl20* (log₂ fold = 6.02), and *Ccr9* (log₂ fold= 6.05) were also found to be among the most downregulated gene expression in neutrophil infiltrated *Cxcr2* flox compared to non-neutrophil infiltrated *Cxcr2* flox tumour (Table 6.5).

The neutrophil-infiltrated *Cxcr2* flox tumour also showed downregulated expression of *Tlr7* (log₂ fold=-7.06) and pro-inflammatory gene, *Il6* (log₂ fold= -5.05) (Table 6.5).

Csf3 is also known as granulocyte-colony stimulating factor (G-CSF) and is required in the induction of neutrophil recruitment via the STAT3 pathway (Nguyen-Jackson *et al.*, 2010). We observed a downregulation in the expression of *Csf3* (log₂ fold = -6.03) (Table 6.5) in neutrophil infiltrated *Cxcr2* flox tumour compared to non-neutrophil infiltrated *Cxcr2* flox tumour. However, the expression of *Stat3* was upregulated of *Stat3* (log₂ fold = 2.95) along with *Stat1* (log₂ fold= 2) (Table 6.6).

The expression of *Gzmb* was observed as the most upregulated gene expression in neutrophil infiltrated *Cxcr2* flox tumour compared to non-neutrophil infiltrated *Cxcr2* flox tumour and wt tumour (Table 6.6).

Other two genes that showed an upregulation in neutrophil infiltrated *Cxcr2* flox tumour include pro-apoptotic gene, *Bcl2* (log₂ fold = 3.99) and immunosuppressive factor, *Mif* (log₂ fold = 2.02) (Table 6.6).

Table 6.5. Tumour-infiltrating neutrophils associated with the downregulation of genes linked with cancer and inflammation in Cxcr2 flox. The expression of genes expressed in non-and neutrophil infiltrated Cxcr2 flox tumour (n=1 each) was compared to non-neutrophil infiltrated wt tumour (n=2). Fold changes was calculated based on $2^{-\Delta\Delta Ct}$ method and presented as log2 value with the mean of endogenous control samples set to 0. Their function as related to immune cells in cancer development and progression context was as listed in the last column. ↓ means downregulation and ↑ upregulation.

Gene	Biological function	Log2 fold (non-neutrophil infiltrated Cxcr2 flox vs wt)	Log2 fold (neutrophil infiltrated Cxcr2 flox vs wt)	Differences in Log2 fold	Function
Ctla4	Immunosuppressive factor	0.49 ± 0.79	-7.55 ± 0.72	↓ 8.04	Immune-suppressive (Zou, 2005).
Tlr7	Toll-like receptor signalling	0.51 ± 0.73	-6.55 ± 0.73	↓ 7.06	Induce protective immune responses (Cheadle et al., 2017).
Ccl28	Chemokine	0.50 ± 0.69	-6.54 ± 0.69	↓ 7.04	Chemoattractant for both CD4 ⁺ and CD8 ⁺ T cells (Wang et al., 2000).
Ccr9	Chemokine receptor	1.49 ± 0.69	-4.55 ± 0.69	↓ 6.05	T-cells development and tissue-specific homing (Tu et al., 2016).
Csf3	Growth factor	-0.51 ± 0.73	-6.53 ± 0.73	↓ 6.03	Production and activation of monocyte (Turner et al., 2014).
Ccl2	Chemokine	2.50 ± 0.72	-3.53 ± 0.72	↓ 6.02	Tumour-derived chemotactic factor for monocyte (Yoshimura, 2018).
Ccl20	Chemokine	1.50 ± 0.70	-4.52 ± 0.72	↓ 6.02	Promotes tumour growth and metastasis through tumour-associated macrophages (TAM) (Samaniego et al., 2018).
Il6	Interleukin	0.49 ± 0.69	-4.56 ± 0.69	↓ 5.05	Associated with the phenotypic changes of macrophages from anti to pro-tumorigenic (Martinez & Gordon, 2014).
Cxcl5	Chemokine	2.01 ± 0.01	-2.06 ± 0.01	↓ 4.07	Promotes tumour angiogenesis (Chen et al., 2019).

Pdcd1	Immunosuppressive factor	1.48 ± 0.68	-2.53 ± 0.68	↓ 4.01	Immune checkpoint to control inflammation and self-reactivity (Highfill et al., 2014).
Cd274 (Pdl1)	Immunosuppressive factor	0.51 ± 0.72	1.51 ± 0.72	↓ 2.01	Ligand for Pd-1 (Highfill et al., 2014).
Cxcr2	Chemokine receptor	-0.02 ± 0.00	-1.99 ± 0.01	↓ 1.97	Neutrophils recruitment (Roth & Hebert, 2000).

Table 6.6. Upregulated genes associated with cancer and inflammation in the presence of tumour-infiltrating neutrophils in Cxcr2 flox. The fold changes were calculated in relation to the expression in non-neutrophil infiltrated wt tumour.

Gene	Biological function	Log2 fold (non-neutrophil infiltrated Cxcr2 flox vs wt)	Log2 fold (neutrophil infiltrated Cxcr2 flox vs wt)	Differences in Log2 fold	Function
Gzmb	Enzymatic modulator of inflammation & immunity	-11.00 ± 0.00	-7.55 ± 0.02	↑ 4.00	Immune-stimulatory, cytotoxicity effect of CD8 ⁺ T-cells (Shresta <i>et al.</i> , 1998).
Bcl2	Anti-apoptotic	-8.00 ± 0.01	-4.00 ± 0.01	↑ 3.99	Pro-apoptosis linked to chemoresistance (De Graaff <i>et al.</i> , 2016).
Stat3	Transcription factor	-6.00 ± 0.03	-3.04 ± 0.03	↑ 2.95	Promotes tumour cell proliferation, survival, invasion, angiogenesis and immunosuppression (Yu <i>et al.</i> , 2014).
Mif	Immunosuppressive factor	1.00 ± 0.01	3.02 ± 0.01	↑ 2.02	Immunosuppressive, pro-inflammatory (Dumitru <i>et al.</i> , 2011; Zhou <i>et al.</i> , 2008).
Stat1	Interferon-responsive gene, transcription factor	-4.52 ± 0.70	-2.52 ± 0.70	↑ 2.00	Promotes inflammation-associated tumorigenesis (Ernst <i>et al.</i> , 2008).

6.2.15 Validation of Ccr2 expression in the tumour

Our RNA array data showed high variability in Ccr2 expression between the biological replicates of Cxcr2 flox and wt (Figure 6.7C). Therefore, the expression of Ccr2 was further evaluated using TaqMan qRT-PCR. Three neutrophils infiltrated tumour, each from Cxcr2 flox and wt were used.

Ccr2 expression was elevated with fold change ≥ 2 in all three Cxcr2 flox tumour in comparison to wt tumours (Figure 6.10).

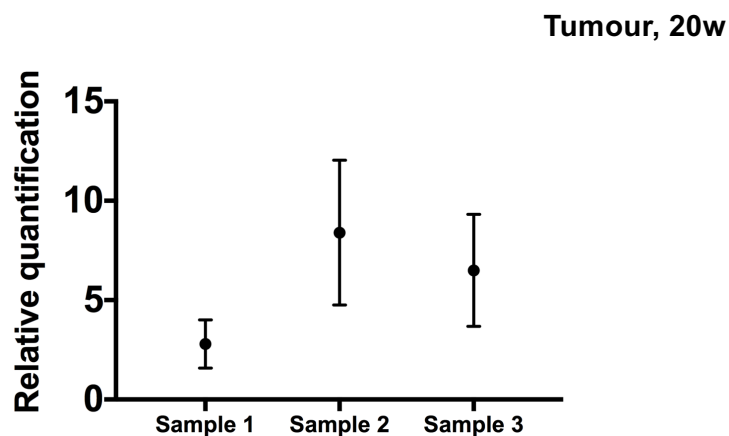
Ccr2 Expression (Cxcr2 flox vs wt)

Figure 6.10. Expression of Ccr2 by qRT-PCR analysis. The fold change in Cxcr2 flox tumour samples (n=3) was calculated in related to the expression in wt tumour samples (n=3). The data express as average value of triplicates (\pm standard deviation) and presented in log₂ unit. Each dot represent data from individual mouse.

6.2.16 Comparisons of gene expression levels between 2 weeks and 20 weeks sample

The difference in gene expression between the pre-tumour bladders (6.2.1, Table 6.1) and the bladder tumours (6.2.9, Table 6.4) were examined by comparing the data of 2 weeks and 20 weeks, respectively (Table 6.7).

Cxcr2 expression was downregulated at both time points (Table 6.7).

Among the most altered genes associated with immune-suppression, Cxcr2 flox showed an upregulation of Ido1 at 2 weeks, but downregulation of Ctla4 at 20 weeks (Table 6.7).

Table 6.7. Comparison of gene expression at 2 weeks and 20 weeks from the start of carcinogen treatment. The 10 genes with the most altered expression comparing 2 weeks 20 weeks samples. ↓ indicates downregulation and ↑ upregulation.

Most altered gene expression at 2 weeks	Most altered gene expression at 20 weeks	Genes with an altered expression at both 2 weeks and 20 weeks
Ido1 (↑)	Gzmb (↑)	Cxcr2 (↓)
Cxcl1 (↑)	Bcl2 (↑)	
Il13 (↑)	Stat3 (↑)	
Il5 (↑)	Mif (↑)	
Tlr3 (↑)	Stat1 (↑)	
Egf (↓)	Ctla4 (↓)	
Il10 (↓)	Tlr7 (↓)	
Il1r1 (↓)	Ccl28 (↓)	
Cxcr2 (↓)	Ccr9 (↓)	
	Csf3 (↓)	
	Cxcr2 (↓)	

6.2.18 Tgf- β expression in tumour

We have analysed the mRNA expression of Tgf- β using RNAscope in an attempt to identify the factor that could lead to higher tumour-infiltrating neutrophils in the absence of Cxcr2 (Chapter 5). Tgf- β was chosen as a targeted gene as it is associated with the polarisation and activation of neutrophils (Coffelt et al., 2016) as well as regulation of other immune cell infiltration into the tumour area (Yang et al., 2010).

We have performed semi-quantitative analysis on the expression of Tgf- β in the urothelium, stroma and tumour, as well as the tumour-leading edge. The scoring criteria used were; 0 = none/minimum, 1= low, 2= medium and 3 = high expression of the randomly placed 100 μ m X 100 μ m box.

Majority of the samples showed only low expression (score 1) of Tgf- β in the urothelium and in the stroma (Figure 6.11D, E). The level of expression in Cxcr2 flox was comparable to that of wt.

Half (n=4/8) of the Cxcr2 flox tumour showed high expression and another half showed medium expression of Tgf- β . Meanwhile, two out of three wt samples showed medium expression and another one showed low expression of Tgf- β (Figure 6.11F). Hence, in general, it is likely that Tgf- β expression is slightly higher in the tumour of Cxcr2 flox compared to wt samples.

At the tumour leading-edge, half of the Cxcr2 flox samples and two out of three wt samples showed score 3 expression of Tgf- β (Figure 6.11G). Therefore, the expression of Tgf- β appeared to be higher in the tumour, but similar in the leading edge of Cxcr2 flox compared to wt.

TGF- β expression by RNAscope

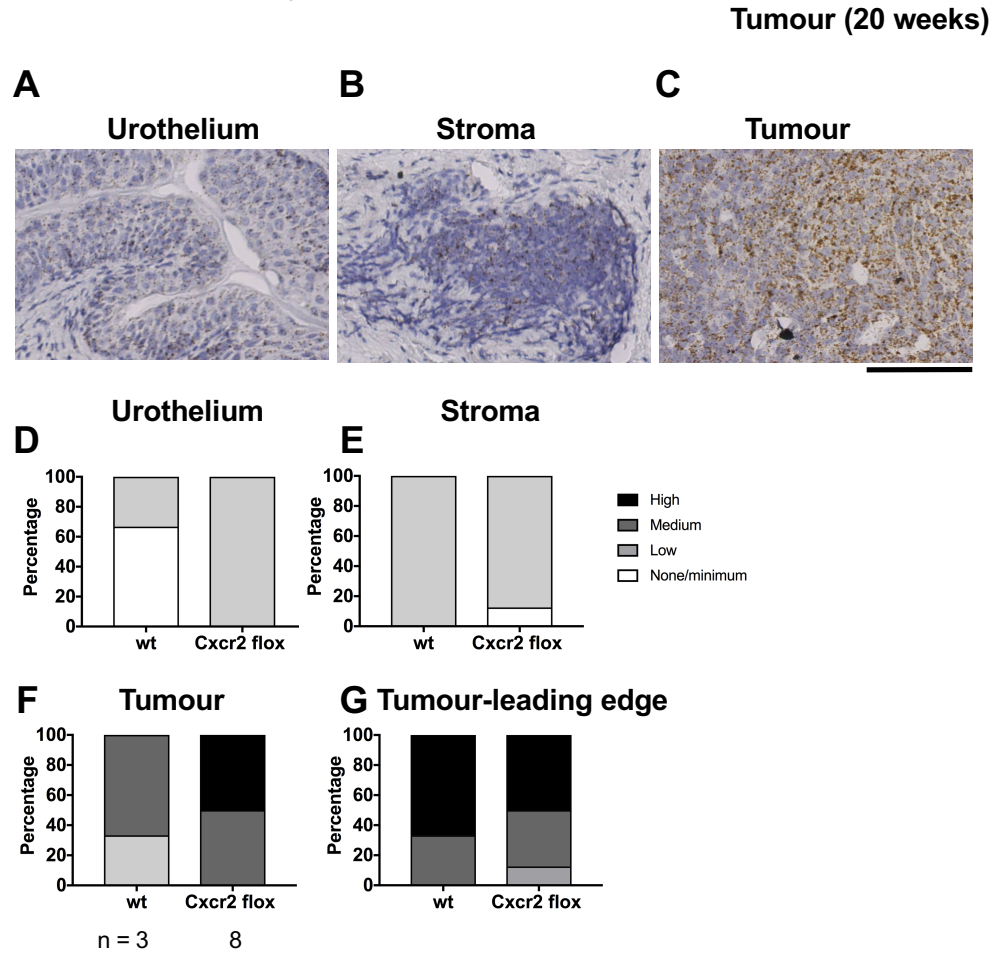


Figure 6.11. Tgf- β expression in bladder tumour samples of Cxcr2 flox and wt. The *in-situ* mRNA expression of Tgf-beta was quantified in urothelium, stroma and tumour area using RNAscope with the brown staining considered as positive signals for the probe used (A-C). Scale bar represent 200 μ m in A-C. Number of samples (n) analysed are as indicated below graph.

6.3 Discussion

6.3.1 Summary of results

The key observations from the expression study were:

- 1) At the acute inflammation stage (2 weeks of OH-BBN treatment), deletion of *Cxcr2* on the myeloid cells led to an alteration of genes associated with immunity and inflammation (Figure 6.1-6.4, Table 6.2).
- 2) Clear differences in the expression of genes associated with immunity and inflammation were also observed between neutrophil infiltrated and non-neutrophil infiltrated *Cxcr2* flox tumour samples (Figure 6.5-6.8, Table 6.5, 6.6).
- 3) The expression of Tgf- β was higher in the tumour leading-edge of wt and *Cxcr2* flox (Figure 6.11).

6.3.2 Differences in RNA analysis using RNA array-based and TaqMan-Assay based qRT-PCR

We have observed inconsistent gene expression measurement between the RNA array and TaqMan qRT-PCR analysis for the samples taken at 2 weeks after OH-BBN treatment. Out of 4 genes tested (*Egf*, *Ido1*, *Spp1* and *Nos2*), only *Egf* expression gave similar data for both RNA array analysis and qRT-PCR (Figure 6.2, 6.5, Table 6.3).

We have also further confirmed the expression of *Ccr2* in tumour samples of *Cxcr2* flox and wt. For the RNA analysis, the expression of *Ccr2* showed great variation in the two biological replicates of neutrophil infiltrated *Cxcr2* flox tumour (Figure 6.7C). Our analysis using TaqMan qRT-PCR gave more consistent data with all (n=3/3) neutrophil infiltrated *Cxcr2* flox tumours used showed an upregulation of more than 2-log₂ fold in comparison to wt tumour samples (Figure 6.10).

The inconsistency in the results obtained by RNA array and qRT-PCR analyses could be mainly due to the differences in the principle of detection of these two methods. The RNA array used SYBR Green dye in which this dye binds onto double-stranded DNA in detecting the amplification of the targeted genes. In contrast, qRT-PCR was performed using TaqMan-assay. This assay utilises the dual-labelled fluorogenic hybridisation probes with a quencher on the 3' end and the FAM or VIC dye label on the 5' end. The SYBR Green-based assay is considered as less specific than TaqMan-based assay due to the possibility of SYBR Green binding onto primer dimer, creating a false-positive signal (Tajadini et al., 2014; Arikawa et al., 2008).

Choices of the housekeeping genes may also contribute to the inconsistency of the gene expression data between RNA array and qRT-PCR. For RNA array, Hsp90 was used for the normalisation, while Gapdh was used for the qRT-PCR analysis.

The RNA used was extracted from the whole bladder tissue rather than the tumour area. Therefore, the changes in gene expression observed could be due to the non-tumour area. The number of samples used was low (n= 2 to 4) that may lead to imprecise estimation in the gene alterations between the Cxcr2 flox and wt samples. Further confirmation in a larger cohort, for example, n=10 tumour samples for each cohort is needed.

6.3.3 Differences in the expression level of genes at acute inflammation compared to late bladder tumorigenesis

Two main factors could contribute to the differences in the gene expression observed at acute inflammation stage and late stage of bladder tumorigenesis; 1) differences in the factor provoking the inflammatory response, and 2) the phenotypic differences of the immune cells present at these two stages.

During the acute inflammation stage (2 weeks from the start of carcinogen treatment), inflammation was provoked by the induction of the carcinogen (OH-BBN). However, at late bladder tumorigenesis stage, the tumour microenvironment could be the source of persistence inflammatory signalling.

Tumour microenvironment encompasses different type of immune cells that interact with each other as well as with the cancer cells, and the cells in the tumour stroma including tumour-associated fibroblasts to support the tumour growth and progression (Grivennikov et al., 2010b; Gajewski et al., 2013; De Visser et al., 2006). It was reported in murine lung carcinoma model that neutrophils in the early stage possess anti-tumour properties with a high level of pro-inflammatory factors, in contrast to the pro-tumour properties in the late stage of the tumour (Mishalian et al., 2013).

6.3.4 Altered gene expression associated with tumour-infiltrating neutrophils in Cxcr2 flox

The downregulation of Cxcl5 in the Cxcr2 flox neutrophil-infiltrated tumour samples might be associated with the downregulation of its receptor, Cxcr2. Alternative signalling coming from the tumour microenvironment may likely to have attracted the neutrophils, independent to Cxcr2 pathway, to facilitate their growth and progression (discussed in more depth in 8.2.4). Due to limitation of samples and time, not all genes could be validated. However, it will be good to validate the level of RNA and protein expression of Cxcl5 in the future studies.

We have observed a mixed level of expression of immunostimulatory and immunosuppressive factors in neutrophil infiltrated Cxcr2 flox tumour.

Our results may indicate that altered signalling in the tumour microenvironment may involve in the recruitment of tumour-infiltrating neutrophils in the absence of Cxcr2 expression in the bladder (discussed in Chapter 8 in more depth).

6.3.5 Tgf- β expression was associated with the presence of tumour cells

The role of Tgf- β in recruiting tumour-infiltrating neutrophils was observed in other studies (Coffelt et al., 2016; Yang et al., 2010). Tgf- β was associated with cancer cell invasion and metastatic progression (Drabsch & Ten Dijke, 2011). Tgf- β could negatively regulate the Cxcr2 signalling in the chemotaxis of the granulocyte population (Gr-1+CD11b+) (Yang et al., 2008). Genetic ablation of its receptor, Tgfbr2, led to an increase in the chemotactic activities of Cxcr2 (Yang et al., 2008). The high expression of the Tgf- β in the leading-edge of the tumour could be associated with the ability of Tgf- β in promoting cancer cell invasion and metastatic progression (Drabsch & Ten Dijke, 2011).

This highlighted the importance of tissue-based analysis in localizing the gene expression in order to understand the biological impact of the targeted gene.

6.4 Future directions

The RNA works were preliminary studies that we performed with small number of samples (n=2 for each cohort) to have a general view on the differences in the gene expression between Cxcr2 flox and wt. Due to the limitation of sample and time, we could not proceed to further validate our results.

The use of RNA array and qRT-PCR- based for the detection of the gene expression is limited to selected genes and therefore, biased. They may not be specific and sensitive enough to detect weakly expressed gene. Alternatively, the use of RNA-seq, which is a higher throughput method with wider coverage will allow detection of the novel transcript.

The expression of the genes associated with inflammation and cancer immunity can be further analysed by an improved strategy based on:

- 1) Use of the non-OH-BBN treated as control of baseline expression.
- 2) Increase the number of samples to at least n=3 in all experimental cohort.
- 3) It will be useful to perform further analysis on the RNA array data using Kyoto Encyclopaedia of Genes and Genomes (KEGG) and Ingenuity Pathway Analysis (IPA). KEGG/IPA analysis could be used for identification of pathway related to molecular

interactions, upstream regulators, network markers and other functional biological insight (Cirillo et al., 2017).

In-situ RNA hybridization (such as RNAScope) can be used to directly visualise the level of Tgf- β RNA in the tumour. Alternatively, specific cell population or tissue area could be dissected out from heterogenous tissue section using laser-capture microdissection (LCM). LCM is a histology-based tissue microdissection using direct microscopic visualisation and excision by laser beam (Simone et al., 2000). The isolated cells or tissue could be used for downstream analysis to quantitate the expression of specific RNA, DNA or protein. By micro-dissecting the tumour edge vs tumour core using LCM the expression of Tgf- β could be better analysed quantitatively considering the tissue-context.

Chapter 7

Effects of neutrophil depletion

7.1.1 Hypotheses

- 1) Targeting neutrophils using monoclonal antibody Ly6G (clone 1A8) will suppress levels of neutrophils induced by carcinogen treatment both in circulating and in the bladder tissue. In the absence of anti-tumour neutrophils in early inflammation that eliminate urothelial cells with tumour-causing DNA damages, there may be an enhanced tumour pathogenesis as we seen in *FGFR3^{S249C}* and *Cxcr2* flox models.
- 2) In well-established tumours, 1A8 treatment will suppress the recruitment of tumour-infiltrating neutrophils, that are presumably pro-tumour, thereby leading to tumour regression.

7.1.2 Aim and Objectives

This chapter aimed to evaluate the effects of neutrophil depletion in bladder tumorigenesis using anti-Ly6G monoclonal antibody (1A8), and the clinical relevance of targeting neutrophils in the tumour.

The Ly6G (1A8 clone) monoclonal antibody used in this study was an antibody that binds specifically on mouse Ly6 complex locus G (Ly6G) antigen. Ly6G, also known as Gr-1, is a glycosylphosphatidylinositol (GPI)-anchored protein which is expressed on the surface of neutrophils (Wang et al., 2012; Fleming et al., 1993). The Ly6G is associated with the recruitment and migration of neutrophil via β 2-integrin pathway (Wang et al., 2012). The anti-Ly6G antibody (1A8 clone) has been extensively used to deplete circulating neutrophils in mouse models (Moynihan et al., 2016; Steele et al., 2016; Coffelt et al., 2015; Finisguerra et al., 2015; Jamieson et al., 2012).

The specific objectives were:

- 1) To evaluate the effects of neutrophil depletion at acute inflammation stage onto the tumour.
- 2) To determine whether neutrophil depletion could lead to regression of bladder tumour.

7.2 Results

7.2.1 WBC levels in OH-BBN- and 1A8-treated mice at 2 weeks of treatments

To further understand the roles of neutrophils in the bladder tumour initiation and progression, we have used monoclonal antibody against Ly-6G⁺ (clone 1A8) to deplete the neutrophil population. Ly6G is a small glycosylphosphatidylinositol (GPI)-linked protein on the surface of neutrophils (Fleming and Malek, 1993)(Fleming et al., 1993)(Fleming et al., 1993)(Fleming et al., 1993). The function of Ly6G strongly associates with the chemotactic activities of neutrophils (Wang et al., 2012).

Treatment regimens were a simultaneous application of 0.05% OH-BBN in the drinking water and intraperitoneal injection (i.p) of 1A8 or its isotype control, 2A3, for 10 weeks, followed by another 10 weeks with normal drinking water (Figure 7.1A). The sampling of the whole blood and bladder were performed at 2 weeks and 20 weeks from the start of the treatments.

At 2 weeks, 1A8-treated mice had significantly lower circulating neutrophils compared to 2A3-treated mice ($p = 0.0065$, Mann-Whitney) (Figure 7.1D). The NLR significantly increased in 1A8-treated compared to 2A3-treated mice ($p = 0.0173$, Mann-Whitney) (Figure 7.1F).

Changes in the level of monocytes, eosinophils and basophils were not prominent among 1A8-, 2A3- and OH-BBN treated cohorts (Figure 7.1G-L).

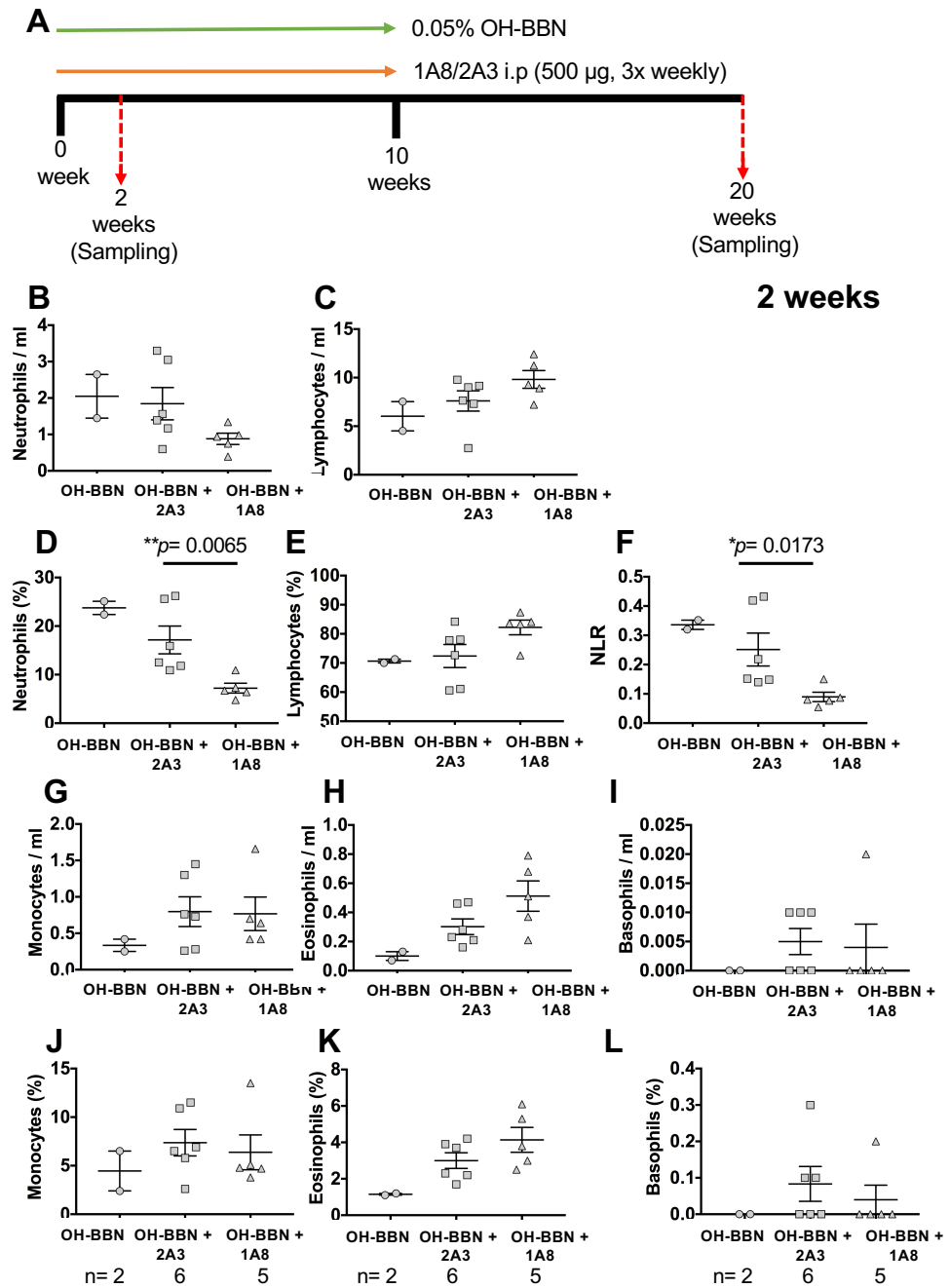


Figure 7.1. Depletion of neutrophils in wt mice. Schematic presentation of the neutrophil depletion studies (A). 1A8/2A3 (500 µg) i.p injection was done in concurrent with OH-BBN treatment. Number of cells within blood (cells/ml) (B, C, G-I) and cell population within WBC (%) (D, E, J-L) for samples taken at 2 weeks of treatment. Number of samples used was as indicated below each column. *P* values (Mann-Whitney) are indicated where significant ($*p<0.05$, $**p<0.01$).

7.2.2 WBC levels in 1A8-treated mice at 20 weeks

In contrast to observations at two weeks, circulating neutrophils at 20 weeks was significantly increased in 1A8-treated mice compared to OH-BBN control group ($p=0.0317$, Figure 7.2C). The decrease in circulating lymphocytes was also observed in 1A8-treated mice, in comparison to both 2A3-treated and OH-BBN mice ($p = 0.0317$, Mann-Whitney) (Figure 7.2D). Accordingly, NLR was significantly higher in 1A8-treated compared to 2A3-treated and OH-BBN mice ($p = 0.0317$, Mann-Whitney) (Figure 7.2E).

Circulating monocytes were also significantly increased in 1A8-treated mice compared to 2A3- and OH-BBN-treated mice (Figure 7.2F).

The levels of eosinophils and basophils were comparable among the treatment groups (Figure 7.2G, H, J, K).

20 weeks

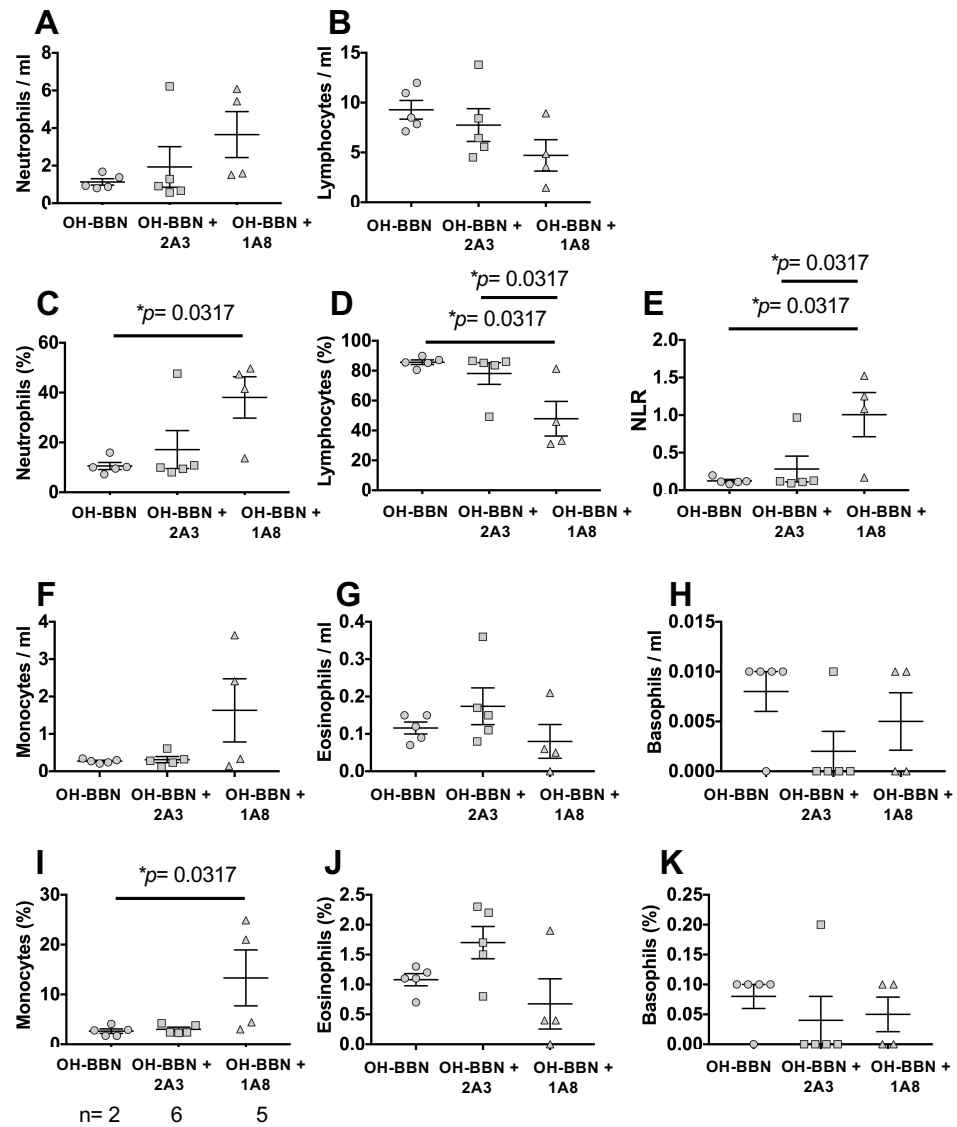


Figure 7.2. WBC analysis of samples at 20 weeks from the start of OH-BBN and 1A8/2A3 treatments. Each WBC population is presented in cell density/ml (A, B, F-H) and in percentage (C, D, I-K). Neutrophil-to-lymphocyte ratio (NLR) (E). The p-values (Mann-Whitney) are indicated where $p^* < 0.05$ were considered significant.

7.2.3 Effects of neutrophil depletion in bladder tumorigenesis

We have evaluated the effects of 1A8-neutrophil depletion at the tissue level.

At 2 weeks from the start of OH-BBN treatment, the neutrophil infiltration was not significantly different in the urothelium, stroma and muscle in 1A8-, 2A3- and OH-BBN-treated mice (Figure 7.3A-C).

Similarly, at 20 weeks from the treatments, the levels of neutrophil infiltration were also comparable in the areas of tumour and stroma of 1A8-, 2A3- and OH-BBN-treated mice (Figure 7.3D, E).

We next scored the pathogenesis of the bladders taken at 20 weeks from the treatments. While statistically not significant, the results indicated an enhanced severity of bladder pathogenesis in 1A8-treated mice compared to 2A3 and OH-BBN treated mice (Figure 7.3F).

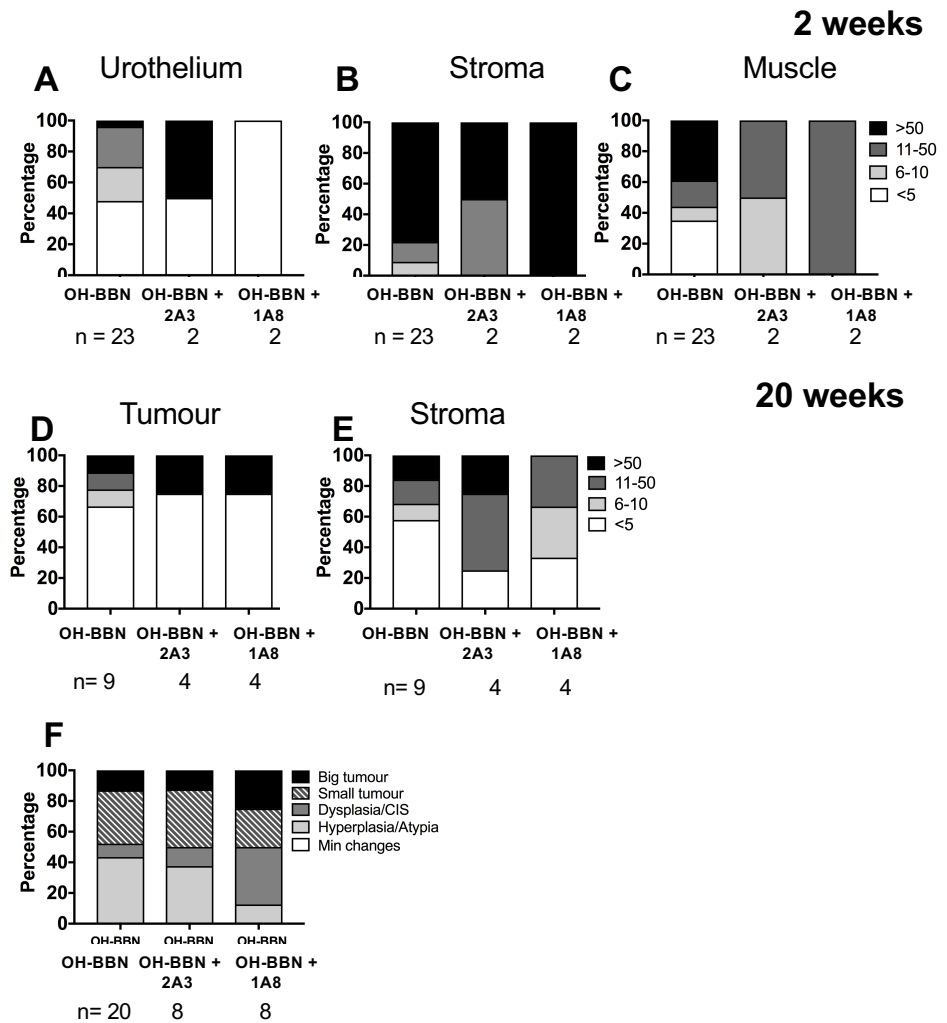


Figure 7.3. Effects of neutrophil depletion in the bladder tissues at 2 and 20 weeks. Infiltrations of neutrophils at 2 weeks (A-C) and 20 weeks (D, E) from the start of OH-BBN treatment. Pathogenesis of bladder tissue at 20 weeks (F). No significant different was observed (Mann-Whitney test).

7.2.4 Effects of neutrophil depletion in tumour-bearing mice

We hypothesized that, in established tumours, depletion of neutrophils by 1A8 will (1) suppress the recruitment of tumour-infiltrating neutrophils, and (2) lead to tumour regression.

Mice were treated with 0.05% OH-BBN in the drinking water for 10 weeks and replaced with normal drinking water (Figure 7.4 A). Ultrasound imaging was used to monitor tumour formation, starting from 18 weeks from the start of OH-BBN treatment. Tumour size was determined by volumetric analysis using data from Vevo3100. Mice harbouring a tumour of approximately 20 mm³ (as measured by bladder volume, see p202) or more were selected. The 1A8 or 2A3 was applied for 2 weeks.

Blood analysis showed comparable number of neutrophils in 1A8-treated mice (1.11 ± 0.44 cells/ml) compared to 2A3-treated mice (1.51 ± 0.54 cells/ml) (Figure 7.4B). Levels of lymphocytes were comparable between 1A8 and 2A3-treated mice (6.00 ± 3.32 cells/ml, 6.41 ± 3.32 cells/ml, respectively) (Figure 7.4C). Accordingly, the NLR was mildly decreased in 1A8-treated mice (0.20 ± 0.047) in comparison to 2A3-treated mice (0.27 ± 0.15) (Figure 7.4D).

The number of monocytes were comparable in 1A8-treated mice (0.40 ± 0.21 cells/ml) compared to the 2A3-treated (0.64 ± 0.40 cells/ml) (Figure 7.4E). Similar observation was obtained for the number of eosinophils and basophils in 1A8-treated mice (0.27 ± 0.16 , 0.01 ± 0.00 cells/ml, respectively) compared to 2A3-treated mice (0.12 ± 0.04 , 0.00 ± 0.00 /ml, respectively) (Figure 7.4F, G).

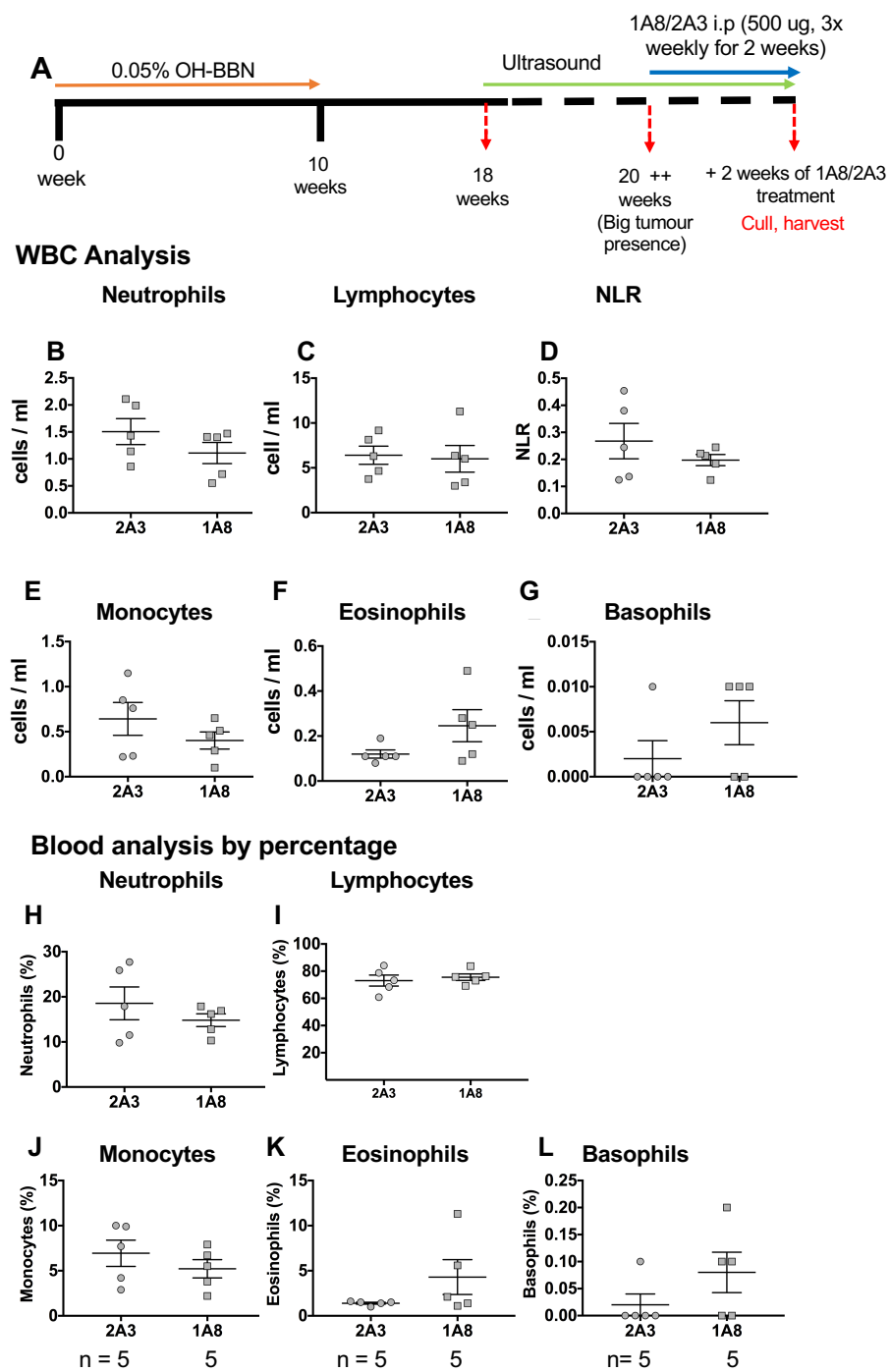


Figure 7.4. WBC analysis of 1A8/2A3-treated mice. Schematic presentation of the neutrophil depletion in mice bearing tumour. Mice were injected i.p with 1A8/2A3 (500 μ g) for three times weekly for two week (A). Number of circulating immune cells (cells/ml); neutrophils (B), lymphocytes (C), NLR (D), monocytes (E), eosinophils (F) and basophils (G). Percentage of each circulating immune cells to the WBCs (H-K). No significant difference was observed (Mann-Whitney test).

7.2.5 The effects of neutrophil depletion in tumour-bearing mice

Next, we analysed the levels of neutrophil infiltration in the tumour and the stroma adjacent to the tumour area in H&E-stained tissue section from mice treated with 1A8 and 2A3, and in the non-1A8/2A3 treated mice (“untreated”) (Figure 7.5).

In general, the level of infiltrated neutrophils was comparable among 1A8- 2A3-treated and non-1A8/2A3 treated (Figure 7.5A and B).

Only one out of six 1A8-treated mice showed a relatively higher number of tumour-infiltrated neutrophils (590 cells/mm²) compared to the 2A3-treated mice (54 ± 115 cells/mm², n=5) (Figure 7.5A).

In the adjacent stroma, two out of six 1A8-treated mice showed a higher number of neutrophils (590 and 440 cells/mm²) compared to 2A3-treated mice (120 ± 79 cells/mm², n=5) (Figure 7.5B).

In summary, the results showed that while there was an indication that neutrophil depletion had some effects in reducing the levels of neutrophils from the blood circulation (Figure 7.4), the levels of neutrophils in the tumour tissue were comparable among 1A8 and 2A3-treated and non-1A8/2A3 treated (Figure 7.5).

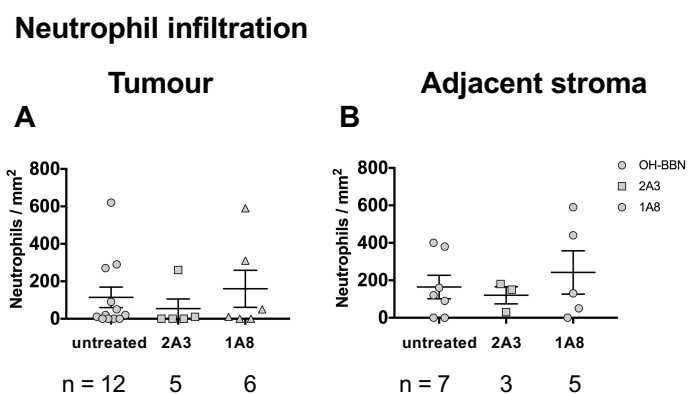


Figure 7.5. Tissue-infiltrated neutrophils in 1A8/2A3-treated and non-1A8/2A3 treated mice. Mice bearing bladder tumour were treated with 1A8/2A3 for two weeks. Neutrophil density (cells/mm²) was evaluated in tumour and adjacent stroma area (A, B). No significant difference was observed (Mann-Whitney test).

7.2.6 Association between circulating and tissue-infiltrated neutrophils in 1A8/2A3 treated mice

In order to better understand the effects of 1A8/2A3 treatment applied to tumour-bearing mice, we have evaluated the association between the levels of neutrophils in circulation and the tissues.

We have observed that mice that showed a high number of circulating neutrophils showed low or no tissue-infiltrated neutrophils (n=4/5 in 2A3-treated and n=3/5 in 1A8-treated mice) (Figure 7.6A). In contrast, n=2/5 of 1A8-treated mice with a lower level of circulating neutrophils displayed a higher level of tissue-infiltrated neutrophils (Figure 7.6A).

A similar association was observed when comparing the levels of circulating neutrophils with neutrophils in the stroma (Figure 7.6 B).

Taken together, the levels of neutrophils in the tissue were not reflected in the levels in circulation, and it showed a negative correlation. It remained unclear whether the application of 1A8 for 2 weeks in the tumour-bearing mice had efficiently suppressed the levels of neutrophils in the tumour tissue.

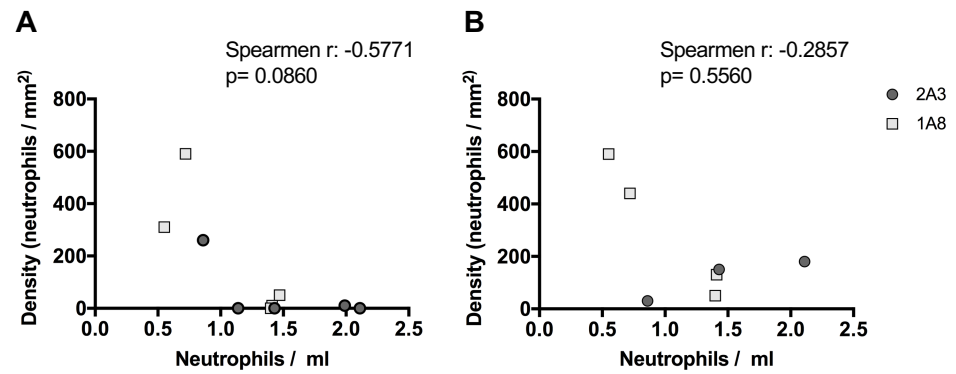


Figure 7.6. Association between circulating neutrophils and tissue-infiltrated neutrophils in 1A8/2A3-treated mice. Number of circulating neutrophils compared to tumour-infiltrating neutrophils (A) and to infiltrated neutrophils in the adjacent stroma (B). N=5 for 1A8- and 2A3-treated was used for the evaluation of tumour-infiltrating samples. N=4 for 1A8-treated and n=3 for 2A3-treated was used for the evaluation of neutrophil in the adjacent stroma. The correlation between circulating and tissue-infiltrated neutrophils were measured using Spearman rank order for non-parametric data distribution.

7.2.7 The effects of neutrophil depletion on the tumour size

The effects of neutrophil depletion by 1A8 on the bladder volumes were monitored during the treatment. The ultrasound images were analysed using Vevo LAB software (Fujifilm VisualSonics Inc, Canada).

The bladder volume was calculated by;

the whole bladder (indicated by white dots in Figure 7.7A) – lumen (indicated by green dots).

In 2A3-treated mice (Figure 7.7B), one showed a continuous increase of the bladder volume, one showed a slight increase, and the last showed an increase observed after one week, followed by a decrease after two weeks.

In 1A8-treated mice (Figure 7.7C), two showed a decrease in bladder volume after two weeks, and one showed a similar volume retained during the treatment.

Overall, the bladder volume remained more constant in 1A8 treated mice, while the bladder volume showed a continuous increase upon 2A3 treatment. However, this was an observation from n=3 only.

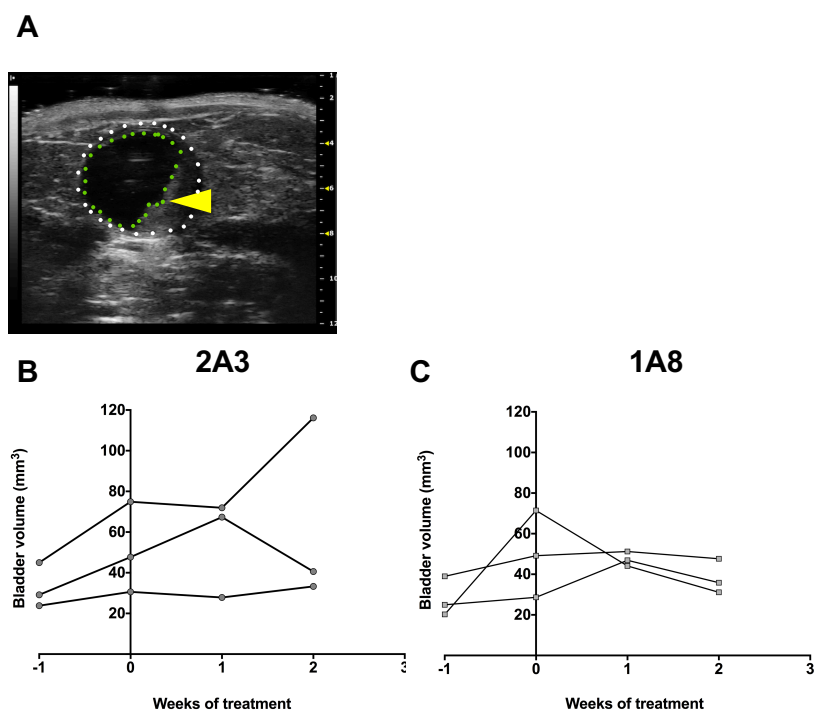


Figure 7.7. Bladder volumetric analysis of tumour-bearing mice treated with 1A8/2A3 for 2 weeks. Representative ultrasound image of the bladder (A). Yellow arrowhead indicates tumour mass of the bladder (white dots). Green dots indicate the lumen. Bladder volume from one-week prior to treatment start up to 2 weeks after treatment by 2A3 (B) and 1A8 (C).

7.3 Discussion

7.3.1 Summary of results

The results from this chapter indicated that:

1. The suppression of neutrophil recruitment during the first 10 weeks in which carcinogen had been applied, may have resulted in an increase of tumour in the bladder at a later stage.
2. The effects of 1A8 treatment on the bladder tumour growth was variable and may require further analysis using an increased number of mice.

7.3.2 Neutrophil depletion at acute inflammation stage enhanced inflammation at the later stage of bladder tumorigenesis

Based on the results, I speculate that the neutrophils depletion at acute inflammation stage might lead to chronic inflammation at the later stage by altering the immune cells balance systemically. This could then enhance the severity of bladder tumour pathogenesis.

7.3.3 Potential causes of the lack of clear neutrophil depletion in tumour-bearing mice

Several factors may cause a lack of clear neutrophil depletion using 1A8 in the mice bearing tumour.

Firstly, the dosage of 1A8 antibody used (500 µg, three times a week) which was based on the literature (Jamieson *et al.*, 2012), may not have been the optimum in depleting the circulating and tissue-infiltrated neutrophils.

Secondly, the level of neutrophils may have been adjusted constantly by an increase in immature neutrophils released from the bone marrow in 1A8-treated mice. This was previously reported (Faget *et al.*, 2018). It was also reported that the effects of 1A8 treatment were not on the number of circulating neutrophils but on the chemotaxis of neutrophils (Wang *et al.*, 2012).

Thirdly, the mouse strain used in this study (C57Bl/6) could have also contributed to the efficacy. For example, it was found that 1A8 treatment significantly reduced neutrophils in BALB/c and FVB/N but not in C57Bl/6 (Faget *et al.*, 2018). This could be due to the immunological variant between C57Bl/6 compared to BALB/C and FVB/N mice. BALB/c and FVB/N mice have T helper cell type 2 (Th2)-biased immune response compared to C57Bl/6 (Disis and Palucka, 2014; Kim *et al.*, 2012; Chen *et al.*, 2005). Differences in haematopoiesis was also observed between the C57Bl/6 and BALB/C mice with the

former have lower level of haematopoietic stem cells in the bone marrow (Mfiuer-sieburg & Roy, 1996)

Finally, treatment with 1A8 treatment was reported to cause changes in the phenotype of neutrophils in the bloodstream of mice with developed lung cancer (Faget *et al.*, 2018).

Our experimental approach was limited in terms of monitoring the levels of tissue-infiltrated neutrophils, as it was post-mortem histopathological analysis.

7.4 Future direction

I propose the following in targeting neutrophil recruitment in the tumour.

1. Inhibitors targeting the neutrophil populations should be tested. One of the candidates for this is Reparixin (also known as Repertaxin). Reparixin is a CXCR1/CXCR2 small molecule inhibitor that is being clinically tested in cancer and inflammation diseases (Schott *et al.*, 2017); <https://www.drugbank.ca/drugs/DB12614>). Reparixin has been shown to reduce tissue infiltrated neutrophils in lung and hepatocellular mouse models (Zarbock *et al.*, 2008; Bertini *et al.*, 2004). Data from this study indicated the important of Cxcr2-axis in the bladder tumour initiation and progression. Thus, Reparixin might work in the bladder cancer model and could help us to better understand the tumour stage-dependent effects of Cxcr2 suppression. Mouse bearing bladder tumour could be treated with Reparixin to evaluate whether inhibition of Cxcr2 might lead to tumour regression.
2. The use of combination treatment should also be considered to increase the efficacy in targeting neutrophil recruitment. Combining 1A8 with a secondary antibody has been shown to increase the efficacy of 1A8-mediated neutrophil depletion (Faget *et al.*, 2018). Other studies have used the anti-CXCR2 monoclonal antibody in combination with PD-L1/PD1 and demonstrate apparent anti-tumour effects (Highfill *et al.*, 2014; Steele *et al.*, 2016).
3. Improved mouse models in testing the above inhibitors should be considered, such as:
 - I. Use of another mouse strain than C57Bl/6 (BALB/C or FVB/N).
 - II. Use of other genetically modified mouse models with potential of monitoring tissue-infiltrating neutrophils more real-time and accurately such as Catchup mice which express specific neutrophil-protein Ly6G promoter (discussed in more depth in 8.4.1).
 - III. Increase number of mouse samples (at least n=10 each for 1A8-treated and 2A3-treated mice).

Chapter 8

General discussion

8.1 Overall summary of the findings

This study set out to investigate the roles of neutrophils in carcinogen-dependent bladder tumorigenesis. Two different GEM models, *FGFR3* mutants and *Cxcr2* flox, and neutrophil depletion approach were used in this study.

The overall findings from this study were:

1. Carcinogen-dependent bladder tumorigenesis was increased in mutationally activated *FGFR3*^{S249C} mice. The tumour phenotype in *FGFR3*^{S249C} mice was more advanced with a modest increase in neutrophil infiltration compared to wt mice. Acute inflammatory response was suppressed at the early time-point of carcinogen treatment (Chapter 3).
2. *Cxcr2* deletion in myeloid cells led to a significant increase in tumour formation compared to wt mice. The *Cxcr2* flox tumours were bigger and more invasive. Senescence-associated proteins, γ -H2aX, p53 and p21 expression were maintained in *Cxcr2* flox at acute inflammation stage. However, tumour cell proliferation occurred regardless of senescence-associated protein expression at a later stage of bladder tumorigenesis in the absence of *Cxcr2* expression (Chapter 4).
3. At acute inflammation stage, recruitment of neutrophils, macrophages and T-cells was suppressed in *Cxcr2* flox. In contrast, an influx of neutrophil population with lack of expression of neutrophils-common markers was observed in *Cxcr2* flox. The increase of tumour-infiltrating neutrophils in *Cxcr2* flox coincided with the increase of CD3⁺ T-cells. A transient increase in circulating and infiltrating macrophages was observed at tumour initiation stage (16 weeks), but not at the later tumour progression stage (20 weeks) (Chapter 5).
4. Alteration of cytokines, chemokines and growth factors were observed in the *Cxcr2* flox and differently regulated at acute inflammation compared to the late stage of bladder tumorigenesis (Chapter 6).
5. Neutrophil depletion at acute inflammation stage led to an increased level of neutrophils in circulation at a later time point, which may reflect the enhanced tumour pathogenesis (Chapter 7).

8.2 Proposed mechanism of inflammation-induced bladder tumour and progression

I propose the following model of how inflammation could induce and promote tumours in Cxcr2 flox mice in three sequential stages. Firstly, suppression of acute inflammatory responses, secondly, an increase in local inflammation associated with tumour initiation, and thirdly, infiltration of pro-tumour neutrophils that altered immune and inflammatory signalling, resulting in an exaggeration of tumour progression (Figure 8.1).

8.2.1 Suppression of acute inflammatory responses

Our results support the accumulating evidence on the importance of myeloid cells and Cxcr2 in regulating inflammatory responses. The defects in neutrophil and macrophage recruitment were reported in other cancer mouse models with genetic ablation of Cxcr2 (Dyer et al., 2017; Steele et al., 2016; Jamieson et al., 2012; Devalaraja et al., 2000b). For example, Cxcr2 knockout mice induced with skin inflammation using 2-O-tetradecanoyl phorbol-13-acetate (TPA) showed reduction of MPO⁺ neutrophils compared to wt mice (Jamieson et al., 2012). Cxcr2 deletion also led to a reduction of skin thickness that indicated impairment in inflammatory response when exposed to TPA (Dyer *et al.*, 2017).

The findings from this study further supported the notion that deficiency in immune cell populations increased the susceptibility to carcinogen-induced carcinogenesis in mouse models (Vesely et al., 2011). For example, an increase in the occurrence of sarcoma induced by carcinogen methylcholanthrene (MCA) was observed in mice that lack eosinophils, T cells and B cells (Engel et al., 1997; Girardi et al., 2003).

8.2.2 An increase in local inflammation associated with tumour initiation in Cxcr2-deficient mice

I propose here that the transient increase in macrophage infiltration could serve as the turning point from acute to chronic inflammation hence initiating the tumour development in Cxcr2 deficient mice. Other studies have also shown that the present and persistent activation of macrophages predispose chronic inflammation to malignant neoplasm (Balkwill & Mantovani, 2001; Lin et al., 2001; Arwert et al., 2018). Macrophages were associated with the tumour initiation and promotion by creating a paracrine/autocrine loop with the tumour cells that induce inflammation, angiogenesis and immunosuppression (Saccani et al., 2006; Poh & Ernst, 2018).

Our results were also in line with the report by Dyer and colleagues (2016) in skin inflammation mouse model. They have observed an increase in macrophage infiltration in the absence of neutrophils at the acutely inflamed sites with exaggerated cutaneous inflammation.

I also propose here that the increase of macrophage infiltration at the tumour initiation stage in Cxcr2 flox may lead to an increase in neutrophil infiltration. This is in accordance with a report that showed resident macrophages in the bladder could induce the production of chemokines and cytokines such as Cxcl1 and Cxcl2 for the recruitment of inflammatory neutrophils from the bone marrow (Schiwon et al., 2014).

8.2.3 Recruitment of pro-tumour neutrophils and tumour progression

We have observed an increase in tumour-infiltrating neutrophils which may lack expression of MPO and NIMP in *Cxcr2* flox at tumour progression stage. The increase in tumour-infiltrating neutrophils observed in *Cxcr2* flox supported the notion that the persistent presence of neutrophils could lead to tumour progression (Powell & Huttenlocher, 2016b).

The effects of the increase in neutrophil infiltration were also shown to be dependent on the stage of the cancer (Eruslanov et al., 2014; Singhal et al., 2016; Steele et al., 2016; Fridlender et al., 2009; Mishalian et al., 2013). For example, in an early stage of lung cancer, neutrophils in the tumour displayed characteristic of APC-like cells (macrophages and dendritic cells) with high expression of CD14, HLA-DR, CCR7, CD86, and CD206 and are tumour suppressive (Singhal *et al.*, 2016). However, this APC-like neutrophil population was largely reduced in large tumour with the presence of hypoxia.

Taking into account that *Cxcr2* flox has a worse tumour phenotype and lacks expression of neutrophil common marker, it is likely that tumour-infiltrating neutrophils observed in this cohort were pro-tumour immature neutrophils. A single-cell analysis on the tumour-associated neutrophils population may help further determining the nature of tumour-infiltrating neutrophils in *Cxcr2* flox. These could be done by isolating the neutrophil population from the peripheral blood or from the tumour tissue of *Cxcr2* flox bearing tumour. The neutrophils could be separated from the other white blood cell populations based on density gradients or by the positive selection using microbeads (Sionov et al., 2015). The phenotype of the tumour-associated neutrophils can be analyzed using RNAseq or flow cytometry (Sagiv et al., 2015; Fridlender et al., 2009; Mishalian et al., 2014).

Previous studies have also associated tumour-infiltrating neutrophils with the immunosuppressive G-MDSC phenotype. Eruslanov and colleagues (2012) have elegantly shown that the tumour microenvironment could alter the functions of myeloid cells in bladder cancer patients. They identified a subset of G-MDSC (CD15^{High} CD33^{Low}) isolated from the peripheral blood and tumour tissue of bladder cancer patients using magnetic cell isolation technique. The isolated G-MDSC population had a high expression of inflammatory factors, including the chemokines (CCL2-4), growth stimulating factor (G-CSF) and interleukins (IL-6, IL-8). When cultured *in vitro*, the G-MDSC showed inhibition of CD4 proliferation but an increase in the T-regulatory cell population (FoxP3) (Eruslanov et al., 2012). Furthermore, there have been several studies reported on the isolation and phenotyping of neutrophils; (Sagiv et al., 2015; Fridlender et al., 2009; Mishalian et al., 2014).

However, the findings of this study did not support the previous *in vitro* and clinical studies in bladder cancer (Zhang et al., 2017; Gao et al., 2015). Zhang and colleagues (2017) found that CXCR2 was highly expressed in the infiltrated MDSC population (CD33⁺CD11b⁺HLA-DR⁻) from bladder cancer patients compared to in the circulation and to the healthy individuals. The expression of CXCL5 was also higher in the bladder tumour tissue (Gao et al., 2015). Interaction between CXCR2 and its ligand, CXCL5, led to the activation of PI3K/AKT signaling pathways that later promoted bladder cancer cell migration and invasion (Gao et al., 2015). One of the reasons that could contribute to the differences is due to the fact that their studies were performed using established tumour samples taken from the bladder cancer patients and mouse bladder cell lines. Hence, the measurement on the CXCR2 effects may be observed at a point where cancer cells have already escaped early immunosurveillance mechanisms, thus lacks the evaluations on the impact of CXCR2 on the early tumorigenic events. The studies also may not have taken into account the inter-tumour, and intra-tumour heterogeneity possessed by the bladder tumour tissue.

Our results were also in contrast to the studies using different cancer mouse model, including melanoma (Singh et al., 2009), colon (Yamamoto et al., 2008), intestinal adenocarcinoma (Jamieson *et al.*, 2012), breast cancer (Acharyya et al., 2012), and pancreatic ductal adenocarcinoma (Chao et al., 2016; Steele et al., 2016). Inhibition of *Cxcr2* genetically and pharmacologically prevents TAN accumulation and suppresses of tumour growth in pancreatic ductal adenocarcinoma (Chao et al., 2016; Steele et al., 2016). *Cxcr2* was found to play roles in promoting metastasis via its signalling on myeloid cells (Steele *et al.*, 2016).

In contrast, the increase of tumour-infiltrating neutrophils in *Cxcr2* flox in our studies coincided with the increase of CD3⁺ T-cells. This could reciprocate the “inflamed tumour” phenotype, which is the type with high infiltration of T-cells in the tumour and its surroundings but are inactive in killing tumour cells (Chen & Mellman, 2013). This “inflamed tumour” phenotype is typically observed in bladder cancer as well as melanoma and lung cancer, which are the cancer types that possess high mutational burden and most likely to respond well to immunotherapies such as anti-PD-L1 and anti-CTLA4 (Gajewski et al., 2013; Chen & Mellman, 2013). However, our findings are in apparent contrast to other studies that showed an increase of tumour-infiltrating T effector cells was observed with a decrease in tumour-infiltrating neutrophils in *Cxcr2*-deficient mice (Chao et al., 2016; Steele et al., 2016).

The above contradictions may imply a heterogeneity of immune cells between different cancer types. Tissue-specific characteristics could also be in-part responsible for determining the mechanisms through which tumours influence the immune cells in

favouring its growth. Indeed, the differences in the tumour occurrence and bladder pathogenesis observed between *Cxcr2* flox and *Cxcr2* ko (Chapter 4) gave a further indication that CXCR2 could possess opposing roles in bladder tumorigenesis in a tissue-context dependent manner.

8.2.4 Potential regulators of neutrophil recruitment to the tumour microenvironment in the absence of *Cxcr2*

Based on the results from the protein expression and RNA expression studies (Chapter 5 and 6), I propose three hypotheses on what may have contributed to compensate the lack of *Cxcr2* in recruiting neutrophils to the tumours. Firstly, this could be by the changes in the expression of chemotactic surface receptors on neutrophils. Secondly, alternative signalling coming from the tumour microenvironment may likely to have attracted the neutrophils to facilitate their growth and progression. Thirdly, due to the tumour pressure, immature neutrophils may likely to have been released from the bone marrow, and the tumour pressure also has led to the granulocytic expansion and prolonged neutrophil lifespan.

The changes in the expression of chemotactic surface receptors on neutrophils:

This study showed that the expression of *Ccr2*, a chemotactic factor mostly expressed by monocytes, was found to be upregulated in the neutrophil infiltrated *Cxcr2* flox tumour (Figure 6.10). This is in agreement with the report that showed an upregulation of CC receptors on neutrophils with the downregulation of their classical receptors (CXCR1 and CXCR2) (Eruslanov et al., 2014). It was shown in a pancreatic adenocarcinoma mouse model that depletion of CXCR2 led to a compensatory increase in an alternative subset of CCR2+ tumour-associated neutrophils (Nywening et al., 2018). Furthermore, bone marrow-derived neutrophils could express surface, and intracellular CCR2 and the trafficking of these neutrophils to the blood is CCR2 and monocyte-dependent (Fujimura et al., 2015). Thus, it may be that that tumour-infiltrating neutrophils in *Cxcr2* flox have an increase in *Ccr2* expression to compensate for the loss of *Cxcr2* expression.

Alternative signalling coming from the tumour microenvironment may likely to have attracted the neutrophils to facilitate their growth and progression:

We have observed an upregulation of *Mif*, *Stat1*, *Stat3*, and downregulation of *Csf3* (G-CSF) in neutrophil-infiltrated *Cxcr2* flox tumours compared to non-neutrophil infiltrated *Cxcr2* flox (Figure 6.6 and 6.7). *Mif* is a cytokine reported in neutrophil activation and recruitment (Schiwon et al., 2014; Dumitru et al., 2011). It has been shown that tumour-derived *Mif* could enhance the survival and activation of pro-tumorigenic neutrophils (Dumitru et al., 2011). Tumour-derived *Mif* was also reported to suppress CD8⁺ activities (Zhou et al., 2008). In bladder cancer, *Mif* was shown to promote the aggressiveness of bladder

cancer cells by increasing cell proliferation and angiogenesis (Choudhary et al., 2013). Stat1 and Stat3 were associated with the pro-inflammatory tumour microenvironment that could promote tumour cell proliferation, survival, invasion angiogenesis and immunosuppression (Yu et al., 2014; Ernst et al., 2008). Tumour could escape the cytotoxic effects of immunity by inducing the anti-apoptotic mechanism, which includes persistent upregulation of STAT3 (Schreiber et al., 2011). In contrast, it has been shown that Csf3 (also known as G-CSF) could negatively regulate CXCR2-mediated neutrophil recruitment (Bajrami et al., 2016). Blocking of G-CSF in mice induced with inflammation led to an elevation of circulating neutrophils (Bajrami et al., 2016). Therefore, I hypothesise that the upregulation of Stat1, Stat3 and Mif, together with the downregulation of G-CSF may lead to the changes in the inflammatory signalling to create an influx of tumour-infiltrating neutrophils.

Due to the tumour pressure, immature neutrophils may likely to have been released from the bone marrow, and the tumour pressure also has led to the granulocytic expansion and prolonged neutrophil lifespan: The expansion and prolongation of neutrophil lifespan could be driven by the secretion of inflammatory chemokines by the tumour cells alone or together with their associated stroma cells (Grivennikov et al., 2010a). Tumour microenvironment could alter the chemokine expressions on tumour-infiltrating neutrophils and prolong their survival via secretion of IL-8 that later helps to recruit more neutrophils (Eruslanov et al., 2014). In the presence of the tumour, the half-life of circulating neutrophils increased to 17 hours compared to only 7 hours in normal conditions (Steinbach et al., 1979; Coffelt et al., 2016).

Immature neutrophil populations were associated with low expression of Ly6G and lack of CXCR2 expression (Ly6G^{lo}/+CXCR2⁻) (Evrard et al., 2018). Furthermore, low expression of granule-related proteins, including MPO, was observed in tumour-infiltrating neutrophils compared to bone marrow-naïve neutrophils (Shaul et al., 2016). Hence, it may be that the persistence of inflammation induced by carcinogen treatment in combination with the lack of Cxcr2 in this study could have driven to neutrophil exhaustion which later led to the release of the immature neutrophil population, a condition known as left shift (Leach et al., 2017; Honda et al., 2016; Sagiv et al., 2015; Behrman et al., 1981). In the left-shift condition, the demand of the neutrophils surpass the amount that been produced by the bone marrow, thus lead to the release of immature phenotype of neutrophils; myelocytes, metamyelocytes, and band neutrophils in the peripheral blood (Honda et al., 2016; Harvey et al., 2012). The increase in the immature neutrophil population has been observed in samples taken from human and mouse bearing breast cancer, lung cancer and head and neck cancer (Moses et al., 2016; Sagiv et al., 2015).

8.2.5 Cxcr2 loss may dysregulate senescence leading to bladder tumorigenesis

We found that the senescence pathway was dysregulated in the absence of Cxcr2 at the later stage of bladder tumorigenesis (Figure 4.9). High expression of p53 observed in Cxcr2 flox, and Cxcr2 ko did not lead to the same amount of p21 expression. In these two cohorts, p21 either failed to be activated in the areas of DNA damage or even when p21 is expressed, tumour cells were still able to undergo proliferation.

In normal cellular responses, DNA damage leads to either cell cycle arrest, to allow the lesions to be repaired, or apoptosis. In DNA damage response pathway that leads to cell cycle arrest, p53 will be stabilised and transcriptionally activated, which then leads to activation of its downstream, p21. This downstream factor is an important inhibitor for cyclin-dependent kinases (CDKs) to induce senescence/cell cycle arrest at G1/S phase (Bartek & Lukas, 2001). Tumour cells in the Cxcr2 flox and Cxcr2 ko mice may have evaded the senescence by manipulating the defective in p53-transcriptional activated p21.

Increase in cell proliferation has long been associated with tumour progression (Ventura et al., 2007). This was also observed in the tumour area of Cxcr2 flox, indicated by the increased expression of Ki67. The expression of Ki67 has been suggested to be used as a prognostic marker for tumour recurrence and progression in NMIBC (Ding et al., 2014). Its expression is associated with higher grade and risk of recurrence of this cancer (Ding et al., 2014).

The roles of Cxcr2 in regulating senescence-associated protein expressions were reported by Acosta and colleagues (2009). In their study, senescence accumulated in the premalignant stage of prostate cancer was associated with a high level of Cxcr2 and loss of Cxcr2 expression lead to a reduction in the severity of the arrest (Acosta & Gil, 2009; Acosta et al., 2008).

It was also reported previously that tumour suppression by senescence was accompanied by the presence of tumour-infiltrating neutrophils, macrophages and natural killer cells (Xue et al., 2007). Under conditions that favour acute activation of senescence via p53, an innate immune response will be subsequently elicited, resulting in the regression of the tumour (Xue *et al.*, 2007). Taken together, I hypothesise that Cxcr2 may have a role in the activation of the senescence-associated pathway in association with its roles in the recruitment of immune cells.

8.3 Targeted therapy in bladder cancer

The main goal of pre-clinical cancer research is to provide new therapies in treating cancer patients. Based on the results in this study and previous studies, below, it would

be useful to evaluate whether targeting of FGFR3 signalling, neutrophils and CXCR2, could be beneficial for bladder cancer patients.

8.3.1 FGFR3-targeted therapy in bladder cancer

Pre-clinical studies have shown promising results in targeting FGFR3 with the effects on reducing bladder cancer cell proliferation (Di Martino et al., 2016). Dovitinib, an FGFR3 tyrosine kinase inhibitor, has been tested in a phase II clinical trial on NMIBC patients that were non-responsive to BCG treatment (Hahn et al., 2017). One out of three patients with FGFR3 mutation showed a complete response, while all patients without FGFR3 mutation were non-responsive (n= 9/9). FGFR3 S249C mutation was associated with resistant towards pazopanib, a selective multi-targeted receptor tyrosine kinase inhibitor (Pinciroli et al., 2016).

Drugs targeting FGFR3 are now being pursued in clinical trials with the combination of checkpoint inhibitors (Ibrahim et al., 2019). Several studies have examined the relationship between FGFR3 alteration and leukocyte infiltration (Borcoman et al., 2019; Sweis et al., 2016). Sweis and colleagues (2016), for example, have found out that FGFR3 mutation alongside β -Catenin and PPAR- γ were associated with T cell exclusion in MBIC.

Targeting FGFR3 mutation using small molecule inhibitors may bring more benefit in NMIBC compared to MBIC given the ability of FGFR3 to stabilize the tumour phenotype in NMIBC (Iyer & Milowsky, 2013).

8.3.2 Neutrophil-targeted therapy in bladder cancer

The BCG treatment given to the intermediate and high risk of NMIBC was associated with neutrophil activities in inducing the production of tumour necrosis factor-related apoptosis-inducing ligand (TRAIL) to suppress tumour cells (Simons et al., 2008; Saban et al., 2007; Suttman et al., 2006; Ludwig et al., 2004).

NLR has been shown as a prognostic marker for disease recurrence, but not disease progression, in NMIBC (Mano et al., 2015; Favilla et al., 2016). It was shown that tumour inflammation influenced the alterations of NLR in NMIBC (Favilla et al., 2016). Lower NLR and low expression of immune gene signature were observed in NMIBC compared to MIBC (Borcoman et al., 2019; Madonia et al., 2018). However, some NMIBC patients showed high NLR, and this was associated with poor prognosis of bladder cancer (Kaiser et al., 2018; Madonia et al., 2018). In the NMIBC patients with low NLR, an agonist for a neutrophil function could aid the induction of local anti-tumour immune response.

In contrast, MIBC was shown to have a high expression of immune gene signature, which could make it susceptible to neutrophil therapy target (Borcman et al., 2019). In MIBC patients, high NLR at pre- and mid neoadjuvant chemotherapy was associated with lower disease-free survival and median overall survival (Kaiser et al., 2018). A high NLR post adjuvant treatment was shown to be a predictive marker for tumour recurrence in MIBC (Kawahara et al., 2016; Morizawa et al., 2016). An increase in immunosuppressive, granulocytic MDSC subset was observed in the peripheral blood and tumour tissue of NMIBC and MIBC patients that did not undergo any BCG therapy (Eruslanov et al., 2012).

G-CSF is a regulator for neutrophil haematopoiesis and chemotaxis (Roberts, 2005). Combination with G-CSF reduces the toxicity of methotrexate, vinblastine, doxorubicin, and cisplatin (MVAC) treatment in inoperable or metastatic bladder cancer (Bellmunt et al., 2014; Bamias et al., 2004).

8.3.3 CXCR2-targeted therapy in bladder cancer

CXCR2-CXCL1 axis was associated with recurrence of NMIBC through activation of PI3K signalling (Chen et al., 2017). Strikingly, a high expression of CXCL1 was observed in the tumour tissue and urine of bladder cancer patients and correlates with high grade and invasiveness (Burnier et al., 2015; Miyake, Lawton, et al., 2013; Miyake, Goodison, et al., 2013; Kawanishi et al., 2008). In addition, a high expression of IL8 (also known as CXCL8), another CXCR2 dominant ligand, also correlates with poor prognosis for bladder cancer patients (Reis et al., 2012).

In contrast, in NMIBC, the level of IL8 could be used as a marker of early prognostic response for the BCG treatment (Thalmann et al., 2000). Patients with recurrence after BCG treatment have a lower level of IL8 compared to non-recurrence (Thalman *et al.*, 2000).

Cxcr2 ligands are classified as ELR⁺ chemokines, meaning they are angiogenic factors, in contrast to ELR⁻ chemokines, which inhibit angiogenesis (Jaffer & Ma, 2016). IL8, for example, has been shown to regulate the angiogenesis that leads to metastasis progression in human bladder cancer (Inoue et al., 2000). Therefore, targeting CXCR2 function is likely to inhibit the ligation of the angiogenic factor that favoured the tumour growth in bladder cancer patients.

One of the challenges in targeting neutrophils is that neutrophils may acquire compensatory receptor from Cxcr2 to Ccr2 in the presence of tumour pressure. Combination of small molecule CXCR2 inhibitor (SB225002) (Tocris Bioscience, UK) and small molecule CCR2 inhibitor (RS504393) (Tocris Bioscience, UK) was reported to

improve chemotherapeutic responses in pancreatic cancer mouse model (Nywening et al., 2018).

It was recently shown that bladder cancer patients treated with gemcitabine have high expression of CCR2 that promoted the recruitment of immunosuppressive monocytic-MDSC population (Mu et al., 2019).

It was also reported that anti-neutrophil and CXCR2 inhibitor could be used to augment the response of checkpoint inhibitors such as the PD-1 axis inhibitor (Steele et al., 2016). Zhou et al (2017) investigated the association of neutrophil infiltration and immune status in tumour samples taken from MIBC patients. Patients with low tumour-infiltrating neutrophils have higher activated cytotoxic T cells (CD8⁺) cells in the tumour and higher overall survival compared to patients with high tumour-infiltrating neutrophils. An increase in the number of tumour-infiltrating neutrophils was associated with a decrease in the chemokines associated for the recruitment and activation of T cells and natural killer cells, thus lack anti-tumoral response.

The response towards anti-neutrophils or CXCR2 inhibitor may depend on the quality and quantity of the tumour-infiltrating immune cells. The potential usage of anti-neutrophil and CXCR2 inhibitor on bladder cancer patients should be evaluated based on; 1) The grade and stage of the bladder cancer and, 2) the status of systemic and local inflammation, such as the number of tumour-infiltrating neutrophils, tumour-infiltrating leukocytes (TILs), as well as the NLR, and the level of macrophages.

Prolonged inhibition of neutrophils could lead to neutropenia, a life-threatening condition. Hence, a question remains to be addressed is how to effectively target only the pro-tumour neutrophils without compromising the innate immunity response.

8.4 Limitations

8.4.1 The use of *LysM Cre* mouse model in studying the functions of neutrophils.

The *LysM* activity also affects mature macrophages and CD11c⁺ splenic dendritic cells (Clausen et al., 1999), therefore not specific to neutrophil lineage. For a better specificity to this lineage, it would be useful to use the Catchup mouse model. It is a model with neutrophil-selective genetic ablation via locus Ly6G with a knock-in allele expressing Cre recombinase (Hasenberg et al., 2015). The Catchup model also expresses the red fluorescent protein tdTomato that could aid visualizing and tracking the neutrophils movement (Hasenberg *et al.*, 2015). Moses and colleague (2016) have reported the use of Catchup model to study about the efficacy of neutrophil depletion using anti Gr-1 or anti Ly6G antibodies in the head and neck cancer model. The use of Catchup model has

allowed them to track the distribution and expansion of immature neutrophils during the course of neutrophil depletion in mice bearing tumours.

8.4.2 Lack of metastasis formation

In a pancreatic cancer model, neutrophils recruitment by *Cxcr2* was shown to be pro-tumorigenic and served as the primary source for metastasis colonization (Steele et al., 2016). We were unable to investigate the effects of *Cxcr2* depletion on establishment and progression of metastasis, as none of the mice in this study developed metastasis.

Our preliminary data on the lymph nodes harvested from *Cxcr2* flox mice with bladder tumour showed a higher presence of neutrophil population compared to lymph nodes from wt mice with a bladder tumour (unpublished). An increase in the neutrophil population was considered as a pre-metastatic condition (Jablonska et al., 2017). It will be interesting to evaluate whether the long-term suppression of *Cxcr2* has an impact on metastasis progression in bladder tumour.

Two potential approaches in establishing the metastatic model of bladder cancer are firstly by prolonging the carcinogen course and secondly, by orthotopic xenograft of *Cxcr2* flox tumour cells into immunocompetent C57Bl/6 mice. Several studies using transgenic mice treated with 0.05% (v/v) OH-BBN between 12 to 45 weeks have shown distant metastasis in the lymph nodes and lung (Said et al., 2013; Overdevest et al., 2012; Vasconcelos-nóbrega et al., 2012). For example, Said and colleagues (2013) have reported metastasis in the para-aortic lymph nodes (13%, n=46) and lung (5.8%, n=46) in the mice with genetic ablation of secreted protein acidic and rich in cysteine (SPARC) treated with 0.05% OH-BBN for 15 - 25 weeks. Thus, *Cxcr2* flox mice could be treated with OH-BBN for the same duration (15-25 weeks) and with the humane endpoints of survival as follows; mouse displaying discomfort, distress or impair mobility such as hunching, ruffling of coat, reluctant to move and weight loss of ≥ 20 of initial weight.

The use of organoid culture in mouse bladder cancer model has been reported previously (Saito et al., 2018). Saito and colleagues have managed to generate transplantable cell lines from OH-BBN-induced bladder cancer tumour which then engraft into C57Bl/6 mice, in order to study the significance of tumour-immune cell infiltration and the effect on PD-1 axis inhibition.

8.5 Overall conclusions

1. FGFR3 mutation and *Cxcr2* deletion on myeloid lineage enhanced carcinogen-dependent bladder tumorigenesis by suppressing acute inflammatory responses.

2. FGFR3 and CXCR2 are both upstream of PI3K pathway (Ornitz and Itoh, 2015; Gavard et al., 2009; Chen et al., 2005). PI3K signalling has been regarded as an important pathway for neutrophil recruitment and migration towards inflammatory sites (Cheng et al., 2019; Hawkins et al., 2010).

3. It is likely that neutrophils played the key immune regulator in exaggerating the effects observed in FGFR3-mutated and *Cxcr2* flox mouse models at the acute inflammation stage as well as tumour-initiation, promotion and progression stages.

4. Defect in acute inflammatory responses together with the accumulation of DNA damage due to the failure in the maintenance of senescence led to failure in resolving pathogenic inflammation.

5. The transient increase in circulating and tissue-infiltrating macrophages at tumour initiation stage led to the establishment of the inflamed microenvironment in *Cxcr2* flox.

6. The inflamed microenvironment was sustained as the tumour progress in *Cxcr2* flox with the possibilities of phenotypic changes of neutrophils recruited to the tumour microenvironment.

7. The established tumour induced pro-inflammatory signalling to aid their growth and progression.

8. Targeting neutrophils and *Cxcr2* in a murine model of bladder tumour is possible but need further optimization to enhance the efficacy of drug/anti-monoclonal antibody deliveries.

8.6 Future directions

The questions that need to be addressed in the future include:

1) What may have caused the discrepancy in the number of neutrophils identified based on morphology (H&E) with the neutrophils' IHC markers (1A8, NIMP, MPO)?

The discrepancy between the H&E and IHC markers at 20 weeks of the tumour samples might indicate a population of immature neutrophils that might lack the granular morphology. Further analysis and profiling of the neutrophils using multiplex immunohistochemistry for simultaneous identification of multiple neutrophil surface markers for immature neutrophils such as Cd101, c-KIT/Cd117 and Cd34 (Mackey et al., 2019).

2) Can we distinguish the pro-tumoral and anti-tumoral neutrophils in Cxcr2 flox tumour by specific markers or gene expression?

It will be useful to isolate and phenotype the tumour infiltrated neutrophils from Cxcr2 flox tumour by performing single-cell analysis such as RNAseq or by the analysing protein expression related to immune activities using flow cytometry (as discussed in 8.2.3) Additionally, the suppression activities of the isolated tumour-associated neutrophils from the Cxcr2 flox could be assessed by culturing the cells in vitro and perform the T-cell proliferation assay (Sionov et al., 2015).

3) Does Cxcr2 has any roles in the metastasis in bladder cancer?

As discussed in Section 8.4.2, the next task will be to find ways to induce metastatic progression in our bladder cancer model by using potential approaches such as by prolonging the carcinogen course and/or by orthotopic xenograft of highly metastatic tumour cells. Treatment with Cxcr2 inhibitor in mice bearing tumour and before the time-point for metastasis will allow us to determine whether Cxcr2 play any roles in the initiation and metastatic progression.

4) What contributes to the bladder tissue-specific role of CXCR2 and the neutrophils?

Bladder-specific effects of Cxcr2 deletion can be assessed by using UroII Cre for the conditional deletion of Cxcr2 allele.

References

- Abraham, S.N. & Miao, Y. (2015) The nature of immune responses to urinary tract infections. *Nature Reviews Immunology*, 15 (10), pp.655–663. Available from: <<http://dx.doi.org/10.1038/nri3887>>.
- Acharyya, S., Oskarsson, T., Vanharanta, S., Malladi, S., Kim, J., Morris, P.G., Manova-Todorova, K., Leversha, M., Hogg, N., Seshan, V.E., Norton, L., Brogi, E. & Massagué, J. (2012) A CXCL1 paracrine network links cancer chemoresistance and metastasis. *Cell*, 150 (1), pp.165–178.
- Acosta, J.C. & Gil, J. (2009) A role for CXCR2 in senescence, but what about in cancer? *Cancer Research*, 69 (6), pp.2167–2170.
- Acosta, J.C., O’Loghlen, A., Banito, A., Guijarro, M. V., Augert, A., Raguz, S., Fumagalli, M., Da Costa, M., Brown, C., Popov, N., Takatsu, Y., Melamed, J., d’Adda di Fagagna, F., Bernard, D., Hernandez, E. & Gil, J. (2008) Chemokine Signaling via the CXCR2 Receptor Reinforces Senescence. *Cell*, 133 (6), pp.1006–1018.
- Ahmad, I., Singh, L.B., Foth, M., Morris, C.A., Taketo, M.M., Wu, X.R., Leung, H.Y., Sansom, O.J. & Iwata, T. (2011) K-Ras and β -catenin mutations cooperate with Fgfr3 mutations in mice to promote tumorigenesis in the skin and lung, but not in the bladder. *DMM Disease Models and Mechanisms*, 4 (4), pp.548–555.
- Ahmad, I., Sansom, O.J. & Leung, H.Y. (2012) Exploring molecular genetics of bladder cancer: Lessons learned from mouse models. *DMM Disease Models and Mechanisms*, 5 (3), pp.323–332.
- Akagi, K., Sandig, V., Vooijs, M., Van Der Valk, M., Giovannini, M., Strauss, M. & Berns, A. (1997) Cre-mediated somatic site-specific recombination in mice. *Nucleic Acids Research*, 25 (9), pp.1766–1773.
- Altzner, F., Martinelli, S., Yousefi, S., Thürig, C., Schmid, I., Conway, E.M., Schöni, M.H., Vogt, P., Mueller, C., Fey, M.F., Zangemeister-Wittke, U. & Simon, H.U. (2004) Inflammation-associated cell cycle-independent block of apoptosis by survivin in terminally differentiated neutrophils. *Journal of Experimental Medicine*, 199 (10), pp.1343–1354.
- American Cancer Society 2020, Immunotherapy for Bladder cancer, viewed 24 April 2020, <<https://www.cancer.org/cancer/bladder-cancer/treating/immunotherapy-for-bladder-cancer.html>>.
- Andzinski, L., Wu, C.F., Lienenklaus, S., Kröger, A., Weiss, S. & Jablonska, J. (2015) Delayed apoptosis of tumor associated neutrophils in the absence of endogenous IFN- β . *International Journal of Cancer*, 136 (3), pp.572–583.
- Antoni, S., Ferlay, J., Soerjomataram, I., Znaor, A., Jemal, A. & Bray, F. (2017) Bladder Cancer Incidence and Mortality: A Global Overview and Recent Trends. *European Urology*, 71 (1), pp.96–108. Available from: <<http://dx.doi.org/10.1016/j.eururo.2016.06.010>>.
- Aras, S. & Raza Zaidi, M. (2017) TAMEless traitors: Macrophages in cancer progression and metastasis. *British Journal of Cancer*, 117 (11), pp.1583–1591. Available from: <<http://dx.doi.org/10.1038/bjc.2017.356>>.

- Arikawa, E., Sun, Y., Wang, J., Zhou, Q., Ning, B., Dial, S.L., Guo, L. & Yang, J. (2008) Cross-platform comparison of SYBR® Green real-time PCR with TaqMan PCR, microarrays and other gene expression measurement technologies evaluated in the MicroArray Quality Control (MAQC) study. *BMC Genomics*, 9, pp.1–12.
- Arwert, E.N., Harney, A.S., Entenberg, D., Wang, Y., Sahai, E., Pollard, J.W. & Condeelis, J.S. (2018) A Unidirectional Transition from Migratory to Perivascular Macrophage Is Required for Tumor Cell Intravasation. *Cell Reports*, 23 (5), pp.1239–1248. Available from: <<https://doi.org/10.1016/j.celrep.2018.04.007>>.
- AU Guidelines. Edn. presented at the EAU Annual Congress Barcelona 2019. ISBN 978-94-92671-04-2.
- Baggiolini, M. & Loetscher, P. (2000) Chemokines in inflammation and immunity. *Immunology Today*, 21 (9), pp.418–420.
- Bajrami, B., Zhu, H., Kwak, H.J., Mondal, S., Hou, Q., Geng, G., Karatepe, K., Zhang, Y.C., Nombela-Arrieta, C., Park, S.Y., Loison, F., Sakai, J., Xu, Y., Silberstein, L.E. & Luo, H.R. (2016) G-CSF maintains controlled neutrophil mobilization during acute inflammation by negatively regulating CXCR2 signaling. *Journal of Experimental Medicine*, 213 (10), pp.1999–2018.
- Baker, S.C. & Southgate, J. (2011) Electrospinning for Tissue Regeneration. *Electrospinning for Tissue Regeneration*, pp.225–241. Available from: <<http://www.sciencedirect.com/science/article/pii/B9781845697419500112>>.
- Balkwill, F. & Mantovani, A. (2001) Inflammation and cancer: Back to Virchow? *Lancet*, 357 (9255), pp.539–545.
- Bamias, A., Aravantinos, G., Deliveliotis, C., Bafaloukos, D., Kalofonos, C., Xiros, N., Zervas, A., Mitropoulos, D., Samantas, E., Pectasides, D., Papakostas, P., Gika, D., Kourousis, C., Koutras, A., Papadimitriou, C., Bamias, C., Kosmidis, P. & Dimopoulos, M.A. (2004) Docetaxel and cisplatin with granulocyte colony-stimulating factor (G-CSF) versus MVAC with G-CSF in advanced urothelial carcinoma: A multicenter, randomized, phase III study from the Hellenic Cooperative Oncology Group. *Journal of Clinical Oncology*, 22 (2), pp.220–228.
- Bardoel, B.W., Kenny, E.F., Sollberger, G. & Zychlinsky, A. (2014) The balancing act of neutrophils. *Cell Host and Microbe*, 15 (5), pp.526–536. Available from: <<http://dx.doi.org/10.1016/j.chom.2014.04.011>>.
- Bartek, J. & Lukas, J. (2001) Mammalian G1- and S-phase checkpoints in response to DNA damage. *Current Opinion in Cell Biology*, 13 (6), pp.738–747.
- Bartek, J., Hodny, Z. & Lukas, J. (2008) Cytokine loops driving senescence. *Nature Cell Biology*, 10 (8), pp.887–889.
- Behrman, R.E., Christensen, R.D., Bradley, P.P. & Rothstein, G. (1981) The leukocyte left shift in clinical and experimental neonatal sepsis. *The Journal of Pediatrics*, 98 (1), pp.101–105.
- Bellmunt, J., De Wit, R., Vaughn, D.J., Fradet, Y., Lee, J.L., Fong, L., Vogelzang, N.J., Climent, M.A., Petrylak, D.P., Choueiri, T.K., Necchi, A., Gerritsen, W., Gurney, H., Quinn, D.I., Culine, S., Sternberg, C.N., Mai, Y., Poehlein, C.H., Perini, R.F. & Bajorin, D.F. (2017) Pembrolizumab as second-line therapy for advanced urothelial carcinoma. *New England Journal of Medicine*, 376 (11), pp.1015–1026.

- Bellmunt, J., Orsola, A., Leow, J.J., Wiegel, T., De Santis, M. & Horwich, A. (2014) Bladder cancer: ESMO practice guidelines for diagnosis, treatment and follow-up. *Annals of Oncology*, 25 (June), pp.iii40–iii48.
- Ben-Sasson, S.Z., Hogg, A., Hu-Li, J., Wingfield, P., Chen, X., Crank, M., Caucheteux, S., Ratner-Hurevich, M., Berzofsky, J.A., Nir-Paz, R. & Paul, W.E. (2013) IL-1 enhances expansion, effector function, tissue localization, and memory response of antigen-specific CD8 T cells. *Journal of Experimental Medicine*, 210 (3), pp.491–502.
- Berger, A. (2000) Science commentary: Th1 and Th2 responses: What are they? *British Medical Journal*, 321 (7258), p.424.
- Bernard-Pierrot, I., Brams, A., Dunois-Lardé, C., Caillault, A., Diez de Medina, S.G., Cappellen, D., Graff, G., Thiery, J.P., Chopin, D., Ricol, D. & Radvanyi, F. (2006) Oncogenic properties of the mutated forms of fibroblast growth factor receptor 3b. *Carcinogenesis*, 27 (4), pp.740–747.
- Bertini, R., Allegretti, M., Bizzarri, C., Moriconi, A., Locati, M., Zampella, G., Cervellera, M.N., Di Cioccio, V., Cesta, M.C., Galliera, E., Martinez, F.O., Di Bitondo, R., Troiani, G., Sabbatini, V., D'Anniballe, G., Anacardio, R., Cutrin, J.C., Cavaliere, B., Mainiero, F., Strippoli, R., Villa, P., Di Girolamo, M., Martin, F., Gentile, M., Santoni, A., Corda, D., Poli, G., Mantovani, A., Ghezzi, P. & Colotta, F. (2004) Noncompetitive allosteric inhibitors of the inflammatory chemokine receptors CXCR1 and CXCR2: Prevention of reperfusion injury. *Proceedings of the National Academy of Sciences of the United States of America*, 101 (32), pp.11791–11796.
- Billerey, C., Chopin, D., Bralet, M., Lahaye, J., Abbou, C.C., Bonaventure, J., Zafrani, S., Kwast, T. Van Der, Thiery, J.P. & Radvanyi, F. (2001) Short Communication. , 158 (6), pp.1955–1959.
- Bizzarri, C., Beccari, A.R., Bertini, R., Cavicchia, M.R., Giorgini, S. & Allegretti, M. (2006) ELR+ CXC chemokines and their receptors (CXC chemokine receptor 1 and CXC chemokine receptor 2) as new therapeutic targets. *Pharmacology and Therapeutics*, 112 (1), pp.139–149.
- Blum, J.S., Wearsch, P.A. & Cresswell, P. (2013) IY31CH16-Cresswell Pathways of Antigen Processing. Available from: <www.annualreviews.org>.
- Borcoman, E., De La Rochere, P., Richer, W., Vacher, S., Chemlali, W., Krucker, C., Sirab, N., Radvanyi, F., Allory, Y., Pignot, G., Barry de Longchamps, N., Damotte, D., Meseure, D., Sedlik, C., Bieche, I. & Piaggio, E. (2019) Inhibition of PI3K pathway increases immune infiltrate in muscle-invasive bladder cancer. *Oncolmmunology*, 8 (5).
- Brandau, S., Dumitru, C.A. & Lang, S. (2013) Protumor and antitumor functions of neutrophil granulocytes. *Seminars in Immunopathology*, 35 (2), pp.163–176.
- Bronte, V., Apolloni, E., Cabrelle, A., Ronca, R., Serafini, P., Zamboni, P., Restifo, N.P. & Zanovello, P. (2000) Identification of a CD11b+/Gr-1+/CD31+ myeloid progenitor capable of activating or suppressing CD8+ T cells. *Blood*, 96 (12), pp.3838–3846.
- Burger, M., Catto, J.W.F., Dalbagni, G., Grossman, H.B., Herr, H., Karakiewicz, P., Kassouf, W., Kiemenev, L. a., La Vecchia, C., Shariat, S. & Lotan, Y. (2013)

Epidemiology and risk factors of urothelial bladder cancer. *European Urology*, 63, pp.234–241. Available from: <<http://dx.doi.org/10.1016/j.eururo.2012.07.033>>.

- Burnier, A., Shimizu, Y., Dai, Y., Nakashima, M., Matsui, Y., Ogawa, O., Rosser, C.J. & Furuya, H. (2015) CXCL1 is elevated in the urine of bladder cancer patients. *SpringerPlus*, 4 (1), pp.1–6.
- Burt, R.K. & Verda, L. (2004) *Immune Reconstitution*. Elsevier Inc. Available from: <<http://dx.doi.org/10.1016/B978-0-12-436643-5.50158-9>>.
- Campbell, L.M., Maxwell, P.J. & Waugh, D.J.J. (2013) Rationale and means to target pro-inflammatory interleukin-8 (CXCL8) signaling in cancer.
- Cancer Research UK 2019, Bladder cancer, viewed 26 October 2019, <<http://www.cancerresearchuk.org/about-cancer/type/bladder-cancer/>>.
- Cancilla, B., Ford-Perriss, M.D. & Bertram, J.F. (1999) Expression and localization of fibroblast growth factors and fibroblast growth factor receptors in the developing rat kidney. *Kidney International*, 56 (6), pp.2025–2039.
- Caruso, R.A., Bellocco, R., Pagano, M., Bertoli, G., Rigoli, L. & Inferrera, C. (2002) Prognostic value of intratumoral neutrophils in advanced gastric carcinoma in a high-risk area in Northern Italy. *Modern Pathology*, 15 (8), pp.831–837.
- Cassetta, L., Fragkogianni, S., Sims, A.H., Swierczak, A., Forrester, L.M., Zhang, H., Soong, D.Y.H., Cotechini, T., Anur, P., Lin, E.Y., Fidanza, A., Lopez-Yrigoyen, M., Millar, M.R., Urman, A., Ai, Z., Spellman, P.T., Hwang, E.S., Dixon, J.M., Wiechmann, L., Coussens, L.M., Smith, H.O. & Pollard, J.W. (2019) Human Tumor-Associated Macrophage and Monocyte Transcriptional Landscapes Reveal Cancer-Specific Reprogramming, Biomarkers, and Therapeutic Targets. *Cancer Cell*, 35 (4), pp.588-602.e10. Available from: <<https://doi.org/10.1016/j.ccell.2019.02.009>>.
- Castillo-Martin, M., Domingo-Domenech, J., Karni-Schmidt, O., Matos, T. & Cordon-Cardo, C. (2010) Molecular pathways of urothelial development and bladder tumorigenesis. *Urologic Oncology: Seminars and Original Investigations*, 28 (4), pp.401–408. Available from: <<http://dx.doi.org/10.1016/j.urolonc.2009.04.019>>.
- Centers for Disease Control and Prevention (US); National Center for Chronic Disease Prevention and Health Promotion (US); Office on Smoking and Health (US). *How Tobacco Smoke Causes Disease: The Biology and Behavioral Basis for Smoking-Attributable Disease: A Report of the Surgeon General*. Atlanta (GA): Centers for Disease Control and Prevention (US); 2010. Available from: <https://www.ncbi.nlm.nih.gov/books/NBK53017/>
- Chao, T., Furth, E.E. & Vonderheide, R.H. (2016) CXCR2-dependent accumulation of tumor-associated neutrophils regulates T-cell immunity in pancreatic ductal adenocarcinoma. *Cancer Immunology Research*, 4 (11), pp.968–982.
- Cheadle, E.J., Lipowska-Bhalla, G., Dovedi, S.J., Fagnano, E., Klein, C., Honeychurch, J. & Illidge, T.M. (2017) A TLR7 agonist enhances the antitumor efficacy of obinutuzumab in murine lymphoma models via NK cells and CD4 T cells. *Leukemia*, 31 (7), pp.1611–1621. Available from: <<http://dx.doi.org/10.1038/leu.2016.352>>.
- Chen, J., Williams, I.R., Lee, B.H., Duclos, N., Huntly, B.J.P., Donoghue, D.J. & Gilliland, D.G.

- (2005) Constitutively activated FGFR3 mutants signal through PLC γ -dependent and -independent pathways for hematopoietic transformation. *Blood*, 106 (1), pp.328–337.
- Chen, C., Xu, Z.Q., Zong, Y.P., Ou, B.C., Shen, X.H., Feng, H., Zheng, M.H., Zhao, J.K. & Lu, A.G. (2019) CXCL5 induces tumor angiogenesis via enhancing the expression of FOXD1 mediated by the AKT/NF- κ B pathway in colorectal cancer. *Cell Death and Disease*, 10 (3). Available from: <<http://dx.doi.org/10.1038/s41419-019-1431-6>>.
- Chen, D.S. & Mellman, I. (2013) Review Oncology Meets Immunology: The Cancer-Immunity Cycle. *Immunity*, 39 (step 3), pp.1–10.
- Chen, J., Williams, I.R., Lee, B.H., Duclos, N., Huntly, B.J.P., Donoghue, D.J. & Gilliland, D.G. (2005) Constitutively activated FGFR3 mutants signal through PLC γ -dependent and -independent pathways for hematopoietic transformation. *Blood*, 106 (1), pp.328–337.
- Chen, L., Pan, X.W., Huang, H., Gao, Y., Yang, Q.W., Wang, L.H., Cui, X.G. & Xu, D.F. (2017) Epithelial-mesenchymal transition induced by GRO- α -CXCR2 promotes bladder cancer recurrence after intravesical chemotherapy. *Oncotarget*, 8 (28), pp.45274–45285.
- Chen, X., Oppenheim, J. J, and Howard, O. M. Z (2005) BALB/c mice have more CD4+CD25+ T regulatory cells and show greater susceptibility to suppression of their CD4+CD25- responder T cells than C57BL/6 mice. *Journal of Leukocyte Biology*, 78 (1), pp.114–121.
- Cheng, Y., Ma, X. lei, Wei, Y. quan & Wei, X.W. (2019) Potential roles and targeted therapy of the CXCLs/CXCR2 axis in cancer and inflammatory diseases. *Biochimica et Biophysica Acta - Reviews on Cancer*, 1871 (2), pp.289–312. Available from: <<https://doi.org/10.1016/j.bbcan.2019.01.005>>.
- Cheung, G., Sahai, A., Billia, M., Dasgupta, P. & Khan, M.S. (2013) Recent advances in the diagnosis and treatment of bladder cancer. *BMC medicine*, 11, p.13.
- Choudhary, S., Hegde, P., Pruitt, J.R., Sielecki, T.M., Choudhary, D., Scarpato, K., DeGraff, D.J., Pilbeam, C.C. & Taylor, J.A. (2013) Macrophage migratory inhibitory factor promotes bladder cancer progression via increasing proliferation and angiogenesis. *Carcinogenesis*, 34 (12), pp.2891–2899.
- Chow, A., Brown, B.D. & Merad, M. (2011) Studying the mononuclear phagocyte system in the molecular age. *Nature Reviews Immunology*, 11 (11), pp.788–798.
- Christoffersson, G., Vågesjö, E., Vandooren, J., Lidén, M., Massena, S., Reinert, R.B., Brissova, M., Powers, A.C., Opdenakker, G. & Phillipson, M. (2012) VEGF-A recruits a proangiogenic MMP-9-delivering neutrophil subset that induces angiogenesis in transplanted hypoxic tissue. *Blood*, 120 (23), pp.4653–4662.
- Cirillo, E., Parnell, L.D. & Evelo, C.T. (2017) A review of pathway-based analysis tools that visualize genetic variants. *Frontiers in Genetics*, 8 (NOV), pp.1–11.
- Clark, R. & Kupper, T. (2005) Old meets new: The interaction between innate and adaptive immunity. *Journal of Investigative Dermatology*, 125 (4), pp.629–637.

- Clausen, B.E., Burkhardt, C., Reith, W., Renkawitz, R. & Förster, I. (1999) Conditional gene targeting in macrophages and granulocytes using LysMcre mice. *Transgenic Research*, 8 (4), pp.265–277.
- Clouston, D. & Lawrentschuk, N. (2013) Metaplastic conditions of the bladder. *BJU International*, 112 (SUPPL. 2), pp.27–31.
- Coelho, F.M., Pinho, V., Amaral, F.A., Sachs, D., Costa, V. V., Rodrigues, D.H., Vieira, A.T., Silva, T.A., Souza, D.G., Bertini, R., Teixeira, A.L. & Teixeira, M.M. (2008) The chemokine receptors CXCR1/CXCR2 modulate antigen-induced arthritis by regulating adhesion of neutrophils to the synovial microvasculature. *Arthritis and Rheumatism*, 58 (8), pp.2329–2337.
- Coffelt, S.B., Kersten, K., Doornebal, C.W., Weiden, J., Vrijland, K., Hau, C.S., Verstegen, N.J.M., Ciampricotti, M., Hawinkels, L.J.A.C., Jonkers, J. & De Visser, K.E. (2015) IL-17-producing $\gamma\delta$ T cells and neutrophils conspire to promote breast cancer metastasis. *Nature*, 522 (7556), pp.345–348.
- Coffelt, S.B., Wellenstein, M.D. & De Visser, K.E. (2016) Neutrophils in cancer: Neutral no more. *Nature Reviews Cancer*, 16 (7), pp.431–446. Available from: <<http://dx.doi.org/10.1038/nrc.2016.52>>.
- Coussens, L.M. & Werb, Z. (2002) Inflammation and cancer. *Nature*, 420 (6917), pp.860–867. Available from: <<https://doi.org/10.1038/nature01322>>.
- Courtney, A.H., Lo, W.L. & Weiss, A. (2018) TCR Signaling: Mechanisms of Initiation and Propagation. *Trends in Biochemical Sciences*, 43 (2), pp.108–123. Available from: <<http://dx.doi.org/10.1016/j.tibs.2017.11.008>>.
- Cross, M., Mangelsdorf, I., Wedel, A. & Renkawitz, R. (1988) Mouse lysozyme M gene: Isolation, characterization, and expression studies. *Proceedings of the National Academy of Sciences of the United States of America*, 85 (17), pp.6232–6236.
- Cumberbatch, M.G.K., Jubber, I., Black, P.C., Esperto, F., Figueroa, J.D., Kamat, A.M., Kiemenev, L., Lotan, Y., Pang, K., Silverman, D.T., Znaor, A. & Catto, J.W.F. (2018) Epidemiology of Bladder Cancer: A Systematic Review and Contemporary Update of Risk Factors in 2018. *European Urology*, 74 (6), pp.784–795. Available from: <<https://doi.org/10.1016/j.eururo.2018.09.001>>.
- Daley, J.M., Thomay, A.A., Connolly, M.D., Reichner, J.S. & Albina, J.E. (2008) Use of Ly6G-specific monoclonal antibody to deplete neutrophils in mice. *Journal of Leukocyte Biology*, 83 (1), pp.64–70.
- Dancey, J.T., Deubelbeiss, K.A. & Harker and Finch, L.A.C.A. (1976) Neutrophil kinetics in man. *Journal of Clinical Investigation*, 58 (3), pp.705–715.
- Davies, L.C., Jenkins, S.J., Allen, J.E. & Taylor, P.R. (2013) Tissue-resident macrophages. *Nature Immunology*, 14 (10), pp.986–995.
- De Graaff, M.A., De Rooij, M.A.J., Van Den Akker, B.E.W.M., Gelderblom, H., Chibon, F., Coindre, J.M., Marino-Enriquez, A., Fletcher, J.A., Cleton-Jansen, A.M. & Bovée, J.V.M.G. (2016) Inhibition of Bcl-2 family members sensitises soft tissue leiomyosarcomas to chemotherapy. *British Journal of Cancer*, 114 (11), pp.1219–1226.
- De La Peña, F.A., Kanasaki, K., Kanasaki, M., Tangirala, N., Maeda, G. & Kalluri, R. (2011) Loss of p53 and acquisition of angiogenic microRNA profile are

insufficient to facilitate progression of bladder urothelial carcinoma in situ to invasive carcinoma. *Journal of Biological Chemistry*, 286 (23), pp.20778–20787.

- De Visser, K.E., Eichten, A. & Coussens, L.M. (2006) Paradoxical roles of the immune system during cancer development. *Nature Reviews Cancer*, 6 (1), pp.24–37.
- Devalaraja, R.M., Nanney, L.B., Qian, Q., Du, J., Yu, Y., Devalaraja, M.N. & Richmond, A. (2000) Delayed wound healing in CXCR 2 knockout mice. *Journal of Investigative Dermatology*.
- Di Martino, E., L'He, C.G., Kennedy, W., Tomlinson, D.C. & Knowles, M.A. (2009) Mutant fibroblast growth factor receptor 3 induces intracellular signaling and cellular transformation in a cell type-and mutation-specific manner. *Oncogene*, 28 (48), pp.4306–4316.
- Di Martino, E., Tomlinson, D.C., Williams, S. V. & Knowles, M.A. (2016) A place for precision medicine in bladder cancer: Targeting the FGFRs. *Future Oncology*, 12 (19), pp.2243–2263.
- Ding, W., Gou, Y., Sun, C., Xia, G., Wang, H., Chen, Z., Tan, J., Xu, K. & Qiang, D. (2014) Ki-67 is an independent indicator in non-muscle invasive bladder cancer (NMIBC); Combination of EORTC risk scores and Ki-67 expression could improve the risk stratification of NMIBC. *Urologic Oncology: Seminars and Original Investigations*, 32 (1), pp.42.e13-42.e19.
- Ding, W., Gou, Y., Sun, C., Xia, G., Wang, H., Chen, Z., Tan, J., Xu, K. & Qiang, D. (2014) Ki-67 is an independent indicator in non-muscle invasive bladder cancer (NMIBC); Combination of EORTC risk scores and Ki-67 expression could improve the risk stratification of NMIBC. *Urologic Oncology: Seminars and Original Investigations*, 32 (1), pp.42.e13-42.e19.
- Disis, M.L. & Palucka, K. (2014) Evaluation of cancer immunity in mice. *Cold Spring Harbor Protocols*, 2014 (3), pp.231–234.
- Drabsch, Y. & Ten Dijke, P. (2011) TGF- β signaling in breast cancer cell invasion and bone metastasis. *Journal of Mammary Gland Biology and Neoplasia*, 16 (2), pp.97–108.
- Dumitru, C.A., Gholaman, H., Trelakis, S., Bruderek, K., Dominas, N., Gu, X., Bankfalvi, A., Whiteside, T.L., Lang, S. & Brandau, S. (2011) Tumor-derived macrophage migration inhibitory factor modulates the biology of head and neck cancer cells via neutrophil activation. *International Journal of Cancer*, 129 (4), pp.859–869.
- Dunn, G.P., Bruce, A.T., Ikeda, H., Old, L.J. & Schreiber, R.D. (2002) Cancer immunoediting: from immunosurveillance to tumor escape. *Nature Immunology*, 3 (11), pp.991–998. Available from: <<https://doi.org/10.1038/ni1102-991>>.
- Dunn, G.P., Old, L.J. & Schreiber, R.D. (2004) The immunobiology of cancer immunosurveillance and immunoediting. *Immunity*, 21 (2), pp.137–148.
- Dyer, D.P., Pallas, K., Ruiz, L.M., Schuette, F., Wilson, G.J. & Graham, G.J. (2017) CXCR2 deficient mice display macrophage-dependent exaggerated acute inflammatory responses. *Scientific Reports*, 7 (May 2016), pp.1–11. Available from: <<http://dx.doi.org/10.1038/srep42681>>.

- Eash, K.J., Greenbaum, A.M., Gopalan, P.K. & Link, D.C. (2010) CXCR2 and CXCR4 antagonistically regulate neutrophil trafficking from murine bone marrow. *Journal of Clinical Investigation*, 120 (7), pp.2423–2431.
- Engel, A., Svane, I. M., Rygaard, J. & Werdelin, O. MCA sarcomas induced in scid mice are more immunogenic than MCA sarcomas induced in congenic, immunocompetent mice. *Scand. J. Immunol.* 45, 463–470 (1997).
- Ernst, M., Najdovska, M., Grail, D., Lundgren-May, T., Buchert, M., Tye, H., Matthews, V.B., Armes, J., Bhathal, P.S., Hughes, N.R., Marcusson, E.G., Karras, J.G., Na, S., Sedgwick, J.D., Hertzog, P.J. & Jenkins, B.J. (2008) STAT3 and STAT1 mediate IL-11-dependent and inflammation-associated gastric tumorigenesis in gp130 receptor mutant mice. *Journal of Clinical Investigation*, 118 (5), pp.1727–1738.
- Ernst, M., Najdovska, M., Grail, D., Lundgren-May, T., Buchert, M., Tye, H., Matthews, V.B., Armes, J., Bhathal, P.S., Hughes, N.R., Marcusson, E.G., Karras, J.G., Na, S., Sedgwick, J.D., Hertzog, P.J. & Jenkins, B.J. (2008) STAT3 and STAT1 mediate IL-11-dependent and inflammation-associated gastric tumorigenesis in gp130 receptor mutant mice. *Journal of Clinical Investigation*, 118 (5), pp.1727–1738.
- Eruslanov, E., Neuberger, M., Daurkin, I., Perrin, G.Q., Algood, C., Dahm, P., Rosser, C., Vieweg, J., Gilbert, S.M. & Kusmartsev, S. (2012) Circulating and tumor-infiltrating myeloid cell subsets in patients with bladder cancer. *International Journal of Cancer*, 130 (5), pp.1109–1119.
- Eruslanov, E.B., Bhojnagarwala, P.S., Quatromoni, J.G., Stephen, T.L., Ranganathan, A., Deshpande, C., Akimova, T., Vachani, A., Litzky, L., Hancock, W.W., Conejo-garcia, J.R., Feldman, M., Albelda, S.M. & Singhal, S. (2014) Neut_Tumor-Ass_LK_JCI2015. *The Journal of Clinical Investigation*, 124 (12).
- Evrard, M., Kwok, I.W.H., Chong, S.Z., Teng, K.W.W., Becht, E., Chen, J., Sieow, J.L., Penny, H.L., Ching, G.C., Devi, S., Adrover, J.M., Li, J.L.Y., Liong, K.H., Tan, L., Poon, Z., Foo, S., Chua, J.W., Su, I.H., Balabanian, K., Bachelier, F., Biswas, S.K., Larbi, A., Hwang, W.Y.K., Madan, V., Koeffler, H.P., Wong, S.C., Newell, E.W., Hidalgo, A., Ginhoux, F. & Ng, L.G. (2018) Developmental Analysis of Bone Marrow Neutrophils Reveals Populations Specialized in Expansion, Trafficking, and Effector Functions. *Immunity*, 48 (2), pp.364-379.e8.
- Faget, J., Boivin, G., Ancey, P.-B., Gkasti, A., Mussard, J., Engblom, C., Pfirschke, C., Vazquez, J., Bendriss-Vermare, N., Caux, C., Vozenin, M.-C., Pittet, M.J., Gunzer, M. & Meylan, E. (2018) Efficient and specific Ly6G+ cell depletion: A change in the current practices toward more relevant functional analyses of neutrophils. *bioRxiv*, p.498881. Available from: <<https://www.biorxiv.org/content/10.1101/498881v1>>.
- Fantini, D., Glaser, A.P., Rimar, K.J., Wang, Y., Schipma, M., Varghese, N., Rademaker, A., Behdad, A., Yellapa, A., Yu, Y., Sze, C.C.L., Wang, L., Zhao, Z., Crawford, S.E., Hu, D., Licht, J.D., Collings, C.K., Bartom, E., Theodorescu, D., Shilatfard, A. & Meeks, J.J. (2018) A Carcinogen-induced mouse model recapitulates the molecular alterations of human muscle invasive bladder cancer. *Oncogene*, 37 (14), pp.1911–1925. Available from: <<http://dx.doi.org/10.1038/s41388-017-0099-6>>.
- Favilla, V., Castelli, T., Urzì, D., Reale, G., Privitera, S., Salici, A., Russo, G.I., Cimino, S. & Morgia, G. (2016) Neutrophil to lymphocyte ratio, a biomarker in non-muscle

invasive bladder cancer: A single-institutional longitudinal study. *International Braz J Urol*, 42 (4), pp.685–693.

- Finisguerra, V., Di Conza, G., Di Matteo, M., Serneels, J., Costa, S., Thompson, A.A.R., Wauters, E., Walmsley, S., Prenen, H., Granot, Z., Casazza, A. & Mazzone, M. (2015) MET is required for the recruitment of anti-tumoural neutrophils. *Nature*, 522 (7556), pp.349–353.
- Fleming, T.J., Fleming, M.L. & Malek, T.R. (1993) Selective expression of Ly-6G on myeloid lineage cells in mouse bone marrow. RB6-8C5 mAb to granulocyte-differentiation antigen (Gr-1) detects members of the Ly-6 family. *Journal of immunology (Baltimore, Md. : 1950)*, 151 (5), pp.2399–408. Available from: <<http://www.ncbi.nlm.nih.gov/pubmed/8360469>>.
- Foth, M., Ahmad, I., Van Rhijn, B.W.G., Van Der Kwast, T., Bergman, A.M., King, L., Ridgway, R., Leung, H.Y., Fraser, S., Sansom, O.J. & Iwata, T. (2014) Fibroblast growth factor receptor 3 activation plays a causative role in urothelial cancer pathogenesis in cooperation with Pten loss in mice. *Journal of Pathology*, 233 (2), pp.148–158.
- Foth, M., Ismail, N.F.B., Kung, J.S.C., Tomlinson, D., Knowles, M.A., Eriksson, P., Sjö Dahl, G., Salmond, J.M., Sansom, O.J. & Iwata, T. (2018) FGFR3 mutation increases bladder tumorigenesis by suppressing acute inflammation. *Journal of Pathology*, 246 (3), pp.331–343.
- Frazier, K.S., Seely, J.C., Hard, G.C., Betton, G., Burnett, R., Nakatsuji, S., Nishikawa, A., Durchfeld-Meyer, B. & Bube, A. (2012) Proliferative and Nonproliferative Lesions of the Rat and Mouse Urinary System.
- Freedman, N.D., Silverman, D.T., Hollenbeck, A.R., Schatzkin, A. & Abnet, C.C. (2011) Association between smoking and risk of bladder cancer among men and women. *JAMA - Journal of the American Medical Association*, 306 (7), pp.737–745.
- Freire M.O. & van Dyke T.E. (2013) Natural resolution of inflammation. *Periodontol 2000* 63(1), pp.149-164. Available from: <<https://doi.org/10.1111/prd.12034>>.
- Fridlender, Z.G. & Albelda, S.M. (2012a) Tumor-associated neutrophils: Friend or foe? *Carcinogenesis*, 33 (5), pp.949–955.
- Fridlender, Z.G., Sun, J., Kim, S., Kapoor, V., Cheng, G., Ling, L., Worthen, G.S. & Albelda, S.M. (2009) Polarization of Tumor-Associated Neutrophil Phenotype by TGF- β : 'N1' versus 'N2' TAN. *Cancer Cell*, 16 (3), pp.183–194. Available from: <<http://dx.doi.org/10.1016/j.ccr.2009.06.017>>.
- Fridlender, Z.G., Sun, J., Mishalian, I., Singhal, S., Cheng, G., Kapoor, V., Horng, W., Fridlender, G., Bayuh, R., Worthen, G.S. & Albelda, S.M. (2012b) Transcriptomic analysis comparing tumor-associated neutrophils with granulocytic myeloid-derived suppressor cells and normal neutrophils. *PLoS ONE*, 7 (2).
- Fujimura, N., Xu, B., Dalman, J., Deng, H., Aoyama, K. & Dalman, R.L. (2015) CCR2 inhibition sequesters multiple subsets of leukocytes in the bone marrow. *Scientific Reports*, 5, pp.1–13. Available from: <<http://dx.doi.org/10.1038/srep11664>>.
- Futosi, K., Fodor, S. & Mócsai, A. (2013) Neutrophil cell surface receptors and their intracellular signal transduction pathways. *International Immunopharmacology*,

17 (3), pp.638–650. Available from:
<<http://dx.doi.org/10.1016/j.intimp.2013.06.034>>.

- Gajewski, T.F., Schreiber, H. & Fu, Y.X. (2013) Innate and adaptive immune cells in the tumor microenvironment. *Nature Immunology*, 14 (10), pp.1014–1022.
- Gandhi, D., Molotkov, A., Baturina, E., Schneider, K., Dan, H., Reiley, M., Laufer, E., Metzger, D., Liang, F., Liao, Y., Sun, T.T., Aronow, B., Rosen, R., Mauney, J., Adam, R., Rosselot, C., VanBatavia, J., McMahon, A., McMahon, J., Guo, J.J. & Mendelsohn, C. (2013) Retinoid signaling in progenitors controls specification and regeneration of the urothelium. *Developmental Cell*, 26 (5), pp.469–482. Available from: <<http://dx.doi.org/10.1016/j.devcel.2013.07.017>>.
- Gao, Y., Guan, Z., Chen, J., Xie, H., Yang, Z., Fan, J., Wang, X. & Li, L. (2015) CXCL5/CXCR2 axis promotes bladder cancer cell migration and invasion by activating PI3K/AKT-induced upregulation of MMP2/MMP9. *International Journal of Oncology*, 47 (2), pp.690–700.
- Gavard, J., Hou, X., Qu, Y., Masedunskas, A., Martin, D., Weigert, R., Li, X. & Gutkind, J.S. (2009) A Role for a CXCR2/Phosphatidylinositol 3-Kinase γ Signaling Axis in Acute and Chronic Vascular Permeability. *Molecular and Cellular Biology*, 29 (9), pp.2469–2480.
- George, S.K., Tovar-Sepulveda, V., Shen, S.S., Jian, W., Zhang, Y., Hilsenbeck, S.G., Lerner, S.P. & Smith, C.L. (2013) Chemoprevention of BBN-induced bladder carcinogenesis by the selective Estrogen receptor modulator tamoxifen. *Translational Oncology*, 6 (3), pp.244–255.
- Ghatalia, P., Zibelman, M., Geynisman, D. M. and Plimack, E. (2018) Approved checkpoint inhibitors in bladder cancer: which drug should be used when?. *Therapeutic Advances in Medical Oncology*, 10, pp.1–10.
- Gilroy, D. & Lawrence, T. (2008) The resolution of acute inflammation: A 'tipping point' in the development of chronic inflammatory diseases. In: A. G. Rossi & D. A. Sawatzky eds. *The Resolution of Inflammation*. Basel, Birkhäuser Basel, pp.1–18. Available from: <https://doi.org/10.1007/978-3-7643-7506-5_1>.
- Girardi, M., Glusac, E., Filler, R.B., Roberts, S.J., Propperova, I., Lewis, J., Tigelaar, R.E. & Hayday, A.C. (2003) The distinct contributions of murine T cell receptor (TCR) $\gamma\delta$ + and TCR $\alpha\beta$ + T cells to different stages of chemically induced skin cancer. *Journal of Experimental Medicine*, 198 (5), pp.747–755.
- Girardi, M., Oppenheim, D.E., Steele, C.R., Lewis, J.M., Glusac, E., Filler, R., Hobby, P., Sutton, B., Tigelaar, R.E. & Hayday, A.C. (2018) Regulation of cutaneous malignancy by $\gamma\delta$ T cells. *Journal of Immunology*, 200 (9), pp.3031–3035.
- Gluck, G., Hortopan, M., Stănculeanu, D., Chiriță, M., Stoica, R. & Sinescu, I. (2014) Comparative study of conventional urothelial carcinoma, squamous differentiation carcinoma and pure squamous carcinoma in patients with invasive bladder tumors. *Journal of medicine and life*, 7 (2), pp.211–214.
- Gordon, S. (2003) Alternative activation of macrophages_ *Nature Review.* , 3 (January).
- Görgens, A., Radtke, S., Möllmann, M., Cross, M., Dürig, J., Horn, P.A. & Giebel, B. (2013) Revision of the Human Hematopoietic Tree: Granulocyte Subtypes Derive from Distinct Hematopoietic Lineages. *Cell Reports*, 3 (5), pp.1539–1552.

- Grassi, L., Pourfarzad, F., Ullrich, S., Merkel, A., Were, F., Carrillo-de-Santa-Pau, E., Yi, G., Hiemstra, I.H., Tool, A.T.J., Mul, E., Perner, J., Janssen-Megens, E., Berentsen, K., Kerstens, H., Habibi, E., Gut, M., Yaspo, M.L., Linser, M., Lowy, E., Datta, A., Clarke, L., Flicek, P., Vingron, M., Roos, D., van den Berg, T.K., Heath, S., Rico, D., Frontini, M., Kostadima, M., Gut, I., Valencia, A., Ouwehand, W.H., Stunnenberg, H.G., Martens, J.H.A. & Kuijpers, T.W. (2018) Dynamics of Transcription Regulation in Human Bone Marrow Myeloid Differentiation to Mature Blood Neutrophils. *Cell Reports*, 24 (10), pp.2784–2794. Available from: <<https://doi.org/10.1016/j.celrep.2018.08.018>>.
- Greten, T.F., Manns, M.P. & Korangy, F. (2011) Myeloid derived suppressor cells in human diseases. *International Immunopharmacology*, 11 (7), pp.802–807. Available from: <<http://dx.doi.org/10.1016/j.intimp.2011.01.003>>.
- Grivnennikov, S.I., Greten, F.R. & Karin, M. (2010) Immunity, Inflammation, and Cancer. *Cell*, 140 (6), pp.883–899. Available from: <<http://dx.doi.org/10.1016/j.cell.2010.01.025>>.
- Guthrie, G.J.K., Charles, K.A., Roxburgh, C.S.D., Horgan, P.G., McMillan, D.C. & Clarke, S.J. (2013) The systemic inflammation-based neutrophil-lymphocyte ratio: Experience in patients with cancer. *Critical Reviews in Oncology/Hematology*, 88 (1), pp.218–230. Available from: <<http://dx.doi.org/10.1016/j.critrevonc.2013.03.010>>.
- Haddad, L.E., Khzam, L.B., Hajjar, F., Merhi, Y. & Sirois, M.G. (2011) Characterization of FGF receptor expression in human neutrophils and their contribution to chemotaxis. *American Journal of Physiology - Cell Physiology*, 301 (5), pp.1036–1045.
- Hahn, N.M., Bivalacqua, T.J., Ross, A.E., Netto, G.J., Baras, A., Park, J.C., Chapman, C., Masterson, T.A., Koch, M.O., Bihrl, R., Foster, R.S., Gardner, T.A., Cheng, L., Jones, D.R., McElyea, K., Sandusky, G.E., Breen, T., Liu, Z., Albany, C., Moore, M.L., Loman, R.L., Reed, A., Turner, S.A., De Abreu, F.B., Gallagher, T., Tsongalis, G.J., Plimack, E.R., Greenberg, R.E. & Geynisman, D.M. (2017) A phase II trial of dovitinib in BCG-unresponsive urothelial carcinoma with FGFR3 mutations or overexpression: Hoosier Cancer Research Network trial HCRN 12-157. *Clinical Cancer Research*, 23 (12), pp.3003–3011.
- Han, X., Feng, Y., Chen, X., Gerard, C. & Boisvert, W.A. (2015) Characterization of G protein coupling mediated by the conserved D1343.49 of DRY motif, M2416.34, and F2516.44 residues on human CXCR1. *FEBS Open Bio*, 5, pp.182–190. Available from: <<http://dx.doi.org/10.1016/j.fob.2015.03.001>>.
- Han, X., Shi, H., Sun, Y., Shang, C., Luan, T., Wang, D., Ba, X. & Zeng, X. (2019) Correction: CXCR2 expression on granulocyte and macrophage progenitors under tumor conditions contributes to mo-MDSC generation via SAP18/ERK/STAT3. *Cell Death & Disease*, 10 (9), pp.1–15. Available from: <<http://dx.doi.org/10.1038/s41419-019-1837-1>>.
- Hanahan, D. & Weinberg, R.A. (2011) Hallmarks of cancer: The next generation. *Cell*, 144 (5), pp.646–674. Available from: <<http://dx.doi.org/10.1016/j.cell.2011.02.013>>.
- Harvey, J.W. (2012) Evaluation of Leukocytic Disorders. *Veterinary Hematology*, pp.122–176.
- Hasenberg, A., Hasenberg, M., Männ, L., Neumann, F., Borckenstein, L., Stecher, M., Kraus, A., Engel, D.R., Klingberg, A., Seddigh, P., Abdullah, Z., Klebow, S.,

- Engelmann, S., Reinhold, A., Brandau, S., Seeling, M., Waisman, A., Schraven, B., Göthert, J.R., Nimmerjahn, F. & Gunzer, M. (2015) Catchup: A mouse model for imaging-based tracking and modulation of neutrophil granulocytes. *Nature Methods*, 12 (5), pp.445–452.
- Haugstetter, A.M., Loddenkemper, C., Lenze, D., Gröne, J., Standfu, C., Petersen, I., Dörken, B. & Schmitt, C.A. (2010) Cellular senescence predicts treatment outcome in metastasised colorectal cancer. *British Journal of Cancer*, 103 (4), pp.505–509.
- Hayashi, F., Means, T.K. & Luster, A.D. (2003) Toll-like receptors stimulate human neutrophil function. *Blood*, 102 (7), pp.2660–2669. Available from: <<https://doi.org/10.1182/blood-2003-04-1078>>.
- Highfill, S.L., Cui, Y., Giles, A.J., Smith, J.P., Zhang, H., Morse, E., Kaplan, R.N. & Mackall, C.L. (2014) Disruption of CXCR2-mediated MDSC tumor trafficking enhances anti-PD1 efficacy. *Science Translational Medicine*, 6 (237).
- Highfill, S.L., Rodriguez, P.C., Zhou, Q., Goetz, C.A., Koehn, B.H., Veenstra, R., Taylor, P.A., Panoskaltis-Mortari, A., Serody, J.S., Munn, D.H., Tolar, J., Ochoa, A.C. & Blazar, B.R. (2010) Bone marrow myeloid-derived suppressor cells (MDSCs) inhibit graft-versus-host disease (GVHD) via an arginase-1-dependent mechanism that is up-regulated by interleukin-13. *Blood*, 116 (25), pp.5738–5747.
- Honda, T., Uehara, T., Matsumoto, G., Arai, S. & Sugano, M. (2016) Neutrophil left shift and white blood cell count as markers of bacterial infection. *Clinica Chimica Acta*, 457, pp.46–53. Available from: <<http://dx.doi.org/10.1016/j.cca.2016.03.017>>.
- Hsu, B.E., Tabariès, S., Johnson, R.M., Andrzejewski, S., Senecal, J., Lehuédé, C., Annis, M.G., Ma, E.H., Völs, S., Ramsay, L.A., Froment, R., Monast, A., Watson, I.R., Granot, Z., Jones, R.G., St-Pierre, J. & Siegel, P.M. (2019) Immature Low-Density Neutrophils Exhibit Metabolic Flexibility that Facilitates Breast Cancer Liver Metastasis. *Cell Reports*, 27 (13), pp.3902-3915.e6.
- Huang, B., Pan, P.Y., Li, Q., Sato, A.I., Levy, D.E., Bromberg, J., Divino, C.M. & Chen, S.H. (2006) Gr-1+CD115+ immature myeloid suppressor cells mediate the development of tumor-induced T regulatory cells and T-cell anergy in tumor-bearing host. *Cancer Research*, 66 (2), pp.1123–1131.
- Hurst, C.D., Alder, O., Platt, F.M., Droop, A., Stead, L.F., Burns, J.E., Burghel, G.J., Jain, S., Klimczak, L.J., Lindsay, H., Roulson, J.A., Taylor, C.F., Thygesen, H., Cameron, A.J., Ridley, A.J., Mott, H.R., Gordenin, D.A. & Knowles, M.A. (2017) Genomic Subtypes of Non-invasive Bladder Cancer with Distinct Metabolic Profile and Female Gender Bias in KDM6A Mutation Frequency. *Cancer Cell*, 32 (5), pp.701-715.e7. Available from: <<https://doi.org/10.1016/j.ccell.2017.08.005>>.
- Ibrahim, T., Gizzi, M., Bahleda, R. & Loriot, Y. (2019) Clinical Development of FGFR3 Inhibitors for the Treatment of Urothelial Cancer. *Bladder Cancer*, 5 (2), pp.87–102.
- Inoue, K., Slaton, J.W., Kim, S.J., Perrotte, P., Eve, B.Y., Bar-Eli, M., Radinsky, R. & Dinney, C.P.N. (2000) Interleukin 8 expression regulates tumorigenicity and metastasis in human bladder cancer. *Cancer Research*, 60 (8), pp.2290–2299.

- Iwata, T. (2000) A neonatal lethal mutation in FGFR3 uncouples proliferation and differentiation of growth plate chondrocytes in embryos. *Human Molecular Genetics*, 9 (11), pp.1603–1613.
- Iwata, T. (2001) Highly activated Fgfr3 with the K644M mutation causes prolonged survival in severe dwarf mice. *Human Molecular Genetics*, 10 (12), pp.1255–1264.
- Iwata, T. & Hevner, R.F. (2009) Fibroblast growth factor signaling in development of the cerebral cortex. *Development Growth and Differentiation*, 51 (3), pp.299–323.
- Iyer, G. & Milowsky, M.I. (2013) Fibroblast growth factor receptor-3 in urothelial tumorigenesis. *Urologic Oncology: Seminars and Original Investigations*, 31 (3), pp.303–311.
- Iyer, G. & Milowsky, M.I. (2013) Fibroblast growth factor receptor-3 in urothelial tumorigenesis. *Urologic Oncology: Seminars and Original Investigations*, 31 (3), pp.303–311.
- Jablonska, J., Lang, S., Sionov, R.V. & Granot, Z. (2017) The regulation of pre-metastatic niche formation by neutrophils. *Oncotarget*, 8 (67), pp.112132–112144.
- Jacobs, J.P., Ortiz-Lopez, A., Campbell, J.J., Gerard, C.J., Mathis, D. & Benoist, C. (2010) Deficiency of CXCR2, but not other chemokine receptors, attenuates autoantibody-mediated arthritis in a murine model. *Arthritis and Rheumatism*, 62 (7), pp.1921–1932.
- Jaffer, T. & Ma, D. (2016) The emerging role of chemokine receptor CXCR2 in cancer progression. *Translational Cancer Research*, 5 (6), pp.S616–S628.
- Jain, A. & Pasare, C. (2017) Innate Control of Adaptive Immunity: Beyond the Three-Signal Paradigm. *The Journal of Immunology*, 198 (10), pp.3791–3800.
- Jamieson, T., Clarke, M., Steele, C.W., Samuel, M.S., Neumann, J., Jung, A., Huels, D., Olson, M.F., Das, S., Nibbs, R.J.B. & Sansom, O.J. (2012) Inhibition of CXCR2 profoundly suppresses inflammation-driven and spontaneous tumorigenesis. *Journal of Clinical Investigation*, 122 (9), pp.3127–3144.
- Jaye, M., Schlessinger, J. & Dionne, C.A. (1992) Fibroblast growth factor receptor tyrosine kinases: molecular analysis and signal transduction. *BBA - Molecular Cell Research*, 1135 (2), pp.185–199.
- Jebar, A.H., Hurst, C.D., Tomlinson, D.C., Johnston, C., Taylor, C.F. & Knowles, M.A. (2005) FGFR3 and Ras gene mutations are mutually exclusive genetic events in urothelial cell carcinoma. *Oncogene*, 24 (33), pp.5218–5225.
- Johnson, A.M., O'Connell, M.J., Miyamoto, H., Huang, J., Yao, J.L., Messing, E.M. & Reeder, J.E. (2008) Androgenic dependence of exophytic tumor growth in a transgenic mouse model of bladder cancer: A role for thrombospondin-1. *BMC Urology*, 8 (1), pp.1–17.
- Junker, K., Van Oers, J.M.M., Zwarthoff, E.C., Kania, I., Schubert, J. & Hartmann, A. (2008) Fibroblast growth factor receptor 3 mutations in bladder tumors correlate with low frequency of chromosome alterations. *Neoplasia*, 10 (1), pp.1–7. Available from: <<http://dx.doi.org/10.1593/neo.07178>>.

- Kaiser, J., Li, H., North, S.A., Leibowitz-Amit, R., Seah, J.A., Morshed, N., Chau, C., Lee-Ying, R., Heng, D.Y.C., Sridhar, S., Crabb, S.J. & Alimohamed, N.S. (2018) The Prognostic Role of the Change in Neutrophil-to-Lymphocyte Ratio during Neoadjuvant Chemotherapy in Patients with Muscle-Invasive Bladder Cancer: A Retrospective, Multi-Institutional Study. *Bladder Cancer*, 4 (2), pp.185–194.
- Kang, H.W., Kim, Y.H., Jeong, P., Park, C., Kim, W.T., Ryu, D.H., Cha, E.J., Ha, Y.S., Kim, T.H., Kwon, T.G., Moon, S.K., Choi, Y.H., Yun, S.J. & Kim, W.J. (2017) Expression levels of FGFR3 as a prognostic marker for the progression of primary pT1 bladder cancer and its association with mutation status. *Oncology Letters*, 14 (3), pp.3817–3824.
- Karni-Schmidt, O., Castillo-Martin, M., HuaiShen, T., Gladoun, N., Domingo-Domenech, J., Sanchez-Carbayo, M., Li, Y., Lowe, S., Prives, C. & Cordon-Cardo, C. (2011) Distinct expression profiles of p63 variants during urothelial development and bladder cancer progression. *American Journal of Pathology*, 178 (3), pp.1350–1360.
- Kawahara, T., Furuya, K., Nakamura, M., Sakamaki, K., Osaka, K., Ito, H., Ito, Y., Izumi, K., Ohtake, S., Miyoshi, Y., Makiyama, K., Nakaigawa, N., Yamanaka, T., Miyamoto, H., Yao, M. & Uemura, H. (2016) Neutrophil-to-lymphocyte ratio is a prognostic marker in bladder cancer patients after radical cystectomy. *BMC Cancer*, 16 (1), pp.1–8. Available from: <<http://dx.doi.org/10.1186/s12885-016-2219-z>>.
- Kawanishi, H., Matsui, Y., Ito, M., Watanabe, J., Takahashi, T., Nishizawa, K., Nishiyama, H., Kamoto, T., Mikami, Y., Tanaka, Y., Jung, G., Akiyama, H., Nobumasa, H., Guilford, P., Reeve, A., Okuno, Y., Tsujimoto, G., Nakamura, E. & Ogawa, O. (2008) Secreted CXCL1 Is a potential mediator and marker of the tumor invasion of bladder cancer. *Clinical Cancer Research*, 14 (9), pp.2579–2587.
- Kilgour, E., Angell, H., Smith, N.R., Ahdesmaki, M., Barrett, J.C., Harrington, E.A., Hurst, C. & Knowles, M.A. (2016) Fibroblast growth factor receptor 3 (FGFR3) mutant muscle invasive bladder cancers (MIBC) are associated with low immune infiltrates. *Annals of Oncology*, 27 (suppl_6), p.2016.
- Kim, E., Bae, Y. M., Choi, M. & Hong, S. (2012) Cyst formation, increased anti-inflammatory cytokines and expression of chemokines support for *Clonorchis sinensis* infection in FVB mice. *Parasitology International*, 61, pp. 124–129.
- Kipp, B.R., Tanasescu, M., Else, T.A., Bryant, S.C., Jeffrey Karnes, R., Sebo, T.J. & Halling, K.C. (2009) Quantitative fluorescence in situ hybridization and its ability to predict bladder cancer recurrence and progression to muscle-invasive bladder cancer. *Journal of Molecular Diagnostics*, 11 (2), pp.148–154. Available from: <<http://dx.doi.org/10.2353/jmoldx.2009.080096>>.
- Kiriluk, K.J., Prasad, S.M., Patel, A.R., Steinberg, G.D. & Smith, N.D. (2012) Bladder cancer risk from occupational and environmental exposures. *URO*, 30, pp.199–211.
- Kitamura, H. & Tsukamoto, T. (2006) Early bladder cancer: Concept, diagnosis, and management. *International Journal of Clinical Oncology*, 11 (1), pp.28–37.
- Knowles, M.A. (2008) Molecular pathogenesis of bladder cancer. *International Journal of Clinical Oncology*, 13 (4), pp.287–297.

- Kobayashi, T., Owczarek, T.B., McKiernan, J.M. & Abate-Shen, C. (2015) Modelling bladder cancer in mice: Opportunities and challenges. *Nature Reviews Cancer*, 15 (1), pp.42–54. Available from: <<http://dx.doi.org/10.1038/nrc3858>>.
- Köhler, A., De Filippo, K., Hasenberg, M., Van Den Brandt, C., Nye, E., Hosking, M.P., Lane, T.E., Männ, L., Ransohoff, R.M., Hauser, A.E., Winter, O., Schraven, B., Geiger, H., Hogg, N. & Gunzer, M. (2011) G-CSF-mediated thrombopoietin release triggers neutrophil motility and mobilization from bone marrow via induction of Cxcr2 ligands. *Blood*, 117 (16), pp.4349–4357.
- Kotas, M.E. & Medzhitov, R. (2015) Homeostasis, Inflammation, and Disease Susceptibility. *Cell*, 160 (5), pp.816–827. Available from: <<http://dx.doi.org/10.1016/j.cell.2015.02.010>>.
- Kuper, H., Boffetta, P. & Adami, H.O. (2002) Tobacco use and cancer causation: Association by tumour type. *Journal of Internal Medicine*, 252 (3), pp.206–224.
- Lawrence, S.M., Corriden, R. & Nizet, V. (2018) The Ontogeny of a Neutrophil: Mechanisms of Granulopoiesis and Homeostasis. *Microbiology and Molecular Biology Reviews*, 82 (1), pp.1–22.
- Lawrence, T. & Natoli, G. (2011) Transcriptional regulation of macrophage polarization: Enabling diversity with identity. *Nature Reviews Immunology*, 11 (11), pp.750–761.
- Leach, J., Morton, J.P. & Sansom, O.J. (2017) Neutrophils: Homing in on the myeloid mechanisms of metastasis. *Molecular Immunology*, 110 (December), pp.69–76.
- Lee, H. J., Song, I. C., Yun, H. J., Jo, D. Y. & Kim, S. (2014) CXC chemokines and chemokine receptors in gastric cancer: from basic findings towards therapeutic targeting. *World journal of gastroenterology* 20(7), pp.1681-93. Available from: <<https://doi.org/10.3748/wjg.v20.i7.1681>>.
- Le, Y. & Sauer, B. (2001) Conditional gene knockout using Cre recombinase. *Applied Biochemistry and Biotechnology - Part B Molecular Biotechnology*, 17 (3), pp.269–275.
- Lee, S.M., Russell, A. & Hellawell, G. (2015) Predictive value of pretreatment inflammation-based prognostic scores (Neutrophil-to-lymphocyte ratio, platelet-to-lymphocyte ratio, and lymphocyte-to-monocyte ratio) for invasive bladder carcinoma. *Korean Journal of Urology*, 56 (11), pp.749–755.
- Lesina, M., Schmid, R.M., Algül, H., Lesina, M., Wörmann, S.M., Morton, J., Diakopoulos, K.N., Korneeva, O., Wimmer, M., Einwächter, H., Sperveslage, J., Demir, I.E., Kehl, T., Saur, D., Sipos, B., Heikenwälder, M., Steiner, J.M., Wang, T.C., Sansom, O.J., Schmid, R.M. & Algül, H. (2016) RelA regulates CXCL1 / CXCR2-dependent oncogene-induced senescence in murine Kras - driven pancreatic carcinogenesis Find the latest version : RelA regulates CXCL1 / CXCR2-dependent oncogene-induced senescence in murine Kras -driven pancreatic carcinogene. , 126 (8), pp.2919–2932.
- Letašiová, S., Medved'ová, A., Šovčíková, A., Dušinská, M., Volkovová, K., Mosoiu, C. & Bartonová, A. (2012) Bladder cancer, a review of the environmental risk factors. *Environmental Health*, 11, p.S11.
- Li, G., Yu, J., Song, H., Zhu, S., Sun, L., Shang, Z. & Niu, Y. (2017) Squamous differentiation in patients with superficial bladder urothelial carcinoma is

- associated with high risk of recurrence and poor survival. *BMC Cancer*, 17 (1), pp.1–9.
- Lievens, P.M.J., Mutinelli, C., Baynes, D. & Liboi, E. (2004) The kinase activity of fibroblast growth factor receptor 3 with activation loop mutations affects receptor trafficking and signaling. *Journal of Biological Chemistry*, 279 (41), pp.43254–43260.
- Lim, K., Hyun, Y.M., Lambert-Emo, K., Capece, T., Bae, S., Miller, R., Topham, D.J. & Kim, M. (2015) Neutrophil trails guide influenzaspecific CD8+ T cells in the airways. *Science*, 349 (6252).
- Lin, E.Y., Nguyen, A. V., Russell, R.G. & Pollard, J.W. (2001) Colony-stimulating factor 1 promotes progression of mammary tumors to malignancy. *Journal of Experimental Medicine*, 193 (6), pp.727–739.
- Liu, K., Zhao, K., Wang, L. & Sun, E. (2018) The prognostic values of tumor-infiltrating neutrophils, lymphocytes and neutrophil/lymphocyte rates in bladder urothelial cancer. *Pathology Research and Practice*, 214 (8), pp.1074–1080. Available from: <<https://doi.org/10.1016/j.prp.2018.05.010>>.
- Liu, L.P., Darnall, L., Hu, T., Choi, K., Lane, T.E. & Ransohoff, R.M. (2010) Myelin repair is accelerated by inactivating CXCR2 on nonhematopoietic cells. *Journal of Neuroscience*, 30 (27), pp.9074–9083.
- Lombard, R., Doz, E., Carreras, F., Epardaud, M., Le Vern, Y., Buzoni-Gatel, D. & Winter, N. (2016) IL-17RA in non-hematopoietic cells controls CXCL-1 and 5 critical to recruit neutrophils to the lung of mycobacteria-infected mice during the adaptive immune response. *PLoS ONE*, 11 (2).
- Lotan, Y., Shariat, S.F., Berger, Y., Bock, D., Brady, J., Collini, M.P., Dineen, M., Grossman, H.B., Kassabian, V., Katz, G., Maralani, S., Messing, E., Salup, R., Soloway, M., Stein, B., Tomera, K. & Treiman, A. (2008) Impact of risk factors on the performance of the nuclear matrix protein 22 point-of-care test for bladder cancer detection. *BJU International*, 101 (11), pp.1362–1367.
- Ludwig, A.T., Moore, J.M., Luo, Y., Chen, X., Saltzgaver, N.A., O'Donnell, M.A. & Griffith, T.S. (2004) Tumor necrosis factor-related apoptosis-inducing ligand: A novel mechanism for *Bacillus Calmette-Guérin*-induced antitumor activity. *Cancer Research*, 64 (10), pp.3386–3390.
- Madonia, M., Paliogiannis, P., Solinas, T., Mangoni, A.A., Carru, C. & Zinellu, A. (2018) Neutrophil to lymphocyte ratio and muscular invasion in early-stage bladder cancer: A meta-analysis. *European Journal of Oncology*, 23 (2), pp.65–71.
- Mano, R., Baniel, J., Shoshany, O., Margel, D., Bar-On, T., Nativ, O., Rubinstein, J. & Halachmi, S. (2015) Neutrophil-to-lymphocyte ratio predicts progression and recurrence of non-muscle-invasive bladder cancer. *Urologic Oncology: Seminars and Original Investigations*, 33 (2), pp.67.e1-67.e7. Available from: <<http://dx.doi.org/10.1016/j.urolonc.2014.06.010>>.
- Mantovani, A., Cassatella, M. a, Costantini, C. & Jaillon, S. (2011) Neutrophils in the activation and regulation of innate and adaptive immunity. *Nature reviews. Immunology*, 11 (8), pp.519–531. Available from: <<http://dx.doi.org/10.1038/nri3024>>.

- Mantovani, A., Sozzani, S., Locati, M., Allavena, P. & Sica, A. (2002) Macrophage polarization: Tumor-associated macrophages as a paradigm for polarized M2 mononuclear phagocytes. *Trends in Immunology*, 23 (11), pp.549–555.
- Martinez, F.O. & Gordon, S. (2014) The M1 and M2 paradigm of macrophage activation: Time for reassessment. *F1000Prime Reports*, 6 (March), pp.1–13.
- Massari, F., Di Nunno, V., Cubelli, M., Santoni, M., Fiorentino, M., Montironi, R., Cheng, L., Lopez-Beltran, A., Battelli, N. & Ardizzoni, A. (2018) Immune checkpoint inhibitors for metastatic bladder cancer. *Cancer Treatment Reviews*, 64, pp.11–20. Available from: <<https://doi.org/10.1016/j.ctrv.2017.12.007>>.
- Massena, S., Christoffersson, G., Vågesjö, E., Seignez, C., Gustafsson, K., Binet, F., Hidalgo, C.H., Giraud, A., Lomei, J., Weström, S., Shibuya, M., Claesson-Welsh, L., Gerwins, P., Welsh, M., Kreuger, J. & Phillipson, M. (2015) Identification and characterization of VEGF-A-responsive neutrophils expressing CD49d, VEGFR1, and CXCR4 in mice and humans. *Blood*, 126 (17), pp.2016–2026.
- McComb, S., Thiriot, A., Krishnan, L. & Stark, F. (2013) Introduction to the Immune System. In: K. M. Fulton & S. M. Twine eds. *Immunoproteomics: Methods and Protocols*. Totowa, NJ, Humana Press, pp.1–20. Available from: <https://doi.org/10.1007/978-1-62703-589-7_1>.
- McConkey, D.J., Lee, Sangkyou, Choi, W., Tran, M., Majewski, T., Lee, Sooyong, Siefker-Radtke, A., Dinney, C. & Czerniak, B. (2010) Molecular genetics of bladder cancer: Emerging mechanisms of tumor initiation and progression. *Urologic Oncology: Seminars and Original Investigations*, 28 (4), pp.429–440. Available from: <<http://dx.doi.org/10.1016/j.urolonc.2010.04.008>>.
- Medzhitov, R. (2008) Origin and physiological roles of inflammation. *Nature*, 454 (7203), pp.428–435.
- Meyera, C., Sevko, A., Ramacher, M., Bazhin, A. V., Falk, C.S., Osen, W., Borrello, I., Kato, M., Schadendorf, D., Baniyash, M. & Umanskaya, V. (2011) Chronic inflammation promotes myeloid-derived suppressor cell activation blocking antitumor immunity in transgenic mouse melanoma model. *Proceedings of the National Academy of Sciences of the United States of America*, 108 (41), pp.17111–17116.
- Mfuer-sieburg, B.C.E. & Roy, P. (1996) Genetic Control of the Frequency of Hematopoietic Stem Cells in Mice: Mapping of a Candidate Locus to Chromosome 1 By Christa E. Mfuer-Sieburg and Roy P. Libby. *Journal of Experimental Medicine*, 183 (March).
- Michaud, D.S. & Sc, D. (2007) Chronic inflammation and bladder cancer. *Journal of Cellular Biochemistry*, 25, pp.260–268.
- Michie, A.M. & Zúñiga-Pflücker, J.C. (2002) Regulation of thymocyte differentiation: pre-TCR signals and β -selection. *Seminars in Immunology*, 14 (5), pp.311–323. Available from: <<http://www.sciencedirect.com/science/article/pii/S1044532302000647>>.
- Mihara, K., Smit, M.J., Krajnc-Franken, M., Gossen, J., Rooseboom, M. & Dokter, W. (2005) Human CXCR2 (hCXCR2) takes over functionalities of its murine homolog in hCXCR2 knockin mice. *European Journal of Immunology*, 35 (9), pp.2573–2582.

- Milatovic, S., Nanney, L.B., Yu, Y., White, J.R. & Richmond, A. (2003) Impaired healing of nitrogen mustard wounds in CXCR2 null mice. *Wound Repair and Regeneration*, 11 (3), pp.213–219.
- Mishalian, I., Bayuh, R., Eruslanov, E., Michaeli, J., Levy, L., Zolotarov, L., Singhal, S., Albelda, S.M., Granot, Z. & Fridlender, Z.G. (2014) Neutrophils recruit regulatory T-cells into tumors via secretion of CCL17 - A new mechanism of impaired antitumor immunity. *International Journal of Cancer*, 135 (5), pp.1178–1186.
- Mishalian, I., Bayuh, R., Levy, L., Zolotarov, L., Michaeli, J. & Fridlender, Z.G. (2013) Tumor-associated neutrophils (TAN) develop pro-tumorigenic properties during tumor progression. *Cancer Immunology, Immunotherapy*, 62 (11), pp.1745–1756.
- Miyake, M., Goodison, S., Urquidi, V., Gomes Giacoia, E. & Rosser, C.J. (2013) Expression of CXCL1 in human endothelial cells induces angiogenesis through the CXCR2 receptor and the ERK1/2 and EGF pathways. *Laboratory Investigation*, 93, pp.768–778.
- Miyake, M., Lawton, A., Goodison, S., Urquidi, V., Gomes-Giacoia, E., Zhang, G., Ross, S., Kim, J. & Rosser, C.J. (2013) Chemokine (C-X-C) ligand 1 (CXCL1) protein expression is increased in aggressive bladder cancers. *BMC Cancer*, 13, pp.1–7.
- Miyamoto, H., Yang, Z., Chen, Y.T., Ishiguro, H., Uemura, H., Kubota, Y., Nagashima, Y., Chang, Y.J., Hu, Y.C., Tsai, M.Y., Yeh, S., Messing, E.M. & Chang, C. (2007) Promotion of bladder cancer development and progression by androgen receptor signals. *Journal of the National Cancer Institute*, 99 (7), pp.558–568.
- Morizawa, Y., Miyake, M., Shimada, K., Hori, S., Tatsumi, Y., Nakai, Y., Anai, S., Tanaka, N., Konishi, N. & Fujimoto, K. (2016) Neutrophil-to-lymphocyte ratio as a detection marker of tumor recurrence in patients with muscle-invasive bladder cancer after radical cystectomy. *Urologic Oncology: Seminars and Original Investigations*, 34 (6), pp.257.e11-257.e17. Available from: <<http://dx.doi.org/10.1016/j.urolonc.2016.02.012>>.
- Moser, B. & Loetscher, P. (2001) Lymphocyte traffic control by chemokines. *Nature Immunology*, 2 (2), pp.123–128.
- Moser, B., Dewald, B., Barella, L., Schumacher, C., Baggiolini, M. & Clark-Lewis, I. (1993) Interleukin-8 antagonists generated by N-terminal modification. *Journal of Biological Chemistry*, 268 (10), pp.7125–7128.
- Moses, K., Klein, J.C., Männ, L., Klingberg, A., Gunzer, M. & Brandau, S. (2016) Survival of residual neutrophils and accelerated myelopoiesis limit the efficacy of antibody-mediated depletion of Ly-6G + cells in tumor-bearing mice . *Journal of Leukocyte Biology*, 99 (6), pp.811–823.
- Mosser, D.M. & Edwards, J.P. (2008) Exploring the full spectrum of macrophage activation. *Nature Reviews Immunology*, 8 (12), pp.958–969. Available from: <<http://dx.doi.org/10.1038/nri2448>>.
- Mostafa, M.H., Sheweita, S.A. & O'Connor, P.J. (1999) Relationship between schistosomiasis and bladder cancer. *Clinical Microbiology Reviews*, 12 (1), pp.97–111.
- Movahedi, K., Guilliams, M., Van Den Bossche, J., Van Den Bergh, R., Gysemans, C., Beschin, A., De Baetselier, P. & Van Ginderachter, J.A. (2008) Identification of

discrete tumor-induced myeloid-derived suppressor cell subpopulations with distinct T cell suppressive activity. *Blood*, 111 (8), pp.4233–4244.

- Moynihan, K.D., Opel, C.F., Szeto, G.L., Tzeng, A., Zhu, E.F., Engreitz, J.M., Williams, R.T., Rakhra, K., Zhang, M.H., Rothschilds, A.M., Kumari, S., Kelly, R.L., Kwan, B.H., Abraham, W., Hu, K., Mehta, N.K., Kauke, M.J., Suh, H., Cochran, J.R., Lauffenburger, D.A., Wittrup, K.D. & Irvine, D.J. (2016) Eradication of large established tumors in mice by combination immunotherapy that engages innate and adaptive immune responses. *Nature Medicine*, 22 (12), pp.1402–1410.
- Mu, X.Y., Wang, R.J., Yao, Z.X., Zheng, Z., Jiang, J.T., Tan, M.Y., Sun, F., Fan, J., Wang, X., Zheng, J.H., Wu, K. & Liu, Z.H. (2019) RS 504393 inhibits M-MDSCs recruiting in immune microenvironment of bladder cancer after gemcitabine treatment. *Molecular Immunology*, 109 (April), pp.140–148.
- Multhoff, G., Molls, M. & Radons, J. (2012) Chronic inflammation in cancer development. *Frontiers in Immunology*, 2 (JAN), pp.1–17.
- Murdoch, C., Muthana, M., Coffelt, S.B. & Lewis, C.E. (2008) The role of myeloid cells in the promotion of tumour angiogenesis. *Nature reviews. Cancer*, 8 (8), pp.618–631. Available from: <<http://www.ncbi.nlm.nih.gov/pubmed/18633355>%5Cn<http://www.nature.com/doi/inder/10.1038/nrc2444>>.
- Murphy, C., McGurk, M., Pettigrew, J., Santinelli, A., Mazzucchelli, R., Johnston, P.G., Montironi, R. & Waugh, D.J.J. (2005) Nonapical and cytoplasmic expression of interleukin-8, CXCR1, and CXCR2 correlates with cell proliferation and microvessel density in prostate cancer. *Clinical Cancer Research*, 11 (11), pp.4117–4127.
- Murphy, P.M. (1994) The molecular biology of leukocyte chemoattractant receptors. *Annual review of immunology*, 12, pp.593–633. Available from: <<http://www.annualreviews.org/doi/pdf/10.1146/annurev.iy.12.040194.003113>>.
- Murphy, P.M., Baggiolini, M., Charo, I.F., Hebert, C.A., Horuk, R., Matsushima, K., Miller, L.H., Oppenheim, J.J. & Power, C.A. (2000) International union of pharmacology. XXII. Nomenclature for chemokine receptors. *Pharmacological Reviews*, 52 (1), pp.145–176.
- Murray, P.J. & Wynn, T.A. (2011) Protective and pathogenic functions of macrophage subsets. *Nature Reviews Immunology*, 11 (11), pp.723–737.
- Nathan, C. & Ding, A. (2010) Nonresolving Inflammation. *Cell*, 140 (6), pp.871–882. Available from: <<http://dx.doi.org/10.1016/j.cell.2010.02.029>>.
- Ng, L.G., Ostuni, R. & Hidalgo, A. (2019) Heterogeneity of neutrophils. *Nature Reviews Immunology*, 19 (4), pp.255–265. Available from: <<http://dx.doi.org/10.1038/s41577-019-0141-8>>.
- Nieder, A.M., Soloway, M.S. & Herr, H.W. (2007) Should We Abandon the FISH Test? *European Urology*, 51 (6), pp.1469–1471.
- Nguyen-Jackson, H., Panopoulos, A.D., Zhang, H., Li, H.S., and Watowich, S.S. (2010) STAT3 controls the neutrophil migratory response to CXCR2 ligands by direct activation of G-CSF-induced CXCR2 expression and via modulation of CXCR2 signal transduction. *Blood* 115, pp.3354–3363. Available from: <<https://doi.org/10.1182/blood-2009-08-240317>>.

- Nywening, T.M., Belt, B.A., Cullinan, D.R., Panni, R.Z., Han, B.J., Sanford, D.E., Jacobs, R.C., Ye, J., Patel, A.A., Gillanders, W.E., Fields, R.C., DeNardo, D.G., Hawkins, W.G., Goedegebuure, P. & Linehan, D.C. (2018) Targeting both tumour-associated CXCR2+ neutrophils and CCR2+ macrophages disrupts myeloid recruitment and improves chemotherapeutic responses in pancreatic ductal adenocarcinoma. *Gut*, 67 (6), pp.1112–1123.
- Ok, J.H., Meyers, F.J. & Evans, C.P. (2005) Medical and surgical palliative care of patients with urological malignancies. *Journal of Urology*, 174 (4 I), pp.1177–1182.
- Okajima, E., Hiramatsu, T., Iriya, K., Ijuin, M., Matsushima, S., and Yamada, K (1975) The effects of sex hormones on development of urinary bladder tumors in rats induced by N-butyl-N-(4-hydroxybutyl) nitrosamine. *Urological Research*, 3 (2), pp.73–79.
- Ornitz D.M. & Itoh N. (2015) The Fibroblast Growth Factor signaling pathway. *Wiley Interdiscip Rev Dev Biol* 4, pp.215–266. Available from: <<https://doi.org/10.1002/wdev.176>>.
- Orthgiess, J., Gericke, M., Immig, K., Schulz, A., Hirrlinger, J., Bechmann, I. & Eilers, J. (2016) Neurons exhibit Lyz2 promoter activity in vivo: Implications for using LysM-Cre mice in myeloid cell research. *European Journal of Immunology*, 46 (6), pp.1529–1532.
- Overdevest, J.B., Knubel, K.H., Duex, J.E., Thomas, S., Nitz, M.D., Harding, M.A., Smith, S.C., Frierson, H.F., Conaway, M. & Theodorescu, D. (2012) CD24 expression is important in male urothelial tumorigenesis and metastasis in mice and is androgen regulated. *Proceedings of the National Academy of Sciences of the United States of America*, 109 (51).
- Pillay, J., Den Braber, I., Vrisekoop, N., Kwast, L.M., De Boer, R.J., Borghans, J.A.M., Tesselaar, K. & Koenderman, L. (2010) In vivo labeling with 2H2O reveals a human neutrophil lifespan of 5.4 days. *Blood*, 116 (4), pp.625–627.
- Pinciroli, P., Won, H., Iyer, G., Canevari, S., Colecchia, M., Giannatempo, P., Raggi, D., Pierotti, M.A., De Braud, F.G., Solit, D.B., Rosenberg, J.E., Berger, M.F. & Necchi, A. (2016) Molecular Signature of Response to Pazopanib Salvage Therapy for Urothelial Carcinoma. *Clinical Genitourinary Cancer*, 14 (1), pp.e81–e90. Available from: <<http://dx.doi.org/10.1016/j.clgc.2015.07.017>>.
- Plowright, E.E., Li, Z., Bergsagel, P.L., Chesi, M., Barber, D.L., Branch, D.R., Hawley, R.G. & Stewart, A.K. (2000) Ectopic expression of fibroblast growth factor receptor 3 promotes myeloma cell proliferation and prevents apoptosis. *Blood*, 95 (3), pp.992–998.
- Poh, A.R. & Ernst, M. (2018) Targeting macrophages in cancer: From bench to bedside. *Frontiers in Oncology*, 8 (MAR), pp.1–16.
- Powell, D.R. & Huttenlocher, A. (2016) Neutrophils in the Tumor Microenvironment. *Trends in Immunology*, 37 (1), pp.41–52. Available from: <<http://dx.doi.org/10.1016/j.it.2015.11.008>>.
- Powers, C.J., McLeskey, S.W. & Wellstein, A. (2000) Fibroblast growth factors, their receptors and signaling. *Endocrine-Related Cancer*, 7 (3), pp.165–197.

- Ptaschinski, C. & Lukacs, N.W. (2017) Acute and chronic inflammation induces disease pathogenesis. *Molecular Pathology: The Molecular Basis of Human Disease*, pp.25–43.
- Qing, J., Du, X., Chen, Y., Chan, P., Li, H., Wu, P., Marsters, S., Stawicki, S., Tien, J., Totpal, K., Ross, S., Stinson, S., Dornan, D., French, D., Wang, Q.R., Stephan, J.P., Wu, Y., Wiesmann, C. & Ashkenazi, A. (2009) Antibody-based targeting of FGFR3 in bladder carcinoma and t(4;14)-positive multiple myeloma in mice. *Journal of Clinical Investigation*, 119 (5), pp.1216–1229.
- Rankin, S.M. (2010) The bone marrow: a site of neutrophil clearance. *Journal of Leukocyte Biology*, 88 (2), pp.241–251.
- Redondo-Gonzalez, E., de Castro, L.N., Moreno-Sierra, J., Maestro de Las Casas, M.L., Vera-Gonzalez, V., Ferrari, D.G. & Corchado, J.M. (2015) Bladder carcinoma data with clinical risk factors and molecular markers: a cluster analysis. *BioMed research international*, 2015, p.168682. Available from: <<http://www.ncbi.nlm.nih.gov/pubmed/25866762>>.
- Reis, S.T., Leite, K.R.M., Piovesan, L.F., Pontes-Junior, J., Viana, N.I., Abe, D.K., Crippa, A., Moura, C.M., Adonias, S.P., Srougi, M. & Dalloglio, M.F. (2012) Increased expression of MMP-9 and IL-8 are correlated with poor prognosis of Bladder Cancer. *BMC Urology*, 12, pp.1–5.
- Roberts, A.W. (2005) G-CSF: A key regulator of neutrophil production, but that's not all! *Growth Factors*, 23 (1), pp.33–41.
- Robinson, B.D., Vlachostergios, P.J., Bhinder, B., Liu, W., Li, K., Moss, T.J., Bareja, R., Park, K., Tavassoli, P., Cyta, J., Tagawa, S.T., Nanus, D.M., Beltran, H., Molina, A.M., Khani, F., Miguel Mosquera, J., Xylinas, E., Shariat, S.F., Scherr, D.S., Rubin, M.A., Lerner, S.P., Matin, S.F., Elemento, O. & Faltas, B.M. (2019) Upper tract urothelial carcinoma has a luminal-papillary T-cell depleted contexture and activated FGFR3 signaling. *Nature Communications*, 10 (1), pp.1–11. Available from: <<http://dx.doi.org/10.1038/s41467-019-10873-y>>.
- Rosales, C. (2018) Neutrophil: A cell with many roles in inflammation or several cell types? *Frontiers in Physiology*, 9 (FEB), pp.1–17.
- Rosenberg, J.E. & Hahn, W.C. (2009) Bladder cancer: Modeling and translation. *Genes and Development*, 23 (6), pp.655–659.
- Rosenberg, J.E., Hoffman-Censits, J., Powles, T., Van Der Heijden, M.S., Balar, A. V., Necchi, A., Dawson, N., O'Donnell, P.H., Balmanoukian, A., Loriot, Y., Srinivas, S., Retz, M.M., Grivas, P., Joseph, R.W., Galsky, M.D., Fleming, M.T., Petrylak, D.P., Perez-Gracia, J.L., Burris, H.A., Castellano, D., Canil, C., Bellmunt, J., Bajorin, D., Nickles, D., Bourgon, R., Frampton, G.M., Cui, N., Mariathasan, S., Abidoye, O., Fine, G.D. & Dreicer, R. (2016) Atezolizumab in patients with locally advanced and metastatic urothelial carcinoma who have progressed following treatment with platinum-based chemotherapy: A single-arm, multicentre, phase 2 trial. *The Lancet*, 387 (10031), pp.1909–1920. Available from: <[http://dx.doi.org/10.1016/S0140-6736\(16\)00561-4](http://dx.doi.org/10.1016/S0140-6736(16)00561-4)>.
- Roth, I. & Hebert, C. (2000) CXCR1 and CXCR2. *Discovery*, 4, pp.1–10.
- Saban, M.R., Simpson, C., Davis, C., Wallis, G., Knowlton, N., Frank, M.B., Centola, M., Gallucci, R.M. & Saban, R. (2007) Discriminators of mouse bladder response to intravesical *Bacillus Calmette-Guerin* (BCG). *BMC Immunology*, 8, pp.1–18.

- Saccani, A., Schioppa, T., Porta, C., Biswas, S.K., Nebuloni, M., Vago, L., Bottazzi, B., Colombo, M.P., Mantovani, A. & Sica, A. (2006) p50 nuclear factor- κ B overexpression in tumor-associated macrophages inhibits M1 inflammatory responses and antitumor resistance. *Cancer Research*, 66 (23), pp.11432–11440.
- Sadik, C.D., Kim, N.D. & Luster, A.D. (2011) Neutrophils cascading their way to inflammation. *Trends in Immunology*, 32 (10), pp.452–460. Available from: <<http://dx.doi.org/10.1016/j.it.2011.06.008>>.
- Sagiv, J.Y., Michaeli, J., Assi, S., Mishalian, I., Kisos, H., Levy, L., Damti, P., Lumbroso, D., Polyansky, L., Sionov, R. V., Ariel, A., Hovav, A.H., Henke, E., Fridlender, Z.G. & Granot, Z. (2015) Phenotypic diversity and plasticity in circulating neutrophil subpopulations in cancer. *Cell Reports*, 10 (4), pp.562–573.
- Said, N., Frierson, H.F., Sanchez-Carbayo, M., Brekken, R.A. & Theodorescu, D. (2013) Loss of SPARC in bladder cancer enhances carcinogenesis and progression. *Journal of Clinical Investigation*, 123 (2), pp.751–766.
- Saintigny, P., Massarelli, E., Lin, S., Ahn, Y.H., Chen, Y., Goswami, S., Erez, B., O'Reilly, M.S., Liu, D., Lee, J.J., Zhang, L., Ping, Y., Behrens, C., Soto, L.M.S., Heymach, J. V., Kim, E.S., Herbst, R.S., Lippman, S.M., Wistuba, I.I., Hong, W.K., Kurie, J.M. & Koo, J.S. (2013) CXCR2 expression in tumor cells is a poor prognostic factor and promotes invasion and metastasis in lung adenocarcinoma. *Cancer Research*, 73 (2), pp.571–582.
- Saito, R., Smith, C.C., Utsumi, T., Bixby, L.M., Kardos, J., Wobker, S.E., Stewart, K.G., Chai, S., Manocha, U., Byrd, K.M., Damrauer, J.S., Williams, S.E., Vincent, B.G. & Kim, W.Y. (2018) Molecular subtype-specific immunocompetent models of high-grade urothelial carcinoma reveal differential neoantigen expression and response to immunotherapy. *Cancer Research*, 78 (14), pp.3954–3968.
- Samaniego, R., Gutierrez-Gonzalez, A., Gutierrez-Seijo, A., Sanchez-Gregorio, S., García-Gimenez, J., Mercader, E., Marquez-Rodas, I., Aviles, J.A., Relloso, M. & Sanchez-Mateos, P. (2018) CCL20 Expression by tumor-associated macrophages predicts progression of human primary cutaneous melanoma. *Cancer Immunology Research*, 6 (3), pp.267–275.
- Sansbury, B.E. & Spite, M. (2016) Resolution of acute inflammation and the role of resolvins in immunity, thrombosis, and vascular biology. *Circulation Research*, 119 (1), pp.113–130.
- Sauer, B. & Henderson, N. (1988) Site-specific DNA recombination in mammalian cells by the Cre recombinase of bacteriophage P1. *Proceedings of the National Academy of Sciences of the United States of America*, 85 (14), pp.5166–5170.
- Sawanobori, Y., Ueha, S., Kurachi, M., Shimaoka, T., Talmadge, J.E., Abe, J., Shono, Y., Kitabatake, M., Kakimi, K., Mukaida, N. & Matsushima, K. (2008) Chemokine-mediated rapid turnover of myeloid-derived suppressor cells in tumor-bearing mice. *Journal of Cellular Physiology*, 111, pp.5457–5466.
- Schiwon, M., Weisheit, C., Franken, L., Gutweiler, S., Dixit, A., Meyer-Schwesinger, C., Pohl, J.M., Maurice, N.J., Thiebes, S., Lorenz, K., Quast, T., Fuhrmann, M., Baumgarten, G., Lohse, M.J., Opdenakker, G., Bernhagen, J., Bucala, R., Panzer, U., Kolanus, W., Gröne, H.J., Garbi, N., Kastenmüller, W., Knolle, P.A., Kurts, C. & Engel, D.R. (2014) Crosstalk between sentinel and helper

macrophages permits neutrophil migration into infected uroepithelium. *Cell*, 156 (3), pp.456–468.

- Schott, A.F., Goldstein, L.J., Cristofanilli, M., Ruffini, P.A., McCanna, S., Reuben, J.M., Perez, R.P., Kato, G. & Wicha, M. (2017) Phase Ib pilot study to evaluate reparixin in combination with weekly paclitaxel in patients with HER-2–negative metastatic breast cancer. *Clinical Cancer Research*, 23 (18), pp.5358–5365.
- Schraufstatter, I.U., Trieu, K., Zhao, M., Rose, D.M., Terkeltaub, R.A. & Burger, M. (2003) IL-8-Mediated Cell Migration in Endothelial Cells Depends on Cathepsin B Activity and Transactivation of the Epidermal Growth Factor Receptor. *The Journal of Immunology*, 171 (12), pp.6714–6722.
- Schreiber, R.D., Old, L.J. & Smyth, M.J. (2011) Cancer immunoediting: Integrating immunity's roles in cancer suppression and promotion. *Science*, 331 (6024), pp.1565–1570.
- Schuh, J.M., Blease, K. & Hogaboam, C.M. (2002) CXCR2 Is Necessary for the Development and Persistence of Chronic Fungal Asthma in Mice. *The Journal of Immunology*, 168 (3), pp.1447–1456.
- Selders, G.S., Fetz, A.E., Radic, M.Z. & Bowlin, G.L. (2017) An overview of the role of neutrophils in innate immunity, inflammation and host-biomaterial integration. *Regenerative Biomaterials*, 4 (1), pp.55–68.
- Semerad, C.L., Christopher, M.J., Liu, F., Short, B., Simmons, P.J., Winkler, I., Levesque, J.P., Chappel, J., Ross, F.P. & Link, D.C. (2005) G-CSF potently inhibits osteoblast activity and CXCL12 mRNA expression in the bone marrow. *Blood*, 106 (9), pp.3020–3027.
- Shaul, M.E., Levy, L., Sun, J., Mishalian, I., Singhal, S., Kapoor, V., Horng, W., Fridlender, G., Albelda, S.M. & Fridlender, Z.G. (2016) Tumor-associated neutrophils display a distinct N1 profile following TGF β modulation: A transcriptomics analysis of pro- vs. antitumor TANs. *Oncolmmunology*, 5 (11), pp.1–14. Available from: <<http://dx.doi.org/10.1080/2162402X.2016.1232221>>.
- Sherwood, J., Bertrand, J., Nalesso, G., Poulet, B., Pitsillides, A., Brandolini, L., Karystinou, A., De Bari, C., Luyten, F.P., Pitzalis, C., Pap, T. & Dell'Accio, F. (2015) A homeostatic function of CXCR2 signalling in articular cartilage. *Annals of the Rheumatic Diseases*, 74 (12), pp.2207–2215.
- Shresta, S., Pham, C.T., Thomas, D.A., Graubert, T.A. & Ley, T.J. (1998) How do cytotoxic lymphocytes kill their targets? *Current Opinion in Immunology*, 10 (5), pp.581–587.
- Sica, A. & Bronte, V. (2007) Altered macrophage differentiation and immune dysfunction in tumor development Find the latest version : Review series Altered macrophage differentiation and immune dysfunction in tumor development. *Journal of Clinical Investigation*, 117 (5), pp.1155–1166.
- Sica, A., Porta, C., Morlacchi, S., Banfi, S., Strauss, L., Rimoldi, M., Totaro, M.G. & Riboldi, E. (2012) Origin and functions of Tumor-Associated Myeloid Cells (TAMCs). *Cancer Microenvironment*, 5 (2), pp.133–149.
- Silvestre-Roig, C., Hidalgo, A. & Soehnlein, O. (2016) Neutrophil heterogeneity: Implications for homeostasis and pathogenesis. *Blood*, 127 (18), pp.2173–2181.

- Simone, N.L., Remaley, A.T., Charboneau, L., Petricoin, E.F., Glickman, J.W., Emmert-Buck, M.R., Fleisher, T.A. & Liotta, L.A. (2000) Sensitive immunoassay of tissue cell proteins procured by laser capture microdissection. *American Journal of Pathology*, 156 (2), pp.445–452. Available from: <[http://dx.doi.org/10.1016/S0002-9440\(10\)64749-9](http://dx.doi.org/10.1016/S0002-9440(10)64749-9)>.
- Simons, M.P., O'Donnell, M.A. & Griffith, T.S. (2008) Role of neutrophils in BCG immunotherapy for bladder cancer. *Urologic Oncology: Seminars and Original Investigations*, 26 (4), pp.341–345.
- Singel, K.L. & Segal, B.H. (2016) Neutrophils in the tumor microenvironment: trying to heal the wound that cannot heal. *Immunological Reviews*, 273 (1), pp.329–343.
- Singh, S., Sadanandam, A., Nannuru, K.C., Varney, M.L., Mayer-Ezell, R., Bond, R. & Singh, R.K. (2009) Small-molecule antagonists for CXCR2 and CXCR1 inhibit human melanoma growth by decreasing tumor cell proliferation, survival, and angiogenesis. *Clinical Cancer Research*, 15 (7), pp.2380–2386.
- Singhal, S., Bhojnagarwala, P.S., O'Brien, S., Moon, E.K., Garfall, A.L., Rao, A.S., Quatromoni, J.G., Stephen, T.L., Litzky, L., Deshpande, C., Feldman, M.D., Hancock, W.W., Conejo-Garcia, J.R., Albelda, S.M. & Eruslanov, E.B. (2016) Origin and Role of a Subset of Tumor-Associated Neutrophils with Antigen-Presenting Cell Features in Early-Stage Human Lung Cancer. *Cancer Cell*, 30 (1), pp.120–135. Available from: <<http://dx.doi.org/10.1016/j.ccell.2016.06.001>>.
- Sionov, R.V., Assi, S., Gershkovitz, M., Sagiv, J.Y., Polyansky, L., Mishalian, I., Fridlender, Z.G. & Granot, Z. (2015) Isolation and characterization of neutrophils with anti-tumor properties. *Journal of Visualized Experiments*, 2015 (100), pp.1–12.
- Sjödahl, G., Lauss, M., Lövgren, K., Chebil, G., Gudjonsson, S., Veerla, S., Patschan, O., Aine, M., Fernö, M., Ringnér, M., Månsson, W., Liedberg, F., Lindgren, D. & Höglund, M. (2012) A molecular taxonomy for urothelial carcinoma. *Clinical Cancer Research*, 18 (12), pp.3377–3386.
- Smith, L. (2011) Good planning and serendipity: Exploiting the Cre/Lox system in the testis. *Reproduction*, 141 (2), pp.151–161.
- Smyth, M.J., Dunn, G.P. & Schreiber, R.D. (2006) Cancer Immunosurveillance and Immunoediting: The Roles of Immunity in Suppressing Tumor Development and Shaping Tumor Immunogenicity. *Advances in Immunology*, 90 (06), pp.1–50.
- Smyth, M.J., Godfrey, D.I. & Trapani, J.A. (2001) A fresh look at tumor immunosurveillance and immunotherapy. *Nature Immunology*, 2 (4), pp.293–299.
- Spivak-Kroizman, T., Lemmon, M.A., Dikic, I., Ladbury, J.E., Pinchasi, D., Huang, J., Jaye, M., Crumley, G., Schlessinger, J. & Lax, I. (1994) Heparin-induced oligomerization of FGF molecules is responsible for FGF receptor dimerization, activation, and cell proliferation. *Cell*, 79 (6), pp.1015–1024.
- Stadtmann, A. & Zarbock, A. (2012) CXCR2: From bench to bedside. *Frontiers in Immunology*, 3 (AUG), pp.1–12.
- Steele, C.W., Karim, S.A., Foth, M., Rishi, L., Leach, J.D.G., Porter, R.J., Nixon, C., Jeffrey Evans, T.R., Carter, C.R., Nibbs, R.J.B., Sansom, O.J. & Morton, J.P. (2015) CXCR2 inhibition suppresses acute and chronic pancreatic inflammation. *Journal of Pathology*, 237 (1), pp.85–97.

- Steinbach, K.H., Schick, P., Trepel, F., Raffler, H., Döhrmann, J., Heilgeist, G., Heltzel, W., Li, K., Past, W., van der Woerd-de Lange, J.A., Thöml, H., Fließner, T.M. & Begemann, H. (1979) Estimation of kinetic parameters of neutrophilic, eosinophilic, and basophilic granulocytes in human blood. *Blut*, 39 (1), pp.27–38. Available from: <<https://doi.org/10.1007/BF01008072>>.
- Stromnes, I.M., Greenberg, P.D. & Hingorani, S.R. (2014) Molecular pathways: Myeloid complicity in cancer. *Clinical Cancer Research*, 20 (20), pp.5157–5170.
- Sturla, L.M., Merrick, A.E. & Burchill, S.A. (2003) FGFR3IIIS: A novel soluble FGFR3 spliced variant that modulates growth is frequently expressed in tumour cells. *British Journal of Cancer*, 89 (7), pp.1276–1284.
- Sui, X., Lei, L., Chen, L., Xie, T. & Li, X. (2017) Inflammatory microenvironment in the initiation and progression of bladder cancer. *Oncotarget*, 8 (54), pp.93279–93294.
- Sun, L., Guo, R.F., Newstead, M.W., Standiford, T.J., Macariola, D.R. & Shanley, T.P. (2009) Effect of IL-10 on neutrophil recruitment and survival after *Pseudomonas aeruginosa* challenge. *American Journal of Respiratory Cell and Molecular Biology*, 41 (1), pp.76–84.
- Suttman, H., Riemensberger, J., Bentien, G., Schmaltz, D., Stöckle, M., Jocham, D., Böhle, A. & Brandau, S. (2006) Neutrophil granulocytes are required for effective *Bacillus Calmette-Guérin* immunotherapy of bladder cancer and orchestrate local immune responses. *Cancer Research*, 66 (16), pp.8250–8257.
- Sweis, R.F., Spranger, S., Bao, R., Paner, G.P., Stadler, W.M., Steinberg, G. & Gajewski, T.F. (2016) Molecular drivers of the non- T-cell-inflamed tumor microenvironment in urothelial bladder cancer. *Cancer Immunology Research*, 4 (7), pp.563–568.
- Sylvester, R.J., Van Der Meijden, A.P.M., Oosterlinck, W., Witjes, J.A., Bouffoux, C., Denis, L., Newling, D.W.W. & Kurth, K. (2006) Predicting recurrence and progression in individual patients with stage Ta T1 bladder cancer using EORTC risk tables: A combined analysis of 2596 patients from seven EORTC trials. *European Urology*, 49 (3), pp.466–477.
- Tajadini, M., Panjehpour, M. & Javanmard, S. (2014) Comparison of SYBR Green and TaqMan methods in quantitative real-time polymerase chain reaction analysis of four adenosine receptor subtypes. *Advanced Biomedical Research*, 3 (1), p.85.
- Takahashi, H., Ogata, H., Nishigaki, R., Broide, D.H. & Karin, M. (2010) Tobacco Smoke Promotes Lung Tumorigenesis by Triggering IKK β - and JNK1-Dependent Inflammation. *Cancer Cell*, 17 (1), pp.89–97. Available from: <<http://dx.doi.org/10.1016/j.ccr.2009.12.008>>.
- Takahashi, S., Ikeda, Y., Kimoto, N., Okochi, E., Cui, L., Nagao, M., Ushijima, T. & Shirai, T. (2000) Mutation induction by mechanical irritation caused by uracil-induced urolithiasis in Big Blue $\text{\textcircled{R}}$ rats. *Mutation Research - Fundamental and Molecular Mechanisms of Mutagenesis*, 447 (2), pp.275–280.
- Takeuchi, A., Dejima, T., Yamada, H., Shibata, K., Nakamura, R., Eto, M., Nakatani, T., Naito, S. & Yoshikai, Y. (2011) IL-17 production by $\gamma\delta$ T cells is important for the antitumor effect of *Mycobacterium bovis* bacillus Calmette-Guérin treatment against bladder cancer. *European Journal of Immunology*, 41 (1), pp.246–251.

- Tesi, R.J. (2019) MDSC; the Most Important Cell You Have Never Heard Of. *Trends in Pharmacological Sciences*, 40 (1), pp.4–7.
- Thalmann, G.N., Sermier, A., Rentsch, C., Möhrle, K., Cecchini, M.G. & Studer, U.E. (2000) Urinary interleukin-8 and 18 predict the response of superficial bladder cancer to intravesical therapy with bacillus Calmette-Guerin. *Journal of Urology*, 164 (6), pp.2129–2133.
- Tsujikawa, T., Kumar, S., Borkar, R.N., Azimi, V., Thibault, G., Chang, Y.H., Balter, A., Kawashima, R., Choe, G., Sauer, D., El Rassi, E., Clayburgh, D.R., Kulesz-Martin, M.F., Lutz, E.R., Zheng, L., Jaffee, E.M., Leyshock, P., Margolin, A.A., Mori, M., Gray, J.W., Flint, P.W. & Coussens, L.M. (2017) Quantitative Multiplex Immunohistochemistry Reveals Myeloid-Inflamed Tumor-Immune Complexity Associated with Poor Prognosis. *Cell Reports*, 19 (1), pp.203–217. Available from: <<http://dx.doi.org/10.1016/j.celrep.2017.03.037>>.
- Tu, Z., Xiao, R., Xiong, J., Tembo, K.M., Deng, X., Xiong, M., Liu, P., Wang, M. & Zhang, Q. (2016) CCR9 in cancer: Oncogenic role and therapeutic targeting. *Journal of Hematology and Oncology*, 9 (1), pp.1–9. Available from: <<http://dx.doi.org/10.1186/s13045-016-0236-7>>.
- Turner, M.D., Nedjai, B., Hurst, T. & Pennington, D.J. (2014) Cytokines and chemokines: At the crossroads of cell signalling and inflammatory disease. *Biochimica et Biophysica Acta - Molecular Cell Research*, 1843 (11), pp.2563–2582. Available from: <<http://dx.doi.org/10.1016/j.bbamcr.2014.05.014>>.
- Turner, N. & Grose, R. (2010) Fibroblast growth factor signalling: From development to cancer. *Nature Reviews Cancer*, 10 (2), pp.116–129.
- Ugel, S., De Sanctis, F., Mandruzzato, S. & Bronte, V. (2015) Tumor-induced myeloid deviation: When myeloid-derived suppressor cells meet tumor-Associated macrophages. *Journal of Clinical Investigation*, 125 (9), pp.3365–3376.
- Ugel, S., Delpozzi, F., Desantis, G., Papalini, F., Simonato, F., Sonda, N., Zilio, S. & Bronte, V. (2009) Therapeutic targeting of myeloid-derived suppressor cells. *Current Opinion in Pharmacology*, 9 (4), pp.470–481.
- van den Berg, T.K. & Kraal, G. (2005) A function for the macrophage F4/80 molecule in tolerance induction. *Trends Immunol*, 26, pp. 506-509. Available from: <<https://doi.org/10.1016/j.it.2005.07.008>>.
- Van Rhijn, B.W.G., Catto, J.W., Goebell, P.J., Knüchel, R., Shariat, S.F., Van Der Poel, H.G., Sanchez-Carbayo, M., Thalmann, G.N., Schmitz-Dräger, B.J. & Kiemeny, L.A. (2014) Molecular markers for urothelial bladder cancer prognosis: Toward implementation in clinical practice. *Urologic Oncology: Seminars and Original Investigations*, 32, pp.1078–1087.
- Vasconcelos-Nóbrega, C., Colaço, A., Lopes, C. & Oliveira, P.A. (2012) BBN as an urothelial carcinogen. *In Vivo*, 26 (4), pp.727–739.
- Ventura, A., Kirsch, D.G., McLaughlin, M.E., Tuveson, D.A., Grimm, J., Lintault, L., Newman, J., Reczek, E.E., Weissleder, R. & Jacks, T. (2007) Restoration of p53 function leads to tumour regression in vivo. *Nature*, 445 (7128), pp.661–665.
- Vesely, M.D., Kershaw, M.H., Schreiber, R.D. & Smyth, M.J. (2011) Natural Innate and Adaptive Immunity to Cancer. *Annual Review of Immunology*, 29 (1), pp.235–271.

- Wang, J.X., Bair, A.M., King, S.L., Shnayder, R., Huang, Y.F., Shieh, C.C., Soberman, R.J., Fuhlbrigge, R.C. & Nigrovic, P.A. (2012) Ly6G ligation blocks recruitment of neutrophils via a β 2-integrin- dependent mechanism. *Blood*, 120 (7), pp.1489–1498.
- Wang, W., Soto, H., Oldham, E.R., Buchanan, M.E., Homey, B., Catron, D., Jenkins, N., Copeland, N.G., Gilbert, D.J., Nguyen, N., Abrams, J., Kershenovich, D., Smith, K., McClanahan, T., Vicari, A.P. & Zlotnik, A. (2000) Identification of a novel chemokine (CCL28), which binds CCR10 (GPR2). *Journal of Biological Chemistry*, 275 (29), pp.22313–22323.
- Wu, X.R., Kong, X.P., Pellicer, A., Kreibich, G. & Sun, T.T. (2009) Uroplakins in urothelial biology, function, and disease. *Kidney International*, 75 (11), pp.1153–1165.
- Wu, Y., Wang, S., Farooq, S.M., Castelveter, M.P., Hou, Y., Gao, J.L., Navarro, J. V., Oupicky, D., Sun, F. & Li, C. (2012) A chemokine receptor CXCR2 macromolecular complex regulates neutrophil functions in inflammatory diseases. *Journal of Biological Chemistry*, 287 (8), pp.5744–5755.
- Wynn, T.A. (2003) IL-13 Effector Functions. *Annual Review of Immunology*, 21 (1), pp.425–456.
- Xiao, X., Zhao, P., Rodriguez-Pinto, D., Qi, D., Henegariu, O., Alexopoulou, L., Flavell, R.A., Wong, F.S. & Wen, L. (2009) Inflammatory Regulation by TLR3 in Acute Hepatitis. *The Journal of Immunology*, 183 (6), pp.3712–3719.
- Xue, W., Zender, L., Miething, C., Dickins, R.A., Hernando, E., Krizhanovskiy, V., Cordon-Cardo, C. & Lowe, S.W. (2007) Senescence and tumour clearance is triggered by p53 restoration in murine liver carcinomas. *Nature*, 445 (7128), pp.656–660.
- Yamamoto, M., Kikuchi, H., Ohta, M., Kawabata, T., Hiramatsu, Y., Kondo, K., Baba, M., Kamiya, K., Tanaka, T., Kitagawa, M. & Konno, H. (2008) TSU68 prevents liver metastasis of colon cancer xenografts by modulating the premetastatic niche. *Cancer Research*, 68 (23), pp.9754–9762.
- Yang, F., Feng, C., Zhang, X., Lu, J. & Zhao, Y. (2017) The Diverse Biological Functions of Neutrophils, Beyond the Defense Against Infections. *Inflammation*, 40 (1), pp.311–323.
- Yang, L., Huang, J., Ren, X., Gorska, A.E., Chytil, A., Aakre, M., Carbone, D.P., Matrisian, L.M.M., Richmond, A., Lin, P.C. & Moses, H.L. (2008) Abrogation of TGF β Signaling in Mammary Carcinomas Recruits Gr-1+CD11b+ Myeloid Cells that Promote Metastasis. *Cancer Cell*, 13 (1), pp.23–35.
- Yang, L., Pang, Y. & Moses, H.L. (2010) TGF- β and immune cells: an important regulatory axis in the tumor microenvironment and progression. *Trends in Immunology*, 31 (6), pp.220–227. Available from: <<http://dx.doi.org/10.1016/j.it.2010.04.002>>.
- Yazbek-Hanna, M., Whelan, P. & Jain, S. (2016) Bladder cancer. *Medicine*, 44(1):52–5.
- Ye, M., Iwasaki, H., Laiosa, C. V., Stadtfeld, M., Xie, H., Heck, S., Clausen, B., Akashi, K. & Graf, T. (2003) Hematopoietic stem cells expressing the myeloid lysozyme gene retain long-term, multilineage repopulation potential. *Immunity*, 19 (5), pp.689–699.

- Ye, X.Z., Yu, S.C. & Bian, X.W. (2010) Contribution of myeloid-derived suppressor cells to tumor-induced immune suppression, angiogenesis, invasion and metastasis. *Journal of Genetics and Genomics*, 37 (7), pp.423–430. Available from: <[http://dx.doi.org/10.1016/S1673-8527\(09\)60061-8](http://dx.doi.org/10.1016/S1673-8527(09)60061-8)>.
- Yoshimura, T. (2018) The chemokine MCP-1 (CCL2) in the host interaction with cancer: A foe or ally? *Cellular and Molecular Immunology*, 15 (4), pp.335–345.
- Yu, H., Lee, H., Herrmann, A., Buettner, R. & Jove, R. (2014) Revisiting STAT3 signalling in cancer: New and unexpected biological functions. *Nature Reviews Cancer*, 14 (11), pp.736–746. Available from: <<http://dx.doi.org/10.1038/nrc3818>>.
- Yuan, X.K., Zhao, X.K., Xia, Y.C., Zhu, X. & Xiao, P. (2011) Increased circulating immunosuppressive CD14+HLA-DR-/low cells correlate with clinical cancer stage and pathological grade in patients with bladder carcinoma. *Journal of International Medical Research*, 39 (4), pp.1381–1391.
- Zarbock, A., Allegretti, M. & Ley, K. (2008) Therapeutic inhibition of CXCR2 by Reparixin attenuates acute lung injury in mice. *British Journal of Pharmacology*, 155 (3), pp.357–364.
- Zhai, Q.J., Black, J., Ayala, A.G. & Ro, J.Y. (2007) Histologic variants of infiltrating urothelial carcinoma. *Archives of Pathology and Laboratory Medicine*, 131 (8), pp.1244–1256.
- Zhang, H., Ye, Y.L., Li, M.X., Ye, S.B., Huang, W.R., Cai, T.T., He, J., Peng, J.Y., Duan, T.H., Cui, J., Zhang, X.S., Zhou, F.J., Wang, R.F. & Li, J. (2017) CXCL2/MIF-CXCR2 signaling promotes the recruitment of myeloid-derived suppressor cells and is correlated with prognosis in bladder cancer. *Oncogene*, 36 (15), pp.2095–2104.
- Zhang, J.M. & An, J. (2007) Cytokines, inflammation, and pain, *Int Anesthesiol Clin* 45 (2), pp.27-37. Available from: <<https://doi.org/10.1097/AIA.0b013e318034194e>>.
- Zhang, Q., Raoof, M., Chen, Y., Sumi, Y., Sursal, T., Junger, W., Brohi, K., Itagaki, K. & Hauser, C.J. (2010) Circulating mitochondrial DAMPs cause inflammatory responses to injury. *Nature*, 464 (7285), pp.104–107.
- Zhang, Y., Fu, J., Shi, Y., Peng, S., Cai, Y., Zhan, X., Song, N., Liu, Y., Wang, Z., Yu, Y., Wang, Y., Shi, Q., Fu, Y., Yuan, K., Zhou, N., Joshi, R., Ichim, T.E. & Min, W. (2018) A new cancer immunotherapy via simultaneous DC-mobilization and DC-targeted IDO gene silencing using an immune-stimulatory nanosystem. *International Journal of Cancer*, 143 (8), pp.2039–2052.
- Zhang, Z.T., Pak, J., Shapiro, E., Sun, T.T. & Wu, X.R. (1999) Urothelium-specific expression of an oncogene in transgenic mice induced the formation of carcinoma in situ and invasive transitional cell carcinoma. *Cancer Research*, 59 (14), pp.3512–3517.
- Zhou, L., Xu, L., Chen, L., Fu, Q., Liu, Z., Chang, Y., Lin, Z. & Xu, J. (2017) Tumor-infiltrating neutrophils predict benefit from adjuvant chemotherapy in patients with muscle invasive bladder cancer. *OncolImmunology*, 6 (4).
- Zhou, Q., Yan, X., Gershan, J., Orentas, R.J. & Johnson, B.D. (2008) Expression of Macrophage Migration Inhibitory Factor by Neuroblastoma Leads to the Inhibition of Antitumor T Cell Reactivity In Vivo. *The Journal of Immunology*, 181 (3), pp.1877–1886.

- Zlotnik, A., Burkhardt, A.M. & Homey, B. (2011) Homeostatic chemokine receptors and organ-specific metastasis. *Nature Reviews Immunology*, 11 (9), pp.597–606. Available from: <<http://dx.doi.org/10.1038/nri3049>>.
- Zou, W. (2005) Immunosuppressive networks in the tumour environment and their therapeutic relevance. *Nature Reviews Cancer*, 5, p.263. Available from: <<http://dx.doi.org/10.1038/nrc1586>>.
- Zúñiga-Pflücker, J.C. (2004) T-cell development made simple. *Nature Reviews Immunology*, 4 (1), pp.67–72.